

**RELATIONSHIP BETWEEN SYSTEMIC AND CENTRAL NERVOUS SYSTEM
MONOCYTE/MACROPHAGE INFECTION IN SIMIAN IMMUNODEFICIENCY
VIRUS ENCEPHALITIS**

by

Stephanie Jane Bissel

BS, University of North Dakota, 1994

Submitted to the Graduate Faculty of

Graduate School of Public Health in partial fulfillment

of the requirements for the degree of

Doctor of Philosophy

University of Pittsburgh

2005

UNIVERSITY OF PITTSBURGH
GRADUATE SCHOOL OF PUBLIC HEALTH

This dissertation was presented

by

Stephanie Jane Bissel

It was defended on

November 29, 2005

and approved by

Clayton A. Wiley, MD, PhD
Graduate Advisor, Professor
Department of Pathology
School of Medicine
University of Pittsburgh

Simon Barratt-Boyes, BVSc, PhD
Committee Member, Associate Professor
Department of Infectious Diseases and Microbiology
Graduate School of Public Health
University of Pittsburgh

Ronald C. Montelaro, PhD
Committee Member, Professor
Department of Molecular Genetics and Biochemistry
School of Medicine
University of Pittsburgh

Michael Murphey-Corb, PhD
Committee Member, Professor
Department of Molecular Genetics and Biochemistry
School of Medicine
University of Pittsburgh

Clayton A. Wiley, M.D., Ph.D

**RELATIONSHIP BETWEEN PERIPHERAL AND CENTRAL NERVOUS SYSTEM
MONOCYTE/MACROPHAGE INFECTION IN SIMIAN IMMUNODEFICIENCY
VIRUS ENCEPHALITIS**

Stephanie Jane Bissel, PhD

University of Pittsburgh, 2005

Approximately $\frac{1}{4}$ of AIDS patients develop HIVE, the pathologic entity associated with cognitive, motor, and behavioral deficits attributed to synaptic damage and neuronal loss. It still remains unclear why only a subset of HIV-infected individuals develops abundant central nervous system (CNS) macrophage/microglia infection that characterizes HIVE. The overarching hypothesis of this body of work is that simian immunodeficiency virus (SIV) encephalitis (SIVE) is the CNS manifestation of a systemic increase in SIV infection and activation of monocyte/macrophage elements. Specifically, we examined the relationship of infected and activated monocyte/macrophage elements outside of the CNS during the evolution of lentiviral encephalitis to the presence of infected macrophages in the CNS. We studied three models of SIV infection: SIV-infection of rhesus and pigtailed macaques and SIV-infection of CD8⁺ T cell depleted macaques. Antibody-mediated CD8⁺ T cell depletion did not increase the incidence of SIVE in infected rhesus macaques. In SIV-infected rhesus macaques, we examined whether presence of activated macrophages or SIV-infected macrophages is associated with the presence of neuronal damage. The presence of abundant infected macrophages in the CNS is related to postsynaptic neuronal damage in macaques with SIVE. At the same time cerebrospinal fluid viral load increased in SIV-infected CD8-depleted rhesus and non-depleted pigtailed macaques that developed encephalitis, monocyte-derived macrophages produced more virus *ex vivo* than macaques that did not develop encephalitis. Compared to pigtailed macaques

that did not develop SIVE, the monocyte associated SIV-DNA load of monocytes was elevated in macaques that developed SIVE. Pigtailed macaques with SIVE had more infected macrophages in peripheral organs, with the exception of lymph nodes, than macaques without SIVE. Longitudinal analysis of phenotypic markers of monocyte activation show that increases in proportion of CD14⁺/CD16⁺ monocytes is associated with chronic disease. Brains with SIVE have greater numbers of T cells with cytotoxic potential. In conclusion, these findings suggest that inherent differences in host macrophage viral production or immune response to macrophage infection are associated with development of encephalitis. Further understanding of the differential role monocyte/macrophages have in the development of lentiviral encephalitis will identify therapeutic targets to halt this public health epidemic.

ACKNOWLEDGEMENTS

I would like to show my deep appreciation and gratitude to my mentor Dr. Clayton Wiley for his guidance, support, and encouragement during my graduate career. He exemplifies strong scientific integrity and insight that has given me confidence and the foundation to develop scientific independence. I would also like to thank my committee members, Drs. Simon Barratt-Boyes, Ronald Montelaro, and Michael Murphey-Corb. The committee has been supportive of my project. Mickey Corb, in particular, has aided me greatly with technical support and ideas.

I am also indebted to my co-workers for providing me not only with scientific discussion, but support, encouragement, the ability to vent my frustrations and share my successes, laughter, and best of all, friendship. These lifelong friends are Wanda Wang, Kelly Jordan-Sciutto, Sriram Venneti, Arlene Carbone-Wiley, Claudia Grossmann, Jonette Werley, Mariel Jais, Susan Slagel, Gokul Kandala, Rafael Medinas-Flores, Sharon Harrold, Karen Weber, Kathleen Morgan, and Jessica Garver. I will miss everyone dearly and wish them happiness in the journey of life.

I would also like to acknowledge past and present member of the Corb lab, Dawn McClemens-McBride, Anita Trichel, Premi Rajakumar, Holly Cassamassa, Stephanie Casino, and Rachel Taber, for their professional and comedic support. Enormous thanks for the support, advice and knowledge from the faculty, staff, and students of IDM and Neuropathology.

The completion of this work was supported by the patience and love of my husband, Aki. He was always there to cheer me up through hard times and made my good times even better. I could never thank him enough. This appreciation is extended to my friends and family. Mom, Dad, Ryan, and Heather have given so much support and love over the years and have encouraged me to achieve my goals. Thank you! I love you all.

TABLE OF CONTENTS

1. INTRODUCTION.....	1
1.1. The AIDS epidemic.....	1
1.2. Lentiviruses and lentiviral infection.....	3
1.2.1. Retroviruses.....	3
1.2.2. Lentiviruses.....	4
1.2.3. HIV infection in humans.....	4
1.2.4. HIV virion.....	8
1.2.5. HIV life cycle.....	8
1.2.6. Viral entry and viral tropism.....	12
1.2.7. Infected tissue macrophages in HIV pathogenesis.....	13
1.3. HIV and CNS infection.....	14
1.3.1. HIV-associated dementia.....	14
1.3.2. HIV encephalitis.....	14
1.3.3. Infected cells in the CNS.....	15
1.3.4. HIV entry into CNS.....	16
1.3.5. Mechanisms of nervous system damage.....	18
1.3.6. Effect of HAART on CNS disease.....	19
1.3.7. Blood brain barrier defects during HIV infection.....	21
1.4. SIV-infected macaque model for HIV infection in humans.....	22
1.4.1. SIV-infection of natural hosts.....	22

1.4.2. SIV-infection in Asian macaques.....	23
1.4.3. Disease progression rates in SIV-infected macaques.....	23
1.4.4. CNS disease in SIV-infected macaques.	24
1.4.5. CNS disease in animal retroviral infection.....	25
1.5. Immune response to primate lentivirus infection	27
1.6. The role of host factors in susceptibility of cells to lentiviral infection.	28
2. SPECIFIC AIMS	29
3. RESULTS	32
3.1. Chapter 1	32
3.1.1. Abstract.....	33
3.1.2. Introduction.....	34
3.1.3. Materials and Methods	36
3.1.4. Results	47
3.1.5. Discussion.....	58
3.1.6. Acknowledgements	65
3.2. Chapter 2	66
3.2.1. Abstract.....	67
3.2.2. Introduction.....	68
3.2.3. Materials and Methods	71
3.2.4. Results	80
3.2.5. Discussion.....	101
3.2.6. Acknowledgements	108

3.3. Chapter 3	109
3.3.1. Abstract.....	110
3.3.2. Introduction.....	111
3.3.3. Materials and Methods	113
3.3.4. Results	121
3.3.5. Discussion.....	134
3.3.6. Acknowledgements	140
3.4. Chapter 4	141
3.4.1. Abstract.....	142
3.4.2. Introduction.....	143
3.4.3. Materials and Methods	145
3.4.4. Results	147
3.4.5. Discussion.....	162
3.4.6. Acknowledgements	166
4. DISCUSSION	167
CNS macrophage infection relates neuronal damage in lentiviral encephalitis	168
Antibody-mediated CD8 ⁺ T cell depletion of rhesus macaques.....	170
Monocyte-associated SIV DNA and capability to produce virus during development of SIVE.....	171
Phenotypic monocyte-activation markers during the development of SIVE	173
Peripheral macrophage infection in macaques with SIVE.....	174
Immune response to CNS macrophage infection	174

Summary of correlates of SIVE.....	175
Summary of factors that did not correlates with development of SIVE	176
Future directions	176
Summary	179
BIBLIOGRAPHY	180

LIST OF TABLES

Table 1. Macaque Infection Parameters.....	45
Table 2. Clinical Symptoms and Peripheral Blood Studies	46
Table 3. Rhesus macaque Age, Sex, Infection Parameters, and Neuropathological and Clinical Diagnosis.....	84
Table 4. Pigtailed Macaque Age, Sex, Infection Parameters, and Neuropathological and Clinical Diagnosis.....	123
Table 5. Description of activation markers analyzed on monocyte subsets during the course of SIV infection.	148-149

LIST OF FIGURES

Figure 1. Genomic organization of HIV-1.....	5
Figure 2. Typical Clinical Course of HIV Infected Patients.....	7
Figure 3. HIV Life Cycle.....	11
Figure 4. Mechanisms of Neurodegeneration During AIDS.....	20
Figure 5. Macaques with histological evidence of SIVE had brain SIV RNA concentrations 5 orders of magnitude greater than macaques without SIVE.....	48
Figure 6. Immunofluorescent staining for macrophages and SIV envelope protein showed extensive co-localization in SIVE.....	50
Figure 7. Quantitation of immunohistochemical staining for macrophages (CD68) and SIV envelope protein shows a 4- to 25-fold increase in brain regions with encephalitis versus those without encephalitis.....	52
Figure 8. Macaques with SIVE show decreased staining for MAP-2 and synaptophysin.....	55
Figure 9. MAP-2 staining is decreased in the brains of macaques with SIVE, whereas synaptophysin staining is decreased in the brains of SIV-infected macaques with and without encephalitis.....	57
Figure 10. Triple-label immunofluorescent staining for macrophage marker SIV envelope protein (red, Cy5), CD68 (green, Alexa488), and astrocyte marker GFAP (blue, Alexa Fluor 555) shows infected macrophages in a microglial nodule from a CD8 ⁺ T cell-depleted rhesus macaque with SIVE.....	83

Figure 11. Longitudinal peripheral blood counts for CD4⁺ lymphocytes (a), CD8⁺ lymphocytes (b), and monocytes (c) of eight CD8 depleted rhesus macaques infected with SIV/DeltaB670. 85

Figure 12. SIV RNA of eight *CD8* depleted rhesus macaques infected with SIV/DeltaB670... 87

Figure 13. Analysis of blood monocyte SIV DNA and SIV p27 production in MDM and nonadherent PBMC from CD8 T cell-depleted rhesus macaques during SIV/DeltaB670 infection. 89

Figure 14. Double-label immunofluorescent staining for macrophage marker CD68 or T cell marker CD3 and SIV envelope protein shows macaques with SIVE have more infected macrophages in the spinal cord but less infected macrophages in the thymus and lung than macaques without encephalitis..... 93

Figure 15. Necropsy survey of the number of infected macrophages and T lymphocytes observed in peripheral organs from eight *CD8* depleted rhesus macaques infected with SIV/DeltaB670..... 95

Figure 16. Analysis of post- and presynaptic proteins and macrophages in the brains from eight *CD8* depleted rhesus macaques infected with SIV/DeltaB670 at necropsy. 98

Figure 17. Mean longitudinal peripheral blood counts for CD4⁺ T cells and CD8⁺ T cells of six pigtailed macaques infected with SIV/DeltaB670. 122

Figure 18. Plasma SIV RNA of six pigtailed macaques infected with SIV/DeltaB670..... 125

Figure 19. Longitudinal analysis of blood monocyte SIV DNA and SIV p27 production in MDM and nonadherent PBMC from six pigtailed macaques infected with SIV/DeltaB670. 126

Figure 20. Longitudinal biopsy survey of the number of infected macrophages and T lymphocytes observed in lymph nodes from six pigtailed macaques infected with SIV/DeltaB670.....	130
Figure 21. Pigtailed macaques with SIV encephalitis have more infected macrophages in peripheral organs than macaques without encephalitis.	131
Figure 22. Pigtailed macaques with SIV encephalitis have more CD3 ⁺ TIA-1 ⁺ cells in the CNS than macaques without encephalitis.	133
Figure 23. CD14 expression on monocytes can be divided into two subsets. Whole blood was stained with anti-CD14 and one of the antibodies listed in Table 1.....	150
Figure 24. Proportion of CD14 ^{hi} cells that expressed phenotypic markers of activation during the course of infection in six pigtailed macaques infected with SIV/DeltaB670.	151
Figure 25. Proportion of CD14 ^{lo} cells that expressed phenotypic markers of activation during the course of infection in six pigtailed macaques infected with SIV/DeltaB670.	153
Figure 26. Mean fluorescent intensity (MFI) of activation markers on CD14 ^{hi} cells during the course of infection in six pigtailed macaques infected with SIV/DeltaB670.	159
Figure 27. The proportion of CD14 ^{hi} /CD16 ⁺ cells increased while the percentage of CD14 ^{lo} /CD16 ^{hi} cells decreased during the course of infection in six pigtailed macaques infected with SIV/DeltaB670 regardless of development of encephalitis.	160

1. INTRODUCTION

1.1. The AIDS epidemic.

As of 2004, the Joint United Nations Programme on HIV/AIDS (UNAIDS) estimates that 39.4 million people are infected with Human Immunodeficiency Virus (HIV), the etiologic agent that causes acquired immune deficiency syndrome (AIDS) (see <http://www.unaids.org>) (372). Children under 15 years of age comprise 2.2 million of the people living with HIV/AIDS (372). Approximately 4.9 million people were expected to acquire HIV infections in 2004, and 3.1 million people were expected to die as the result of AIDS in 2003 (372). The HIV/AIDS epidemic shows no sign of abating and remains a global public health epidemic. Sub-Saharan Africa is the most severely affected region, with an astonishing average adult prevalence of 7.4% (372). HIV prevalence among pregnant women in sub-Saharan Africa ranges from almost 40% in Botswana and Swaziland to ~3% in Angola (372). Antiretroviral treatment in sub-Saharan Africa is unavailable to most infected individuals. Lack of effective prevention programs, social inequality, and social traditions of the region combine to make effective policies and practices to combat HIV/AIDS challenging. A small glimpse of hope exists in Uganda where HIV prevalence has fallen from 13% to 4.1% during the last decade (372). Disturbingly, several other regions such as China, Indonesia, Viet Nam, Russia, the Baltic States, Papua New Guinea, and North Africa are experiencing growing epidemics. In the United States and other high-income countries, the total number of people infected with HIV continues to increase especially among minority populations such as African-American females. It appears that effective prevention programs have been given less priority in recent years leading to resurgence of high-risk sexual behaviors in several high-income countries.

In the United States, it is estimated that there are ~40,000 newly acquired infections each year (372). African Americans currently bear the brunt of the epidemic. ~25% of all AIDS cases and over 50% of new HIV diagnoses have been reported in African Americans despite comprising only 12% of the United States population (372). African American women account for a staggering 72% of new HIV diagnoses in all US females (372). Whereas the proportion of AIDS cases have declined among Caucasians and remained stable for Hispanics, AIDS is one of the top three causes of death for some African American age groups. This may be partly due to decreased access to antiretroviral therapy which has decreased AIDS-related deaths in Caucasians (372). It is clear the poverty and socioeconomic status in the United States and the rest of the world increase risk for HIV infection.

The expanding HIV/AIDS epidemic threatens the health and economy of the human population. Despite enormous advances made in understanding this virus, there is currently no licensed vaccine to prevent or eliminate HIV infection. Fortunately, there are effective antiretroviral drug regimens that prolong lives of people infected with HIV, but these regimens do not clear HIV from infected individuals, do not work for all individuals, and are not available to all individuals. Ultimately, until treatments that eliminate HIV infection are available, all HIV-infected people will die from AIDS. It is imperative that implementation of efficacious prevention programs and innovative study of HIV infection be continued in order to curb this pandemic.

1.2. Lentiviruses and lentiviral infection.

1.2.1. Retroviruses.

In 1904, one of the first viruses discovered was the equine infectious anemia virus (EIAV) (357, 375). This virus was identified decades later as a retrovirus. Retroviruses are a large family of enveloped RNA viruses containing reverse transcriptase that share structural, genomic, and replicative characteristics (57). Most known retroviruses infect vertebrates but have been found in invertebrates such as insects and mollusks. Retroviral infection can result in a broad spectrum of diseases such as malignancies, wasting diseases, neurological diseases, and most famously immunodeficiencies. The most unique characteristic of retroviruses is it contains an enzyme, reverse transcriptase (RT), which is able to convert its single stranded RNA to linear double stranded DNA (18, 358, 359). Isolation of reverse transcriptase in 1970 transformed the field of molecular biology, providing a means to convert RNA to cDNA (357). After reverse transcription, the viral double-stranded DNA is able to stably integrate into the host DNA.

The family *Retroviridae* consists of 7 genera: *Alpharetrovirus*, *Betaretrovirus*, *Gammaretrovirus*, *Deltaretrovirus*, Type D Retrovirus group, spumaviruses, and lentiviruses (68, 69, 357). *Alpharetrovirus*, *Betaretrovirus*, *Gammaretrovirus*, and *Deltaretrovirus* infection can cause leukemia, lymphoma, sarcomas, and other malignancies (68, 357). Spumaviruses are apparently benign. Lentivirus infection typically exhibits a chronic course of disease resulting in immunodeficiency, autoimmunity, pneumonitis, and neurological disease (193).

1.2.2. Lentiviruses.

Members of this genus of retroviruses historically appeared to result in a slow (Latin: *lentus*, slow) viral infection. Examples of lentiviruses include HIV-1 and -2, simian immunodeficiency virus (SIV), feline immunodeficiency virus (FIV), bovine immunodeficiency virus (BIV), visna/maedi virus, caprine arthritis-encephalitis virus, and EIAV (193). Infection with lentiviruses usually leads to an assortment of neurological and/or immunological disease in their host (193). The CNS is prone to infection by lentiviruses. In addition to the retroviral genes *gag*, *protease*, *polymerase*, *integrase*, and *envelope*, lentiviral genomes contain a complex combination of accessory genes that aid in regulating viral mRNA and protein expression, increasing virus infectivity and transmission, transactivation, inhibition of host's immune response, and viral release (Figure 1) (193).

1.2.3. HIV infection in humans.

In 1983, a retrovirus later called HIV-1 (referred to as HIV from this point) was identified as the cause of AIDS in humans (21). HIV-2 infection was discovered in 1986 (65) and is genetically closer to SIV from sooty mangabeys. HIV is transmitted through contact with infected blood or blood products, sexual fluids, or mother-child transmission (193).

During acute infection, HIV infected individuals experience headaches, rash, retro-orbital pain, muscle aches, sore throats, fevers, nausea, lethargy, or lymphadenopathy (9). Acute infection lasts ~9-10 weeks and is associated with high levels of viral replication, dissemination of virus throughout the body, increased CD8⁺ T cell counts, and decreased CD4⁺ T cell counts (193, 275).

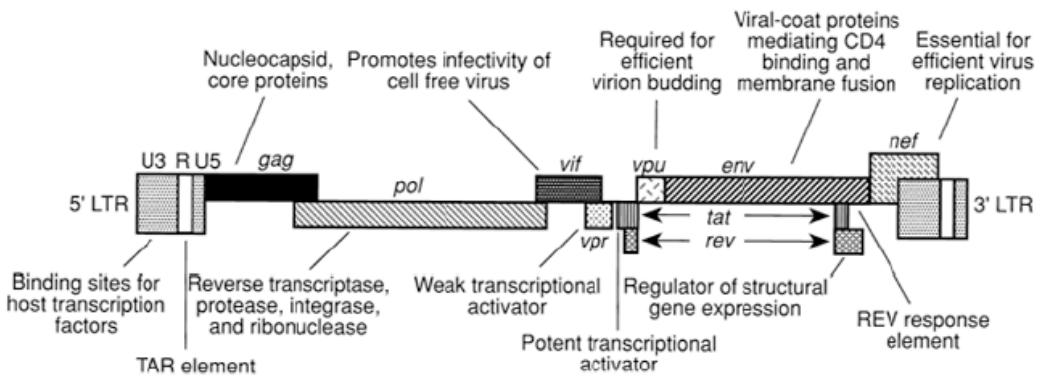


Figure 1. Genomic organization of HIV-1. Typical elements of retroviral genomes include the LTRs and genes for core proteins (*gag*), reverse transcriptase (*pol*), and the viral envelope (*env*). Genes encoding accessory proteins are also depicted with descriptions of some of their known functions. (Reproduced with permission from Cohen et. al. (70)© Lippincott Williams and Wilkins).

Following acute infection, patients experience a long clinically asymptomatic stage (clinical latency) where viral replication continues, but viremia is reduced by the host immune response (Figure 2). This lasts from many months to years. The decrease in the number of blood virions plateaus to a 'set point' which is a prognostic indicator of the survival time of the infected individual (237). Individuals with lower set points generally have greater survival length than those with higher set points. The number of CD4⁺ T cells generally rebounds; however, CD4⁺ T cell counts gradually decline during this stage.

AIDS is the final stage of infection. During this stage, CD4⁺ T cell counts are reduced to a level where viral replication cannot be effectively controlled (Figure 2). Once AIDS develops, lymphadenopathy, fever, diarrhea, cachexia, and other symptoms can be chronic. The patient easily acquires opportunistic infections such as *P. carinii* pneumonia, toxoplasmosis, cryptosporidiosis, candidiasis, *Mycobacterium* spp., listeriosis, Kaposi's sarcoma, Burkitt's lymphoma, progressive multifocal leukoencephalopathy, histoplasmosis, and others. Eventually, the patient succumbs to these infections.

The disease course of HIV infection varies from patient to patient, even when the primary infection is acquired from the same source (201). About 5% of infected individuals are termed long-term non-progressors (chronic infection for greater than 7 years without development of AIDS) whereas others have a rapid progression of disease. Determinants of progression are related to host factors (e.g. competence of immune system in combating HIV infection and genetic factors) and less frequently the virulence of the primary source of HIV (171).

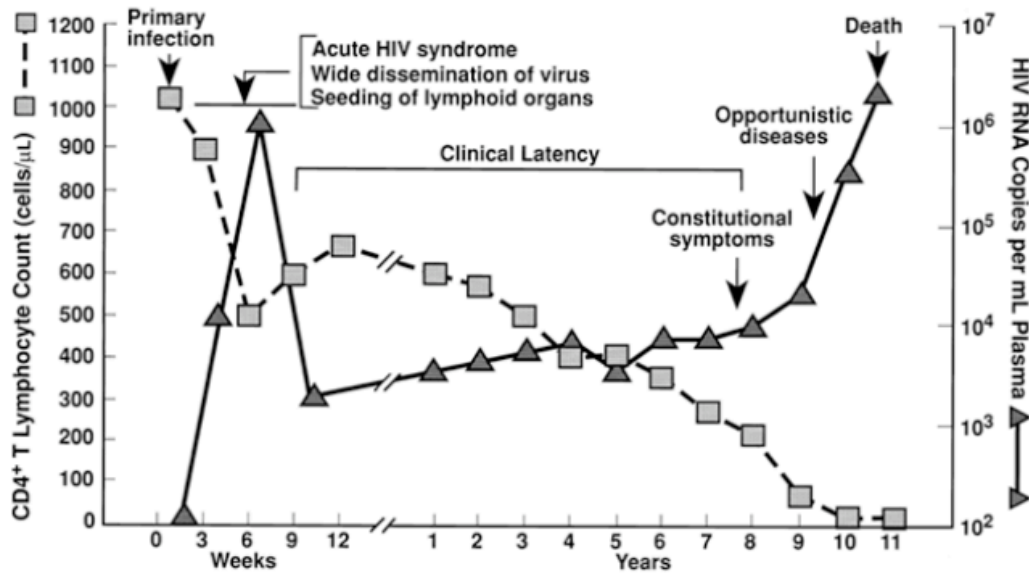


Figure 2. Typical Clinical Course of HIV Infected Patients. After primary HIV infection, a burst of plasma viremia occurs in concert with a transient decline in the CD4⁺ T-cell count. Partial immune control over viral replication ensues, resulting in a variable period of clinical latency. As the CD4⁺ T-cell count declines, the risk of developing constitutional symptoms and opportunistic diseases increases. (Reproduced with permission from Cohen et. al. (70)© Lippincott Williams and Wilkins).

1.2.4. HIV virion.

Retroviral virions are 80-100 nm in diameter with outer envelopes derived from the host cell membrane. There are two viral glycoproteins and various host proteins of unknown significance incorporated into the outer envelope. The glycoprotein complexes are trimers of external glycoprotein gp120 and membrane spanning protein gp41 (193). Host proteins such as human leukocyte antigen (HLA) class I and II proteins and ICAM-1 adhesion protein are incorporated into the membrane during the budding process. The outer envelope surrounds the internal cone-shaped nucleocapsid that contains several viral proteins and surrounds the virion RNA. RT, integrase, and protease are contained in the virion. The viral genome consists of two linear, nonsegmented single strands of RNA with positive polarities that are 7-12 kb long. Retroviral genomes contain gene coding domains *gag-pro-pol-env* that encode for structural, protease, polymerase, and envelope proteins, respectively (Figure 1) (68). These coding domains are flanked by noncoding long terminal repeats (LTR) that include redundant repeats (R) along with unique sequences, U5 on the 5' end and U3 on the 3' end.

1.2.5. HIV life cycle.

The replication cycle of HIV-1 is completed in ~28-32 hours and can be separated into early and late steps (Figure 3). The first step of HIV infection is attachment of gp120, the envelope glycoprotein, to the host cell surface receptor CD4 (or alternative receptor). Attachment induces a conformational change in gp120 allowing subsequent binding to a co-receptor (CCR5 or CXCR4) and fusion of viral envelope protein gp41 with the host cell membrane (68). The viral RNA associated with the nucleocapsid is released into the cytoplasm where initiation of reverse transcription occurs after partial uncoating of the nucleocapsid. Host-

derived tRNA^{lys} binds to the primer binding site downstream of the 5' LTR to initiate reverse transcription using viral RNA-dependent DNA polymerase and RNase H activity (68, 193). Viral cDNA is produced and duplicated into double-stranded DNA structures. Early steps of the life cycle are completed when noncovalently bound circular viral cDNA is transported in a preintegration complex with integrase matrix proteins to the nucleus, where it is randomly integrated into host chromosomal DNA (193). Integration is required for production of infectious progeny.

The late steps of HIV infection proceed with production of viral mRNA and viral genomic RNA from the integrated proviral DNA. Transcription is initiated by host RNA polymerase II at a TATA box on the U3 region of the LTR (68). The LTR contains binding sites for other transcription factors such as NF- κ B, Sp1, AP-1, NFAT-1, Ets-1, USF-1, LEF, and C/EBP/ β (68, 383). The transactivating regulatory protein, Tat, increases transcription initiation and elongation. Regulatory proteins Tat, Rev, and Nef are the earliest mRNA species found in infected cells.

Transcription results in full-length RNA species that are polyadenylated at the 3' end and capped at the 5' end. Doubly spliced transcripts are detected at 12-16 hours post-infection (p.i.) followed by full-length genomic RNA and unspliced mRNA at 24 hours p.i. (168). Precursor HIV structural proteins are synthesized as polyproteins and incorporated into the immature virions at the cell surface (68). Viral genomic RNA is incorporated into the capsid proteins that assemble at the cell membrane. These immature nucleocapsids associate with envelope proteins that are incorporated in the host cell membrane. The virion buds through the cell membrane with a coat of viral glycoproteins and host membrane proteins. Gag and Gag-Pol polyproteins are cleaved by viral protease into individual proteins to generate mature virions (68).

Productive infection of macrophages differs in many respects from CD4⁺ T cells. Whereas CD4⁺ T cells require cellular DNA synthesis to produce virus, macrophages are productively infected without cell division or DNA synthesis (390). It is thought that productive HIV infection can only be supported in macrophages that maintain some form of proliferative capacity because macrophage activation is required for completion of reverse transcription (177, 326). Some reports state integration of provirus can occur without cellular activation (326); whereas others observe HIV nuclear import is blocked in freshly isolated monocytes, but not macrophages (260). C/EBP/β transcription factor is necessary for HIV replication in macrophages but not in T cells (141, 192). Inhibitory isoforms of C/EBP/β are potentially expressed in response to interferon-β (148, 389). HIV accessory genes appear to function differently in macrophages and T cells (352, 353). Viral assembly and budding can occur in cytoplasmic vacuoles in macrophages (271).

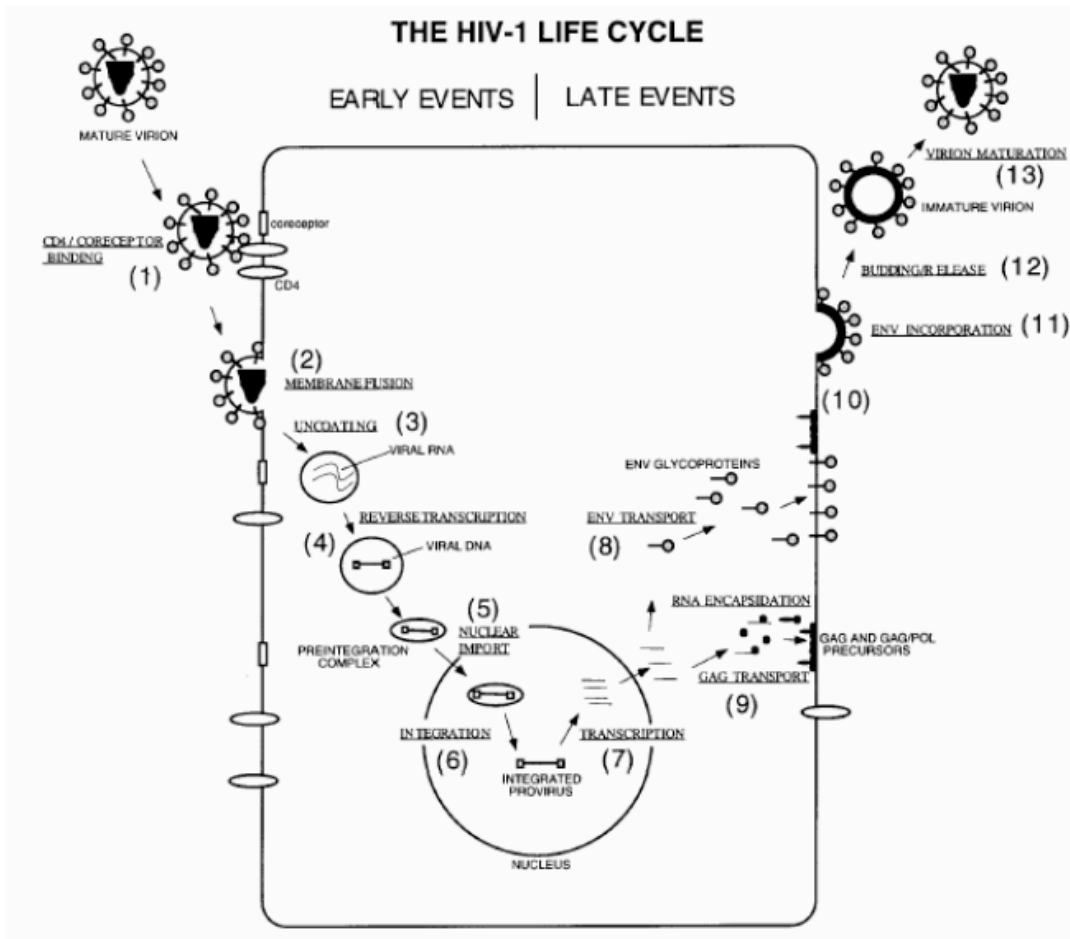


Figure 3. HIV Life Cycle. (Reproduced with permission from Freed, E.O. (108) © 1998 Elsevier)

1.2.6. Viral entry and viral tropism.

Initial studies showed that HIV bound to and infected cells bearing the CD4 receptor (76, 173). Subsequently, it was discovered that infection was more efficient in the context of a co-receptor. The designation of receptor versus co-receptor is arbitrary and predominantly based upon historical considerations that CD4 was discovered first (167, 403). HIV and SIV coreceptors include the chemokine receptors CXCR4 (105) or CCR5 (86, 91). In the case of SIV, CCR5 appears to play a greater role in promoting infection than the originally discovered CD4 molecule (93, 98, 217). *In vitro*, it was recognized that viral strains utilizing CCR5 are macrophage tropic (7), while strains utilizing CXCR4 are T cell-tropic (91). Most viral strains are able to use both receptors for entry with varying efficiency. Other co-receptors, including CCR2, CCR3, CCR8, BOB, and AJP, can be used by some viral strains *in vitro* (Reviewed in ((64))). These latter co-receptors have reduced infection efficiency compared to CCR5, and it is still debatable whether they are important during *in vivo* infection (For review, see (25, 273)).

HIV infects and replicates in CD4⁺ T cells and monocyte/macrophages. These primary cellular targets are believed to be the predominant viral producers throughout the course of infection (72). Several other hematopoietic cell types have been reported to be infected, including dendritic cells (299), CD8⁺ T cells (202), natural killer cells (374), and natural killer T cells (107). Many non-hematopoietic cells have also been reported to be infected by HIV including: epithelia (216, 261, 387), endothelia (83, 250), cardiomyocytes (306), striated myocytes (328), podocytes (309), hepatocytes (50), and others. However, it is unclear what role infection of these cell types may play *in vivo*. The number of peripheral blood mononuclear cells that harbor HIV DNA is variable (338) (~0.1%-15% [(16, 280)]). It has been estimated using PCR techniques that asymptomatic patients carry 1 in 100 to 40,000 infected CD4⁺ T cells

(39, 292, 325), while patients with AIDS carry ~1 in 100 to 10,000 infected CD4⁺ T cells (325) or up to 10% of blood CD4⁺ T cells (149). Using in situ PCR, others have observed that either 0.2% to 69% of CD4⁺ T cells (17) or 4% to 15% of peripheral blood mononuclear cells (280) harbor proviral DNA. Of the few reports that have examined blood monocyte infection, it seems relatively few peripheral monocytes are infected (17). This issue has never been fully illuminated.

1.2.7. Infected tissue macrophages in HIV pathogenesis.

During early stages of HIV infection, it is widely thought that macrophages and dendritic cells are the key tissue elements that propagate virus due to their migratory properties (49, 380, 412). However, others have recently observed that CD4⁺ T cells are the predominant infected cells in lymphoid tissues during acute infection (321, 346). During early time points in infection, it is estimated that a median of 90% of productively infected lymphoid cells are CD4⁺ T cells, while a median of 7% are macrophages. The frequency of productively infected cells per gram of lymphoid tissue has been reported to be ~500,000 to 5,000,000 (321). During late stages of infection, most of the remaining CD4⁺ T cells in the lymph nodes are infected (266). In early and late stages of infection, variable numbers of latently infected CD4⁺ T cells and macrophages are found throughout all lymphoid tissues (99).

In opposition to CD4⁺ T cells, viability of HIV-infected macrophages seems to be unaffected by the virus. However, lentiviral infection may alter or impair macrophage functions. For these reasons, it is believed that macrophages might act as a reservoir for persistent viral infection and produce chronic inflammation and tissue damage.

1.3. HIV and CNS infection.

1.3.1. HIV-associated dementia.

Approximately 25% of immunosuppressed AIDS patients develop a neurodegenerative disorder clinically characterized as HIV-associated dementia complex (HIVDC) (6, 38, 61, 77, 90, 232). This syndrome is associated with cognitive, motor, and behavioral abnormalities that are thought to arise from subcortical damage (125, 241, 286, 287). Symptoms include impaired short-term memory, concentration deficits, leg weakness, personality changes, apathy, and social withdrawal. During life, diagnosis of HIVDC is generally attained after excluding numerous potential central nervous system (CNS) opportunistic infections and neoplasms such as toxoplasmosis, cryptococcal meningitis, cytomegalovirus encephalitis, malignant lymphoma, and progressive multifocal leukoencephalopathy. No consensus has been established regarding the pathologic substrate of HIVDC. This might be due to differences in clinical and pathological definitions and because not all studies concerning HIVDC are followed up by autopsy confirmation of clinical diagnoses. However, autopsy findings have shown that AIDS patients who become demented for reasons other than opportunistic infections demonstrate HIV encephalitis (HIVE) by immunohistochemistry (3).

1.3.2. HIV encephalitis.

After the development of severe immunodeficiency, ~1/4 of HIV infected individuals develop HIVE (15, 79, 209, 223). HIVE is a pathological disease that develops when HIV invades the brain parenchyma. Consensus regarding the diagnostic criteria for HIVE has been published (42). HIVE is characterized by the presence of microglial nodules, multinucleated giant cells, and abundant HIV-infected macrophages as determined by immunohistochemistry, in situ hybridization, or quantitative HIV RNA assessment (42, 43, 259, 395). Abundant

activated macrophages are found distributed throughout deep gray and white matter structures (138, 238, 265, 282, 296, 404). Multinucleated giant cells are thought to form when infected cells bearing viral envelope glycoproteins fuse with other cells bearing receptors for the virus (332, 392).

The frequency of HIV in these brain macrophages is controversial (3, 30, 124, 125) because variation in probes used to detect virus and variation in tissue preservation brought about inconsistent estimates of the abundance of virus. Some of these early studies concluded that the amount of virus in the brain could not account for the extent of clinical symptoms or neuropathology; therefore, it was suggested that neuronal damage was mediated by presence of activated brain macrophages rather than amount of viral infected macrophages (124). The preponderance of studies argue that neuronal damage in lentiviral encephalitis is linked to regional presence of both activated and infected macrophages (22, 213, 287, 371, 394, 395). It is still unexplained why only a fraction of individuals develop HIV encephalitis, though length of survival with severe immunosuppression may be a factor (343, 391).

1.3.3. Infected cells in the CNS.

In the brain, potential cellular targets for HIV infection include perivascular and parenchymal macrophages/microglia, neurons, astrocytes, oligodendrocytes, and endothelia. The literature is replete with confusing and conflicting reports claiming HIV infection of brain cells of multiple lineages. There is consensus that microglia/macrophages are the predominant infected cell in brains with HIV (44). Endothelia and neurons derived from fetal tissue have all been shown to be susceptible to productive HIV infection *in vitro* (8, 100, 139, 249, 349), but there is little pathological evidence to support that these cells are susceptible *in vivo* (30, 364,

369, 393). Astrocytes may be susceptible to HIV infection *in vivo* but do not support productive infection (267, 298, 354, 363, 369). This makes HIVE unlike most previously described viral encephalitides since the virus predominantly infects microglia/macrophages rather than neurons or macroglia (156).

There is some controversy as to whether perivascular or parenchymal microglia/macrophages comprise the majority of infected cells (73, 398). Using the simian model for HIV infection, a report concluded that perivascular macrophages and not parenchymal microglia are infected by SIV (398). This report relies on using CD14 and CD45 to distinguish macrophages and microglia, respectively, but this distinction is highly problematic (reviewed in (30)). Studies of human autopsy tissues suggest that while there is an angiocentricity to the brain lesions, at least 2/3 of HIV p24⁺ cells in HIVE brains are parenchymal microglia (73). Since microglia and macrophages are derived from the same monocyte lineage precursors, this distinction may be more a question of semantics.

1.3.4. HIV entry into CNS.

The brain is separated from the rest of the body (periphery) by the blood-brain barrier (BBB), while the cerebrospinal fluid (CSF) is separated from the periphery by the epithelium of the choroid plexus (produces CSF). In order for encephalitis to develop, virus must cross the BBB. Soon after lentiviral infection, virus or viral DNA can be recovered from the CSF and brain in addition to most body compartments (9, 11, 62, 80, 101, 121, 180, 302, 341). The source of this early virus is not clear, and it is unknown whether the early virus detected in the CNS is cleared or remains as a potential viral reservoir. Studies that have looked at CNS viral load during acute and asymptomatic infection support both scenarios (9, 66, 395). It is well

accepted that virus enters in the end stages of infection, so the small potential proviral reservoir might have limited contribution to the development of encephalitis. Others have hypothesized that HIV enters the CNS at distinct time points during the course of infection since different brain regions contain discrete viral variants (331). These data suggest that HIV encephalitis develops as the result of entry of new virus (most likely within monocytic elements) or an uncontrolled recrudescence of the small amount of virus that entered during acute stages of infection.

There are several hypotheses that address the entry of HIV into the brain. The hypothesis with the most supporting evidence is that monocytes act as “Trojan horses” trafficking HIV through the BBB into the brain (80, 281). Evidence supporting this is derived from immunohistochemical studies that have shown viral infected macrophages are often found in perivascular sites with little to no evidence of endothelial cell infection (30, 398). This is consistent with the normal process of immune cells crossing the BBB for immune surveillance in a carefully regulated process (143). Using *in vitro* models, some researchers postulate that endothelial cells (infected or not) are the portals through which cell-free HIV enters the brain (20, 200). HIV is able to transcytose cultured endothelia (200), but little evidence supports this mechanism *in vivo*.

The majority of HIV strains isolated from the CNS are macrophage tropic (110, 133). Phylogenetic analysis of viral sequences show that viruses isolated from the CNS are more genetically related than viruses isolated from other tissue such as blood, lymph nodes, and spleen (175). It has not been established whether the genetic difference seen in the CNS results from independent entry at distinct times or whether HIV genetically adapts to replicate in the microenvironment of the CNS more efficiently.

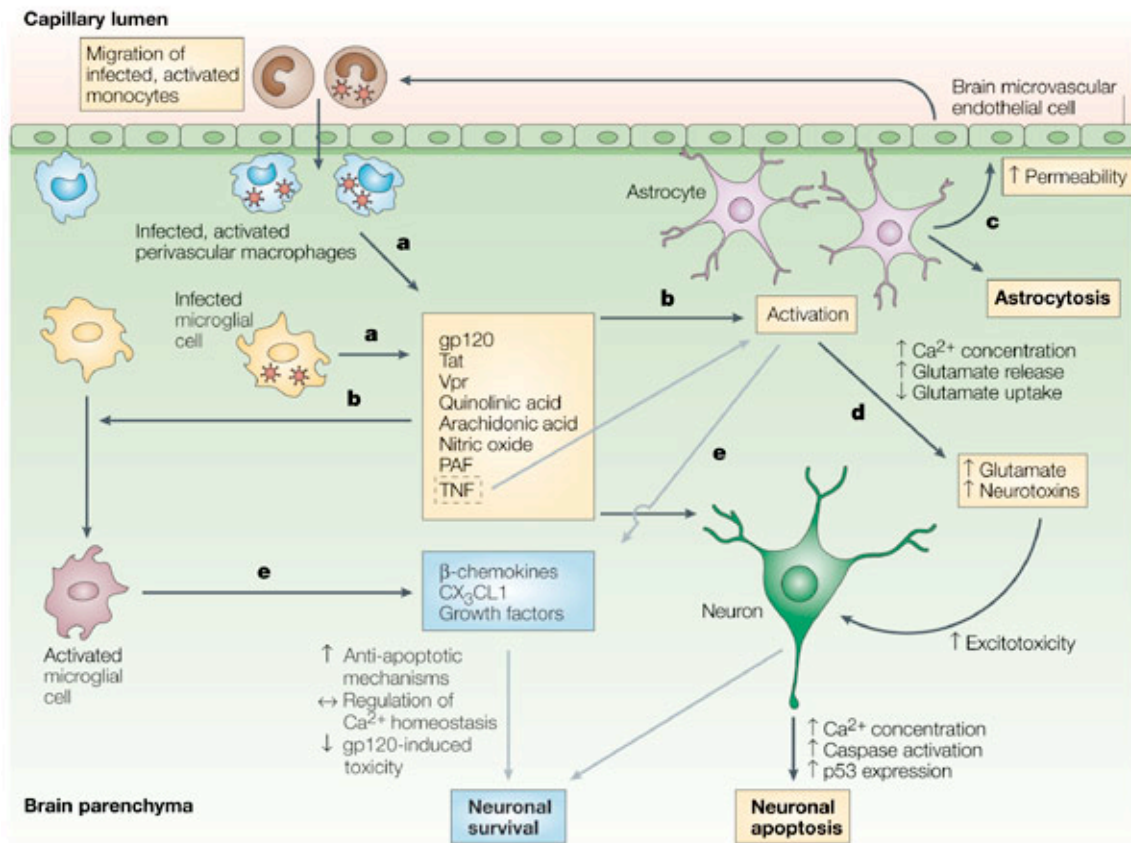
1.3.5. Mechanisms of nervous system damage.

Despite the absence of convincing evidence of neuronal infection, neurodegeneration has been reported in both lentiviral infected and encephalitic individuals (22, 42, 44, 75, 333). Since neurons are not infected, neuronal damage seen in HIV-infected patients is thought to be mediated by indirect mechanisms. Theories regarding the mechanism of neuronal damage can be divided into two groups that are not necessarily mutually exclusive. The first group of theories considers HIV proteins neurotoxic (Figure 4) (81, 92, 122, 196, 207, 257, 289, 294, 320). Neurons in adult human brains express the two co-receptors required for HIV entry, CXCR4 (191, 317) and CCR5 (310), and some neuronal populations possibly express CD4 (110), so it is possible that direct interaction of HIV envelope proteins with neuronal chemokine receptors mediate neurotoxicity (6, 24, 92, 122, 123, 144, 159, 160, 176, 197, 210, 239, 257, 320, 407). Beyond HIV envelope protein, Tat, Vpr, Nef, Vpu, and Rev proteins have also been implicated in initiating neuronal dysfunction (123, 140, 258, 279, 311, 334, 370, 376, 378).

The second group of theories builds on the concept that neuronal dysfunction is caused by the gamut of host factors that are released from brain macrophages (Figure 4) (88, 142, 225). These secreted products might directly act on neurons or indirectly act on supporting glial cells initiating synaptic damage and neuronal death (41, 114, 117, 142, 198, 262, 293, 294). Functions of astrocytes include removal, metabolism, and recycling of excess glutamate (a major excitatory neurotransmitter) from neuronal synapses. Secreted products from macrophages are known to inhibit this critical function of astrocytes (27). Excess glutamate and oxidative stress are thought to contribute to neurodegeneration by an unknown mechanism. It is controversial whether these insults result in neuronal apoptosis or whether degeneration is mediated by other mechanisms (159, 163).

1.3.6. Effect of HAART on CNS disease.

With the advent of highly active antiretroviral therapy (HAART) in 1995, mortality and morbidity have decreased in HIV-infected patients. As with opportunistic infections and HIV-related tumors of the CNS, the incidence of HIVD has decreased to ~10% in patients treated with HAART, although it has been suggested that the prevalence will increase due to patients living longer (373). Many patients treated with HAART clinically exhibit a more mild form of CNS dysfunction termed minor cognitive motor disorder (MCMD). Losses in higher cortical functions such as memory and computational skills are subtler with MCMD compared to HIVD. It is unclear whether this form of dysfunction has become more common, become more obvious because it does not progress to overt dementia, or arisen as a side effect of HAART. Recent estimates suggest MCMD might affect 30% of HIV-infected individuals. Individuals with MCMD have a worse overall prognosis of disease progression (58, 313). As with HIVD, MCMD is associated with neuropathology typical of that seen in HIV. It has been suggested that MCMD may result from a slower progressive neurodegeneration mediated by lower levels of HIV replication in the CNS of patients on HAART.



Nature Reviews | Immunology

Figure 4. Mechanisms of Neurodegeneration During AIDS. **a.** Infected, activated perivascular macrophages/microglia produce HIV and release viral proteins that can be deleterious to the CNS. HIV gp120 envelope protein, Tat, and Vpr have been shown to be toxic *in vitro* to neurons and/or astrocytes. Infected, activated cells also produce other factors – such as cytokines (e.g. TNF), quinolinic and arachidonic acid, platelet-activating factor (PAF) and nitric oxide – that are known to have neurotoxic effects. **b.** These factors promote further activation of macrophages and proliferation and activation of astrocytes. **c.** Activated astrocytes modify permeability of the blood-brain barrier and promote migration of more monocytes into the brain. **d.** Increased release of intracellular Ca²⁺ and glutamate through decreases in glutamate uptake results in excitotoxic death of neurons. (Reproduced with permission from Gonzalez-Scarano, F. et. al. (132) © 2005 [Nature Publishing Group](#))

Despite the observation that few antiretroviral drugs attain effective concentrations in the CNS, the incidence of HIVE has decreased in patients on HAART (137). However, the prevalence of HIVE has increased with some estimates stating 45% of AIDS autopsies demonstrate HIVE (190). With HAART, HIV infection has been reported to be associated with a more subtle degeneration of dendritic arbors and interneuron populations compared to widespread degeneration of excitatory pyramidal neurons (190, 224). A comprehensive pathological survey is needed to verify these reports. Abundant HIV infected macrophages are still observed in brains with HIVE in HAART patients, and more extensive white matter destruction is observed than prior to HAART.

Potential influences of HAART on HIV-associated neuropathology are mediated by suppressed HIV replication, increased cell mediated immunity, increased survival, and interactions of antiretroviral drugs with brain endothelia. Since HAART is probably unable to completely suppress HIV replication in the CNS, the CNS may act as a reservoir (189). Yet, although HAART may alter brain disease, it is unclear whether compartmentalized virus evolving under suboptimal antiretroviral levels in the CNS will be virulent.

1.3.7. Blood brain barrier defects during HIV infection.

The BBB is a selectively permeable layer of brain endothelial cells that are packed tightly together by tight junctions (or zonula occludens). Tight junctions block many molecules from gaining entry into the CNS. Lipid soluble molecules such as oxygen and carbon dioxide cross the BBB readily. There are also selective transport systems for molecules such as sugars and amino acids. Immune cells cross the BBB normally in order to survey the CNS; however, this

process is carefully regulated (143). Several reports show that the BBB is abnormal during HIV-infection (48, 120, 283). Alterations in the BBB are more common in patients with HIVD compared to nondemented AIDS patients and seronegative controls (287). Some investigators believe that deterioration of BBB integrity allows HIV entry into the CNS and subsequent development of HIVE. However, it is difficult to distinguish whether CNS infection leads to BBB breakdown or whether BBB breakdown allows infected cells or free virus to invade the brain. Since BBB breakdown is seen in many patients without HIVE or HIV-associated CNS pathology, BBB alterations probably do not lead to development of encephalitis but might contribute to entry of HIV after initiation of CNS disease.

1.4. SIV-infected macaque model for HIV infection in humans.

1.4.1. SIV-infection of natural hosts.

Primate lentiviruses have been detected in wild African monkeys from the genus *Ceropithecus*, *Chlorocebus* (African green monkeys), *Cercocebus* (mangabeys), *Colobus*, and *Pan* (chimpanzees) (145, 251). These primate lentiviruses are divided into at least six distinct lineages that share 40 to 50% identity in Gag and Pol proteins (145). HIV is closely related to SIV-chimpanzee strains. Most SIV strains used in research were derived from sooty mangabeys and are closely related to HIV-2. In wild African monkeys, SIV infection does not result in immunodeficiency despite active ongoing viral replication at comparable levels to macaques experimentally infected with pathogenic SIV (55). Natural hosts generally have asymptomatic infection that has been attributed to a much more mild immune activation than seen in hosts with pathogenic disease (56, 337).

1.4.2. SIV-infection in Asian macaques.

After HIV was determined to be the cause of AIDS in humans, SIV was isolated from captive Asian macaques (78, 251). Originally named STLV-III, SIV was determined to be a lentivirus that caused a chronic, lethal infection similar to AIDS in humans. A variety of macaque species are susceptible to pathogenic SIV infection (145, 170, 186), and rhesus macaques (*Macaca mulatta*), pigtailed macaques (*M. nemestrina*), and cynomolgus macaques (*M. fascicularis*) are the common species utilized to study the pathogenesis of AIDS when experimentally infected with SIV. Lentivirus infection in Asian macaques or orangutans has not been detected in the wild.

The disease course of SIV-infected Asian macaques has considerable interspecies and intraspecies variation even when infected with identical SIV strains. SIV causes disease within months to years after infection. As seen in humans, but with shorter lengths of time, SIV-infected macaques exhibit rare, long-term non-progression of disease as well as rapid progression to disease in a period of less than six months post-inoculation (146). The pathogenesis of SIV infection in Asian macaques is very similar to HIV-induced AIDS in terms of viremia, immune response, progression to AIDS, opportunistic infections, and infection of the CNS.

1.4.3. Disease progression rates in SIV-infected macaques.

Similar to HIV infected humans, SIV-infected macaques have three types of disease progression determined by survival time after inoculation. Rapid progressors succumb to AIDS within six months of infection due to persistent high-level viremia (95, 411). These animals are sometimes coined as ‘non-responders’ because they are often unable to control viremia during

acute infection and have little or no detectable virus-specific immune responses. Intermediate or typical progressors exhibit characteristic disease progression with establishment of clinical latency and development of simian AIDS in 1-3 years (367). Slow progressors stay asymptomatic for long periods after more substantial containment of acute viremia (195). Slow progressors can survive for greater than 5 years.

1.4.4. CNS disease in SIV-infected macaques.

Descriptions of SIV encephalitis (SIVE) have been reported ever since the discovery of simian models of lentiviral infection. SIVE shares many features with HIV in that the neuropathology is similar and only a fraction of infected macaques develop encephalitis. As in humans, microglia/macrophages are the predominant infected cell in the CNS of macaques with SIVE. This is distinct from less immunosuppressive lentiviral encephalitides like Visna that have intense lymphocytic infiltrates (156). In brains with HIV, the distribution of viral infected macrophages is mostly subcortical while the cortical regions are also involved in SIVE. However, both diseases show significant inter-individual variation.

SIV infection of macaques illuminates the importance of viral strain and species differences in determining the neuropathological outcome after infection (75). As seen in humans with HIV, the predominant strain of SIV in the CNS of macaques with SIVE is macrophage-tropic. In order to explain why only a fraction of lentiviral-infected individuals develop encephalitis, it has been theorized that evolution of “neurovirulent” viral strains with certain unknown genetic attributes must be present in the host in order for brain infection to occur. However, it is difficult to tease apart whether these neurovirulent strains developed in the periphery, allowing infection of the brain or whether viral strains that infect and replicate in the

CNS evolve in the microenvironment of the brain to allow more efficient replication. Pigtailed macaques are also known to develop encephalitis at a higher incidence than rhesus macaques. Cynomolgus macaques rarely show lesions associated with SIV-infected macrophages.

Efforts at determining correlates of encephalitis have been made using a variety of primate models. A model of using co-infection with SIV/DeltaB670 and a “neurovirulent” clone (SIV/17E-Fr) that is macrophage-tropic is reported to induce encephalitis in 90% of infected pigtailed macaques (418). This model finds that both CSF and CNS parenchymal viral load are tightly associated with extent of SIVE. This is similar to reports in HIV-infected humans (395, 397). Another model using a different viral strain and macaque species showed no apparent relationship between presence of brain lesions and viral load (32). Rapid disease progression (268, 391), elevated CSF monocyte chemotactic protein (MCP)-1 concentrations (63, 417) and low anti-SIV antibody titers 1 month after infection (268) have also been associated with development of encephalitis.

1.4.5. CNS disease in animal retroviral infection.

Several retroviruses cause neurologic diseases in animals. Non-lentiviral murine leukemia virus (MLV) infection of mice leads to intracellular vacuolization, neuronal loss, and gliosis in absence of an inflammatory response (40). Neurovirulence, or ability to replicate and cause disease in the CNS, of MLV infected mice has been localized to the *env* gene, while incidence of disease and where lesions develop are influenced by the LTR (277). However, unlike HIV, MLV is thought to infect neurons, endothelial cells, and perivascular macrophages although, this is a point of contention (23, 135, 156).

Sheep, horses, cows and cats are affected by lentiviral diseases (156). As with HIV infection, these diseases are characterized by long asymptomatic periods that either progress slowly or relapse/remit. Most lentiviral illnesses have a fatal outcome although horses infected by equine infectious anemia virus can survive. Common complications include lymphadenopathy, pneumonitis, hemolytic anemia, thrombocytopenia, and encephalitis. Ruminant and equine lentiviruses only infect macrophages and are associated with intense inflammatory disease. Feline and primate lentiviruses infect both macrophages and CD4⁺ T cells resulting in immunodeficiency and opportunistic infections.

Within one month of infection, visna virus infection of sheep leads to mononuclear infiltrate in meninges and perivascular spaces (284). Lesions and demyelination are predominantly seen in the white matter (284). Macrophages and their progenitors are reported to be infected and virus-producing macrophages in the CNS leads to cytokine production by T cells that recruit T cells to the CNS (115, 116, 165, 256).

Although some cats infected with feline immunodeficiency virus exhibit neuropathology characteristic of HIV encephalitis (2, 31), SIV infection of macaques have provided the most insight on pathogenesis of HIV encephalitis. Most studies of other animal lentiviruses have shed light on how macrophage infection leads to disease in the CNS in response to cytokines (156).

1.5. Immune response to primate lentivirus infection.

The explosion of viral replication during primary infection in both HIV-infected humans and SIV-infected macaques initiates antibody, cytotoxic T lymphocytes (CTL), and CD4 helper responses that decrease viremia to a set point. It has been suggested that variation in the antiviral immune response influences differences in viral load set points during acute phase of infection (113).

High concentrations of HIV-specific antibodies develop within one to three months of infection (113). Antibodies recognizing linear portions of structural proteins Gag p24 and p17 are developed first with antibodies to Env and Pol detected thereafter (327). Since HIV-infected patients usually show decreased viremia during acute infection prior to appearance of HIV neutralizing antibodies, the role antibodies play in controlling HIV infection is unclear (178). Due to high mutation rates of virus during infection, hindered antibody access to epitopes by V1 and V2 loops, and heavy glycosylation of the envelope (53, 278, 301), HIV and SIV elude antibody responses.

Appearance of HIV-specific CD8⁺ CTL responses coincides with reduction in viremia during acute stages (214). Macaques depleted of CD8⁺ T cells at time of SIV inoculation exhibit substantial sustained increases in viremia (154, 324). CTL control HIV and SIV infection by at least three mechanisms. Virus-specific CTL lyse infected cells after recognition of viral peptides presented in the context of major histocompatibility complex (MHC) class I molecules on cell surfaces (406). In an antigen specific, MHC class I-restricted manner, CTL secrete β chemokines such as MIP-1 α and β and RANTES that can bind HIV co-receptors and block viral entry (385). CD8⁺ T cells secrete CD8⁺ T cell antiviral factor (CAF) that can decrease viral transcription (382) and IFN- γ that initiates anti-viral responses.

1.6. The role of host factors in susceptibility of cells to lentiviral infection.

Since the disease course of SIV-infected Asian macaques has considerable interspecies and intraspecies variation even when infected with identical SIV strains (128, 329), it is apparent that host factors influence the outcome of disease. Several human genes have been associated with susceptibility of HIV infection, disease progression, and clinical outcome. Individuals with a truncation of the HIV co-receptor CCR5 protein due to a homozygous 32-base pair deletion within the CCR5 gene are resistant to HIV infection, while heterozygotes have slower disease progression rates (82, 150, 240, 242, 316). MHC proteins present antigens to lymphocytes and are the most polymorphic human genes. In both humans and macaques, particular MHC alleles are associated with either rapid or slow disease progression (33, 51, 208). Humans with polymorphisms in the promotor region of the IL-10 gene have increased susceptibility to HIV infection and rapid disease progression (336). Individuals with a low number of duplications in MIP-1 α P gene segments have increased susceptibility to HIV infection and disease progression (129). Despite associations of genetic polymorphisms on HIV disease outcome, no consensus of what factors play the greatest role in determining disease outcome has been reached.

2. SPECIFIC AIMS

Human immunodeficiency virus (HIV) associated dementia complex (HIVD) occurs in ~25% of AIDS patients leading to cognitive, motor, and behavioral deficits that are attributed to synaptic damage and neuronal loss. AIDS patients that become demented in absence of opportunistic infection demonstrate brain pathology associated with HIV encephalitis (HIVE). Simian immunodeficiency virus (SIV) infection of macaques is a well-established model of HIV infection as it mimics disease progression and pathogenesis in humans and, most importantly for this study, leads to the development of SIV encephalitis (SIVE) in a fraction of infected macaques. We proposed to use SIV infection of *Macaca mulatta* and *Macaca nemestrina* to study infection and activation markers of peripheral monocyte and macrophages during the evolution of lentiviral encephalitis.

While macrophage/microglia are the predominant infected cell type associated with lentiviral encephalitis, the relationship between the monocyte/macrophage infection within and outside of the brain are not known. Our overarching hypothesis was: **Development of SIV encephalitis and ensuing neurologic damage results from a generalized increase in the numbers of SIV infected and activated monocyte/macrophages both inside and outside of the brain.** To test portions of this global hypothesis, we constructed associated aims that were studied in SIV-infected macaques with and without encephalitis.

Specific Aim 1: Compare quantification of macrophages, virus and presynaptic and postsynaptic proteins in macaques with SIV encephalitis to macaques without SIV encephalitis (Chapter 3.1).

Since neurodegeneration observed in SIVE has been linked to viral-infected and activated CNS macrophages, we examined the relationship between virus, macrophages, and neurologic damage in multiple brain regions in SIV-infected rhesus macaques with and without encephalitis. Formalin-fixed paraffin embedded brain tissue was immunostained for SIV envelope, CD68 (marker for macrophages/microglia), presynaptic protein synaptophysin, and postsynaptic protein microtubule-associated protein-2. Using laser confocal microscopy, pixels corresponding to each stain were quantified and correlated to the presence or absence of SIVE. In addition, brain SIV RNA was quantified in frontal cortical gray and white matter, occipital cortical gray and white matter, caudate, putamen, globus pallidus, hippocampus, and cerebellum.

Specific Aim 2: Examine the relationship between peripheral SIV infection and the development of SIV encephalitis in CD8 depleted rhesus macaques (Chapter 3.2).

CD8 depletion of macaques at the time of infection leads to rapid progression of disease. Since rapid progression is associated with the development of SIVE, we hypothesized that macaques treated with an anti-CD8 antibody would be more likely to develop CNS disease. Using this model, infection of circulating infected monocytes and CD4⁺ T cells were assessed during the course of infection. CD4⁺ T cell, CD4⁺/CD29⁺ T cell, CD8⁺ T cell, and monocyte absolute counts or percentages were monitored in addition to plasma viremia to assess systemic disease progression. CSF viral load was monitored to assess CNS disease progression. Based on histological findings, macaques were retrospectively classified at post-mortem for presence of SIVE and compared to macaques without SIVE. To determine whether SIV macrophage

infection was unique to the CNS in animals that developed encephalitis, a survey of the number of infected macrophages and T cells in the liver, lung, small bowel, spinal cord, spleen, and thymus was performed on necropsy tissue. In addition, analysis of postsynaptic and presynaptic proteins and macrophages in the brains from these macaques was performed to determine the amount of neuronal damage in CD8-depleted SIV infected macaques.

Specific Aim 3: Examine the relationship between peripheral SIV infection and the development of SIV encephalitis in pigtailed macaques (Chapter 3.3 and 3.4).

Using SIV infection of pigtailed macaques, infection of circulating infected monocytes and CD4⁺ T cells, phenotypic markers of monocyte activation, CSF viral load, and lymph node macrophage infection were assessed during the course of infection. In addition to plasma viremia, absolute counts of CD4⁺ T cells, CD8⁺ T cells, and monocytes were monitored to assess systemic disease progression. Based on histological findings, macaques were retrospectively classified at post-mortem for presence of SIVE and compared to macaques without SIVE. To determine whether SIV macrophage infection was unique to the CNS in animals that developed encephalitis, a survey of the number of infected macrophages and T cells in the liver, lung, small bowel, spinal cord, spleen, and thymus was performed on necropsy tissue.

3. RESULTS

3.1. Chapter 1

Published in:

American Journal of Pathology 2002; 160: 927-941

MACROPHAGES RELATE PRESYNAPTIC AND POSTSYNAPTIC DAMAGE IN SIMIAN IMMUNODEFICIENCY VIRUS ENCEPHALITIS

Stephanie J. Bissel,* Guoji Wang,† Mimi Ghosh,* Todd A. Reinhart,* Saverio Capuano III,*
Kelly Stefano Cole,‡ Michael Murphey-Corb,‡ Michael Piatak, Jr.,§ Jeffrey D. Lifson,§ and
Clayton A. Wiley†

From the Department of Infectious Diseases and Microbiology,* Graduate School of Public
Health, and the Departments of Pathology† and Molecular Genetics and Microbiology,‡
University of Pittsburgh School of Medicine, Pittsburgh, Pennsylvania; and the Laboratory of
Retroviral Pathogenesis,§ AIDS Vaccine Program, Science Applications International
Corporation Frederick, National Cancer Institute at Frederick, Frederick, Maryland

3.1.1. Abstract

Neurodegeneration observed in lentiviral-associated encephalitis has been linked to viral-infected and –activated central nervous system macrophages. We hypothesized that lentivirus, macrophages, or both lentivirus and macrophages within distinct microenvironments mediate synaptic damage. Using the simian immunodeficiency virus (SIV)-infected macaque model, we assessed the relationship between virus, macrophages, and neurological damage in multiple brain regions using laser confocal microscopy. In SIV-infected macaques with SIV encephalitis (SIVE), brain tissue concentrations of SIV RNA were 5 orders of magnitude greater than that observed in nonencephalitic animals. In SIVE, staining for postsynaptic protein microtubule associated protein-2 was significantly decreased in the caudate, hippocampus, and frontal cortical gray matter compared to nonencephalitic controls, whereas staining for presynaptic protein synaptophysin was decreased in SIV-infected macaques with and without encephalitis. These data suggest that presynaptic damage occurs independent of pathological changes associated with SIVE, whereas postsynaptic damage is more tightly linked to regional presence of both activated and infected macrophages.

3.1.2. Introduction

Approximately 25% of human immunodeficiency virus (HIV)-infected patients develop human immunodeficiency virus encephalitis (HIVE) (15, 79, 209, 223). A more variable percentage of simian immunodeficiency virus (SIV)-infected macaques develop SIVE, depending on macaque species and viral strain (22, 75, 155, 213, 333, 349, 391, 415). HIVE, the pathological substrate of HIV-associated dementia, generally develops in AIDS patients with advanced immunosuppression (259, 290, 394). Pathologically, HIV-associated dementia is characterized by the presence of microglial nodules, multinucleated giant cells, and abundant HIV-infected macrophages as determined by immunocytochemistry, in situ hybridization, or quantitative HIV RNA assessment (42, 395). Clinically, patients experience cognitive, motor, and behavioral deficits (345) that are attributed to neuronal damage and loss (3, 102, 103, 166, 222, 394, 396).

Despite the absence of convincing evidence of neuronal infection, neurodegeneration has been reported in both HIV and SIV infection (22, 42, 44, 75, 333). Some studies suggest neural damage can occur even in the absence of significant infection within the brain. SIVmac251-infected cynomolgus monkeys exhibit dendritic damage even in the absence of encephalitis or detectable central nervous system (CNS) virus (246). However, the majority of studies link profuse activated and lentiviral-infected brain macrophages to neurodegeneration (3-5, 22, 124, 213, 222, 287, 371, 394, 395, 397, 415). It is unclear whether neurodegeneration is caused by direct effects of the virus, indirect effects of infection, or both. Many studies have suggested the

secreted products of activated macrophages might directly act on neurons or indirectly act on supporting glial cells initiating synaptic damage and neuronal death (41, 74, 114, 123, 142, 159, 199, 204, 289, 291, 293, 294).

Both presynaptic and postsynaptic damage have been reported during HIVE (3, 102, 103, 131, 166, 222, 226, 246, 396). This suggests that there is disruption in neuronal circuitry that could cause neurological deficits and lead to neuronal loss. Synaptophysin (SYN), a 38-kd calcium-binding protein associated with membranes of neuronal presynaptic vesicles and involved in neurotransmitter release, is widely used to mark presynaptic terminals and to approximate synaptic density (96, 229, 231, 247, 314, 396). Loss of synaptophysin immunoreactivity has been interpreted as morphological evidence of presynaptic neuronal damage and is closely associated with signs and symptoms observed in several chronic dementias (47, 131, 185, 227, 228, 315, 339, 355). Similarly, microtubule-associated protein-2 (MAP-2), a high molecular weight protein found in neuronal cell bodies and dendrites, is widely used to mark postsynaptic elements (47, 185, 230, 246, 305). MAP proteins are involved in the polymerization of tubulin into microtubules and help provide physical stability to microtubule formations. Loss of MAP-2 immunoreactivity has been interpreted as morphological evidence of dendritic pathology (230, 305). The universal response of CNS tissue to any nonspecific damage is gliosis. Gliosis is readily identified by immunohistochemical staining for glial fibrillary acidic protein (GFAP), a 52-kd intermediate filament protein found in astrocytes.

There is substantial controversy regarding the relative role of virus and activated macrophages in mediating lentiviral- associated neurodegeneration. Using the SIV-infected macaque model, we assessed the relationship between virus and macrophages and neurological damage by laser confocal microscopy. We found that some regions of the CNS in infected

macaques showed presynaptic damage during systemic infection independent of the presence of encephalitis. However, we observed that lentiviral encephalitis was distinctly associated with severe synaptic damage and tightly linked with the presence of both activated and infected macrophages. The microscopic multifocality of the infectious process was similarly reflected in the focality of the neurological damage.

3.1.3. Materials and Methods

Animals

Rhesus macaques (*Macaca mulatta*) were housed and maintained according to strict American Association of Laboratory Animal Care standards. Macaque infection parameters are described in Table 1. Six rhesus macaques derived from vaccine trials, challenged with viral swarm SIVdeltaB670 (SIV/dB670), and sacrificed were used in this study. Two macaques were involved in vaccine studies. Two macaques were administered PMPA [9-R-(2-phosphonomethoxypropyl)adenine] 24 hours before inoculation with SIV. Macaques were infected intravenously with SIV/deltaB670 (n = 4), via bronchoscope with bronchial alveolar lavage from an animal infected with SIV/dB670 (n = 1), or rectally with SIV/dB670 and a subsequent infection via bronchoscope with bronchoalveolar lavage from an animal infected with SIV/dB670 (n = 1). Because the focus of this study was on CNS manifestations due to CNS SIV infection, the divergent routes of infection and clinical history in this group of animals does not impact directly on the final outcome of CNS disease. Ages of the macaques used in this study ranged from 33 to 100 months. Length of infection varied from 37 to 379 days. Macaques were sacrificed when moribund with AIDS (Table 2). Only two macaques (macaques 603 and 221) exhibited neurological signs consisting of decreased feeding, decreased spontaneous movement,

neglect of novel environmental stimuli, lethargic response to physical stimulation, and variable focal neurological signs. Two noninfected macaques served as controls. Complete necropsies were performed after humane sacrifice.

CD4⁺ Cell Counts

Buffy coats from peripheral blood obtained from SIV-infected macaques immediately before euthanasia were labeled with fluorochrome-conjugated monoclonal antibodies against CD4 (OKT4; Coulter, Hialeah, FL). Two-parameter light-scatter profiles were used to gate the lymphocyte population and to determine the percentage of CD4⁺ lymphocytes. Absolute CD4⁺ cell numbers were calculated using percent CD4⁺ lymphocytes and differential cell counts from the blood as previously described (219).

Tissue

Brains were removed immediately after euthanasia and processed for analysis. The left hemisphere was cut into regional blocks and stored at 80°C. The right hemisphere was fixed in 10% buffered formalin (Fisher Scientific, Pittsburgh, PA). Coronal sections were made, and tissue blocks were paraffin-embedded. Six- μ m sections were made for pathological analysis.

Quantitation of SIV RNA in Brain Tissue

For real-time polymerase chain reaction (PCR) analysis, total RNA was isolated from ~100 mg of frozen (-80°C) brain tissue from frontal neocortical gray and white matter, occipital neocortical gray and white matter, caudate, putamen, globus pallidus, hippocampus, and cerebellum. RNA isolation was performed using Trizol reagent (Life Technologies, Inc., Rockville, MD) according to the manufacturer's recommendations. Pelleted total RNA isolated from brain tissue was dissolved in molecular biology grade water and SIV *gag*-encoding

sequences quantified by real time PCR in an Applied Biosystems Prism 7700 (Applied Biosystems, Foster City, CA) as previously described (418). The threshold sensitivity of this method was 10 copy Eq/reaction, typically corresponding to 1 µg of input total RNA, or the equivalent of ~0.9 mg of brain tissue. The RNA assay was normalized based on input RNA but reported here as copy Eq/mg tissue. The RNA yield from animal to animal was very consistent at 0.87 µg of RNA/mg tissue ± 0.15 (mean ± SD). Region to region RNA yield varied as expected (0.6 to 1.4 µg of RNA/mg tissue) with cerebellum > neocortical gray matter = caudate = putamen = globus pallidus = hippocampus > neocortical white matter.

Quantitation of SIV RNA in Plasma

Quantitation of virion-associated RNA in plasma was performed by real-time PCR in a Prism 7700 (ABI). Virions were pelleted from 1 ml of plasma by centrifugation at 14,000 x g for 1 hour. Total RNA was extracted from the virus pellet using Trizol (Life Technologies, Inc.) and 20 µl of each sample was analyzed in a 96-well plate. Synthesis of cDNA was accomplished in triplicate reactions containing 5.0 nmol/L MgCl₂, 1X PCR buffer II, 0.75 mmol/L of each dNTP, RNase inhibitor, 1.2 U MULV reverse transcriptase, 2.5 µmol/L random hexamers, and 10% of total viral RNA. Samples were mixed and incubated at room temperature for 10 minutes followed by 42°C for 12 minutes and the reaction terminated by heating at 99°C for 5 minutes then cooling to 4°C for 5 minutes. The PCR reaction was then initiated by adding 30 µl of a PCR master mix containing 1X PCR buffer A, 5.5 mmol/L MgCl₂, 2.5 U of AmpliTaq Gold, 200 mmol/L of each dNTP, 450 nmol/L of each primer, and 200 nmol/L of probe. The primers and probe used were: forward primer U5/LTR, 5'AGGCTGGCAGATTGAGCCCTGGGAGGTTTC3'; reverse primer 5' R region of LTR, 5'CCAGGCGGCGACTAGGAGAGATGGGAACAC3'; and probe 6FAM,

5'TTCCCTGCTAGACTCTCACCAGCACTTGG-3' TAMRA. The amplification was performed by heating at 95°C for 10 minutes to activate AmpliTaq Gold (Perkin Elmer), followed by 40 cycles of 95°C for 15 seconds, 55°C for 15 seconds, and 72°C for 30 seconds. Serial dilutions of RNA ranging from 10⁸ to 100 copies/reaction obtained by *in vitro* transcription of a plasmid containing the target LTR region were subjected to RTPCR reaction in triplicate along with the samples to generate the standard curve with a sensitivity threshold of 100 copies/reaction. RNA copy numbers from the unknown plasma samples were calculated from the standard curve and expressed as RNA copies/ml plasma.

Histology

Paraffin sections of brain tissue containing putamen, caudate, neocortical gray and white matter, and hippocampus were stained with hematoxylin and eosin (H&E) and assessed for the presence of SIVE. SIVE was empirically defined as the presence of microglial nodules and multinucleated giant cells, and profuse perivascular mononuclear infiltrates. To assess the distribution and abundance of macrophages and SIV morphologically, we used a monoclonal antibody against a macrophage/ microglia-associated protein CD68 (clone KP1; DAKO, Carpinteria, CA) and a polyclonal antibody against the SIV envelope gp110 (generously provided by Dr. Kelly Stefano Cole and Dr. Ron Montelaro, University of Pittsburgh, Pittsburgh, PA), respectively. Three of the infected macaques showed histological findings of SIVE. The remaining three SIV-infected macaques did not show histopathological features of SIVE, however, neuropathological findings in these three SIV-infected macaques included rare perivascular infiltrates. Each SIV-infected macaque used in this study showed no histopathological abnormalities outside those associated with SIV encephalitis/ infection. The noninfected control macaque brains showed no histopathological abnormalities.

Immunofluorescent Histochemistry

Paraffin sections containing putamen, caudate, neocortical gray and white matter, and hippocampus were deparaffinized in HistoClear (3 x 5 minutes) (National Diagnostics, Atlanta, GA). Sections were rehydrated as follows: 100% ethanol (2 x 5 minutes), 95% ethanol (1 x 5 minutes), 70% ethanol (1 x 5 minutes), and H₂O (1 x 5 minutes). Rehydrated sections were immersed in 3% H₂O₂ (Sigma, St. Louis, MO) in 70% methanol (J. T. Baker, Phillipsburg, NJ) (1 x 30 minutes) to block endogenous peroxidase activity. To unmask antigens, sections were incubated in Target Retrieval Solution (DAKO) at 97°C for 1 hour. Sections were cooled (1 x 30 minutes, room temperature) and blocked with 10% normal goat serum (DAKO). Sections were incubated with mouse monoclonal antibody against a macrophage lysosomal-associated protein CD68 and rabbit polyclonal antibody to the SIV envelope protein SIV-gp110 (1:50,000 and 5 µg/ml dilutions, respectively, at 4°C overnight). The mouse monoclonal antibody CD68 could not be detected by Cy3-conjugated goat anti-mouse IgG at the concentration used in this staining protocol, so the CD68 signal was amplified using the commercially available Tyramide Signal Amplification kit (NEN Life Science Products, Boston, MA) (386). Sections were incubated with biotinylated goat anti-mouse IgG serum (Jackson ImmunoResearch Laboratories, Inc., West Grove, PA) (1:200, room temperature, 1 hour). After being washed with 0.5% Tween-20 buffer, sections were incubated with blocking buffer (room temperature, 30 minutes) followed by horseradish peroxidase-conjugated streptavidin (1:500 in blocking buffer, room temperature, 30 minutes). Sections were washed with 0.5% Tween-20 buffer and incubated with fluorescein-conjugated tyramide (1:100 in 1X Amplification Diluent, room temperature, 10 minutes). After washing with 0.5% Tween-20 buffer, sections were incubated with one of the following mouse

monoclonal antibodies: MAP-2 (1:1500, SMI 52; Sternberger Monoclonals Inc., Lutherville, MD), synaptophysin (1:100, SY 38; DAKO), or GFAP (1:500, 6F2; DAKO). Sections were incubated with Cy5-conjugated goat anti-mouse IgG and Cy3-conjugated goat anti-rabbit IgG (Jackson ImmunoResearch Laboratories, Inc.) (1:200, room temperature, 1 hour). The fluorogen tags used to detect synaptic proteins are noted in the figure legends. Slides were mounted in gelvatol (13) and fluorescence quantified as described below in the laser confocal microscopy quantification section.

Peroxidase Immunohistochemical Staining

Paraffin-embedded tissue sections were deparaffinized by incubation at 60°C for 15 minutes, immersion in xylenes twice for 8 minutes each, and dehydration in graded ethanols. Tissues were pretreated by microwaving at 2-minute intervals for a total of 10 minutes at settings between 60 to 20% maximal power in 0.01 mol/L of citrate buffer (pH 6.0). The buffer was replenished as needed to ensure that the tissue sections did not dry out. Slides were then blocked in 5% nonfat dry milk in 1X phosphate-buffered saline (PBS) for 1 hour. Tissue sections were then incubated with a CD68-specific monoclonal antibody at a 1:50 dilution for 45 minutes and washed with 1X PBS three times, 5 minutes each. The bound monoclonal antibody was then detected using the avidin-biotin complex approach with the Vectastain Elite System (Vector Laboratories, Burlingame, CA). Sections were incubated with biotinylated goat anti-mouse secondary antibody for 30 minutes and washed as before. They were then incubated with an avidin/horseradish peroxidase conjugate for 30 minutes and again washed as before. All incubations were performed at room temperature. Immunohistochemical signal (brown staining) was provided by the action of horseradish peroxidase on the substrate 3,3'-diaminobenzidine. Slides were counterstained with propidium iodide to stain the nuclei by incubating in 1X PBS

containing 10 mg/ml of propidium iodide for 30 minutes at room temperature in the dark. Slides were then washed by rinsing in 1X PBS and double-distilled water, dehydrated in graded ethanols, cleared in xylenes, and mounted with Permount (Fisher).

Laser Confocal Microscopy Quantification

Consecutive sections were stained with H&E or immunohistochemically stained as described above. A dissecting microscope was used to identify anatomical regions on the H&E-stained section. Five regions of the SIV-infected macaque brains containing putamen, caudate, neocortical frontal gray and white matter, and hippocampus were identified on the immunofluorescent stained slides. The marked H&E tissue section was matched with the consecutive, immunostained tissue section, and the marked regions were traced on the immunofluorescent section. Immunohistochemically stained sections containing regions of interest were analyzed by laser confocal microscopy (Molecular Dynamics, Sunnyvale, CA). The illumination was provided by an argon/krypton laser with 488-, 568-, and 647-nm primary emission lines. Each image was scanned along the z-axis and the middle sectional plane was found (262,144 pixels per plane; 1 pixel, 0.25 μm^2). Images were collected on a Silicon Graphics Inc. computer (Operating System Release 5.3, Farmington, MI) and analyzed using the Image Space software (Version 3.2, Molecular Dynamics). All multiple-label immunofluorescent images are 10-section projections.

Each brain region from every macaque was randomly scanned in 10 microscopic areas (40X). The specimen was first scanned for fluorescein isothiocyanate (FITC) and Cy3 signals. Subsequently, the specimen was rescanned for Cy5 signal in the same sectional plane. All

specimens were scanned at the same laser power aperture, gain, and photomultiplier tube settings for each wavelength. The number of pixels emitted by each signal was counted using the same collection parameters. Each area scanned encompasses an area of 67,600 μm^2 .

For quantification of SIV-gp110 or CD68 pixels, pixel counts were obtained from 10 microscopic areas within five brain regions. To compare the pixel counts collected in each brain region, the average pixel count was determined for each brain region within the three SIV-infected macaques without encephalitis. Then for every macaque, each pixel value in a brain region was divided by the average pixel count in the analogous brain region of the SIV-infected macaques. The means of the normalized values were then calculated for each brain region in the SIV-infected macaques with and without encephalitis and control macaques and reported as fold difference in pixel counts. The fold difference in pixel counts for SIV-infected macaques with and without encephalitis each represent three macaques in which 10 areas in each brain region/macaque were scanned, giving a fold pixel count from 30 total areas. Fold difference in pixel counts for control macaques represent two macaques in which 10 areas in each brain region/macaque were scanned, giving a fold pixel count from 20 total areas.

For quantification of MAP-2, synaptophysin, or GFAP pixels, pixel counts were obtained from 10 microscopic areas within five brain regions. To compare the pixel counts collected in each brain region, the average pixel count was determined for each brain region within the three SIV-infected macaques without encephalitis. Then for every macaque, each pixel value in a brain region was divided by the average pixel count in the analogous brain region of the normal, control macaques. The medians of the normalized values were then determined for each brain region in the SIV-infected macaques with and without encephalitis and control macaques, averaged, and reported as fold difference in pixel counts. The fold difference in pixel counts for

SIV-infected macaques with and without encephalitis each represent three macaques in which 10 areas in each brain region/macaque were scanned, giving a total pixel count from 30 total areas. Fold difference in pixel counts for control macaques represent two macaques in which 10 areas in each brain region/macaque were scanned, giving a total pixel count from 20 total areas.

Image Capture and Peroxidase Immunohistochemistry Quantitation

Quantitation of the CD68-specific immunoreactivity of stained tissue sections was performed by capturing bright-field microscopic images in five random fields for each microanatomic location. Images were captured with a Spot RT Camera mounted on a Nikon E600 fluorescence microscope using a 60X Plan Apochromat objective. Image capture and analysis was performed using the Metaview software package (Universal Imaging Corporation). Each image was subjected to red, green, and blue color separation and the green signal was converted to monochrome. The image was then thresholded to highlight immunoreactive areas of the field and the percentage of surface area that was CD68-immunoreactive was measured. For each image the corresponding propidium iodide-stained image was captured using a FITC filter cube and the number of nuclei in each field was counted manually.

Statistical Analysis

Comparisons of pixel count, SIV RNA, and clinical parameter variances among groups were analyzed by two-way, unpaired Student's t-test. A P value of <0.05 was considered significant. Correlation coefficients and t-tests were determined using Microsoft Excel:Mac 2001.

Table 1. Macaque Infection Parameters

Monkey group*	Monkey number	Sex	Age, months	Virus	Inoculation route†	Length of infection, days
Severe SIVE	604	F	33	SIV/dB670	i.v.	116
	603	M	75	SIV/dB670	i.v.	81
	221	M	70	SIV/dB670	BAL	37
SIV without encephalitis	9221	M	100	SIV/dB670	Rectal/BAL	379
	234	M	44	SIV/dB670	i.v.	360
	236	F	42	SIV/dB670	i.v.	367
Control	421	F	66	NA	NA	NA
	422	M	53	NA	NA	NA

*Severe SIVE is defined as the histopathological presence of abundant SIV-infected microglial nodules and multinucleated giant cells. Rare/no microglial nodules and no multinucleated giant cells were observed in SIV-infected macaques without encephalitis. Each macaque used in this study showed no histopathological abnormalities outside those associated with SIV encephalitis/infection. Control noninfected macaques showed no gross or microscopic pathological changes.

†Some macaques were inoculated by intravenous (i.v.) routes. Macaque 221 was inoculated via bronchoscope with the bronchial alveolar lavage (BAL) from another macaque infected with SIV/dB670. Macaque 9221 was initially infected by rectal inoculation followed by another infection with the BAL from a SIV/dB670-infected macaque via bronchoscope.

NA, not applicable; SIV/dB670, SIV/deltaB670.

Table 2. Clinical Symptoms and Peripheral Blood Studies

Monkey group	Monkey number	Peripheral viral load*	Lymphocytes, %	Total % CD4 cells	Clinical symptoms†
Severe SIVE	604	6.00×10^7	21	47	Anorexia, weight loss, electrolytes deteriorating
	603	5.30×10^8	37	37	Anorexia, weight loss, neurological signs
	221	1.90×10^8	14	32	Weight loss, neurological signs
SIV without encephalitis	9221	6.40×10^5	34	20	Weight loss, upper respiratory symptoms
	234	2.06×10^5	43	39	No symptoms
	236	4.70×10^2	32	33	No symptoms
Control	421	NA	NA	NA	No symptoms
	422	NA	NA	NA	No symptoms

*Numbers reflect the total SIV/RNA copies/ml plasma at time of death.

†Neurological signs are described in the Material and Methods section.

NA, not applicable

3.1.4. Results

Total CD4⁺ T Cell Counts Were Not Different in SIV-Infected Macaques with and without Encephalitis, However, Plasma SIV RNA Concentrations Were Higher in Macaques with SIVE

Tables 1 and 2 summarize clinical data from the six SIV-infected and two noninfected rhesus macaques evaluated in this study. Macaques that developed neurological signs had to be euthanized because of declining health after shorter periods of infection ($P = 0.004$) (Table 1). The two macaques (macaques 603 and 221) with neurological signs had SIVE, however, we had no direct means of determining how long they had encephalitis. The plasma viral loads at time of sacrifice for each macaque in the severe SIVE group were 2 to 5 orders of magnitude higher than those measured in SIV-infected macaques without encephalitis ($P = 0.2$) (Table 2, Figure 5B). Absolute CD4 counts between SIV-infected macaques with and without encephalitis were similar (Table 2). However, because of the heterogeneity of the peripheral infection in these macaques (eg, length of infection) these observations have no direct reflection on the CNS infection in these macaques.

SIV-Infected Macaques with Encephalitis Had Concentrations of SIV RNA in Multiple Brain Regions that Were Five Orders of Magnitude Greater than Macaques without Encephalitis

Most brain regions analyzed in macaques with SIVE contained 10^6 to 10^7 copies of SIV RNA/mg brain tissue (Figure 5A). Nonencephalitic SIV-infected macaques with mild

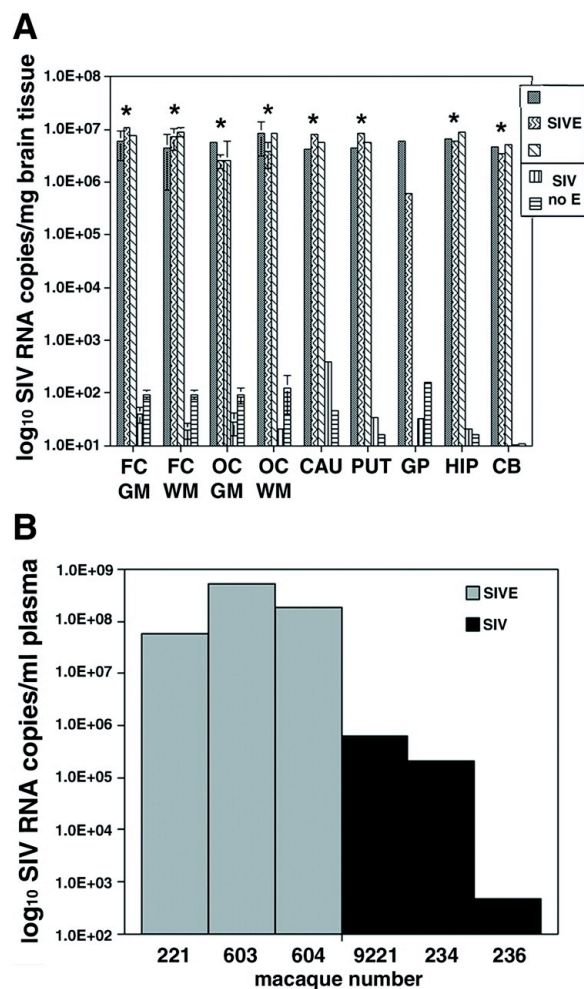


Figure 5. Macaques with histological evidence of SIVE had brain SIV RNA concentrations 5 orders of magnitude greater than macaques without SIVE. **A:** The number of SIV RNA copies/mg tissue extracted from different brain regions is shown for three macaques with SIVE (□ ▨ ▩) and two SIV-infected macaques without encephalitis (▧ ▩). Tissue from the globus pallidus for macaque 604 was not available. Quantitation of SIV RNA copies was determined by RT-PCR as described in the Materials and Methods. SIV-infected macaques without encephalitis contained <200 SIV RNA copies/mg tissue in each brain region (average of 67 and median of 35 SIV RNA copies/mg tissue for all regions analyzed). Error bars for FC GM, FC WM, OC GM, and OC WM indicate the SD of the average of two separate brain areas for each region. **Asterisks** indicate statistically significant differences in number of SIV RNA copies/mg brain tissue between SIVE macaques with and without encephalitis. *, P < 0.05. **B:** Peripheral SIV load in the plasma at time of death. The number of SIV RNA copies/ml plasma for each macaque was determined by RT-PCR. The **gray bars** represent animals with SIVE, whereas the **black bars** correspond to SIV-infected macaques without encephalitis. On average, macaques with encephalitis had 3 orders of magnitude greater concentrations of plasma SIV RNA than SIV-infected macaques without encephalitis. (The individual macaque number is shown on the x axis.)

Abbreviations: SIVE, simian immunodeficiency virus encephalitis; MGN, microglial nodule; MGNC, multinucleated giant cell; FC GM, frontal neocortical gray matter; FC WM, frontal neocortical white matter; OC, occipital cortex; CAU, caudate; PUT, putamen; GP, globus pallidus; HIP, hippocampus; CB, cerebellum.

perivascular chronic inflammation contained $<4 \times 10^2$ SIV RNA copies/mg brain tissue (Figure 5A). Most brain regions from these macaques had significantly less SIV RNA concentrations (10^1 to 10^2 SIV RNA copies/mg brain tissue) ($P < 0.03$) (Figure 5A) than macaques with SIVE.

High Concentrations of SIV RNA in Brains of Macaques with SIVE Correlated with Profuse Microglial Nodules and Multinucleated Giant Cells

H&E staining and immunohistochemical staining for SIV envelope protein gp110 (SIVgp110) and macrophage/microglia-related molecule CD68 were performed on paraffin sections to determine the histological presence of encephalitis. Noninfected macaques showed no histopathological changes or cells stained positively for SIV proteins. Macaques with high CNS tissue concentrations of SIV RNA had profuse microglial nodules, severe perivascular chronic inflammation, and multiple multinucleated giant cells (Figure 6; A, B, and C). SIV-infected macrophages were observed in both parenchymal and perivascular locations.

Although neuropathology was widespread in macaques with high CNS tissue concentrations of SIV RNA, the histopathological changes were most abundant in midfrontal neocortical white and gray matter and caudate regions. Substantial SIV RNA concentrations in the cerebellum were associated with abundant white matter macrophages that stained for SIV and relative sparing of cerebellar cortical foci. Rare SIV-infected perivascular macrophages were seen in macaques with brain SIV RNA concentrations lower than 4×10^2 SIV RNA. In SIV-infected macaques without encephalitis, we observed rare or no monocytic infiltrates.

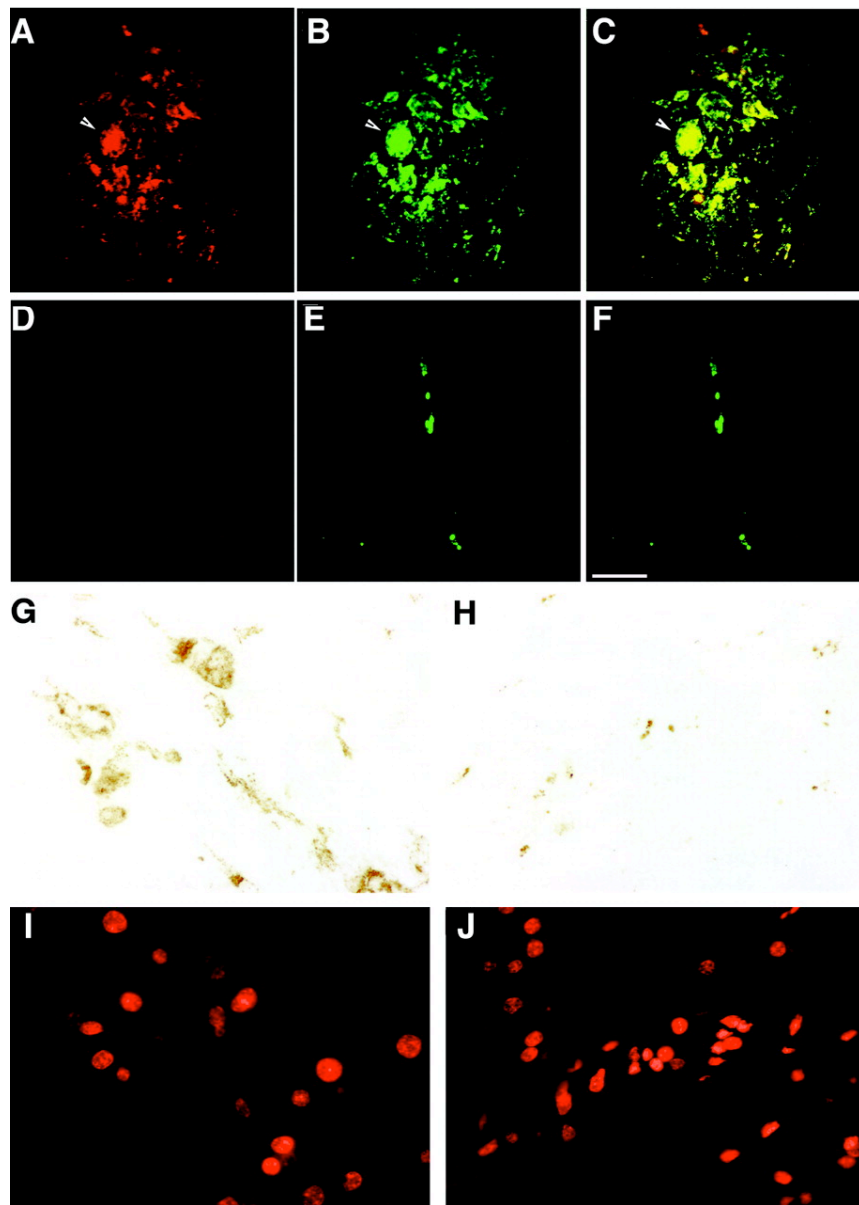


Figure 6. Immunofluorescent staining for macrophages and SIV envelope protein showed extensive co-localization in SIVE. **A**, **B**, and **C**: Histological sections from the white matter of a macaque with SIVE (macaque 221). **D**, **E**, and **F**: Histological sections from the white matter of a SIV-infected macaque without encephalitis (macaque 236). **A** and **D** illustrate immunofluorescent staining for the SIV envelope protein gp110 (red, Cy3), and **B** and **E** show immunofluorescent staining for the macrophage-related protein CD68 (green, FITC) visualized by double-label immunofluorescent confocal microscopy. **C** and **F** show merged images with yellow indicating co-localization of SIV-gp110 and CD68. **A**, **B**, and **C** from a macaque with SIVE demonstrate a microglial nodule containing a multinucleated giant cell (arrow). A rare field in a macaque without SIVE (**D**, **E**, and **F**) shows a perivascular macrophage. Scale bar, 50 μ m. **G–J**: To confirm the immunofluorescent quantification, a peroxidase-based technique was used to quantitate the percent surface area CD68⁺ macrophages cover in macaques with and without encephalitis. **G** and **I** show a histological section from the caudate of a macaque with SIVE (macaque 221). **H** and **J** show a histological section from the caudate of a SIV-infected macaque without encephalitis (macaque 236). **G** and **H** show peroxidase staining for the macrophage-related protein CD68 (reddish-brown, 3,3'-diaminobenzidine), and **I** and **J** show the nuclear counter stain of **G** and **H** (red, propidium iodide) visualized by fluorescence microscopy.

CD68 Staining Was Most Abundant in the Putamen, Caudate, Hippocampus, and Frontal Cortex of Macaques with SIVE

All brain regions of macaques with SIVE showed increased CD68 staining. Quantitation of pixels corresponding to CD68 immunostaining showed the greatest fold increase in the caudate and midfrontal neocortical gray matter (16- and 25-fold increase, respectively) (Figure 7C). SIV-infected macaques without encephalitis showed more pixels corresponding to CD68 than the noninfected control macaques, but this increase was not statistically significant (Figure 7C). Using an enzymatic colorimetric method to quantitate CD68 staining in the same brain regions of the same macaques, we observed that ~1% of the surface area in each brain region was stained for CD68 in macaques with SIVE. The putamen showed the largest percentage of surface area stained for CD68 (1.4%). In SIV-infected macaques without encephalitis, <0.4% of surface area was stained for CD68 in all brain regions (Figure 7A). Compared to SIV-infected macaques without SIVE, all brain regions analyzed in macaques with SIVE showed a 3- to 11-fold increase in the percentage of surface area stained for CD68 (Figure 7, A and B).

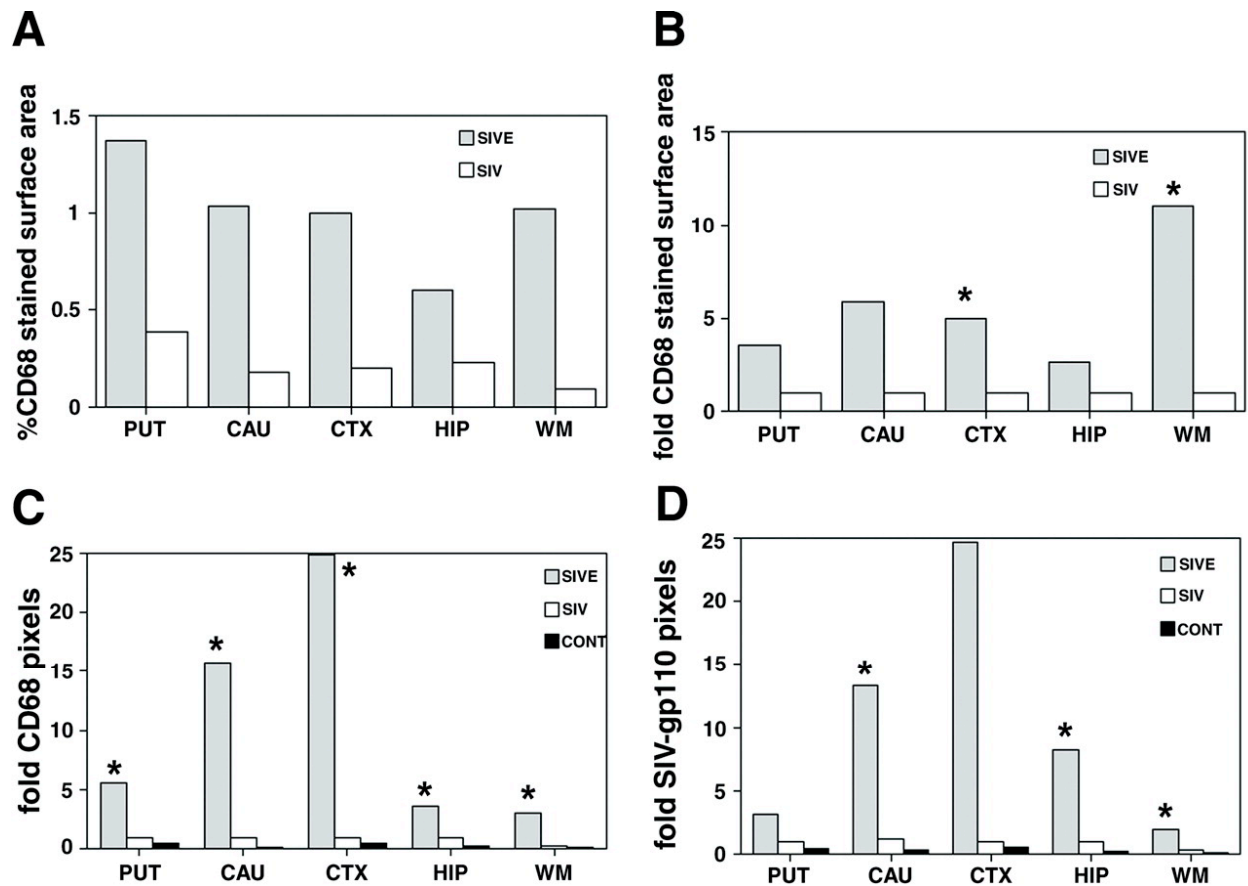


Figure 7. Quantitation of immunohistochemical staining for macrophages (CD68) and SIV envelope protein shows a 4- to 25-fold increase in brain regions with encephalitis versus those without encephalitis. **A:** CD68 staining covers ~1% of the surface area in most brain regions with encephalitis. The average percentage of surface area stained with CD68 was determined for each brain region of the SIVE and SIV without encephalitis groups. **B:** The neocortical white and gray matter exhibit the greatest difference in the percentage of surface area stained for CD68. Histogram plots show the fold increase of surface area stained for CD68 in macaques with or without SIVE compared to SIV-infected macaques without encephalitis. **C:** Quantitation of fluorescent pixels corresponding to CD68 is significantly increased in all brain regions of macaques with SIVE. Pixels were quantified in indicated brain regions using immunofluorescent laser confocal microscopy as described in the Materials and Methods. Average pixels staining for CD68 in each animal group were compared to SIV-infected macaques without encephalitis and reported as fold difference in pixel counts. **D:** The number of pixels corresponding to SIV-gp110 envelope protein is significantly higher in the caudate, hippocampus, and white matter. Average immunofluorescent pixels for SIV-gp110 in each animal group were compared to SIV-infected macaques without encephalitis and reported as fold difference in pixel counts. **Gray bars, SIVE; white bars, SIV without encephalitis; black bars, controls.** Fold pixels listed on y-axes represent fold difference in pixel counts. *, $P < 0.05$.

Macaques with SIVE Had Increased Staining for SIV Envelope Protein in the Caudate, Hippocampus, and Frontal Cortex

Figure 6 shows representative fields used to quantify CD68 and SIVgp110 in five brain regions of SIV-infected macaques with and without encephalitis. Quantitation of pixels corresponding to SIVgp110 staining was 2- to 13-fold higher in the caudate, hippocampus, and white matter of macaques with SIVE compared to nonencephalitic macaques ($P < 0.005$) (Figure 7D). The midfrontal neocortical gray matter exhibited a 25-fold increase in SIVgp110 staining in macaques with SIVE, however, because of large variations in SIVgp110 staining the difference in this region was not statistically significant ($P < 0.05$).

SIVE Is a Multifocal Disease with Tight Correlation between the Presence of Macrophages and SIV Antigen

Wide variation within all brain regions analyzed demonstrated the multifocal nature of SIVE. As an example, the mean \pm SD of the fold increase in SIVgp110 and CD68 staining within the midfrontal neocortical gray matter was 25 ± 86 and 25 ± 60 , respectively. In macaques with SIVE, the majority of cells that were immunostained for CD68 also stained for SIVgp110 (Figure 6C). Pixel quantification of CD68 and SIVgp110 staining showed a correlation coefficient of 0.91 in the putamen, 0.99 in the midfrontal neocortical gray matter, and 0.97 in the hippocampus.

Macaques with SIVE Showed Less Abundant Postsynaptic Protein MAP-2 Staining in the Caudate, Hippocampus, and Frontal Cortical Gray Matter than Macaques without Encephalitis

To determine the relationship between postsynaptic damage and SIVE, quantification of postsynaptic protein MAP-2 staining was performed in gray matter regions from all macaque groups. A representative histological section from the caudate of a macaque with SIVE showed decreased MAP-2 staining (Figure 8A) compared to equivalent sections from SIV-infected macaques without encephalitis (Figure 8E). MAP-2 staining in the caudate, hippocampus, and midfrontal neocortical gray matter was 66 to 70% lower in macaques with SIVE than in both SIV-infected and noninfected macaques without encephalitis (Figure 9A). MAP-2 staining was also 37% lower in the putamen of macaques with SIVE, but this decrease did not achieve statistical significance. SIV-infected macaques without encephalitis exhibited significantly lower staining for MAP-2 in the midfrontal cortical gray matter than noninfected macaques (50% lower), however, the decrease was not as great as that observed in macaques with SIVE (Figure 9A).

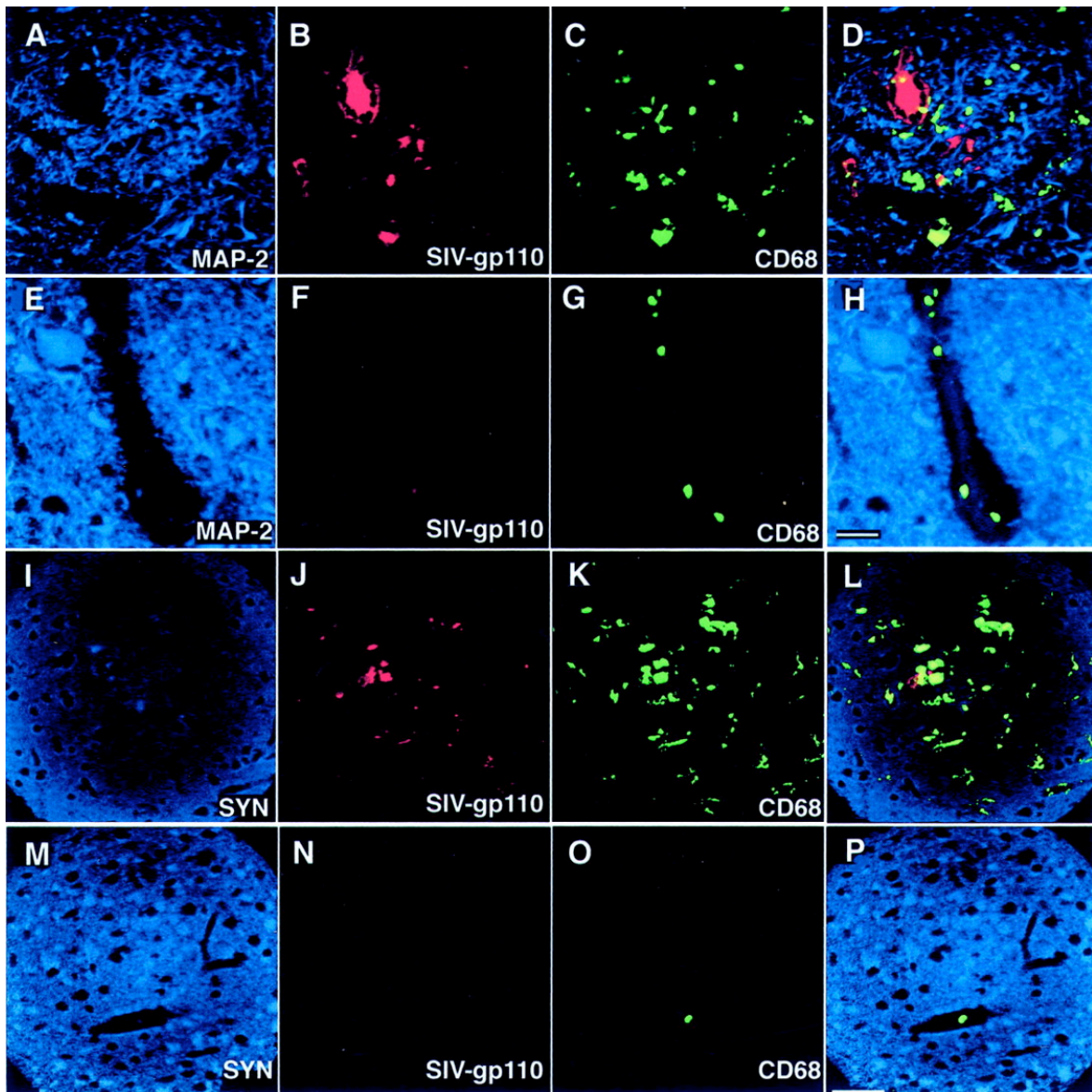


Figure 8. Macaques with SIVE show decreased staining for MAP-2 and synaptophysin. **A–H:** The relationship between MAP-2 staining and the presence of macrophages and SIV can be qualitatively appreciated in this triple label image. Images such as this were quantitated and plotted in Figures 9. **A to D** show histological sections from the caudate of a macaque with SIVE (macaque 603) immunostained for MAP-2 (**A**; blue, Cy5), SIV-gp110 (**B**; red, Cy3), and CD68 (**C**; green, FITC) visualized by triple-label immunofluorescent laser confocal microscopy. **E to H** show histological sections from the caudate of a SIV-infected macaque without SIVE (macaque 236) immunostained for MAP-2 (**E**; blue, Cy5), SIV-gp110 (**F**; red, Cy3), and CD68 (**G**; green, FITC). An overlay of the three preceding images is shown in **D** and **H**. Yellow shows co-localization. Scale bar, 20 μm . **I–L:** The relationship between synaptophysin staining and the presence of macrophages and SIV can be qualitatively appreciated in this triple label image. Images such as this were quantitated and plotted in Figures 9. **I to L** show histological sections from the hippocampus of a macaque with SIVE (macaque 604) immunostained for synaptophysin (SYN) (**I**; blue, Cy5), SIV-gp110 (**J**; red, Cy3), and CD68 (**K**; green, FITC) visualized by triple-label immunofluorescent laser confocal microscopy. **M to P** show histological sections from the hippocampus of a normal uninfected macaque (macaque 421) immunostained for SYN (**M**; blue, Cy5), SIV-gp110 (**N**; red, Cy3), and CD68 (**O**; green, FITC). An overlay of the three preceding images is shown in **L** and **P**. Yellow shows co-localization. Scale bar, 50 μm .

Immunostaining for the Presynaptic Protein Synaptophysin Was Decreased in SIV-Infected Macaques with and without Encephalitis

To determine the relationship between presynaptic damage and SIVE, quantification of presynaptic protein synaptophysin staining was performed in gray matter regions from all macaque groups. A representative histological section from the hippocampus of a macaque with SIVE showed decreased synaptophysin staining (Figure 8I) compared to a noninfected macaque without encephalitis (Figure 8M). In contrast to MAP-2 staining, the number of pixels corresponding to synaptophysin was decreased in both SIV-infected macaques with and without encephalitis compared to noninfected macaques (Figure 9B). The putamen and hippocampus of SIV-infected macaques with and without encephalitis showed 60 to 80% lower synaptophysin staining than noninfected macaques without encephalitis (Figure 9B). Macaques with SIVE exhibited similar fold staining for synaptophysin in the caudate and frontal neocortical gray matter as noninfected controls, whereas SIV-infected macaques without encephalitis showed a significant decrease in synaptophysin staining in the frontal neocortical gray matter compared to noninfected controls (Figure 9B).

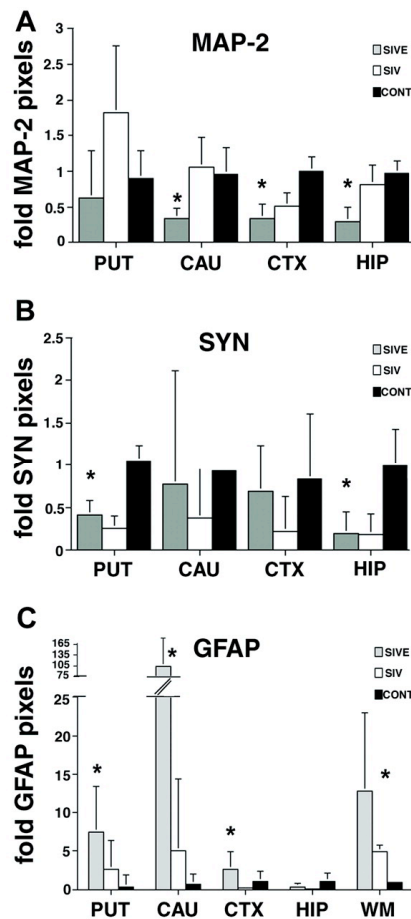


Figure 9. MAP-2 staining is decreased in the brains of macaques with SIVE, whereas synaptophysin staining is decreased in the brains of SIV-infected macaques with and without encephalitis. **A:** The number of pixels corresponding to MAP-2 is significantly decreased in the caudate, neocortical gray matter, and hippocampus of macaques with SIVE compared to nonencephalitic and noninfected controls. Each indicated brain region was immunostained for MAP-2 and visualized by immunofluorescent confocal microscopy. Ten areas in each brain region were quantified for each animal and marker. To obtain the fold difference in pixel counts for MAP-2, the median pixel count for each animal, brain region, and marker was divided by the average pixel count for the corresponding brain region and marker of the control animals. **B:** The number of pixels representing synaptophysin is significantly decreased in the putamen and hippocampus of SIV-infected macaques with and without encephalitis. Each indicated brain region was immunostained for SYN and visualized by immunofluorescent confocal microscopy. Ten areas in each brain region were quantified for each animal and marker. To obtain the fold difference in pixel counts for SYN, the median pixel count for each animal, brain region, and marker was divided by the average pixel count for the corresponding brain region and marker of the control animals. **C:** GFAP staining is increased in the brains of macaques with SIVE. Each indicated brain region was immunostained for GFAP and visualized by immunofluorescent confocal microscopy. Ten areas in each brain region were quantified for each animal and marker. To obtain the fold difference in pixel counts for GFAP, the median pixel count for each animal, brain region, and marker was divided by the average pixel count for the corresponding brain region and marker of the control animals. The number of pixels corresponding to GFAP is significantly increased in the putamen, caudate, and neocortical gray and white matter of macaques with SIVE compared to nonencephalitic and noninfected controls. Error bars reflect positive error. Fold pixels listed on y-axes represent fold difference in pixel counts. Abbreviations are listed in Figure 9. CTX, neocortical frontal gray matter. *, $P < 0.01$.

Quantitative Immunostaining for GFAP Showed Prominent Gliosis in the Putamen, Caudate, and Frontal Cortex of Macaques with SIVE

To determine the relationship between nonspecific CNS damage and SIVE, quantification of GFAP staining was performed in gray and white matter regions from all macaque groups. SIV-infected and noninfected macaques without encephalitis showed 2- to 100-fold lower GFAP staining than macaques with SIVE (Figure 9C). The greatest fold increase in GFAP staining in macaques with SIVE compared to SIV-infected macaques without encephalitis was present in caudate and white matter (100-fold and 8-fold, respectively) (Figure 9C). Surprisingly, the hippocampus showed similar GFAP staining in all macaques. SIV-infected macaques without encephalitis showed up to fivefold higher GFAP staining in putamen, caudate, and white matter than noninfected macaques.

3.1.5. Discussion

In lentiviral-associated dementia there has been considerable controversy regarding the relationship between neurological damage and the abundance of virus in the CNS (3, 32, 85, 124, 125, 157, 187, 288, 394, 395, 397, 415, 418). Because some investigators have found little HIV antigen in the brains of individuals with HIV-associated dementia, it has been suggested that the presence of activated macrophages/microglia in the CNS is a better correlate of dementia than the presence of HIV-infected macrophages (124). Similar observations have been reported in the SIV model in which no clear relationship was discerned between neuropathology and the number of SIV-infected cells (32). However, these reports used nonquantitative methodology, relying on nonquantitative scoring of immunohistochemistry and in situ hybridization in selected brain regions. Preservation and accessibility of viral proteins and nucleic acids using these techniques

is technique-dependent. Several other studies have shown that the severity of HIV and SIV encephalitis correlates with higher viral RNA concentrations in several brain regions using sensitive, quantitative RNA assays (85, 395, 397, 418).

We have confirmed that the histological presence of encephalitis is associated with high concentrations of SIV RNA in most brain regions. Brains of SIV-infected macaques with histological findings of SIVE contained 5 orders of magnitude greater concentrations of SIV RNA than SIV-infected macaques without encephalitis. Because the macaque brains used in this study were not perfused with buffer after sacrifice, brain tissue extracts were necessarily contaminated with blood. Whether blood contamination contributed to the amount of SIV RNA quantified in brain tissue extracts depends on two factors: the level of virus in blood and the amount of blood in the tissue. Blood-borne SIV could be cell-associated or within the plasma. Because CD4 counts in these SIV-infected macaques were low, the amount of viral RNA derived from infected CD4⁺ T cells would not be expected to significantly contribute to the levels of SIV RNA measured in the brain. The SIV RNA load in plasma of macaques with SIVE was 5.3×10^8 SIV RNA copies/ml plasma or less. If we assume the blood contaminating brain tissue extracts contained an upper limit of 1×10^6 SIV RNA copies/ml plasma, we would estimate that blood contamination of brain extracts would account for less than 1×10^4 copies/mg. Thus, the high RNA concentrations observed in most brain regions must be attributed to virus in brain tissue rather than blood contamination. Lastly, we are assured blood contamination was not a factor in quantification of viral RNA in brain tissue extracts because the SIV-infected macaques without encephalitis had greater than 10^5 SIV RNA copies/ml plasma but less than 10^2 SIV RNA copies/mg brain tissue.

It is interesting that regions such as the cerebellum that traditionally have been reported to lack overt histopathology have similar concentrations of SIV RNA as regions with more abundant pathology. It has been reported that cerebellar cortex is not as affected histopathologically as the basal ganglia structures during lentiviral encephalitis (418). We have observed such a pattern in patients with HIV encephalitis (397). It has been reported that the deep cerebellar gray nuclei have abundant macrophages that stained for HIVgp41 (transmembrane protein), whereas infected cells are rare in the cerebellar cortex (181). In the animals used in this study, cerebellar white matter was also heavily infiltrated with SIV-infected macrophages (data not shown). Seemingly conflicting observations in cerebellar viral RNA concentrations might result from sampling different portions of the cerebellum.

Vast differences in viral RNA concentrations between SIV-infected macaques with and without encephalitis makes the readily quantifiable RNA assay an unbiased tool for diagnosing lentiviral encephalitis. However, this approach quantifies the average amount of RNA within 100 mg of brain tissue that contains ~500 million cells with abundant microenvironments potentially disparate in lentiviral presence. Defining proximal relationships between macrophage and viral factors requires more selective analysis than averages derived from measurements of 500 million cells. Using confocal microscopy, we quantified markers of virus and macrophages within discrete microenvironments and assessed the relationship of these markers to neuronal damage.

There are three potential drawbacks to microscopy-based quantification of viral and host cell markers: necessity of using fixed tissue, observer bias in selecting regions for quantitation, and variability within individual microscopic fields. All of the macaque CNS tissues were fixed by immersion in 10% formalin. To control for any potential differences in antigen preservation during immersion fixation, we compared MAP-2 fluorescent staining in cerebellar cortical gray

matter (data not shown). No significant interspecimen variation was observed for this control antigen. To prevent observer bias, brain regions were defined by gross inspection of the slide and then circled. Random selection of microscopic regions within the encircled areas was performed by an observer blinded to animal disease status. Finally, to accommodate variability encountered within individual microenvironments (eg, presence of vessels of various calibers, presence of white matter tracts within basal ganglia structures, intranuclear histological variability), we acquired optical images within 10 fields for each brain region. Individual microenvironments showed the expected variability, however, comparison of the fluorescent-labeling averages between macaques with and without encephalitis showed significant differences.

We compared our technique of quantifying fluorescent markers in microscopic fields to an enzymatic colorimetric quantification method. Using the colorimetric method, white matter of macaques with SIVE had the greatest fold increase in surface area stained for CD68, whereas with the confocal method frontal neocortical gray matter showed the greatest fold increase in fluorescent pixels stained for CD68. However, overall the two methods showed parallel trends in quantifying macrophages.

Both CD68 and SIVgp110 staining were elevated in all brain regions of macaques with SIVE compared to SIV-infected macaques without SIVE. The greatest increases were seen in the midfrontal cortical gray matter and caudate suggesting that neurons in these regions are at greater risk of damage from soluble products secreted by activated and infected macrophages. Regions receiving projections from the caudate and midfrontal cortical gray matter would be at risk of secondary damage because of downstream events initiated at the soma of these neurons.

The majority of activated macrophages in the brains of macaques with SIVE were infected with SIV. Examining individual microscopic fields, we estimated ~70 to 80% of

macrophages stain for SIVgp110. This observation is different from some previous reports. For instance, it has been reported that 16 to 25% of brain macrophages stained for HIV antigen (134). However, this study analyzed a wide variety of neuropathological conditions (eg, opportunistic cytomegalovirus, Toxoplasma, cryptococcus) and was not restricted to assessment of lentiviral encephalitis. Other studies have also suggested that the majority of CD68-positive macrophages did not stain for SIV gp41 (418). Some of the discrepancy between previous studies and ours might be attributed to differing sensitivities of antibodies for transmembrane (gp41) and surface unit glycoprotein (gp110). Additionally, in our studies raw pixel counts indicate that CD68 staining corresponded to more pixels than SIV staining in most microscopic foci. Because CD68 is a marker of lysosomes and the antibody we used to stain SIV-infected cells is specific for viral envelope protein, it may not be appropriate to directly compare absolute CD68 and SIVgp110 pixel counts. Perhaps more meaningful is to compare fold changes in CD68 and SIV immunostaining between encephalitic and nonencephalitic brains.

Lentiviral encephalitis is a multifocal process with significant variation between microscopic regions. This is best shown by the large standard deviations in CD68 and SIVgp110 quantification seen within all brain regions. To assess an individual brain nucleus, an average of numerous fields is required to compensate for microscopic variation. Microscopic foci within brain regions of macaques with abundant macrophage infiltration and viral infection show loss of synaptic proteins. Compared to macaques without encephalitis, macaques with SIVE had significant decreases in MAP-2 staining in the caudate, midfrontal cortical gray matter, and hippocampus suggesting primary postsynaptic damage. Others have also reported decreases in dendritic proteins in SIV-infected cynomolgus macaques soon after infection, but these decreases were independent of concentrations of SIV DNA in the brain (246). It is surprising

that staining for MAP-2 was increased in the putamen of SIV-infected macaques without encephalitis compared to both encephalitic and noninfected controls. It is possible to hypothesize that neurons that have postsynaptic processes in the putamen generate a temporary response to acute damage by dilating postsynaptic processes, but ultimately undergo atrophy because of the chronic insult of encephalitis.

Staining for the presynaptic protein, synaptophysin, was also decreased in the putamen and hippocampus of macaques with SIVE and the putamen, caudate, midfrontal cortical gray matter, and hippocampus of SIV-infected macaques without encephalitis. This finding is consistent with a recent report showing decreased synaptophysin immunoreactivity in macaque brains soon after infection with SIV (131). However, it is puzzling that greater decreases in synaptophysin staining were not observed in the encephalitic macaques in this study. The vast interconnectivity of the brain complicates this analysis by requiring some means of dissecting out synaptic damage distal to affected neuronal soma. In support of indirect mechanisms leading to decreases in synaptic proteins, we have shown that GFAP staining is increased in most brain regions in macaques with SIVE. As we and others have observed, SIV-infected macaques without encephalitis also showed increases in GFAP staining compared to noninfected controls although far less than that observed with encephalitis (131). As the hippocampus is particularly sensitive to hypoxia/ischemia, the absence of increased gliosis in the region suggests that the neuropathological damage observed in SIVE is not related to diffuse ischemic injury, but more specifically related to the encephalitis itself.

Finding presynaptic damage in SIV-infected macaques independent of encephalitis and postsynaptic damage dependent on local presence of encephalitis suggests the following hypothesis: presynaptic components are susceptible to systemic toxins generated as a result of

lentiviral infection, whereas postsynaptic elements are susceptible to degradation by products of locally activated and infected macrophages within the CNS. In support of this hypothesis, we observed less synaptophysin staining in neocortical gray matter, caudate, and putamen of SIV-infected macaques without encephalitis than in SIV-infected macaques with encephalitis. The SIV-infected macaques had longer periods of infection, raising the possibility that presynaptic damage is a consequence of longer peripheral infection. Because synaptophysin is a functional protein and MAP-2 is a structural protein, this hypothesis may extend to functional proteins being susceptible to systemic toxins produced during lentiviral infection, whereas structural proteins are damaged by CNS lentiviral infection. Presynaptic and postsynaptic damage may progress to neuronal loss in the brains of lentiviral encephalitic macaques. MAP-2 functions are modulated by phosphorylation through NMDA receptor-associated signal transduction pathways and subsequent activation of nitric oxide synthase and MAP kinase (203). Secretion of NMDA receptor agonists such as quinolinic acid by activated macrophages might result in hyperphosphorylation of MAP-2 and subsequent destabilization of microtubules leading to neuronal degeneration (59).

In the current study we have attempted to examine the hypothesis that loss of synaptic proteins may spatially correlate with the presence of pathology in macaques with SIVE. We quantified increases in CD68, SIV envelope protein gp110, and GFAP in encephalitic macaques. Presynaptic proteins were decreased in SIV-infected macaques independent of encephalitis, whereas loss of postsynaptic proteins was linked to encephalitis. Quantitation of synaptic proteins in brain regions with abundant SIV-infected and -activated macrophages points to

indirect mechanisms of neuronal damage. Future studies to elucidate mechanisms of neural damage will require compensating for the high degree of microregional variability in neuropathology of lentiviral encephalitis.

3.1.6. Acknowledgements

We thank Jonette Werley for valuable technical assistance; Christopher A. Pittman and Ronald Hamilton for assistance in dissection and banking of the monkey brains; and Premeela Rajakuman, Dawn L. McClemens-McBride, Katy Board, and Karen Norris for assistance in obtaining clinical information for the macaques.

3.2. Chapter 2

Submitted to:

American Journal of Pathology

LONGITUDINAL ANALYSIS OF MONOCYTE/MACROPHAGE INFECTION IN SIMIAN IMMUNODEFICIENCY VIRUS-INFECTED, CD8⁺ T CELL-DEPLETED MACAQUES THAT DEVELOP LENTIVIRAL ENCEPHALITIS

Stephanie J. Bissel,^{*} Guoji Wang,[†] Anita M. Trichel,[§] Michael Murphey-Corb,[§]

Clayton A. Wiley[†]

From the Department of Infectious Diseases and Microbiology,^{*} Graduate School of Public Health and the Departments of Pathology[†] and Molecular Genetics and Biochemistry[§], School of Medicine, University of Pittsburgh, Pittsburgh, Pennsylvania.

Abbreviations: CNS – central nervous system; CSF - cerebral spinal fluid; GFAP – glial fibrillary acidic protein; HAART – highly active antiretroviral therapy; HIVD – Human Immunodeficiency Virus Dementia; HIVE - Human Immunodeficiency Virus Encephalitis; MAP-2 – microtubule-associated protein-2; MDM – monocyte-derived macrophages; PBMC – peripheral blood mononuclear cell; SIV – Simian Immunodeficiency Virus; SIVE- Simian Immunodeficiency Virus Encephalitis

3.2.1. Abstract

The histopathological hallmark of lentiviral-associated encephalitis is an abundance of infected and activated macrophages within the brain. Why a subset of infected hosts develop lentiviral encephalitis and others do not is unknown. Using a CD8⁺ T cell-depletion model of simian immunodeficiency virus (SIV)-infected rhesus macaques, we examined the relationship between peripheral SIV infection of monocyte/macrophages and the development of encephalitis. At the same time CSF viral load increased in macaques that developed encephalitis, we observed that monocyte-derived macrophages from these macaques produced more virus than macaques that did not develop encephalitis. However, during the course of infection, the number of blood monocyte-associated SIV DNA copies did not distinguish macaques that developed SIVE from macaques that did not develop encephalitis. Paradoxically, in this model, macaques that developed encephalitis had fewer SIV-infected macrophages in lungs and thymus at postmortem than macaques that did not develop encephalitis. These findings suggest that inherent differences in host monocyte viral production are related to development of encephalitis.

3.2.2. Introduction

Approximately 1/4 of immunosuppressed AIDS patients develop a neurodegenerative disorder clinically characterized as HIV-associated dementia complex (HIVD) (79). HIVD is a clinical syndrome associated with cognitive, motor, and behavioral deficits that are thought to be mediated by diffuse neuronal damage and loss. In the absence of opportunistic infections of the central nervous system (CNS), HIV encephalitis (HIVE) appears to be the pathological substrate for HIVD (394). The pathological hallmarks of HIVE are microglial nodules, multi-nucleated giant cells, and the presence of abundant activated or HIV-infected macrophages (42). The pathogenesis of neuronal injury is unknown as there is little evidence of convincing neuronal infection. Current hypotheses suggest a myriad of secreted products from infected and activated macrophages might interact with neurons or activate astrocytes to initiate synaptic damage followed by neuronal death (123, 198, 262, 293).

Simian immunodeficiency virus (SIV)-infected macaque models share numerous characteristics with human HIV infection including development of encephalitis in a variable percentage of infected macaques (~25%). Factor(s) determining whether macaques develop simian immunodeficiency virus encephalitis (SIVE) have not been defined; however, incidence of encephalitis and speed of onset (~6-36 months) vary with primate species and viral strains (22, 75, 415). Macrophage-tropic SIV is the predominant virus found in the CNS of macaques with SIVE (155, 213). Abundance of macrophage-tropic variants within the host is necessary, but not sufficient, for development of encephalitis (155, 213) This suggests that either additional viral

determinants or host factors influence the ability of virus to replicate in brain macrophages.

Macaques that exhibit rapid disease progression (391) or low anti-SIV antibody titer one month after infection (268) are more likely to develop encephalitis.

Development of two macaque models that have rapid disease progression are associated with increased incidence of CNS disease (80-90%)(323, 324, 416). One model uses infection of pigtailed macaques with two viral strains that results in immunosuppression and replication in macrophages (416). The second model uses treatment of rhesus macaques with an anti-CD8 antibody at the time of infection resulting in decreased control of viral replication due to depletion of CD8⁺ T cells and NK cells (323, 324). These models suggest innate host factors are important determinants of encephalitis. However, it is still unclear why activated and infected macrophages are abundant in the CNS of only some lentiviral-infected hosts.

Since HIV and SIV can be recovered from the cerebral spinal fluid (CSF) during the acute phase of infection (11, 62, 101, 121, 180, 252, 302, 341), it is possible that virus enters the brain and establishes either a chronic active or a latent infection. Most studies suggest that CNS infection is suppressed while the host has an intact immune response. Both HIV DNA (89, 134, 360) and SIV DNA (66) are present at low levels in brain tissue from asymptomatic individuals. This leaves open the possibility that late stage encephalitis may result from activation of latent CNS virus seeded at the time of primary infection or may result from newly trafficked virus entering the brain within infected macrophages.

It has been reported that the incidence and severity of HIVD (37, 90, 118, 136, 312) and HIVE have decreased since the advent of highly active antiretroviral therapy (HAART) (223). Since HAART is usually not administered during primary infection, a decrease in incidence of HIVE in individuals on HAART suggests that suppression of later plasma viremia decreases the

incidence of encephalitis. Infected macrophages in the brains of HIV- and SIV-encephalitic individuals are predominantly distributed in perivascular areas suggesting recent entry (259, 400). These observations suggest that development of HIVE may be the result of new virus entering the CNS; however, it is unclear whether these recently entered macrophages were infected prior to entering the brain or became infected after entering the brain. Since disruption of the physical blood brain barrier is a late event, cell free plasma virus is unlikely to enter the CNS but rather virus probably enters the CNS within monocytic elements (Trojan Horse Theory) (80, 281). Alternatively, cell free virus may enter the CNS throughout the course of infection or at late stages of infection and only when the immune system fails to curb infection of CNS macrophages does encephalitis develop.

It has been theorized that development of encephalitis may be due to increased trafficking of HIV-infected monocytes. (54, 188) Infection of circulating CD4⁺ T cells has been studied extensively in both HIV and SIV (12, 194, 275), but much less is known regarding infection of circulating monocytes. To begin to understand the role of monocyte infection outside of the CNS during the development of SIVE, it is necessary to longitudinally compare infection of circulating monocytes with the systemic parameters of disease progression and the presence or absence of SIVE at necropsy. We sought to determine whether monocyte/macrophage elements from macaques that develop SIVE harbor more productive infection than macaques that do not develop encephalitis. Using the CD8⁺ T cell-depletion model, we addressed the following questions with the aim to examine the relationship between peripheral SIV infection of macrophages and the development of SIV encephalitis. During the time course of infection do macaques that develop

encephalitis have more circulating infected monocytes or do their monocytes produce more virus after differentiation into macrophages? Is robust macrophage infection unique to the brain or present throughout the body?

3.2.3. Materials and Methods

Animals

Rhesus macaques (*Macaca mulatta*) were housed and maintained according to American Association of Laboratory Animal Care standards. Macaque information is described in table 3. Ten rhesus macaques were treated with CD8 depleting antibody (324) at -3, 0, and 4 days post-infection. Depletion of CD8⁺ T cells was confirmed by flow cytometry. At day 0, macaques were inoculated with SIVDeltaB670 viral swarm by intravenous injection. Macaques were observed daily for clinical signs of anorexia, weight loss, lethargy, or diarrhea. Two of the macaques were humanely sacrificed at two and four weeks post-infection prior to onset of clinical signs. The eight remaining macaques were euthanized upon development of AIDS. A macaque is considered to have AIDS when SIV infection has progressed to the end stage with severely depressed T cell counts and is non-responsive to treatment as determined by clinical observations (e.g. increased body temperature, sustained weight loss of 20% or greater, anorexia, lymphadenopathy and splenomegaly, changes in activity, diarrhea unresponsive to treatment, or opportunistic infections). Animals moribund with AIDS were euthanized. Ages of the macaques ranged from 22 to 46 months (age at time of necropsy). Complete necropsies were performed after humane sacrifice.

Cell counts

Whole peripheral blood samples obtained from SIV-infected macaques at -3, 0, 4, 7, 14 days post-infection and every 2 weeks thereafter were incubated with fluorochrome-conjugated monoclonal antibodies for 30 minutes, 4°C. For CD4⁺ and CD8⁺ T cell count determination: 100-μl of blood was stained with PerCP-conjugated anti-CD4 (clone L200; BD Biosciences Pharmingen, San Diego, CA), fluorescein isothiocyanate (FITC)-conjugated anti-CD3 (clone FN18; Biosource, Camarillo, CA), and phycoerythrin (PE)-conjugated anti-CD8 (clone DK25, DakoCytomation; Carpinteria, CA). For CD4⁺CD29⁺ T cells, 100-μl of blood was stained with PerCP-conjugated anti-CD4, FITC-conjugated anti-CD3, and PE-conjugated anti-CD29 (clone 4B4LDC9LDH8; Beckman Coulter, Hialeah, FL). For monocyte count determination: 100-μl of blood was stained with FITC-conjugated anti-CD14 (clone RM052; Beckman Coulter). Red blood cells were lysed using 2 ml Vitalyse (BioE, Inc., St. Paul, MN), 30 min, room temperature. Cell suspensions were centrifuged and washed with phosphate buffered saline (PBS) containing 4% fetal bovine serum. Cell suspensions were centrifuged and resuspended in PBS containing 1% paraformaldehyde. The percentage of CD8⁺/CD3⁺, CD4⁺/CD3⁺, CD4⁺/CD3⁺/CD29⁺, and CD14⁺ cells was determined on an XL2 flow cytometer (Beckman Coulter). Absolute cell numbers were calculated by multiplying the percentage of cells by the absolute lymphocyte or monocyte counts obtained from blood differential cell counts as previously described (219).

CD8 depletion

The cMT-807 mAb was obtained from Dr. Keith A. Reimann through the National Institutes of Health National Center for Research Resources. Ten rhesus macaques were treated with anti-CD8 monoclonal antibody cM-T807 as previously described (324). Briefly, 3 days before inoculation with SIVDeltaB670, each macaque was administered 10 mg/kg cM-T807 subcutaneously. On day 0 and 4 post-infection, each macaque was administered 5 mg/kg cM-T807 through intravenous injection.

Tissue

Blood samples were obtained immediately pre-infection and on post-infection days 3, 7, 14, 21, 28 and every two weeks thereafter.

CSF draws were attempted every two weeks post-infection. CSF was aliquoted and stored at -80°C .

Brains were removed immediately after euthanasia and processed for analysis. With the exception of M141, who died unexpectedly, all macaques were perfused with saline before necropsy. Regional samples were cut from the left hemisphere, snap-frozen, and stored at -80°C . The right hemisphere was fixed in 10% buffered formalin (Fisher Scientific, Pittsburgh, PA). Coronal sections were made, and tissue blocks were paraffin-embedded. Six- μm sections were made for histopathological analysis.

Portions of liver, lung, small bowel, thymus, spleen, and spinal cord were removed immediately after euthanasia and fixed in 10% buffered formalin. Sections of each organ were made, and tissue blocks were paraffin-embedded. Six- μm sections were made for histopathological analysis.

Histology

To assess each macaque brain for the presence of SIVE, paraffin sections of brain tissue containing neocortical gray and white matter, caudate, putamen, hippocampus, occipital cortex, and cerebellum were stained with hematoxylin and eosin (H&E). SIVE was empirically defined as the presence of microglial nodules, multinucleated giant cells, and profuse perivascular mononuclear infiltrates. The morphological distribution and abundance of macrophage/microglia and SIV-infected cells was assessed using a monoclonal antibody against macrophage/microglia-associated protein CD68 (clone KP1; DakoCytomation) and a polyclonal antibody against the SIV envelope gp110 (generously provided by Dr. Kelly Stefano Cole and Dr. Ron Montelaro, University of Pittsburgh, Pittsburgh, PA), respectively. Three of the ten macaques showed histological findings of SIVE. The remaining seven macaques did not show histopathological features of SIVE. However, some of the macaques showed rare perivascular infiltrates with three of the non-encephalitic macaques showing histological signs of meningitis (Table 3).

Quantitation of SIV RNA in Plasma and CSF

Virions from either 1 ml of plasma or 500 μ l CSF were pelleted by centrifugation at 16,000 x g or 23,586 x g for 1 hour. Total RNA was extracted from the virus pellet using Trizol (Life Technologies, Inc.). Real-time reverse transcriptase (RT)-PCR was performed with 20 μ l of each RNA sample as previously described (28). Primers and probes were specific for the SIV U5/LTR region.

SIV DNA quantitation

PBMC were isolated by density gradient using Ficoll-Paque (Amersham Biosciences, Piscataway, NJ). 10^7 PBMC were incubated with CD14 Microbeads (Miltenyi Biotec, Bergisch Gladbach, Germany). Magnetic separation was performed using MiniMACS Separator with MS Columns (Miltenyi Biotec) according to manufacturer's recommendations. Purified monocytes were obtained from the positive fraction. Purity was evaluated by incubating a portion of the positive fraction with FITC-conjugated anti-human CD14 (clone RM052, Beckman Coulter) and PE-conjugated anti-human CD3 (clone FN18; Biosource) and analyzing using an EPICS XL-2 flow cytometer (Beckman Coulter). Purity ranged from 95-98%. Cells were pelleted at 14,000 rpm for 1 minute and frozen. DNA was isolated from thawed samples using Qiagen DNA Blood Mini Kit (Qiagen, Valencia, CA) and resuspended in 50 μ l of H₂O. The total amount of DNA was measured using the NanoDrop ND-1000 Spectrophotometer (NanoDrop Technologies, Wilmington, DE).

Quantitation of cell-associated DNA was performed by real-time PCR in a Prism 7700 (Applied Biosystems (ABI), Foster City, CA). The PCR reaction was performed in triplicate adding 47 μ l of a PCR master mix containing 5.5 mM MgCl₂, 1X PCR buffer A (ABI), 300 mM of each dNTP, 400 nM of each primer, and 200 nM of probe to 3 μ l of each samples in a 96-well plate. The primers and probe used were described previously (28, 109). To generate a standard curve, serial dilutions of DNA containing the SIV target region, ranging from 10^1 to 10^6 copies/reaction, were subjected to PCR in triplicate along with experimental samples. SIV DNA copy numbers from unknown experimental samples were calculated from the standard curve.

This result was normalized for volume adjustments (# SIV DNA copies/cell), multiplied by the number of circulating monocytes/ml blood as determined by complete blood count and differential, and reported as number of SIV DNA copies from CD14⁺ monocytes/mL blood.

Ex vivo cultures to assess p27 production

PBMC were isolated from whole blood by Ficoll-Paque (Amersham Biosciences). For monocyte-derived macrophage (MDM) cultures, 3×10^6 PBMC were plated in 2-well Lab-Tek Permanox Chamber Slides (Nalge Nunc International, Rochester, NY) in AIM-V media (Invitrogen - Gibco, Carlsbad, CA) supplemented with 20% fetal calf serum (FCS), 10 ng/ml monocyte-colony stimulating factor (Sigma-Aldrich, St. Louis, MO), and 10 ng/ml granulocyte monocyte-colony stimulating factor (Sigma-Aldrich). On day 4 of culture, chamber slides were washed three times with sterile PBS to remove nonadherent cells and maintained in AIM-V supplemented with 20% FCS. Complete media changes were performed at 7, 10 and 14 days post-incubation. Virus production was measured on day 14 supernatants using the SIV Core Antigen ELISA kit (Beckman Coulter) according to manufacturer's recommendations. The MDMs in the chamber slides were washed 3 times with PBS and fixed with 4% paraformaldehyde. In order to assess the purity and infection of MDM cultures, slides were immunofluorescently stained for macrophages as described for formalin fixed paraffin-embedded tissue (28). This affirmed the majority of cells in the culture were MDMs.

For nonadherent cell cultures, 1×10^6 PBMC were added to 12-well plates in RPMI-1640 containing L-Glutamine (Invitrogen – Gibco) supplemented with 10% FCS, 40 U/ml recombinant human interleukin-2 (IL-2) (Roche Diagnostics Corporation, Indianapolis, IN), and 5 µg/ml phytohemagglutinin-L (PHA) (Roche Diagnostics Corporation). On day 4, PHA was

removed by washing the cells in RPMI-1640 containing L-Glutamine supplemented with 10% FCS and 40 U/ml IL-2. Complete media changes were performed at 7, 10 and 14 days post-incubation. Cells were maintained at a concentration of 1×10^6 cells/ml. Virus production was measured on day 14 culture supernatants using the SIV Core Antigen ELISA kit (Beckman Coulter) according to manufacturer's recommendations.

Immunofluorescent Histochemistry

Paraffin sections containing neocortical gray matter, basal ganglia, and hippocampus were stained for macrophage associate lysosomal marker CD68, SIV envelope protein SIVgp110, microtubule-associated protein-2 (MAP-2) (SMI 52; Sternberger Monoclonals Inc., Lutherville, MD), synaptophysin (SY 38; DakoCytomation), or glial fibrillary acidic protein (GFAP) (6F2; DakoCytomation) and detected with fluorogen tags as described previously (28). Double-label immunofluorescence stains using antibodies from the same species were performed using Tyramide Signal Amplification (PerkinElmer Life and Analytical Sciences, Boston, MA) for one of the labels (386).

For triple-label immunofluorescence, double-label immunofluorescence staining without tyramide amplification was performed first followed by incubation with a directly conjugated fluorescent monoclonal antibody. GFAP mouse monoclonal antibodies were conjugated with Alexa Fluor 555 using Zenon Tricolor Mouse IgG₁ Labeling Kit (Molecular Probes, Eugene, OR) according to manufacturer's recommendations. The double- labeled immunofluorescent slides were incubated with the conjugated antibody for 2 hours at room temperature. Slides were washed in 0.5% Tween-20 buffer followed by PBS and fixed in 4% formaldehyde in PBS for 15 minutes at room temperature. Slides were mounted in gelvatol (1).

Double-label immunofluorescence was performed on paraffin sections of liver, lung, small bowel, thymus, spleen, and spinal cord in order to assess the number of SIV-infected T cells and macrophages. Staining of the organs was performed as described for brain. A polyclonal antibody (DakoCytomation) or monoclonal antibody (CD3-12; Abcam, Cambridge, MA) against CD3 was used to visualize T cells. The following monoclonal antibodies against macrophage markers were used in order to determine the identity of SIVgp110⁺ cells that did not co-label with CD68 or CD3: HLA-DR (DK22; DakoCytomation), HAM56 (HAM56; DakoCytomation), and CD163 (Ber-MAC3; DakoCytomation).

Laser Confocal Microscopy Quantification

Quantification of immunofluorescent staining was performed as described previously (28, 158). Regions of macaque brains containing neocortical frontal gray matter, basal ganglia (caudate and putamen), and hippocampus were identified on slides immunofluorescently stained with antibodies to MAP-2, CD68, or synaptophysin. The regions of interest were analyzed by laser confocal microscopy (LSM 510, Zeiss, Jena, Germany). The illumination was provided by Argon (458, 477, 488, 514 nm, 30mW) lasers. Each image was scanned along the z-axis and the middle sectional plane was found (262,144 pixels per plane; 1 pixel, 0.25 μm^2). Digital images were captured and analyzed with LSM 510 3.2 software (Zeiss).

Each brain region from every macaque was randomly scanned by an individual blinded to the status of the macaques in 10 microscopic areas (40X) encompassing 106,100 μm^2 . Scanning parameters such as laser power, aperture, gain and photomultiplier tube settings for each wavelength were kept constant for each macaque specimen. The number of pixels (area) and the intensity of staining (mean fluorescent intensity (MFI)) emitted by each signal were enumerated

using a constant threshold that minimized signal due to autofluorescence. The MFI was multiplied by the area stained to measure the total staining for each label in the scanned area. The total staining value (MFI * area) enumerated from the average of ten scanned areas in a brain region represents a measure of the label in that brain region.

Organ SIV-Infected Cell Counting

Slides with sections of liver, lung, small bowel, thymus, spleen, and spinal cord were immunofluorescently stained with antibodies to CD68 and SIVgp110 or CD3 and SIVgp110. Digital images were captured using the LSM 510 3.2 software (Zeiss). Each organ from every macaque was randomly scanned by an individual blinded to the status of the macaques in 10 microscopic areas (40X) encompassing 106,100 μm^2 . Scanning parameters such as laser power aperture, gain and photomultiplier tube settings for each wavelength were kept constant for each macaque specimen. Three blinded reviewers enumerated the number of double-labeled cells (CD68⁺SIVgp110⁺ or CD3⁺SIVgp110⁺) and single-labeled SIV⁺ cells. The three values from each observer were averaged to represent the number of infected cells in that organ area.

Statistical Analyses

Data were analyzed using PRISM 4.0b software (GraphPad Software, Inc., San Diego, CA). We compared each separate variable in two independent, unpaired groups using two-tailed Mann-Whitney tests for non-parametric independent comparisons with 95% confidence intervals. Data were analyzed comparing macaques with SIVE to macaques without encephalitis at each time point rather than comparing the longitudinal trend within the same group. Since two

macaques were experimentally sacrificed prior to developing symptoms that required humane sacrifice, they were not included in statistical analyses comparing macaques with SIVE to macaques without encephalitis.

3.2.4. Results

CD8 Depletion of SIV-Infected Macaques Led to Rapid Progression and SIVE in Three Macaques.

Table 3 summarizes clinical and pathological data from ten SIV-infected and two non-infected rhesus macaques followed in this study. Two of the ten SIV-infected macaques were sacrificed at pre-determined time points while they were asymptomatic. These macaques were not included in the statistical analysis. The brainstem of one of these macaques (M154) had been accidentally nicked by a needle during a CSF draw. Interestingly, based on immunohistochemical staining, the numerous infiltrating macrophages were not infected with SIV. Inflammation was observed in the choroid plexus of each of the time sacrificed macaques at necropsy. In M152, there were SIV-infected macrophages in the inflamed choroid plexus. The remaining eight macaques were euthanized upon development of clinical AIDS. Three of the eight (38%) macaques developed SIVE (Figure 10). Three other macaques developed meningitis without encephalitis. One macaque (M135) had a mild, focal leukoencephalitis, but this was not classified as SIVE since there were no SIV-infected cells present on immunohistochemical evaluation.

With CD8 depletion, survival time after infection was short for all macaques (range = 56-192 days; mean = 103.4 days; median = 80.5 days). If rapid progression is defined as death from AIDS within 200 days of infection (391), then all eight CD8 depleted macaques were rapid

progressors. The average survival time for macaques that developed SIVE (mean = 71 days; median = 56 days) was shorter than macaques that did not develop SIVE (mean = 122.8 days; median = 81 days), but this was not statistically significant ($P = 0.48$).

Monoclonal antibody against CD8 administered around the time of infection effectively reduced circulating CD8⁺ T cells to ~3% (0-14 days post-infection) and ~15% (21-28 days post-infection) of pre-infection levels (Figure 11b). CD8⁺/CD3⁻ cells were also depleted during this time period (data not shown). Surprisingly, macaques that developed SIVE regained circulating CD8⁺ T cells sooner than macaques that did not develop encephalitis at two weeks post-infection ($P < 0.05$), although they never reached pre-infection levels during the course of infection (Figure 11b). Previous studies treating macaques with the same CD8 depleting antibody or an irrelevant antibody showed preservation of function in other arms of the immune system (323, 324). General immune activation was not observed in non-infected macaques treated with the CD8 depleting antibody. As noted in these previous studies, histological evaluation of lymph node biopsies did not demonstrate evidence of pathological changes associated with antibody treatment.

Peripheral Blood CD4⁺CD29⁺ T Helper Cells Diminished Earlier In Macaques That Developed SIVE.

The average absolute CD4⁺ T cell and monocyte counts between macaques with and without encephalitis were similar (Figure 11a and c). Pre-infection average CD4⁺ T cell counts were lower in macaques that developed SIVE (Figure 11a), but in this small number of animals the difference was not statistically significant. The same trend was observed with average pre-infection CD8⁺ T cell counts (Figure 11b). The peripheral CD4⁺CD29⁺ T cell subset declined

from day 4 to 14 after infection (mean of 24.4% to 3.3%; median of 22.5% to 0%) in macaques that developed encephalitis, while macaques that did not develop encephalitis had a less steep decline (mean of 32.8% to 22%; median of 31.3% to 18.7%) (Figure 11d). The difference in mean percentage of CD4⁺CD29⁺ T cells between macaques that did and did not develop encephalitis approached statistical significance ($P = 0.067$) at 2 weeks post-infection.

Plasma Viremia Was Greater at One and Three Weeks Post-Infection In Macaques That Developed SIVE.

Plasma viremia in all CD8 depleted macaques was high (Figure 12a). In macaques that developed encephalitis, mean/median plasma viremia was 1.5 orders of magnitude higher at 1 and 3 weeks post-infection compared to SIV-infected macaques that did not develop encephalitis ($P < 0.05$). The two macaques that survived for 192 days (M145 and M147) suppressed plasma viremia at six weeks post-infection (1-2 log drop in plasma viremia), while all other macaques exhibited unsuppressed plasma viremia throughout the course of infection.

CSF of Macaques That Developed SIVE Contained More SIV RNA Beginning at Six to Eight Weeks Post-Infection.

CSF viral load was similar in all macaques during the first four weeks after infection (Figure 12b). Between six and eight weeks post-infection, macaques that developed encephalitis showed higher mean/median CSF SIV RNA copies/ml. By eight weeks post-infection, CSF viral loads in macaques that developed SIVE were two orders of magnitude higher than macaques that did not develop encephalitis. Median CSF SIV RNA viral loads were two orders of magnitude higher in macaques that developed SIVE at the time of death (Figure 12c).

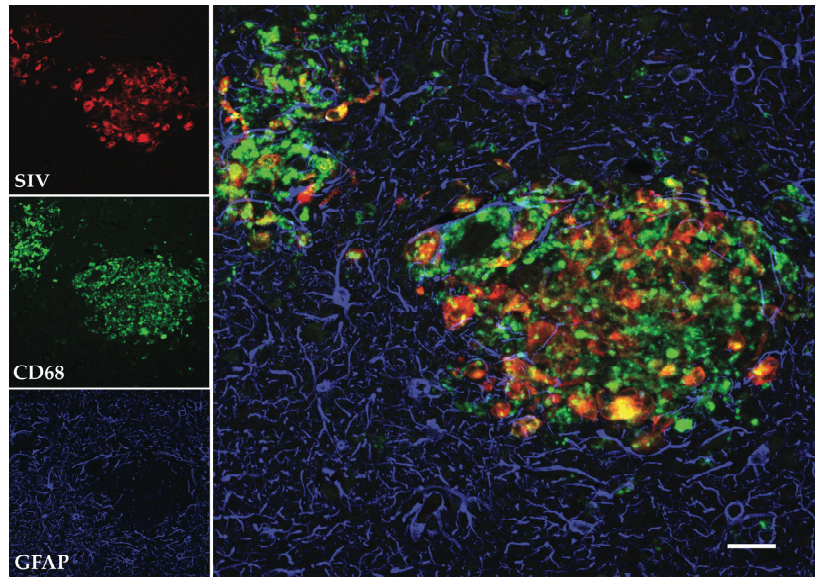


Figure 10. Triple-label immunofluorescent staining for macrophage marker SIV envelope protein (red, Cy5), CD68 (green, Alexa488), and astrocyte marker GFAP (blue, Alexa Fluor 555) shows infected macrophages in a microglial nodule from a CD8⁺ T cell-depleted rhesus macaque with SIVE. Yellow indicates co-localization of CD68 and SIV. Aqua would show co-localization of SIV and GFAP, however no productively infected astrocytes were detected. Scale bar: 20 μ m.

Table 3. Rhesus macaque Age, Sex, Infection Parameters, and Neuropathological and Clinical Diagnosis.

	Monkey Number	Age (mo)	Disease at time of sacrifice	Length of Infection (d) ^{&}	Neuropath Dx	Clinical Dx
SIV encephalitis	M139	34	AIDS	56	SIVE, meningitis, myelitis	SIV open-mouth breathing; anorexia; diarrhea
	M140	46	AIDS	56	SIVE, myelitis	SIV anorexia, diarrhea
	M144	39	AIDS	101	SIVE, myelitis	SIV bloody nose; lethargic; difficulty breathing
SIV without encephalitis	M141	22	AIDS	69	NPC	diarrhea
	M135	34	AIDS	80	leukoencephalitis*, meningitis	scrotal and facial edema
	M158	23	AIDS	81	meningitis	anorexia, diarrhea
	M145	45	AIDS	192	NPC	lymphadenopathy
	M147	41	AIDS	192	NPC	lymphadenopathy
SIV without encephalitis timed sacrifice [%]	M154	32	asymptomatic	16	choroid plexitis	ataxic
	M152	39	asymptomatic	30	meningitis: choroid plexitis	diarrhea
non-infected controls	M405	na	NA	NA	control	NA
	M421	66	NA	NA	control	NA

mo, month; wpi, week post-infection; d, day; NA, not applicable; na, not available; NPC, no pathological changes; Dx, diagnosis

*This monkey had a mild, focal leukoencephalitis that did not contain SIV.

[&] A macaque is considered to have end stages AIDS as determined by clinical observations and T cell subset changes. See Materials and Methods for detailed description.

[%] The two macaques that were sacrificed before developing AIDS were not included in the statistical analyses or displayed in graphs unless noted.

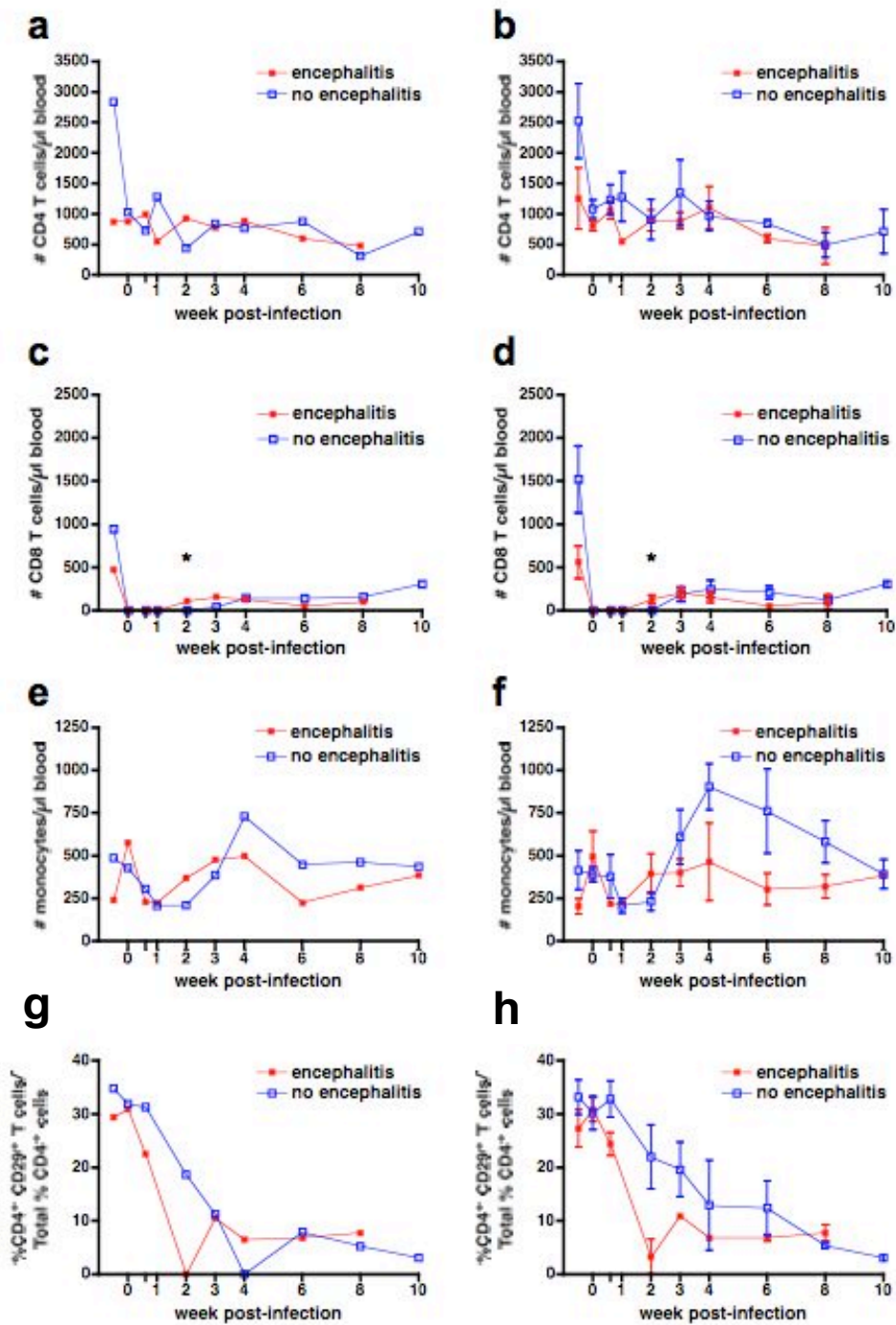


Figure 11. Longitudinal peripheral blood counts for CD4⁺ lymphocytes (a and b), CD8⁺ lymphocytes (c and d), and monocytes (e and f) of eight CD8 depleted rhesus macaques infected with SIV/DeltaB670.

Figure legend continued on next page.

Figure 11 legend continued.

Based on post-mortem histological findings, macaques were retrospectively classified for presence of SIV encephalitis. CD4⁺ and CD8⁺ lymphocyte profiles of animals that did or did not develop encephalitis were similar, however, peripheral blood CD4⁺CD29⁺ T helper lymphocytes (g and h) decreased at two weeks post-infection in macaques that developed encephalitis. Macaques that developed encephalitis had lower average white blood cell count prior to infection or CD8 depletion. **a and b:** Peripheral blood absolute CD4⁺ lymphocyte counts decreased throughout the course of infection. (a) Median peripheral blood absolute CD4⁺ lymphocyte counts for the three macaques with SIVE are shown in **red** and the five macaques without encephalitis are shown in **blue**. (b) Average peripheral blood absolute CD4⁺ lymphocyte counts with standard deviation. **c and d:** Peripheral blood CD8⁺ lymphocytes were suppressed for 2-4 weeks in macaques administered cM-T807 during primary infection. (c) Median peripheral blood absolute CD8⁺ lymphocyte counts for the three macaques with SIVE are shown in **red** and the five macaques without encephalitis are shown in **blue**. The asterisk at day 14 post-infection indicates a statistically significant difference in the peripheral blood absolute CD8⁺ lymphocyte count between macaques with and without encephalitis. *, P<0.05. All other time points are not statistically different. (d) Average peripheral blood absolute CD8⁺ lymphocyte counts with standard deviation. **e and f:** Peripheral blood absolute monocyte counts were not statistically different between macaques with and without encephalitis. (e) Median peripheral blood absolute monocyte counts for the three macaques with SIVE are shown in **red** and the five macaques without encephalitis are shown in **blue**. (f) Average peripheral blood absolute monocyte counts with standard deviation. **g and h:** Peripheral blood CD4⁺CD29⁺ T helper lymphocytes decreased earlier in macaques that developed SIVE. (g) Median percentages of peripheral blood T helper lymphocytes (%CD4⁺CD29⁺/Total % CD4⁺ cells) for the three macaques with SIVE are shown in **red** and the five macaques without encephalitis are shown in **blue**. (h) Average percentages of peripheral blood T helper lymphocytes (%CD4⁺CD29⁺/Total % CD4⁺ cells) with standard deviation.

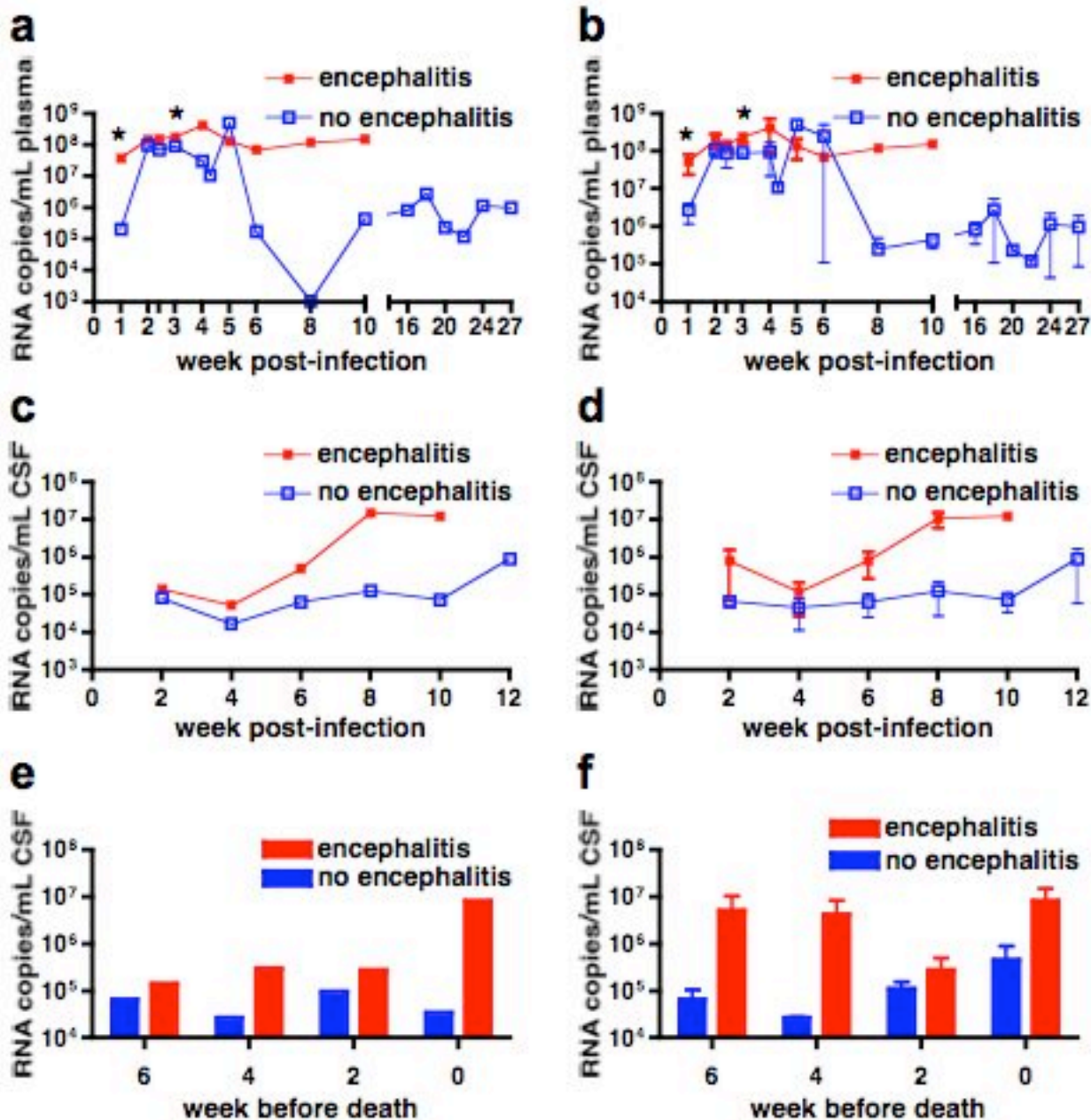


Figure 12. SIV RNA of eight *CD8* depleted rhesus macaques infected with SIV/DeltaB670. Based on necropsy histological findings, macaques were retrospectively classified for presence of SIV encephalitis. Plasma viral load (a-b) in macaques that developed encephalitis was significantly higher at 1 and 3 weeks post-infection compared to macaques that did not develop encephalitis. Between six and eight weeks post-infection, higher CSF viral load (c-f) distinguishes macaques that developed encephalitis from macaques that did not develop encephalitis. **a:** Median longitudinal plasma SIV RNA for the three macaques with SIVE are shown in **red** and the five macaques without encephalitis are shown in **blue**. Plasma SIV RNA of macaques that developed encephalitis was significantly higher than macaques without

Figure legend continues on next page.

Figure 12 legend continued.

encephalitis at one and three weeks post-infection. *, $P < 0.05$. **b**: Average longitudinal plasma SIV RNA with standard deviation. **c**: Median longitudinal CSF SIV RNA for the three macaques with SIVE are shown in **red** and the five macaques without encephalitis are shown in **blue**. CSF SIV RNA of macaques that developed encephalitis was higher than macaques without encephalitis throughout the length of infection, especially during the end stages of infection. Due to unavailable CSF samples, statistical analyses could not be completed for all time points. **d**: Average longitudinal CSF SIV RNA with standard deviation. **e**: Median CSF SIV RNA for macaques with SIVE (**red**) and macaques without encephalitis (**blue**) in weeks before death. Macaques that develop SIVE have more virus in CSF than macaques that do not develop encephalitis in the weeks leading up to death. **f**: Average CSF SIV RNA in weeks before death with standard deviation.

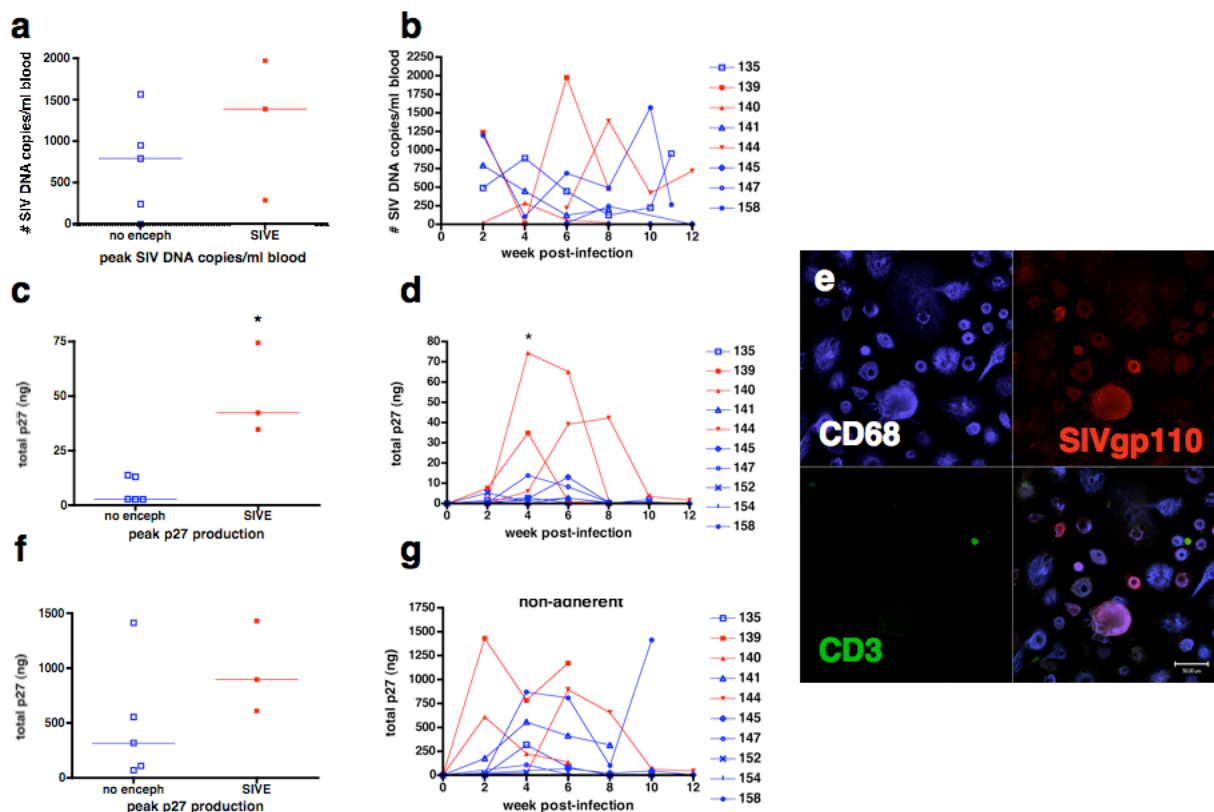


Figure 13. Analysis of blood monocyte SIV DNA and SIV p27 production in MDM and nonadherent PBMC from CD8 T cell-depleted rhesus macaques during SIV/DeltaB670 infection. Based on necropsy histological findings, macaques were retrospectively classified for presence of SIV encephalitis. **a:** Peak number of SIV DNA copies assessed in CD14⁺ blood monocytes. **b:** The number of SIV DNA copies was assessed in CD14⁺ blood monocytes isolated by magnetic bead separation every two weeks post-infection from macaques with SIVE (**red**) and macaques without encephalitis (**blue**). There was a peak in SIV DNA in CD14⁺ monocytes in two of the three macaques with SIVE from 2-8 weeks post-infection and one of five macaques without encephalitis at 2 and 10 weeks post-infection. Regardless of the development of encephalitis, all but one macaque (145) had detectable SIV DNA in CD14⁺ blood monocytes at least one time during infection. **c:** Peak p27 production in MDMs cultured *ex vivo*. **d:** During the course of infection, p27 production of MDMs (adherent PBMC) cultured *ex vivo* for 14 days showed that the three macaques with SIVE (**red**) produce more p27 in culture than the five macaques without encephalitis (**blue**). This graph shows p27 values from MDM of each macaque every two weeks post-infection. SIV p27 production peaked in macaques that developed SIVE for one or two consecutive time points measured between 4-8 weeks post-infection. Average p27 production in MDMs from macaques that developed encephalitis was significantly higher than macaques without encephalitis at four weeks post-infection. *, P<0.05. Since macaques 152 and 154 were experimentally sacrificed, they were not included in statistical analysis. **e:** Representative image of MDM cultures that were assayed for SIV p27 production

Legend continued on next page.

Figure 13 legend continued.

by ELISA. The culture was immunostained for CD68 (upper left, blue, Cy5), SIVgp110 (upper right, red, Cy3), and CD3 (lower left, green, Alexa488) and visualized by triple-label immunofluorescent laser confocal microscopy. An overlay of the three preceding images is shown in the lower right. Purple shows co-localization of MDMs and SIVgp110. Scale: 50 μ m. **f:** Peak p27 production in non-adherent PBMC cultured *ex vivo*. **d:** Longitudinal p27 production of non-adherent PBMC cultured *ex vivo* for 14 days shows that two of three macaques with SIVE (**red**) produce more p27 in culture than the five macaques without encephalitis (**blue**) at week 2 post-infection. Due to unavailable PBMC samples, statistical analyses could not be completed for week 2 post-infection. Since macaques 152 and 154 were experimentally sacrificed, they were not included in statistical analysis.

During the Course of Infection, Monocyte Associated SIV DNA Did Not Distinguish Macaques That Developed SIVE From Those That Did Not Develop Encephalitis.

The infection of monocyte/macrophage elements outside of the brain was compared between macaques that developed SIVE and macaques that did not develop encephalitis. The number of SIV DNA copies associated with CD14⁺ blood monocytes was assessed every two weeks post-infection in each macaque. For all macaques, the number of SIV DNA copies in monocytes varied from 0-1974 SIV DNA copies/ml blood (Figure 13a). One macaque (145) that did not develop encephalitis did not have any detectable monocyte-associated SIV DNA. Two of the three macaques that developed SIVE (139 and 144) had higher numbers of SIV DNA copies in CD14⁺ monocytes at six and eight weeks post-infection than macaques that did not develop SIVE, however one macaque that did not develop encephalitis (158) had comparable monocyte-associated SIV DNA levels as macaques that developed SIVE at two and ten weeks post-infection.

Ex Vivo SIV p27 Production from Monocyte-Derived Macrophages of Macaques That Developed SIVE Was Higher than Macaques That Did Not Develop Encephalitis.

The ability of infected monocytes to replicate virus was assessed *ex vivo*. Cultured monocyte-derived macrophages were monitored for SIV p27 production every other week after infection to assess viral production in each macaque. Adherent peripheral blood MDM of macaques that developed encephalitis produced more p27 *ex vivo* than did MDM of macaques that did not develop encephalitis (Figure 13b and c). This difference was observed within 4-8 weeks of infection. In order to control for potential variability in the number of monocytes plated in each culture, the p27 values were also analyzed by normalizing to the number of input

monocytes. Normalization showed the same trend and statistical differences (data not shown). Figure 13b shows a representative MDM culture used to assess p27 production. Rare non-infected T cells were occasionally observed, however, all infected cells in these cultures were macrophages. Separate non-adherent PBMC cultures were also monitored for viral production. At two weeks post-infection, SIV p27 production in non-adherent PBMC cultures (i.e. cultures with CD4⁺ T cells) was higher in two macaques that developed encephalitis than in macaques that did not develop encephalitis, however, after two weeks there was no difference in PBMC viral production between macaques that did or did not develop encephalitis (Figure 13d).

At Necropsy, Macaques with SIVE Had More SIV-Infected Cells in Small Bowel and Spinal Cord But Less SIV-Infected Cells in Lung and Thymus than Macaques Without Encephalitis.

The number of SIV-infected macrophages and SIV-infected T cells in the liver, lung, small bowel, spinal cord, spleen, and thymus at the time of necropsy were compared between macaques with and without encephalitis. Formalin-fixed paraffin-embedded tissue was fluorescently immunostained for macrophages (CD68), T cells (CD3), and virus (SIVgp110). Three observers enumerated the number of infected macrophages (CD68⁺/SIV⁺ cells), infected T cells (CD3⁺/SIV⁺ cells), and SIV-infected cells that did not co-localize with either CD68 or CD3 (SIV⁺/CD3⁻/CD68⁻ cells). Figure 14 shows representative fields used to enumerate the number of SIV-infected macrophages and CD3⁺ T cells in the spinal cord, lung, and thymus (Figure 15). While many SIV-infected cells in the tissues did not co-label with either CD3 or CD68, of those cells that did double-label for SIV and cell-lineage antigens, macrophages were the most common tissue-based infected cell.

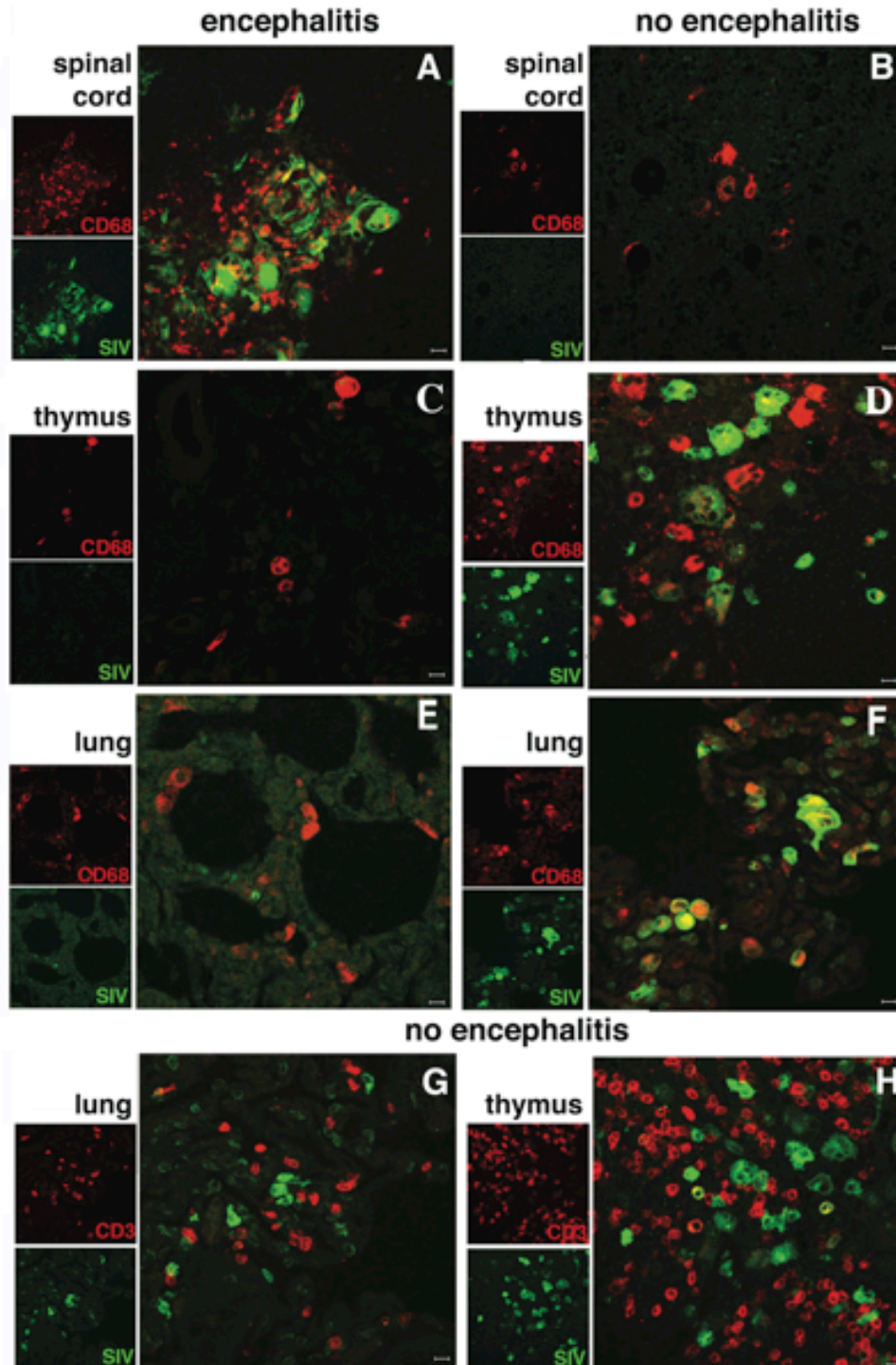


Figure 14. Double-label immunofluorescent staining for macrophage marker CD68 or T cell marker CD3 and SIV envelope protein shows macaques with SIVE have more infected with SIVE macrophages in the spinal cord but less infected macrophages in the thymus and

Legend continued on next page.

Figure 14 legend continued.

lung than macaques without encephalitis. Images such as these were used to count the number of infected macrophages and T cells for tabulation in Figure 15. **A-F:** Small images on the **left** illustrate individual channels for CD68 (red, Cy5) and SIVgp110 (green, Alexa488). The large image on the **right** shows a merged image of the red and green channel with yellow indicating co-localization of CD68 and SIVgp110. **G & H:** Small images on the **left** illustrate individual channels for CD3 (red, Cy5) and SIVgp110 (green, Alexa488). The large image on the **right** shows a merged image of the red and green channel with yellow indicating co-localization of CD3 and SIVgp110. **A** shows a histological section of **spinal cord** from a macaque with SIVE (M139). Macrophages are the predominant SIV-infected cell with rare non-infected T cells. **B** shows a histological section of **spinal cord** from a macaque without encephalitis (M158). Macrophages are less abundant and not infection with SIV. **C and H** show histological sections of **thymus** from a macaque without encephalitis (M135). Some of the infected cells in the thymus of macaques without encephalitis were macrophages, fewer were T cells, but the majority of SIV-infected cells did not co-label with either CD68 or CD3. **D** shows a histological section of **thymus** from a macaque with SIVE (M144). There are few SIV-infected cells and less macrophages than in macaques without encephalitis. **E, F, and G** show histological sections of **lung** from a macaque without encephalitis (M135) (**E and G**) and a macaque with SIVE (M139) (**F**). Some of the infected cells in the lung of macaques without encephalitis were macrophages, but the majority of cells did not co-label with either CD68 or CD3. Macaques with SIVE had few SIV-infected cells in their lungs. Scale bars: 20 μ m.

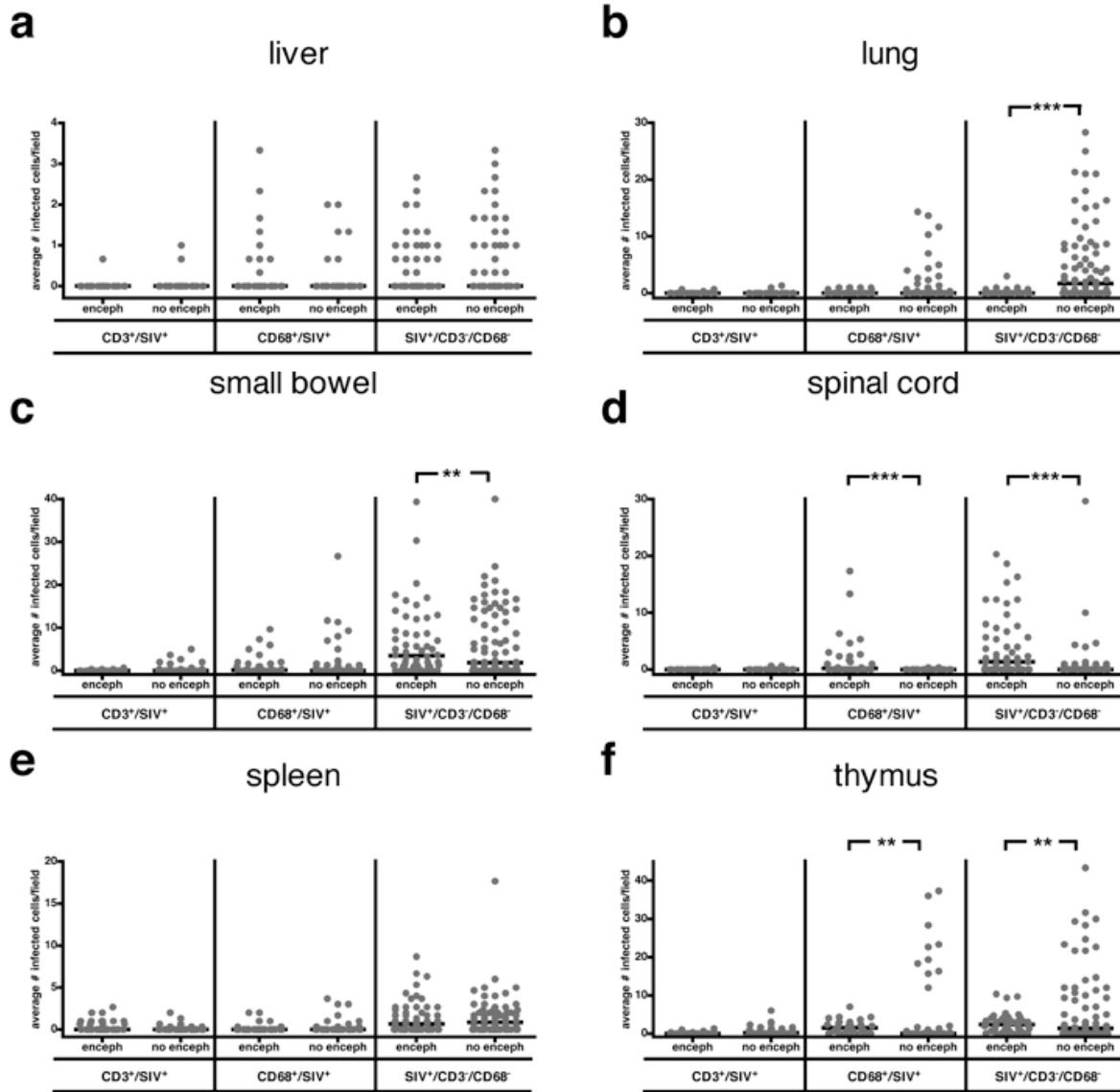


Figure 15. Necropsy survey of the number of infected macrophages and T lymphocytes observed in peripheral organs from eight *CD8* depleted rhesus macaques infected with SIV/DeltaB670. Based on post-mortem histological findings, macaques were retrospectively classified for presence of SIV encephalitis. Each organ was immunostained for both CD3/SIVgp110 and CD68/SIVgp110 and visualized by immunofluorescent confocal microscopy. Three observers enumerated the number of infected macrophages (CD68⁺/SIV⁺ cells), infected T cells (CD3⁺/SIV⁺ cells), and SIV-infected cells that did not co-label with either CD68 or CD3 (SIV⁺/CD3⁻/CD68⁻ cells). The black bars represent the median number of infected cells enumerated for each group (each dot represents the enumeration from an individual field). Macaques with SIVE show more SIV-infected cells in the small bowel and spinal cord but less SIV-infected cells in the lung and thymus than macaques without encephalitis. Many organs have

Legend continued on next page.

Figure 15 legend continued.

SIV-infected cells that do not co-label with CD3 or CD68. Macrophages are the most common SIV-infected cell in these organs. **a: Liver.** Median number of infected T cells and macrophages per field in the liver was similar in macaques with and without encephalitis. **b: Lung.** The median number of infected macrophages and infected cells that did not label with CD68 or CD3 was statistically significantly higher in macaques without encephalitis compared to macaques with SIVE. **c: Small bowel.** Median number of infected cells that did not label with CD3 or CD68 was statistically significantly higher in macaques with SIVE compared to macaques without encephalitis. **d: Spinal cord.** Median number of infected macrophages and infected cells that did not label with CD3 or CD68 was statistically significantly higher in macaques with SIVE compared to macaques without encephalitis. **e: Spleen.** Median number of infected T cells and macrophages per field in the spleen was similar in macaques with and without encephalitis. **f: Thymus.** The median number of infected macrophages and infected cells that did not label with CD3 was statistically significantly higher in macaques without encephalitis compared to macaques with SIVE. *, $P < 0.05$. **, $P < 0.01$. ***, $P < 0.001$.

SIV-infected cells that did not co-label with CD3 or CD68 had a cytomorphology of macrophages with abundant cytoplasm. In an attempt to identify the origin of these cells, we examined sections of lung from a macaque that had several unidentified SIV-infected cells by staining with macrophage markers HLA-DR, HAM56 and CD163 (data not shown). The SIV-infected cells in the lung were mostly located in the stroma (Figure 14E). Of this array of macrophage markers, CD68 identified the most SIV-infected cells; however, as noted above, many SIV-infected cells did not co-label with these markers. Not surprisingly, SIV encephalitic macaques had more abundant SIV-infected cells in the spinal cord than macaques without encephalitis (Figures 14A, 14B and 15d). However, in other organs (i.e. lung and thymus) macaques without encephalitis had more infected cells than encephalitic macaques (Figures 14 C-H, 15b and 15f).

The Number of SIV-Infected Cells in Longitudinal Lymph Node Biopsies Did Not Distinguish Macaques That Developed SIVE From Those That Did Not Develop SIVE.

The number of SIV-infected macrophages and SIV-infected T cells were also enumerated in lymph node biopsies throughout the course of infection. Two of the three macaques that developed SIVE had more CD68⁺/SIV⁺ cells in lymph nodes at six weeks post-infection than macaques that did not develop encephalitis (data not shown). At four weeks after infection, lymph nodes in most macaques had an increase in SIV-infected cells (CD3⁺/SIV⁺ and CD3⁻/CD68⁻/SIV⁺ cells) regardless of development of encephalitis. At death, few SIV-infected cells were present in lymph nodes. Most of these lymph nodes were depleted of cells and involuted.

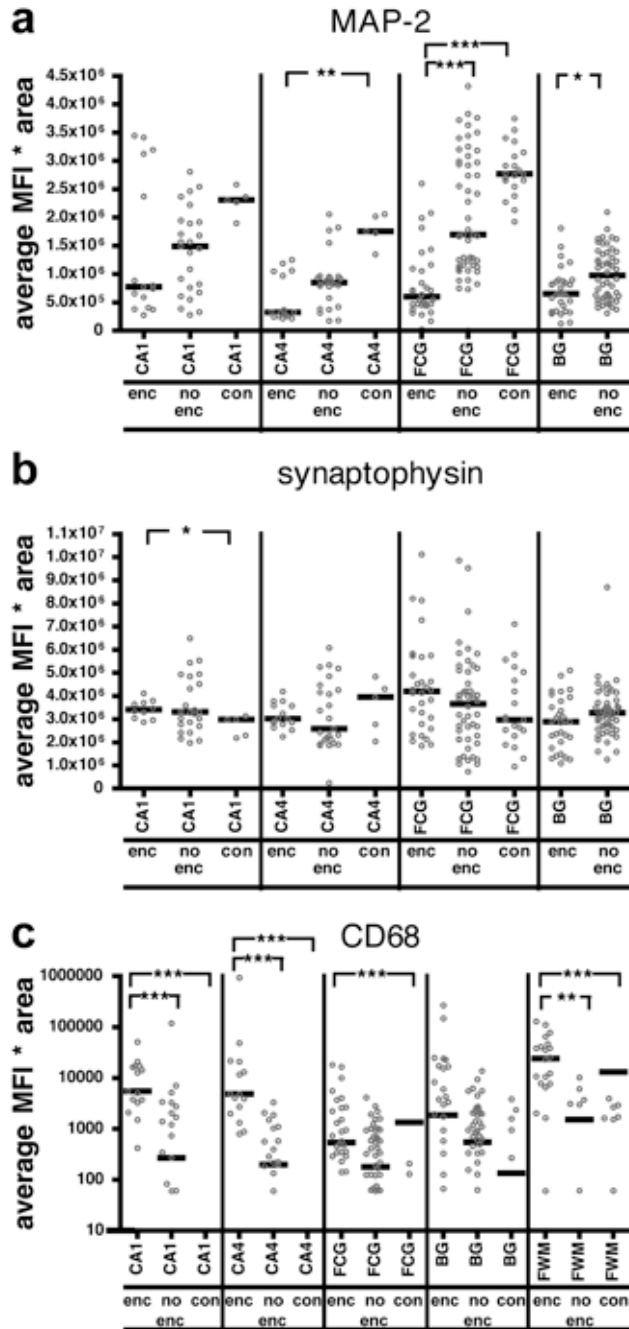


Figure 16. Analysis of post- and presynaptic proteins and macrophages in the brains from eight *CD8* depleted rhesus macaques infected with SIV/DeltaB670 at necropsy. Based on histological findings, macaques were retrospectively classified post-mortem as having SIV encephalitis (enc), without encephalitis (no enc), or non-infected controls (con). Each indicated brain region was immunostained for MAP-2 (a), synaptophysin (b), and CD68 (c) and visualized by immunofluorescent confocal microscopy. Ten microscopic fields in each brain region were quantified for each animal and marker. Mean fluorescent intensity (MFI) multiplied by the number of pixels (area) covered by

Legend continued on next page.

Figure 16 legend continued.

fluorescence was quantified in each brain region using immunofluorescent confocal laser microscopy as described in Materials and Methods. For the basal ganglia region, average MFI and pixels for MAP-2 and synaptophysin were compared to macaques without encephalitis and reported as average MFI * area due to limited availability of basal ganglia tissue from non-infected macaques. The black bars represent the median number of infected cells enumerated for each group, while each dot represents the enumeration from an individual field. Macaques with SIVE showed less postsynaptic protein (MAP-2 staining) but not presynaptic protein (synaptophysin staining) in cortical regions than macaques without encephalitis. Macaques with SIVE showed more CD68 staining in cortical regions than macaques without encephalitis. **a: MAP-2.** MAP-2, post-synaptic protein, staining is decreased in the brains of macaques with SIVE. **b: SYN.** Synaptophysin, pre-synaptic protein, staining is similar in the brains of macaques with and without encephalitis. **c: CD68.** CD68, a macrophage/microglia associated protein, staining is significantly increased in the brain regions of macaques with SIVE. *, $P < 0.05$. **, $P < 0.01$. ***, $P < 0.001$.

Macaques with SIVE Showed More Abundant CD68 Staining in Cortical Regions than Macaques Without Encephalitis.

All brain regions of macaques with SIVE showed increased CD68 macrophage staining compared to non-infected macaques. The greatest fold increase in CD68 staining was seen in the CA1 and CA4 regions of the hippocampus (~11,000- and 10,000-fold, respectively) (Figure 16c). Frontal cortical gray and white matter also exhibited 29- and 25-fold increased CD68 staining respectively, compared to non-infected macaques ($P > 0.001$). Increased CD68 staining was also significantly higher in the hippocampus and frontal cortical gray matter of macaques with SIVE compared to macaques without encephalitis. Macaques with SIVE showed greater CD68 staining in the basal ganglia compared to non-infected macaques, however the increase did not achieve statistical significance.

Macaques with SIVE Showed Less Abundant Postsynaptic Proteins but Not Presynaptic Proteins than Macaques Without Encephalitis.

To determine whether postsynaptic and presynaptic damage was present in CD8 depleted macaques with and without encephalitis, quantification of postsynaptic protein MAP-2 and presynaptic protein synaptophysin (SYN) was performed in gray matter. Average MAP-2 staining in frontal cortical gray matter and basal ganglia was 44 and 57% lower in macaques with SIVE compared to controls ($P < 0.001$ and 0.05 , respectively) (Figure 16a). Average MAP-2 staining in the CA4 region of the hippocampus and frontal cortical gray matter was 69 and 71% lower in macaques with SIVE than non-infected macaques ($P < 0.01$ and $P < 0.001$, respectively) (Figure 16a). Macaques without encephalitis exhibited lower staining for MAP-2 in the CA4

region of the hippocampus and frontal cortical gray matter, but the decrease did not achieve statistical significance. Average presynaptic synaptophysin staining in the CA4 region of the hippocampus, frontal cortical gray matter, and basal ganglia was similar in macaques with and without encephalitis and non-infected macaques (Figure 16b). Macaques with SIVE exhibited a significant increase in synaptophysin staining in the CA1 region of the hippocampus compared to non-infected macaques ($P > 0.05$).

3.2.5. Discussion

Correlates of SIVE.

We examined the development of lentiviral encephalitis using a CD8⁺ T cell-depleted SIV-infected rhesus macaque model. Some previously published correlates of development of lentiviral encephalitis include: elevated CSF viral loads after acute infection (418), rapid disease progression (268, 391), elevated CSF monocyte chemotactic protein (MCP)-1 concentrations (63, 417), and low anti-SIV antibody titer at 1 month after infection (268). It has been proposed that CSF viral loads that exceed 10^6 copies/mL might be a surrogate marker for high viral loads in the brain (397). In this study, we examined the relationship between peripheral SIV infection of monocyte/macrophages and the development of encephalitis with the goal of determining whether macrophage infection is unique to the CNS in animals that develop encephalitis.

Features Distinguishing Macaques That Developed SIVE from Those That Did Not Develop Encephalitis.

MDM from macaques that developed SIVE produced more virus *ex vivo* at 4-8 weeks post-infection. Because the peak viral production of MDM from the three macaques that developed encephalitis occurred at different time points after infection, a statistical difference was only seen at 4 weeks post-infection. Since there are several time points where viral production can be measured from MDM cultures but not from nonadherent PBMC cultures containing lymphocytes, we are confident that the monocytes were not infected in culture by virus derived from peripheral blood lymphocytes. It would be interesting to determine whether development of SIVE is the result of recent entry of infected monocytes that are capable of producing more virus by labeling blood monocytes and following their trafficking. Although there was no observable or statistical difference in SIV p27 production in nonadherent PBMC cultures containing CD4⁺ T cells, SIV production was increased in two of the macaques in the SIVE group at two and six weeks post-infection. This opens the possibility that development of SIVE could be associated with the magnitude of total viral production rather than number of circulating infected monocytes. Differential capability of replicating virus during development of SIVE suggests an inherent difference in the ability of individual host monocytes to become infected and/or to produce virus.

In our study, macaques that developed SIVE had unsuppressed plasma viremia after six weeks of infection and significantly higher plasma viremia at one and three weeks after infection compared to macaques that did not develop SIVE. In the literature, the relationship between high plasma viremia and development of encephalitis is unclear. Some studies have found no correlation between plasma viremia and SIVE (85, 418), while other studies reported 62% of

macaques with elevated antigenemia had SIVE, when only 9% without elevated antigenemia developed SIVE (22). These differences might be attributed to macaque species or differences in evolution of viral strains. For several reasons, we do not believe that the increased plasma viremia is due to increased blood monocyte production of virus. First, although blood monocytes do harbor evidence of multiply spliced mRNA indicating ongoing HIV replication (413), prior to differentiation into macrophages blood monocytes are not active producers of virus *in vitro* (71, 255, 303, 342). Second, although we see increased viral production from adherent cells (macrophages) of macaques with SIVE, the amount of virus the monocytes are producing is unlikely to account for extremely high plasma viremia. Third, activated CD4⁺ T cells found in peripheral tissues and tissue macrophages are thought to be the source of plasma viremia (reviewed in (348)). For two macaques in our study, host ability to suppress plasma viral replication 6-weeks after infection was independent of CD8⁺ T cell reconstitution and predictive of longer survival and protection from developing encephalitis. This suggests there was not complete depletion of tissue CD8⁺ T cells. It is possible that host ability to replicate virus, other arms of the immune system such as antibody responses, or evolution of different genotypic viral strains might be involved in controlling monocyte viral replication. Alternatively, non-CD8-dependent mechanisms might contribute important control of monocyte viral replication and host survival.

CSF viral load was persistently elevated in macaques that developed encephalitis as previously reported by others (85, 418). This highlights a potential difference between the CD8⁺ T cell-depleted rapid progression simian model and human disease. In HIV-infection, virus can be isolated from the CSF during acute infection (179); however, during asymptomatic phases CSF viral load is low. After the development of AIDS, some HIV-infected individuals develop

HIVE associated with increased CSF viral load (62, 233, 397). The persistent elevated CSF viral load and severity of CNS disease observed in CD8⁺ T cell-depleted macaques might indicate SIVE develops at early stages of disease rather than at late stages as seen in humans.

Interestingly, CSF viral load increased during the same time periods after infection (4-8 weeks post-infection) as *ex vivo* production was increased in cultured MDM in macaques that develop SIVE. Further studies are needed to determine if this association is indicative of the time period when encephalitis develops.

Although absolute CD4⁺ T cell counts were not predictors of encephalitis, the CD4⁺CD29⁺ subset of CD4⁺ T cells declined more rapidly in macaques that developed SIVE compared to macaques that did not develop encephalitis. CD4⁺CD29⁺ T cells declined during the same time periods after infection as *ex vivo* production was increased in cultured MDM in macaques that develop SIVE. CD29 (β1 integrin) is part of a heterodimer that binds to vascular cell adhesion molecule-1 (VCAM-1) that is expressed on activated endothelial cells (285). Since expression of CD29 is associated with an activated phenotype (205), macaques that develop encephalitis might selectively lose activated CD4⁺ T cells. Selective loss of this subset of T cells has been shown to be associated with rapid disease progression, another correlate of SIVE (218-220, 329).

Factors Not Distinguishing Macaques That Developed SIVE from Those That Did Not Develop Encephalitis.

In this study, CD8⁺ T cell-depletion at the time of infection led to encephalitis in 38% of the macaques that progressed to AIDS. This percentage is similar to non- CD8⁺ T cell-depleted macaques (22, 391). Williams *et al.* have found a higher incidence of encephalitis in macaques

that remain CD8 depleted for longer than 28 days (399, 401). In our study, CD8⁺ T cells began to reappear in circulation two-three weeks after depletion. We did not monitor the reemergence of NK cells depleted by anti-CD8 antibody treatment. It is possible that other mechanisms of viral suppression (as mentioned above) might be important determinants of encephalitis.

As previous reports (28, 391) have shown no correlation between CD4⁺ T cell count dynamics and development of encephalitis, these CD8⁺ T cell-depleted rhesus macaques also did not show any relationship between total CD4⁺ T cell and monocyte counts and the development of encephalitis.

The number of SIV DNA copies in CD14⁺ blood monocytes was not consistently higher in macaques that developed SIVE compared to macaques that did not develop SIVE. Although two of the three macaques had higher monocyte associated SIV DNA at two time points during infection, one macaque that did not develop SIVE had equivalent monocyte-associated SIV DNA at two other time points. Higher loads of monocyte associated DNA was not associated with increased viral production from *ex vivo* MDM in animals that did not develop SIVE. Williams *et al* observed peak monocyte associated SIV DNA in CD8⁺ T cell-depleted macaques between 7 and 14 days post-infection. (399) Although this analysis did not distinguish macaques with and without encephalitis, it is possible assessing monocyte associated SIV DNA earlier in infection or in subsets of CD14⁺/CD16⁺ cells may better predict development of encephalitis. These data suggest host factors (such as APOBEC family members (211, 408), mutant MCP-1 alleles (130), and TRIM-5alpha(350)) may be more important during the development of encephalitis than the number of circulating infected monocytes.

Unexpectedly we did not observe a clear relationship between systemic macrophage infection and CNS infection. We initially hypothesized that infected macrophages in other solid

organs would correlate with development of encephalitis as reported previously in two animals (87). Since both lentiviral encephalitis and lentiviral pneumonitis are associated with replication in macrophages (14), it is thought that there might be a connection between development of SIV encephalitis and SIV pneumonia. As with previous reports (34), we examined the cell lineage of infected cells in necropsy tissues. In our small study, the lung, thymus and lymph nodes at week six after infection had greater numbers of SIV-infected macrophages in macaques without encephalitis compared to macaques with SIVE. This suggests that development of encephalitis in this model is not associated with a general increase in the number of infected macrophages throughout the body. Few infected CD3⁺ T cells were observed in any organ including secondary lymphoid tissue. This may simply reflect severe depletion of CD4⁺ T cells in tissues at the end stages of disease (276, 308, 381).

A large number of SIV-infected cells that did not co-label with either T cell marker (CD3) or macrophage marker (CD68) were observed in all tissues. It is possible that infected cells might down-regulate cell-lineage proteins, complicating immunodetection. Since many of these infected cells have the morphological appearance of macrophages, an array of antibodies against macrophage proteins was tested to determine if other markers (HLA-DR, HAM56 and CD163) would better identify the lineage of the SIV-infected cells; however CD68 remained the best marker. Interestingly, we do not observe this technical difficulty in tissues from SIV-infected pigtailed macaques (unpublished observations). Because infected cells may assume aberrant morphology, other probes will be needed to identify the lineage of these infected cells.

By chance, the macaque with an accidental needle nick in the brain stem during a routine CSF draw was sacrificed at 16 days post-infection. This animal had 1.9×10^8 RNA

copies/ml plasma. It is remarkable that this three-day old breach in the blood brain barrier did not lead to a robust infection of the infiltrating macrophages. This unplanned experiment implies that some innate immunity is preserved at early stages precluding infection of receptive host cells in the host brain. Although an isolated incident, it hints that development of CNS infection depends upon factors other than blood brain barrier defects, high plasma viremia, and lack of CD8⁺ T cells.

Presynaptic and postsynaptic damage have been reported during HIVE (103, 166, 222, 226, 396). Compared to macaques without encephalitis, macaques with SIVE had significantly lower postsynaptic proteins (MAP-2) in midfrontal cortical gray matter and basal ganglia as we have observed previously (28). Since macaques with encephalitis had short survival times, this suggests that primary postsynaptic damage occurs quickly. Macaques without encephalitis also had decreased MAP-2 staining in hippocampus and frontal cortical gray matter raising the question whether a robust systemic infection may contribute to postsynaptic damage. Staining for presynaptic protein (synaptophysin) was paradoxically increased in the hippocampus and cortical gray matter of macaques with SIVE compared to non-infected macaques. It is possible that presynaptic proteins may increase in SIVE as a temporary response to acute neuronal damage (e.g. perineuronal net disturbance with formation of aberrant synapses (234)).

In this study we focused on the relationship between peripheral SIV infection of monocyte/macrophages and the development of encephalitis. At the same time that CSF viral load increased in macaques that developed encephalitis, we observed that viral replication in MDM from macaques that eventually developed SIVE produced more virus than macaques that did not develop encephalitis independent of CD4⁺ and CD8⁺ T cell counts. However, the number of blood monocyte-associated SIV DNA copies did not distinguish macaques that

developed SIVE from those that did not develop encephalitis. Paradoxically, macaques that did not develop encephalitis had more SIV-infected macrophages in the lungs and thymus than macaques with SIVE. This suggests that there may be inherent differences in the ability of individual host monocytes to become productively infected or produce virus in macaques. Future studies will be needed to elucidate whether monocytes from macaques that develop SIVE have greater susceptibility to be infected, produce virus, or traffic into the brain.

3.2.6. Acknowledgements

We thank Jonette Werley for valuable technical assistance; Dawn L. McClemens-McBride, Premeela Rajakuman, and Afrouz Bazmi for assistance in obtaining clinical data for the macaques; Stephanie Casino and Holly Casamassa for valuable veterinary assistance; Kathleen Morgan for assistance in early surveys of SIV-infected in peripheral organs; and Keith Reimann and the National Cell Culture Center for the CD8-specific Ab (cM-T807) produced with funds provided by NIH grant RR-16001.

3.3. Chapter 3

Manuscript in preparation for publication.

SYSTEMIC MONOCYTE/MACROPHAGE INFECTION IS ASSOCIATED WITH THE DEVELOPMENT OF SIMIAN IMMUNODEFICIENCY VIRUS ENCEPHALITIS IN PIGTAILED MACAQUES

Stephanie J. Bissel,^{*} Guoji Wang,[†] Anita M. Trichel,[§] Michael Murphey-Corb,[§]

Clayton A. Wiley[†]

From the Department of Infectious Diseases and Microbiology,^{*} Graduate School of Public Health and the Departments of Pathology[†] and Molecular Genetics and Biochemistry[§], School of Medicine, University of Pittsburgh, Pittsburgh, Pennsylvania.

3.3.1. Abstract

The brains of individuals with lentiviral-associated encephalitis contain an abundance of infected and activated macrophages. It is hypothesized that encephalitis develops when increased numbers of infected monocytes traffic to the CNS during end stages of immunosuppression. The relationship between development of encephalitis and circulation of infected monocytes and why only a fraction of infected hosts develop lentiviral encephalitis is unknown. We proposed to examine whether monocyte/macrophages from pigtailed macaques that develop simian immunodeficiency virus (SIV) encephalitis (SIVE) contain more replication competent virus than macaques that do not develop SIVE during the course of infection and at necropsy using SIV-infected pigtailed macaques. Compared to macaques that did not develop SIVE, the monocyte associated SIV-DNA load of monocytes and the capability of monocyte-derived macrophages and nonadherent PBMC to produce virus *ex vivo* was increased in macaques that developed SIVE. Macaques with SIVE had more infected macrophages in peripheral organs with the exception of lymph nodes. Brains with SIVE had greater numbers of T cells and NK cells with cytotoxic potential than brains without encephalitis. However, T cell and NK cell infiltration in SIVE was more modest than that observed in classical acute viral encephalitides. These findings support the hypothesis that inherent differences in host monocyte/macrophage viral production are associated with the development of encephalitis.

3.3.2. Introduction

Prior to the era of highly active antiretroviral therapy (HAART), approximately 25% of human immunodeficiency virus (HIV)-infected individuals exhibited the pathological hallmarks of HIV encephalitis (HIVE) at autopsy. These hallmarks are microglial nodules, multinucleated giant cells, and the presence of abundant activated or HIV-infected macrophages (15, 42, 79, 209, 223). As with other HIV-related sequelae since the advent of HAART, the incidence of HIVE is decreasing (137, 190); however, prevalence of HIVE is increasing with one report estimating approximately 45% of AIDS autopsies exhibiting HIVE (190). The pathogenesis of simian immunodeficiency virus (SIV)-infected macaque models is remarkably similar to human HIV infection with a variable percentage of SIV-infected macaques also developing SIV encephalitis (SIVE) with similar pathological changes in the central nervous system (CNS) (22, 75, 155, 213, 333). Both of these lentiviral encephalitides show extensive neuronal damage despite an absence of significant neuronal infection (42, 44, 75, 333). Secreted molecules from abundant activated and infected macrophages are thought to interact directly with neurons or alter supporting glial cell functions to indirectly mediate synaptic damage and subsequent neuronal death (74, 123, 198, 264, 289, 293).

Correlates of lentiviral encephalitis have not been fully identified, and it still remains largely unclear why only a fraction of infected individuals develop encephalitis. Incidence and rate of onset (approximately 6-36 months) vary considerably among different macaque species and with inoculation of different viral strains (22, 75, 415). Virus isolated from the CNS is macrophage-tropic, but inoculation of macaques with macrophage-tropic SIV is not adequate to induce SIVE (155, 213). Retrospective studies show macaques that exhibit rapid disease progression (<6 months) are more likely to develop SIVE (391). Even when inoculated with

identical viral strains, pigtailed macaques develop a greater incidence of SIVE than rhesus macaques (212), while cynomolgus and rhesus macaques of Chinese origin rarely exhibit SIV-related neurologic sequelae. These observations suggest host factors influence the ability of virus to enter the CNS or replicate in CNS macrophages.

The ability to control SIV replication is thought to influence disease progression rates (95, 128, 323, 329, 340, 347, 388) and possibly development of encephalitis (169, 215, 245, 268, 344). Rhesus macaques depleted of CD8⁺ T cells at time of infection fail to reduce acute viremia accompanied by significantly shorter survival times (323). It has been suggested that these macaques have increased incidence of encephalitis (398, 399). Low anti-SIV antibody titers one month after infection are also associated with development of SIVE in pigtailed macaques (268). In the CSF or brain parenchyma of macaques with frequent neurologic symptoms, SIV-specific antibody or antibody-secreting cells are not detected (344). The prevalence of CD8⁺ T cells in the CNS is unclear. Increased numbers of CD8⁺ T cells correlates with CNS impairment or SIVE in SIV-infected rhesus macaques (169, 215). However, rhesus macaques with *gag*-specific CD8⁺ T cells in the CSF had minimal CNS infection (245), however, increased presence of SIV-specific CD8⁺ T cells in the CSF were detected in macaques with slow progression and little neurologic symptoms (344). These data suggest that the ability of CNS macrophages to produce virus or the ability of the immune system to control macrophage viral replication within and outside the CNS influence susceptibility to encephalitis.

Because monocyte/macrophages are the predominant infected cell in the CNS in SIVE and development of SIVE may be due to increased trafficking of SIV-infected monocytes (54, 188), we proposed to determine whether monocyte/macrophages from macaques that develop SIVE harbor more replication competent virus than macaques that do not develop SIVE. Our

previous evidence suggested endogenously infected monocyte-derived macrophages (MDM) from rhesus macaques depleted of CD8⁺ T cells produced more virus than depleted macaques that did not develop encephalitis. Paradoxically, fewer productively infected macrophages were observed in peripheral organs of macaques with SIVE (29). Here, we show that MDM from SIV-infected pigtailed macaques that develop SIVE also produce more virus *ex vivo*, have greater number of SIV-infected monocytes, contain more productively infected macrophages in peripheral organs (but not lymph nodes), and have greater number of activated T cells in the CNS. These findings support the hypothesis that inherent differences in host monocyte/macrophage viral production are related to development of encephalitis.

3.3.3. Materials and Methods

Animals

Pigtailed macaques (*Macaca nemestrina*) were housed and maintained according to American Association of Laboratory Animal Care standards. Macaque information is described in Table 4. Six pigtailed macaques were inoculated with SIVDeltaB670 viral swarm by intravenous injection at day 0. Macaques were observed daily for clinical signs of anorexia, weight loss, lethargy, or diarrhea. Macaques were euthanized upon development of AIDS-like clinical symptoms. Ages of the macaques ranged from 50 to 59 months (age at time of necropsy). Length of infection varied from 83-300 days (median = 128 days). Complete necropsies were performed after humane sacrifice.

Cell counts

Whole peripheral blood samples (100 μ l) obtained from SIV-infected macaques at 0, 7, 14, 21, and 28 days post-infection and every 2 weeks thereafter were stained with fluorochrome-conjugated monoclonal antibodies against CD4 (clone L200; BD Biosciences Pharmingen, San Diego, CA), CD3 (clone FN18; Biosource, Camarillo, CA), and CD8 (clone DK25, DakoCytomation; Carpinteria, CA) for 30 min, 4°C. Red blood cells were lysed using 2 mL Vialyse (BioE, Inc., St. Paul, MN), 30 min, room temperature. Cell suspensions were centrifuged and washed with phosphate-buffered saline (PBS) containing 4% fetal bovine serum. Cell suspensions were centrifuged again and resuspended in PBS containing 1% paraformaldehyde. The percentage of CD8⁺/CD3⁺ and CD4⁺/CD3⁺ cells was determined on an XL2 flow cytometer (Beckman Coulter, Hialeah, FL) within 24 hours of staining. T cells were gated by CD3 fluorescence and side scatter log. At least 10,000 events were analyzed, and the percentage of CD4⁺ and CD8⁺ T cells was determined within the gate. Compensation was done by singly stained peripheral blood mononuclear cells (PBMC) from each animal. Data analysis was performed using FlowJo (Tree Star, Inc., Ashland, OR). Absolute cells numbers were calculated using percentage of cells and differential cell counts from the blood as previously described (219).

Tissue

Blood samples were obtained prior to infection and on post-infection days 7, 14, 21, 28 and every two weeks thereafter.

CSF draws were attempted every two weeks post-infection. CSF was aliquoted and stored at -80°C.

Lymph node biopsies were performed at 2, 4, 12, 16 weeks post-infection and at necropsy under ketamine anesthesia at inguinal or axillary sites. Lymph nodes were fixed in 10% buffered formalin (Fisher Scientific, Pittsburgh, PA) and paraffin-embedded. Six- μ m sections were made for histopathological analysis.

Brains were removed immediately after euthanasia, with the exception of M158 and M159, and processed for analysis. M158 and M159 died unexpectedly and their brains were removed upon discovery. Regional samples were cut from the left hemisphere, snap-frozen, and stored at -80°C . The right hemisphere was fixed in 10% buffered formalin. Coronal sections were made, and tissue blocks were paraffin-embedded. Six- μ m sections were made for histopathological analysis.

Portions of liver, lung, small bowel, thymus, spleen, and spinal cord were removed immediately after euthanasia and fixed in 10% buffered formalin. Samples of these organs were not available for M159. Sections of each organ were made, and tissue blocks were paraffin-embedded. Six- μ m sections were made for histopathological analysis.

Quantitation of SIV RNA in Plasma.

Virions from 1 ml of plasma were pelleted by centrifugation at $16,000 \times g$ or $23,586 \times g$ for 1 hour. Total RNA was extracted from the virus pellet using Trizol (Life Technologies, Inc.). Real-time reverse transcriptase (RT)-PCR was performed with 20 μ l of each RNA sample as previously described (28). Primers and probes were specific for the SIV U5/LTR region.

Histology

To assess each macaque brain for the presence of SIVE, paraffin sections of brain tissue containing neocortical gray and white matter, caudate, putamen, hippocampus, occipital cortex, and cerebellum were stained with hematoxylin and eosin (H&E). SIVE was empirically defined as the presence of microglial nodules, multinucleated giant cells, and profuse perivascular mononuclear infiltrates. The morphological distribution and abundance of macrophage/microglia and SIV-infected cells was assessed using a monoclonal antibody against macrophage/microglia-associated protein CD68 (clone KP1; DakoCytomation) and a polyclonal antibody against the SIV envelope gp110 (generously provided by Dr. Kelly Stefano Cole and Dr. Ron Montelaro, University of Pittsburgh, Pittsburgh, PA), respectively.

Ex vivo cultures to assess p27 production

PBMC were isolated from whole blood by density gradient centrifugation using Lymphocyte Separation Medium (Mediatech, Inc., Herndon, VA). For monocyte-derived macrophage (MDM) cultures, 3×10^6 PBMC were plated in 2-well Lab-Tek Permanox Chamber Slides (Nalge Nunc International, Rochester, NY) in AIM-V media (Invitrogen - Gibco, Carlsbad, CA) supplemented with 20% fetal calf serum (FCS), and 10 ng/ml monocyte-colony stimulating factor (Sigma-Aldrich, St. Louis, MO). On day 4 of culture, cultures were washed three times with sterile PBS to remove nonadherent cells and maintained in AIM-V supplemented with 20% FCS. Complete media changes were performed at 7, 10 and 14 days post-incubation. Virus production was measured on day 14 supernatants using the SIV Core Antigen ELISA kit (Beckman Coulter) according to manufacturer's recommendations. The MDMs in the chamber slides were washed 3 times with PBS and fixed with 4% paraformaldehyde. In order to assess the purity and infection of MDM cultures, slides were

immunofluorescently stained for macrophages (CD68), SIV envelope protein (SIVgp110), and T cells (CD3) as described for formalin-fixed paraffin-embedded tissue (28). This affirmed the majority of cells in the culture were MDMs.

For nonadherent cell cultures, 1×10^6 PBMC were added to 12-well plates in RPMI-1640 with L-Glutamine (Invitrogen – Gibco) supplemented with 10% FCS, 40 U/ml recombinant human interleukin-2 (IL-2) (Roche Diagnostics Corporation, Indianapolis, IN), and 5 $\mu\text{g/ml}$ phytohemagglutinin-L (PHA) (Roche Diagnostics Corporation). On day 4, PHA was removed by washing the cells in RPMI-1640 with L-Glutamine supplemented with 10% FCS and 40 U/ml IL-2. Complete media changes were performed at 7, 10 and 14 days post-incubation. Cells were maintained at a concentration of 1×10^6 cells/ml. Virus production was measured on day 14 culture supernatants using the SIV Core Antigen ELISA kit (Beckman Coulter) according to manufacturer's recommendations.

SIV DNA quantitation

PBMC were isolated by density gradient centrifugation using Lymphocyte Separation Medium (Mediatech, Inc., Herndon, VA). 10^7 PBMC were incubated with CD14 Microbeads (human) (Miltenyi Biotec, Bergisch Gladbach, Germany). Magnetic separation was performed using MiniMACS Separator with MS Columns (Miltenyi Biotec) according to manufacturer's recommendations. Purified monocytes were obtained from the positive fraction. Purity was evaluated by incubating a portion of the positive fraction with FITC-conjugated anti-human CD14 (clone RM052, Beckman Coulter) and PE-conjugated anti-human CD3 (clone FN18; Biosource) and analyzed using an EPICS XL-2 flow cytometer. Purity ranged from 95-98%. The negative fraction was incubated with CD4 Microbeads (human) (Miltenyi Biotec) and

separated using the MiniMACS separation system. Purified CD4⁺ T cells were obtained from the positive fraction and purity evaluated as described for monocyte fraction. Purity ranged from 90-98%. Cells were pelleted at 14,000 rpm for 1 minute and frozen. DNA was isolated from thawed samples using Qiagen DNA Blood Mini Kit (Qiagen, Valencia, CA) and resuspended in 50 μ l of H₂O. The total amount of DNA was measured using the NanoDrop ND-1000 Spectrophotometer (NanoDrop Technologies, Wilmington, DE).

Quantitation of cell-associated DNA was performed by real-time PCR in a Prism 7700 (Applied Biosystems (ABI), Foster City, CA). The PCR reaction was performed in triplicate adding 47 μ l of a PCR master mix containing 5.5 mM MgCl₂, 1X PCR buffer A (ABI), 300 mM of each dNTP, 400 nM of each primer, and 200 nM of probe to 3 μ l of each samples in a 96-well plate. The primers and probe used were described previously (28, 109). To generate a standard curve, serial dilutions of DNA containing the SIV target region, ranging from 10¹ to 10⁶ copies/reaction, were subjected to PCR in triplicate along with experimental samples. SIV DNA copy numbers from unknown experimental samples were calculated from the standard curve. This result was normalized for volume adjustments (# SIV DNA copies/cell), multiplied by the number of circulating monocytes/ml blood as determined by complete blood count and differential, and reported as number of SIV DNA copies from CD14⁺ monocytes/mL blood.

Immunofluorescent Histochemistry

For lymph nodes: Paraffin sections containing biopsy tissue were stained for macrophage associated lysosomal marker CD68 or a polyclonal antibody against CD3 (DakoCytomation) and SIV envelope protein SIVgp110. Double-label immunofluorescent detection was performed with fluorogen tags as described previously (28) in order to assess the number of SIV-infected T cells and macrophages.

For liver, lung, small bowel, thymus, spleen, and spinal cord: Paraffin sections were stained for CD68, SIVgp110, and CD3 in order to assess the number of SIV-infected T cells and macrophages. Triple-label immunofluorescence staining was performed as described previously (28, 386) using Tyramide Signal Amplification (PerkinElmer Life and Analytical Sciences, Boston, MA) for CD68. This was followed by staining for CD3 and SIVgp110.

For brain: Paraffin sections containing midfrontal cortex and basal ganglia were stained for CD3 and TIA-1 (clone 2G9A10F5, Beckman Coulter) in order to assess the number of cytolytic effector cells. Double-label immunofluorescent detection was performed with fluorogen tags as described for lymph node staining.

Counting of SIV-Infected Cells in Organs and Lymph Nodes

Slides with sections of lymph nodes were immunofluorescently stained with antibodies to CD68 and SIVgp110 or CD3 and SIVgp110, while slides with sections of liver, lung, small bowel, thymus, spleen, and spinal cord were immunofluorescently stained with antibodies to CD68, CD3, and SIVgp110. The regions of interest were analyzed by laser confocal microscopy (LSM 510, Zeiss, Jena, Germany). The illumination was provided by Argon (458, 477, 488, 514 nm, 30mW) lasers. Each image was scanned along the z-axis and the middle sectional plane was found (262,144 pixels per plane; 1 pixel, 0.25 μm^2). Digital images were captured and analyzed with LSM 510 3.2 software (Zeiss). Each organ or lymph node from every macaque was randomly scanned by an individual blinded to the status of the macaques in 10 microscopic areas (40X) encompassing 106,100 μm^2 . Scanning parameters such as laser power aperture, gain and photomultiplier tube settings for each wavelength were kept constant for each macaque

specimen. Three or four blinded reviewers enumerated the number of double-labeled cells (CD68⁺SIVgp110⁺ or CD3⁺SIVgp110⁺) and single-labeled SIV⁺ cells. The three or four values from each observer were averaged to represent the number of infected cells in that organ area.

Counting of CD3⁺ and TIA-1⁺ Cells

Slides with sections of midfrontal cortex and basal ganglia were immunofluorescently stained with antibodies to CD3 and TIA-1. The regions of interest were viewed using an epifluorescence microscope (Nikon). Each brain section from every macaque was randomly scanned by an individual blinded to the status of the macaques in 10 microscopic areas (20X) encompassing 212,200 μm^2 . Blinded reviewers enumerated the number of double-labeled cells (CD3⁺TIA-1⁺) and single-labeled cells (CD3⁺ and TIA-1⁺). Values from each observer were averaged to represent the number of cells in the brain.

Statistical Analysis

Data were analyzed using either Microsoft Excel or PRISM 4.0b software (GraphPad Software, Inc., San Diego, CA). We compared each separate variable in two independent, unpaired groups using two-tailed Mann-Whitney tests for non-parametric independent comparisons with 95% confidence intervals. Data were analyzed comparing macaques with SIVE to macaques without encephalitis at each time point rather than comparing the longitudinal trend within the same group.

3.3.4. Results

Four of Six SIV-Infected Pigtailed Macaques Developed Encephalitis.

Six pigtailed macaques were infected with SIVDeltaB670 and followed during the course of infection until clinical symptoms required humane sacrifice. Table 4 summarizes clinical and pathological diagnoses for each macaque. Upon histopathological evaluation, four macaques developed SIVE (67%). One macaque that developed SIVE had concurrent gram-positive bacterial meningitis. Two macaques did not show evidence of SIVE based on immunohistochemical evaluation for SIV-infected cells. One macaque without encephalitis showed acute hypoxic changes in the CA1 region of the hippocampus. The average length of infection for macaques with SIVE was 131 days (median = 128 days; range = 83-185 days) and 191.5 days (median = 191.5 days; range = 83-300 days) for macaques without encephalitis.

CD4⁺ and CD8⁺ T Cells Were Higher During Acute Infection In Macaques That Developed SIVE.

Pre-infection average CD4⁺ and CD8⁺ T cell counts were higher in macaques that developed SIVE compared to SIV-infected macaques that did not develop SIVE (Figures 17a and b) and remained higher until 10 and 18 weeks post-infection for CD4⁺ and CD8⁺ T cells, respectively. In this small number of animals, these differences were not statistically significant. The relative loss of CD4⁺ T cells showed similar trends in both macaques that did and did not develop encephalitis with very few CD4⁺ T cells present at death (Figure 17a).

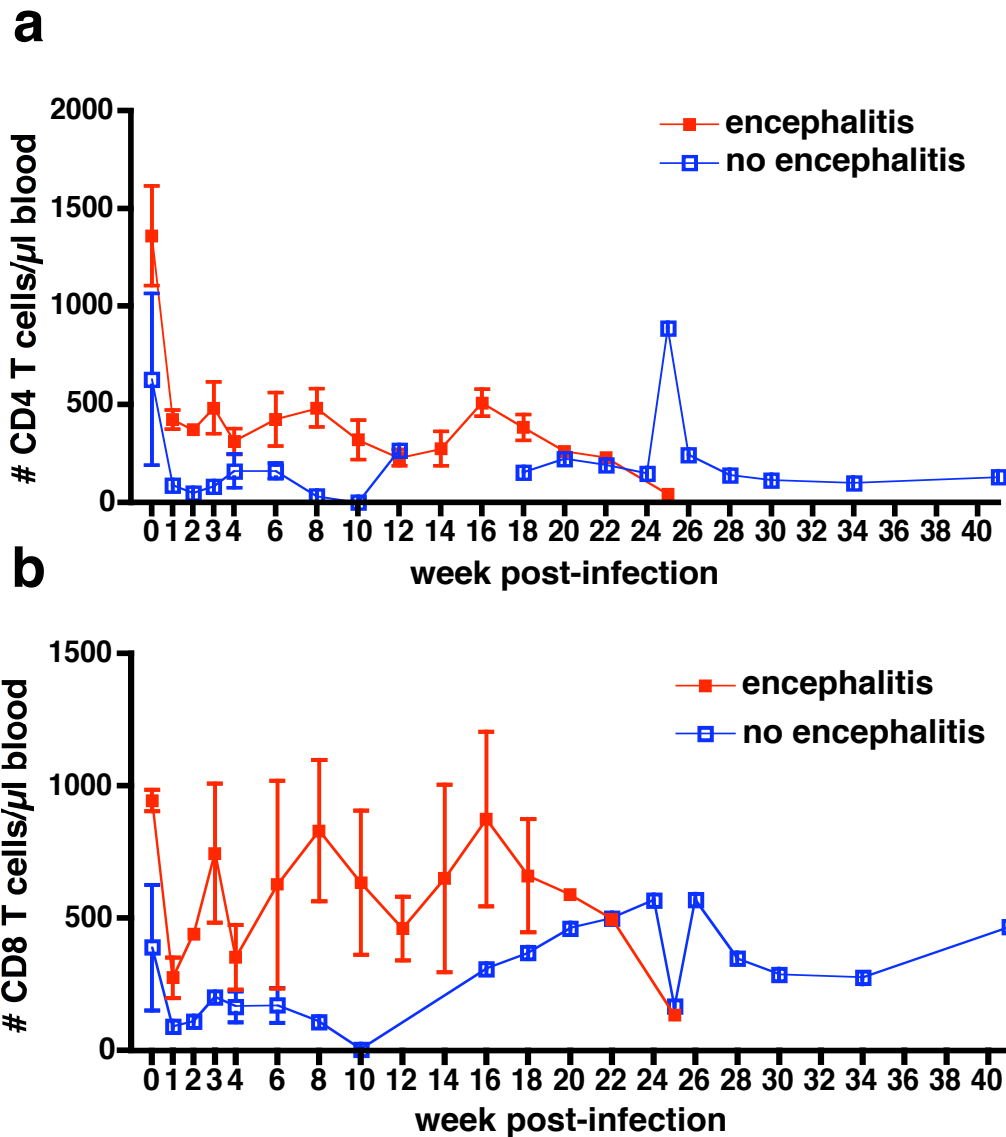


Figure 17. Mean longitudinal peripheral blood counts for CD4⁺ and CD8⁺ T cells of six pigtailed macaques infected with SIV/DeltaB670. Based on histological findings, macaques were retrospectively classified at post-mortem for presence of SIVE. Macaques that developed encephalitis had lower average CD4⁺ and CD8⁺ T cell counts prior to infection and maintained higher average T cell counts. **a:** Mean peripheral blood absolute CD4⁺ T cell counts decreased during the first week post-infection (wpi) and remained decreased for the duration of infection. Macaques that developed SIVE (**red**) had greater average CD4⁺ T cell counts than macaques without encephalitis (**blue**) until 10 wpi. **b:** Mean peripheral blood CD8⁺ T cell counts decreased during the first wpi then made a partial recovery before decreasing again. Macaques that developed SIVE (**red**) had greater average CD8⁺ T cell counts than macaques without encephalitis (**blue**) until 18 wpi.

Table 4. Pigtailed Macaque Age, Sex, Infection Parameters, and Neuropathological and Clinical Diagnosis.

Monkey Number	Age (mo)	Sex	Disease at time of sacrifice	Length of Infection (d)	Neuropath Dx	Clinical Dx
M156	52	m	AIDS	83	normal	Cough, epistaxis, interstitial pneumonia, scrotum & enlarged and necrotic prepuce
M157	50	m	AIDS	137	subacute SIVE with diffuse granulomas, low grade meningitis, poliomyelitis	screaming, orchitis, muscle tics
M158	55	m	AIDS	185	SIV encephalitis, SIV myelitis	died unexpectedly, SIV hepatitis, SIV enteritis
M159	51	m	AIDS	83	SIV encephalitis, severe meningitis (gram-positive bacteria), severe edema with ischemic changes	died unexpectedly, CMV pnemonitis, glomerulosclerosis
M160	52	m	AIDS	300	normal, acute hypoxic changes	hemorrhagic lung, pneumonitis
M161	59	m	AIDS	119	SIV encephalitis, SIV myelitis	ataxia, splenomegaly, severe pneumonia (<i>Pneumocystis carinii</i>)

Plasma Viremia Was Increased From 6-12 Weeks Post-Infection In Macaques That Developed SIVE.

During the first four weeks of infection, both macaques that did and did not develop encephalitis had high plasma viremia (Figures 18a and b). Beginning at six weeks post-infection, mean plasma viremia was approximately 1 order of magnitude higher in macaques that developed SIVE compared to non-encephalitic macaques, but this did not reach statistical significance.

During the Course of Infection, Monocyte-Associated SIV DNA Was Increased At Various Time Points Post-Infection in Three of Four Macaques That Developed SIVE.

In order to compare the viral load of blood monocytes between macaques that did and did not develop SIVE, the number of SIV DNA copies associated with CD14⁺ blood monocytes was assessed at 1, 2, 3, and 4 weeks post-infection and every two weeks thereafter when enough blood was available to isolate the cells. For all macaques, the number of SIV DNA copies in monocytes varied from 0-9823 SIV DNA copies/ml blood (Figure 19a). Three of the macaques that developed SIVE had higher numbers of SIV DNA copies in monocytes at either 2, 4, and 8 weeks post-infection than macaques without SIVE. Monocyte-associated viral loads of macaques that did not develop SIVE were lower than seen in three of the four macaques that developed SIVE.

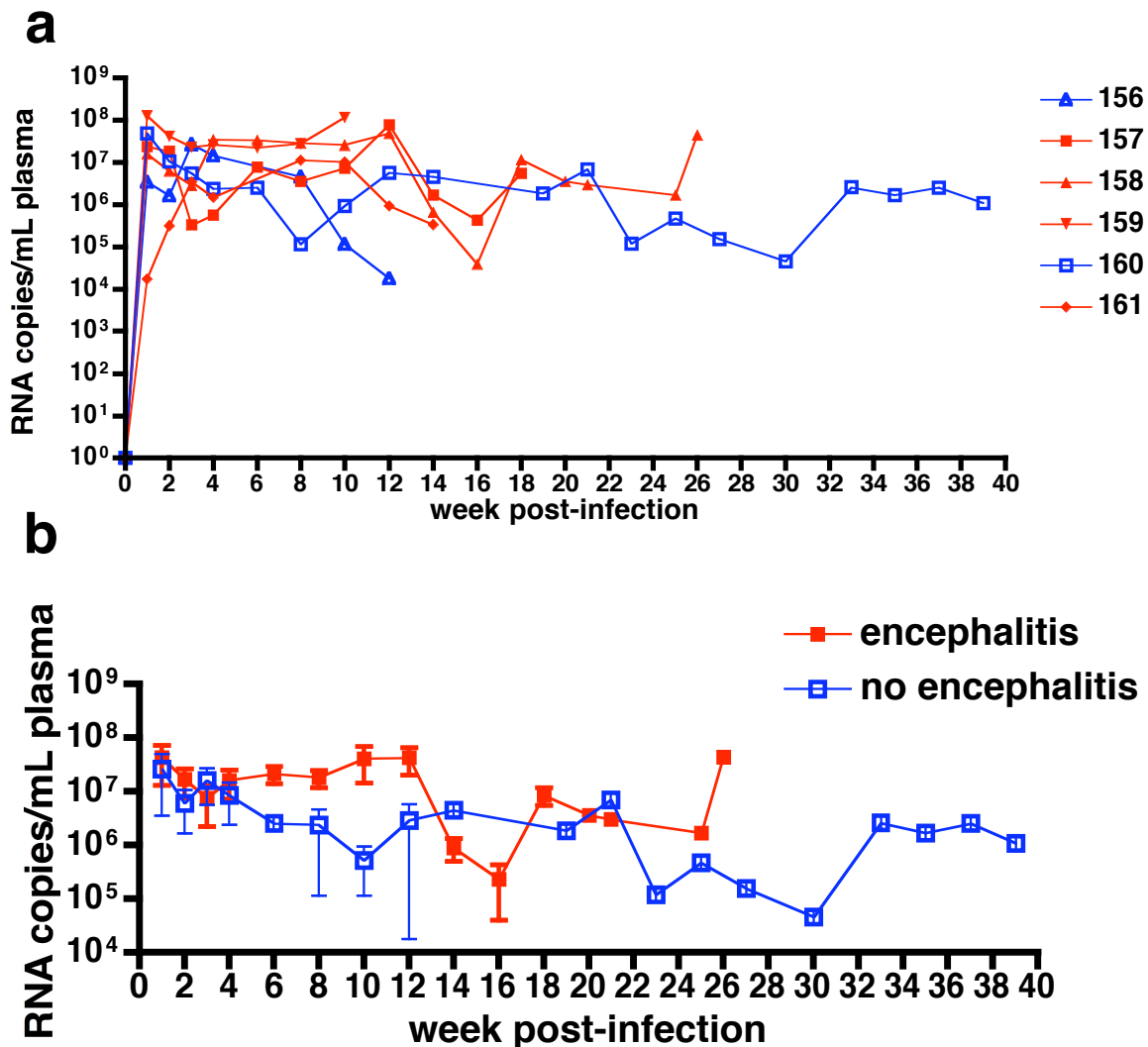


Figure 18. Plasma SIV RNA of six pigtailed macaques infected with SIV/DeltaB670. Based on histological findings, macaques were retrospectively classified at post-mortem for presence of SIV encephalitis. Plasma viral load in macaques that developed encephalitis was higher from 6-12 weeks post-infection compared to macaques that did not develop encephalitis. **a:** Longitudinal plasma SIV RNA for the four macaques with SIVE are shown in **red** and the two macaques without encephalitis are shown in **blue**. **b:** The mean longitudinal plasma SIV RNA for macaques shown in **a**. Plasma viremia was similar for macaques with and without encephalitis during the first four weeks post-infection. From 6-12 weeks post-infection, plasma viremia was higher in macaques that developed encephalitis compared to macaques that did not develop encephalitis.

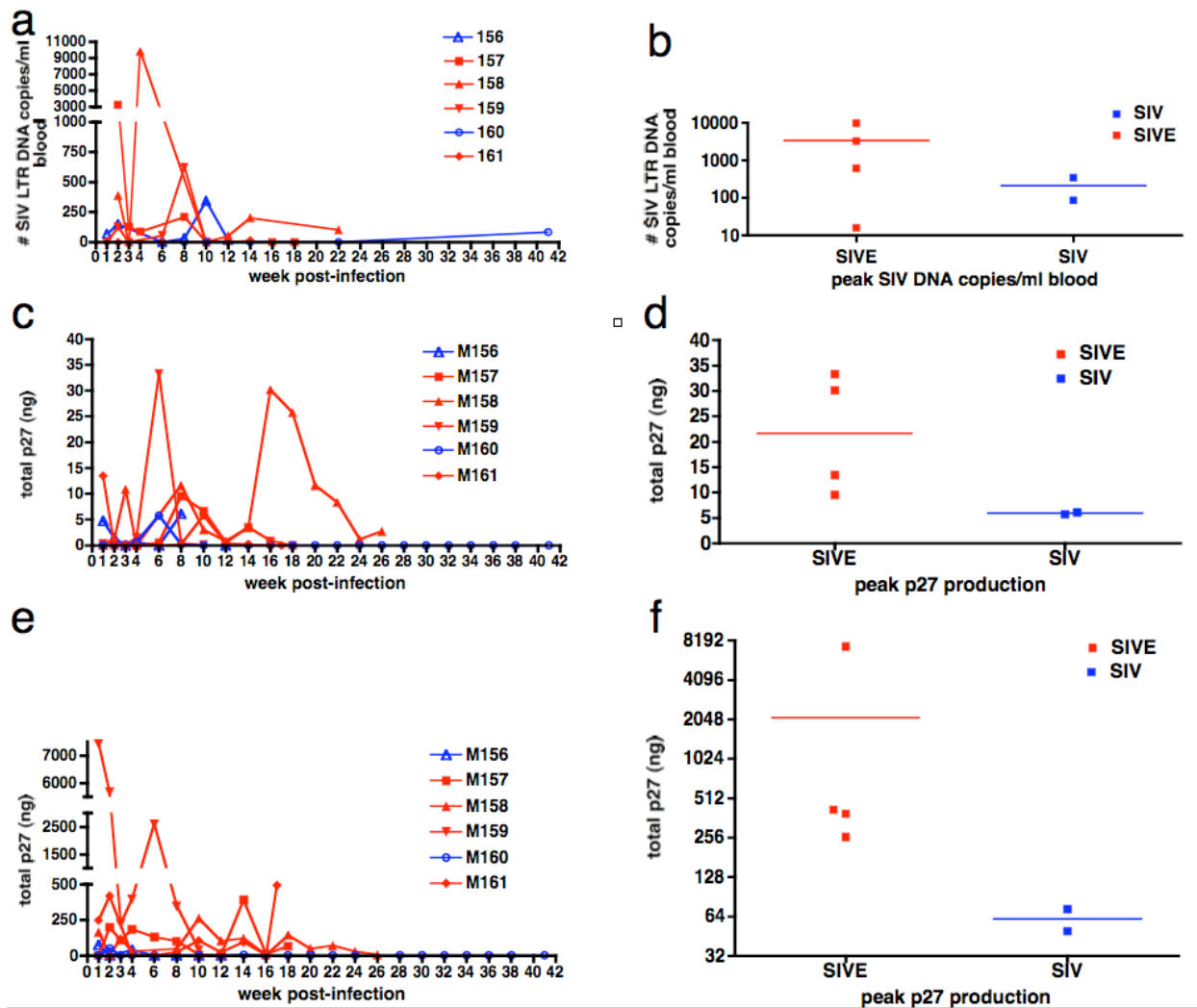


Figure 19. Longitudinal analysis of blood monocyte SIV DNA and SIV p27 production in MDM and nonadherent PBMC from six pigtailed macaques infected with SIV/DeltaB670. Based on necropsy histological findings, macaques were retrospectively classified for presence of SIVE. **a:** The number of SIV DNA copies was higher at various times post-infection in macaques that developed SIVE (**red**) than macaques that did not develop encephalitis (**blue**). The number of SIV DNA copies was assessed in CD14⁺ blood monocytes isolated by magnetic bead separation at 1, 2, 3, 4 weeks post-infection and every two weeks thereafter from macaques with SIVE and macaques without encephalitis. **b:** Peak SIV DNA copies. **c:** At various times during the course of infection, p27 production of MDMs (adherent PBMC) cultured *ex vivo* for 14 days showed that the four macaques that developed SIVE (**red**) produced more p27 in culture than the two macaques without encephalitis (**blue**). MDM from each macaque that developed SIVE had peak *ex vivo* virus production at different times post-infection, mostly within the first eight weeks post-infection. **d:** Peak p27 production from MDMs cultured *ex vivo*. **e:** Longitudinal p27 production of non-adherent PBMC cultured *ex vivo* for 14 days is increased at various times post-infection from the four macaques that developed SIVE (**red**) compared to the two macaques without encephalitis (**blue**). **f:** Peak p27 production from non-adherent PBMC cultured *ex vivo*.

Ex Vivo SIV P27 Production from Monocyte-Derived Macrophages and Nonadherent PBMC of Macaques That Developed SIVE Was Higher than Macaques That Did Not Develop Encephalitis.

The ability of infected monocytes to replicate virus was assessed *ex vivo*. Cultured MDM were monitored for SIV p27 production at 1, 2, 3, and 4 weeks post-infection and every two weeks thereafter when enough blood was available to isolate the cells. Adherent peripheral blood MDM of the four macaques that developed encephalitis produced more p27 *ex vivo* than did MDM of the two SIV-infected macaques that did not develop SIVE (Figure 19b). The time points post-infection that these differences were observed was variable for each macaque. All macaques showed higher *ex vivo* p27 production from MDM within the first eight weeks post-infection. M158 showed peak virus production at 16 weeks post-infection.

Separate non-adherent PBMC cultures were also monitored for viral production. Non-adherent cells were capable of producing more virus than adherent MDM cultures, but there were time points where MDM cultures produced more virus than non-adherent PBMC cultures from the same macaque. Longitudinal p27 production of non-adherent PBMC cultured *ex vivo* for 14 days is increased at various time post-infection from the four macaques that developed SIVE compared to the two SIV-infected macaques that did not develop encephalitis (Figure 19c). As with MDM cultures, the majority of the viral production occurred at earlier time points post-infection.

The numbers of infected cells in lymph nodes from macaques with and without encephalitis are similar.

There were few infected cells in the lymph nodes during the course of infection (Figure 20). The average number of macrophages infected in lymph nodes throughout the course of infection was less than one infected macrophage/field except for M158 at necropsy (average = 4.7 infected macrophage/field). The average number of CD3⁺/SIVgp110⁺ cells was 1-2 infected cells/field at two weeks post-infection and <1 at four, twelve, and sixteen weeks post-infection. There was no distinction between the number of infected cells observed in lymph nodes in macaques that did and did not develop SIVE.

At Necropsy, Macaques with SIVE Had More Productively Infected Macrophages in Liver, Lung, Small Bowel, Spleen, Thymus, and Spinal Cord than Macaques Without Encephalitis.

The number of productively infected macrophages and T cells in the liver, lung, small bowel, spinal cord, spleen, and thymus were compared between macaques with and without SIVE. Formalin-fixed paraffin embedded tissue was fluorescently immunostained for macrophages (CD68), T cells (CD3), and virus (SIVgp110). Four observers enumerated the number of macrophages (CD68⁺/SIV⁺ cells), infected T cells (CD3⁺/SIV⁺ cells), and SIV-infected cells that did not co-localize with either CD68 or CD3 (SIV⁺/CD3⁻/CD68⁻ cells). There were very few cells that did not co-label with either CD3 or CD68 in these tissues (Figure 21). Macrophages were the most common infected cell in lung, small bowel, spleen, and thymus (Figures 21b-f), while similar numbers of macrophages and T cells were infected in the liver (Figure 21a). In all organs examined, the median number of productively infected macrophages was statistically significantly higher in macaques with SIVE compared to SIV-infected

nonencephalitic macaques. The small bowel had the highest number of infected macrophages of all organs examined. The median number of productively infected T cells was statistically significantly higher in liver and spinal cord of macaques with SIVE compared to SIV-infected nonencephalitic macaques (Figures 21a and d) although few infected T cells were observed in the spinal cord.

At Necropsy, Macaques with SIVE Had More CNS T Cells With Cytolytic Potential than Macaques Without Encephalitis.

To begin to examine local immune response to SIV replication in CNS macrophages, the number of CD3⁺ T cells expressing the T cell intracellular antigen 1 (TIA-1) was analyzed in midfrontal cortical and basal ganglia regions of the brain. TIA-1 is a cytoplasmic granule-associated protein expressed in cells with cytolytic potential (10). In the brains of macaques with SIVE, there were statistically significantly more CD3⁺TIA-1⁺ cells than in brains of SIV-infected macaques without SIVE (Figures 22a and 22c). The number of CD3⁺TIA-1⁻ and CD3⁻TIA-1⁺ was also greater in brains of macaques with SIVE, but this did not achieve statistical significance. Compared to SIVE, a human brain exhibiting herpes simplex virus (HSV) encephalitis had a five-fold increase in the number of CD3⁺TIA-1⁺ cells and a 12.8-fold increase in the number of CD3⁺TIA-1⁻ cells. 75% and 66% of CD3⁺ cells co-labeled with TIA-1 in brains of macaques with SIVE and SIV-infected macaques without SIVE, respectively (Figure 22 c and data not shown). Macrophages did not co-label with TIA-1, but TIA-1⁺ cells were adjacent to perivascular cuffs of macrophages in brains of macaques with SIVE.

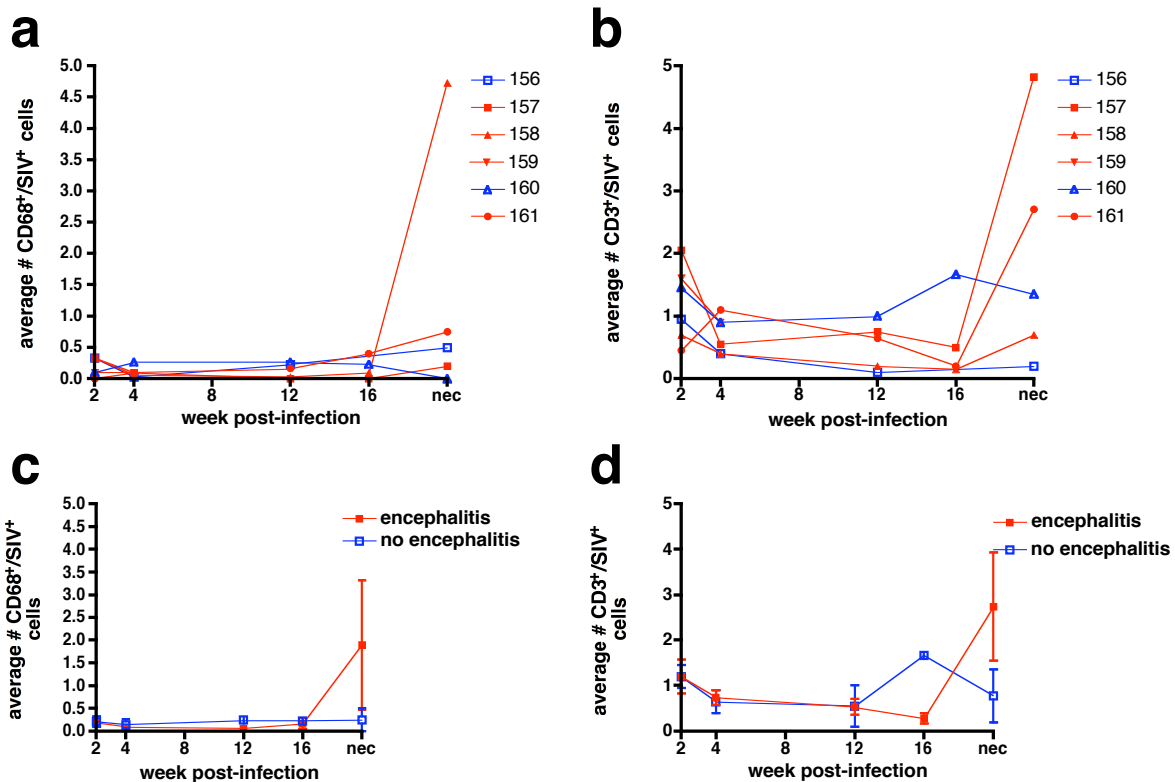


Figure 20. Longitudinal biopsy survey of the number of infected macrophages and T cells observed in lymph nodes from six pigtailed macaques infected with SIV/DeltaB670. Based on histological findings, macaques were retrospectively classified at post-mortem for presence of SIVE. Each lymph node sample was immunostained for both CD3/SIVgp110 and CD68/SIVgp110 and visualized by immunofluorescent confocal microscopy. Three observers enumerated the number of infected macrophages (CD68⁺/SIV⁺ cells) and infected T cells (CD3⁺/SIV⁺ cells). There are few infected cells in the lymph nodes during the course of infection, and there is no distinction between the number of infected cells in lymph nodes from macaques with and without encephalitis. **a:** Average number of infected macrophages per microscopic field for each macaque. Four of five macaques showed slight increases in the number of CD68⁺/SIV⁺ cells at necropsy. Lymph node samples were not available for M159 at 8, 12, 16 weeks post-infection and at necropsy. **b:** Mean number of infected macrophages per microscopic field was similar in macaques with (red) and without encephalitis (blue). **c:** Average number of infected T cells per microscopic field for each macaque. **d:** Mean number of infected T cells per microscopic field was similar in macaques with (red) and without encephalitis (blue).

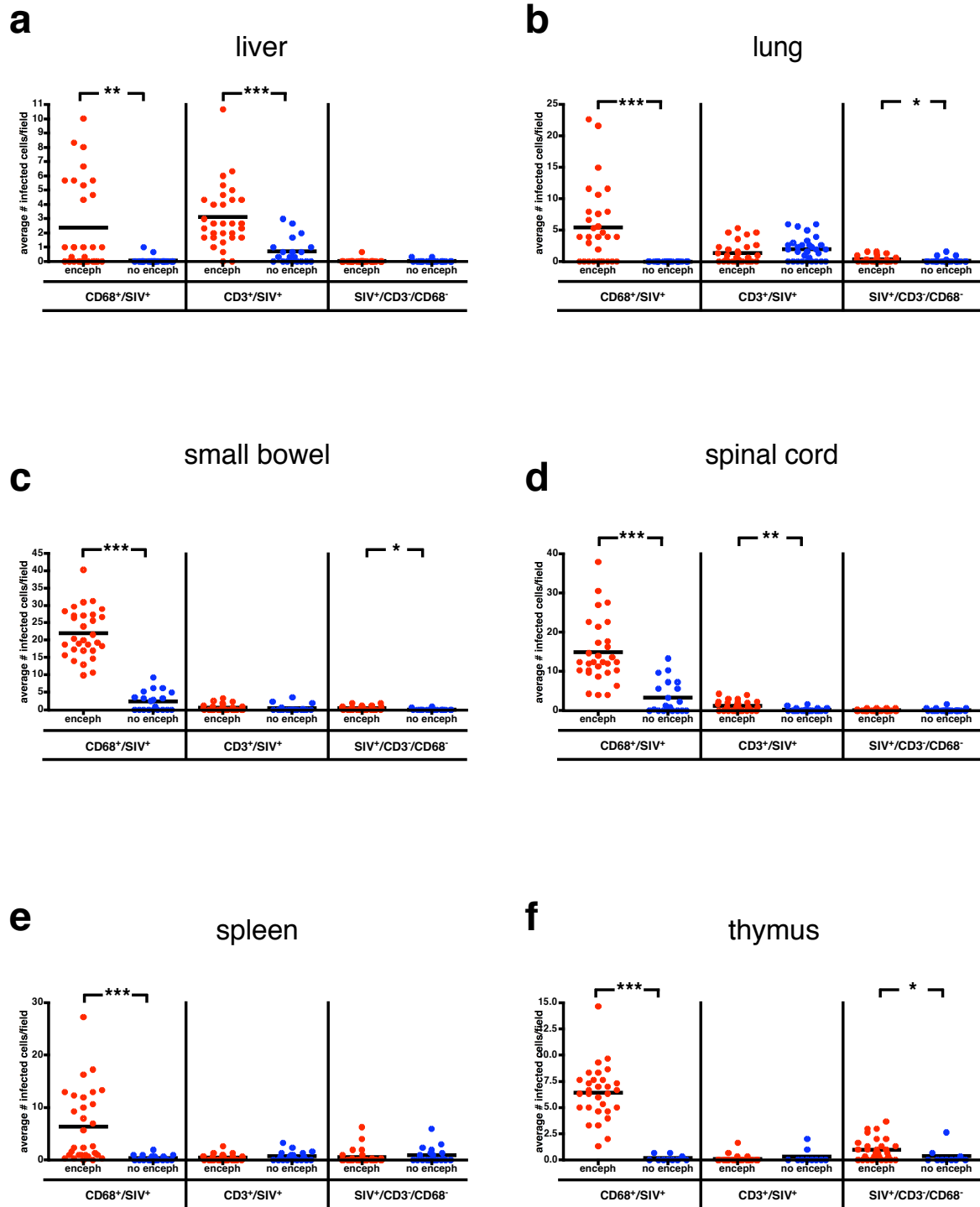


Figure 21. Pigtailed macaques with SIV encephalitis have more infected macrophages in peripheral organs than macaques without encephalitis. Organs obtained at necropsy were immunostained for CD68, CD3, and SIVgp110 and visualized by immunofluorescent confocal microscopy. Four observers

Legend continued on next page.

Figure 21 legend continued.

enumerated the number of infected macrophages ($CD68^+/SIV^+$ cells), infected T cells ($CD3^+/SIV^+$ cells), and SIV-infected cells that did not co-label with either CD68 or CD3 ($SIV^+/CD68^-/CD3^-$ cells). The black bars represent the **median** of infected cells enumerated for each group (each dot represents the enumeration from an individual field). **a and d: Liver and Spinal Cord.** The median of infected macrophages was statistically significantly higher in macaques with SIVE compared to macaques without encephalitis. More infected T cells were also enumerated in macaques with SIVE compared to macaques without encephalitis. Macrophages were the most common SIV-infected cell in the spinal cord. **b, c and f: Lung, Small Bowel and Thymus.** The median number of infected macrophages was statistically significantly higher in macaques with SIVE compared to macaques without encephalitis. A small number of SIV-infected cells that did not co-label with CD68 or CD3 were found in the thymus, small bowel and lung. The small bowel had the highest number of infected macrophages of all organs examined. **e: Spleen.** The median number of infected macrophages was statistically significantly higher in macaques with SIVE compared to macaques without encephalitis. *, $P < 0.05$. **, $P < 0.01$. ***, $P < 0.001$.

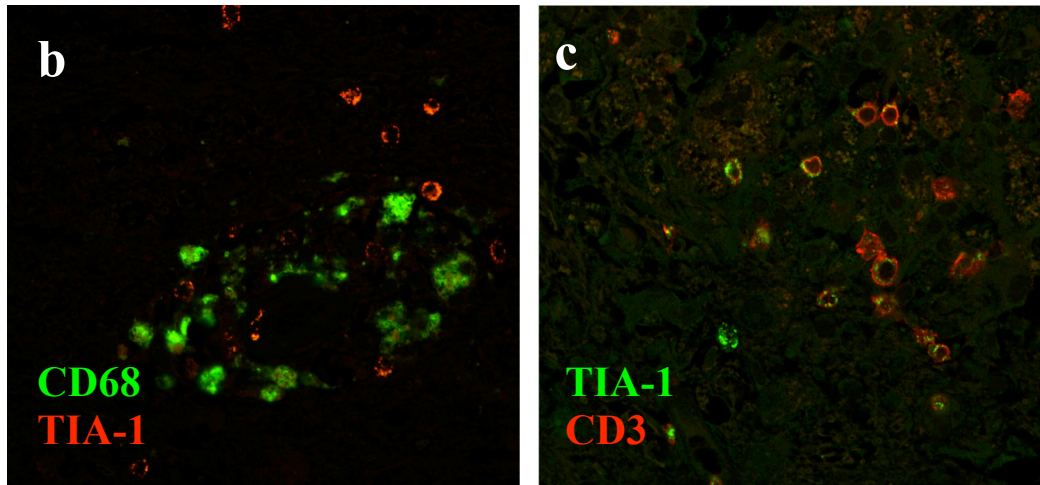
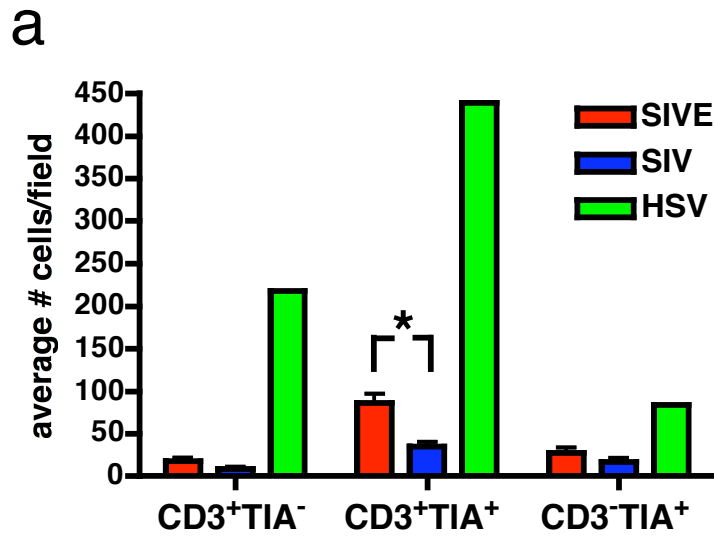


Figure 22. Pigtailed macaques with SIV encephalitis have more CD3⁺TIA-1⁺ cells in the CNS than macaques without encephalitis. For this analysis, we used banked tissue from six macaques with SIVE and six nonencephalitic SIV-infected macaques. Brain tissue obtained at necropsy was immunostained for TIA-1 and CD3 and visualized by immunofluorescent confocal microscopy. Observers enumerated the number of CD3⁺TIA-1⁻ cells, CD3⁺TIA-1⁺ cells, and CD3⁻TIA-1⁺ cells. Human brain tissue obtained from autopsy of a case of herpes simplex virus (HSV) encephalitis was analyzed for comparison. **a:** The number of CD3⁺TIA-1⁺ cells were significantly greater in macaques with SIVE compared to nonencephalitic SIV-infected macaques. However, the number of CD3⁺TIA-1⁺, CD3⁺TIA-1⁻, and CD3⁻TIA-1⁺ cells was more abundant during HSV encephalitis than SIVE. *, *P* < 0.05. **b:** A perivascular cuff containing **macrophages (green, CD68)** abutted by **TIA-1⁺ cells (red)** from a macaque with SIVE. **c:** Most CD3⁺ cells in macaques with SIVE are TIA-1⁺. Cells were stained for **CD3 (red)** and **TIA-1 (green)** with **yellow** indicating co-localization of CD3 and TIA-1.

3.3.5. Discussion

Infection of brain macrophages is the predominant feature of lentiviral encephalitis (15, 42, 79, 209, 223). Infected macrophages can be found in the CNS during acute stages of infection (66); however, productively infected CNS cells during the asymptomatic stage of disease are rare (397). Since not all macaques develop encephalitis upon commencement of immunosuppression, the role these early infected macrophages play in development of encephalitis is not clear. During late stages of immunosuppression, encephalitis is thought to develop when increased numbers of infected monocytes traffic to the CNS (54, 188). It is not known whether macrophage infection is unique to the CNS in animals that develop encephalitis or whether these animals also exhibit abundant blood monocyte and systemic tissue macrophage infection. To begin to determine whether there is an association between systemic and CNS macrophage infection, we analyzed monocyte/macrophage infection during the course of infection in six SIV-infected pigtailed macaques that were retrospectively classified for presence of SIVE.

Monocyte/Macrophage Infection During the Course of Infection

During the course of infection, the viral load of monocytes and their capability to produce virus *ex vivo* was analyzed approximately every two weeks post-infection. Three of the macaques that developed SIVE had higher numbers of SIV DNA copies than the SIV-infected macaques that did not develop SIVE. Each of these three encephalitic macaques had peak monocyte-associated viral load at different time points post-infection indicating there is variability in disease progression even among animals that develop encephalitis. All four

macaques that developed SIVE had MDM that produced more virus *ex vivo* than the SIV-infected macaques that did not develop SIVE. Interestingly, peak monocyte-associated viral loads and peak SIV production from MDM did not temporarily coincide. MDM viral production usually followed 1-2 weeks after peak monocyte-associated viral loads. This suggests that even though infected monocytes are in circulation, they might be poor producers of virus. When MDM are producing high levels of virus, it appears that a few monocytes are capable of producing more virus. These data suggest there are inherent differences in the individual macaque monocytes to harbor virus and to produce virus during the course of infection.

The highest levels of monocyte-associated SIV DNA and SIV production from MDM in macaques that developed SIVE were observed during early or mid stages of infection. It is surprising that peak virus loads and production were not seen at the time points immediately before death when the immune response is ablated. The same trend is seen in the nonadherent PBMC cultures that contain the CD4⁺ T cells. This is most likely due to host cell depletion. As with the *ex vivo* MDM cultures, all four macaques that developed SIVE had nonadherent PBMC that produced more virus *ex vivo* than the SIV-infected macaques that did not develop SIVE. It is not surprising that nonadherent cultures fail to produce virus at end stages of infection since the blood CD4⁺ T cell numbers are drastically reduced. Since MDM produce more virus during earlier stages of infection rather than prior to death, it suggests that ability of cells to produce virus during earlier time points of infection may be more important in the development of encephalitis.

Previously, we analyzed viral load in monocytes and their capability to produce virus *ex vivo* in a group of eight rhesus macaques treated with a CD8⁺ T cell depleting antibody (29). The MDM from the three macaques that developed SIVE in this group also produced more virus

than macaques that did not develop encephalitis; however, the number of blood monocyte-associated SIV DNA copies did not distinguish macaques that developed SIVE from macaques that did not develop encephalitis during the course of infection. Although this could be attributed to species and experimental differences, it suggests that the ability of MDM to produce virus during the course of infection is more tightly associated with the development of SIVE than the number of infected monocytes.

Inguinal or axillary lymph node biopsies at 2, 4, 12, and 16 weeks post-infection were performed to analyze the number of infected macrophages during the course of infection. In both macaques that did and did not develop SIVE, there were few infected macrophages present in lymph nodes at the time points analyzed. More surprising was the small number of infected T cells observed at these time points, less than 2 cells/field. High levels of infected cells are generally seen in lymph nodes of rhesus macaques during asymptomatic infection (300). In this study, the pigtailed macaque lymph nodes might have experienced massive replication and cell death prior to the first lymph node biopsy. This is in agreement with the dramatic decrease in peripheral blood CD4⁺ T cells seen by the first week after infection. Neither macrophage or T cell infection of the lymph nodes correlated with SIVE.

Macrophage Infection At Necropsy

In pigtailed macaques, animals with SIVE exhibit greater numbers of infected macrophages in all peripheral organs (except lymph nodes) than macaques without SIVE. The number of infected T cells was also greater in the liver of the macaques with SIVE than SIV-infected non-encephalitic macaques; however, there are few infected T cells in other peripheral organs at necropsy. This may simply reflect severe depletion of CD4⁺ T cells in tissues at the end stages of

disease (276, 308, 381). It is surprising that the number of infected macrophages in the lymph nodes did not mirror the other organs given that the spleen (another secondary lymphoid tissue) showed abundant macrophage infection in macaques with SIVE. Since most lymph nodes were depleted and involuted by necropsy, it is possible that monocytes were migrating to other organs. This suggests that the ability of pigtailed macaque macrophages to produce virus in the CNS and other organs is related to the development of encephalitis.

Such dramatic differences in macrophage infection in peripheral organs were not observed in the group of eight rhesus macaques treated with a CD8⁺ T cell depleting antibody (29). Paradoxically, in this other model, macaques that developed encephalitis had fewer SIV-infected macrophages in lungs and thymus at postmortem than macaques that did not develop encephalitis. We hypothesized for both species of macaques that infected macrophages in other solid organs would correlate with development of encephalitis. It is possible that rhesus macaques treated with a CD8⁺ T cell depleting antibody have such rapid disease progression that macrophage infection does not have time to develop in every organ. This leaves unexplained why the CNS would be the only organ to show increased macrophage infection in this model.

Immune Response to Macrophage Infection

Although we did not analyze the immune response to peripheral infected monocyte/macrophages during the course of infection, there was no significant difference in the level of CD4⁺ and CD8⁺ T cell decline or plasma viremia between macaques that did and did not develop encephalitis. Macaques that developed SIVE had greater average CD4⁺ and CD8⁺ T cell counts than macaques that did not develop SIVE, but the magnitude of loss of CD4⁺ T cells was similar. Interestingly, the numbers of CD8⁺ T cells in the macaques that develop SIVE

fluctuated greatly during the course of infection even though plasma viremia is similar between macaques that did and did not develop encephalitis. These data confirm other reports that there is no clear relationship between total CD4⁺ T cell or plasma viremia and the development of encephalitis (28, 391).

There are few reports that have examined immune control of viral infected macrophages in humans or macaques with lentiviral encephalitis (95, 169, 335, 340, 347, 388). This is due to lack of reagents to examine the immune response and difficulty in isolating immune cells from autopsy brain tissue. Others have identified and described the distribution of CD8⁺ T cells in association with SIV lesions in the brain (169) and presence of NK cells has been observed by TIA-1 staining (335). We performed a survey of TIA-1⁺ cells in the brain. TIA-1 is a cytoplasmic granule-associated protein expressed in cells with cytolytic potential (10). In macaques with SIVE, the number of T cells with cytotoxic potential was significantly higher than SIV-infected macaques without encephalitis. It is likely that the majority of these cells were CD8⁺ T cells since only a small fraction express TIA-1 and CD4⁺ cells are rare in the brains of macaques with SIVE. There were five times as many T cells with cytolytic potential than T cells that did not co-label with TIA-1. The numbers of NK cells (CD3-TIA-1⁺) in the brains of macaques with SIVE were also increased compared to macaques without SIVE. Presence of T cells and NK cells with cytolytic potential in brains with SIVE indicates that development of SIVE induces an immune response to control CNS viral infection that is not present in the CNS of macaques without SIVE. This suggests that during asymptomatic phases of infection there is insufficient viral production locally in the CNS to induce a substantial immune response. In the future, it will be necessary to determine whether the local CNS immune response during

asymptomatic infection or in animals that do not develop SIVE is sufficient to contain viral production or whether development of encephalitis is determined by factors outside of the CNS.

Comparison of T cells and NK cells with cytolytic potential found in the CNS of macaques with SIVE compared to humans with HSV encephalitis shows that other viral encephalitides induce a much greater local T cell response than SIVE. This was also observed in human brains with West Nile Virus encephalitis (data not shown). These classical acute encephalitides have viral infected neurons, and frequently affect older and immunosuppressed individuals. It will be interesting to determine why the immune responses differ in magnitude in these different encephalitides.

In this study we examined on the relationship between peripheral SIV infection of monocyte/macrophages and the development of encephalitis and the presence of cells with cytolytic potential in macaques with SIVE. Compared to macaques that did not develop SIVE, the monocyte associated SIV-DNA load of monocytes and the capability of MDM and nonadherent PBMC to produce virus *ex vivo* was increased in macaques that developed SIVE. Macaques with SIVE had more infected macrophages in peripheral organs with the important exception of lymph nodes. Brains from encephalitic macaques had more T cells and NK cells with cytotoxic potential than brains from non-encephalitic macaques; however, there were far fewer activated immune cells in SIVE compared to classic acute HSV encephalitis. These results suggest that the inherent differences in host viral production by monocyte/macrophages and T cells during the course of infection and macrophages at the end stages of infection are associated with the development of encephalitis. Future studies will determine what host factors account for these inherent differences and why SIVE does not induce as strong of an immune cell infiltrate as other encephalitides.

3.3.6. Acknowledgements

We thank Gokul Kandala, Jonette Werley and Jessica Garver for valuable technical assistance; Dawn L. McClemens-McBride and Premeela Rajakuman for assistance in obtaining clinical data for the macaques; Holly Casamassa for valuable veterinary assistance.

3.4. Chapter 4

Manuscript in preparation for publication.

LONGITUDINAL ANALYSIS OF ACTIVATION MARKERS ON MONOCYTE SUBSETS DURING THE DEVELOPMENT OF SIMIAN IMMUNODEFICIENCY VIRUS ENCEPHALITIS

Stephanie J. Bissel,^{*} Guoji Wang,[†] Anita M. Trichel,[§] Michael Murphey-Corb,[§]

Clayton A. Wiley[†]

From the Department of Infectious Diseases and Microbiology,^{*} Graduate School of
Public Health and the Departments of Pathology[†] and Molecular Genetics and
Biochemistry[§], School of Medicine, University of Pittsburgh, Pittsburgh,
Pennsylvania.

3.4.1. Abstract

Twenty-five percent of HIV-infected patients develop a clinical syndrome known as HIV-associated dementia (HAD) that is associated with lentiviral encephalitis. Since lentiviral encephalitis has been hypothesized to be associated with monocytes that have the capacity to migrate into the brain, we have prospectively analyzed the percent expression and mean fluorescent intensity of a panel of phenotypic activation markers on CD14^{hi} and CD14^{lo} monocytes from SIV-infected macaques that did or did not develop encephalitis. CD16, CCR5, CD69, HLA-DR, CD62L, CD40, CD64, and CD163 expression were analyzed every two weeks after infection. CD14^{hi}/CD16⁺ and CD14^{lo}/CD16^{hi} monocytes were expanded during acute infection and at various time points during the course of infection; however, this expansion was not unique or greater in macaques that developed encephalitis. The proportion of monocytes that expressed CD62L, HLA-DR, CD16, CD64, and CD40 were either higher or lower in macaques that developed encephalitis at single time points during the course of infection. However, none of the tested phenotypic markers predicted development of encephalitis. Taken together, these results suggest that changes in the proportion of circulating activated monocytes do not directly determine development of encephalitis, but this does not rule out the importance of activated monocytes in the development of encephalitis.

3.4.2. Introduction

Twenty-five percent of HIV-infected patients develop a clinical syndrome known as HIV-associated dementia (HAD) (6, 36, 61, 77, 90, 232). In the absence of opportunistic infections, HIV encephalitis (HIVE) is the pathological correlate of HAD. Within the central nervous system (CNS), the predominant infected cell in HIVE is the macrophage (104, 138, 238, 296, 392). Although virus can be detected in the CNS soon after infection (80), dementia and encephalitis develop late in disease when the patient is severely immunosuppressed (36). Development of encephalitis is thought to be the result of activated infected blood monocytes trafficking into the CNS.

By migrating from blood into tissue, monocytes differentiate into macrophages (377). While trafficking of activated T cells into the CNS has been studied in a variety of diseases, much less is known about monocyte trafficking. Migration of activated T cells is directed by tissue specific chemokines and integrin receptors (97). T cells found in CSF express CXCR3, CCR5, and CCR6 (172), and inflammatory chemokine CXCR3 is thought to be involved in T cell accumulation in the CNS (366). Little is known about the normal turnover of CNS macrophages (microglia) (402) or how this might be augmented during disease (151).

It is reasonable to speculate that migration of activated monocytes is regulated by expression of integrins such as LFA-1 and VLA-4 and chemokine receptors. Monocytes integrins adhere to endothelial cell adhesion molecules ICAM-1 and VCAM-1 in order to migrate into tissue (153, 330). It is largely unknown how monocytes cross the brain endothelium, but it is believed that that VLA-4/VCAM and PECAM/PECAM interactions are important in facilitating transmigration (60, 235, 263, 318, 384). Monocyte $\alpha 4 \beta 1$ integrin and endothelial VCAM-1 interactions are thought to be necessary for transmigration into the CNS

during SIV encephalitis (318). Recent reports indicate that monocytes express high amounts of monocyte chemotactic protein-1 receptor CCR2 (162). Upon differentiation into macrophages, CCR2 expression progressively decreases and CCR1 and CCR5 expression progressively increases (162). In multiple sclerosis, reports suggest CCR1⁺/CCR5⁺/CD14⁺ cells are the sub-population of monocytes able to enter the inflamed CNS (365). CCR1 is thought to play an integral role in the migration of monocytes into CNS (366).

Blood monocytes can be defined on the basis of CD14 and CD16 expression with CD14⁺⁺CD16⁻ monocytes as the major population and CD14⁺CD16⁺ monocytes as the minor population (414). Cross-linking of immunoglobulin receptors expressed on monocytes is thought to either inhibit or activate monocytes. Binding of FcγRIIb inhibits monocytes while activation of FcγRIIa, FcγRI (CD64), and FcγRIII (CD16) activates monocytes (67, 119, 368). Activation of monocytes by CD16 binding IgG immune complexes initiates cellular responses such as phagocytosis, antibody-dependent cellular cytotoxicity, and release of inflammatory molecules such as cytokines (119).

It has been shown that CD14⁺CD16⁺ cells are expanded during pro-inflammatory conditions such as infectious diseases (414), including bacterial infections (161), and other disorders such as patients with coronary artery disease (322), rheumatoid arthritis (164), acute Kawasaki disease (161), and asthma (304). This minor monocyte population is also increased within minutes after exercising (111). HIV-infected patients also have increased percentage of CD14/CD16 cells (94, 362), and patients with HAD have increased proportion of CD14⁺CD16⁺ and CD14⁺CD69⁺ blood monocytes (183, 295).

Since lentiviral infection of the brain has been hypothesized to be associated with augmented monocyte migration into the CNS and an increased proportion of blood monocytes that express CD16 and CD69 has been reported during HAD, we prospectively analyzed the percent expression and mean fluorescent intensity (MFI) of a panel of phenotypic markers on CD14⁺ monocytes during disease progression using a primate model. Blood monocytes from SIV-infected macaques that did or did not develop encephalitis were retrospectively analyzed for CD16, CCR5, CD69, HLA-DR, CD62L, CD40, CD64, and CD163 expression. We hypothesized that blood monocytes from macaques that developed encephalitis would have increased proportion of cells expressing these activation markers compared to macaques that would not develop encephalitis during the course of infection.

3.4.3. Materials and Methods

Monkeys and blood

Six male pigtailed macaques (*Macaca nemestrina*) were inoculated intravenously with the viral swarm SIVDeltaB670. Whole blood was collected from each monkey in heparinized tubes once weekly through the first month of infection and every two weeks thereafter. Activity, stool consistency, appetite, and general condition were observed daily. Physical examinations were performed at each blood draw. Examinations consisted of body temperature and weight measurements, palpation and size grading of lymph nodes and spleen, abdominal palpation, and assessment of general condition. Macaques were provided full supportive care and humanely euthanized when they became non-responsive to treatment. The presence of SIV encephalitis was determined for each macaque brain by assessing hematoxylin and eosin stained brain sections for the presence of microglial nodules, multinucleated giant cells, and profuse

perivascular infiltrates followed by immunohistochemical detection of macrophages (CD68; clone KP1; DakoCytomation) and SIV gp110 (generously provided by Dr. Kelly Stefano Cole and Dr. Ron Montelaro, University of Pittsburgh, Pittsburgh, PA). (28)

Preparation of peripheral blood monocytes for flow cytometry

100 μ L whole heparinized blood was incubated with fluorescein isothiocyanate (FITC)-conjugated anti-CD14, clone RM052 (Beckman Coulter, Hialeah, FL), phycoerythrin (PE)-Cy5-conjugated anti-CD16, clone 3G8 (Beckman Coulter), and one of the following: PE-conjugated anti-human CCR5, clone 3A9 (BD PharMingen, San Diego, CA), CD69, clone TP1.55.3 (Beckman Coulter), HLA-DR, clone G46-6 (BD PharMingen), CD62L, clone SK11 (BD PharMingen), CD64, clone 22 (Beckman Coulter), CD40, clone MAB89 (Beckman Coulter), CD163, clone GHI/61 (BD PharMingen) for 30 min, 4°C. Red blood cells were lysed using 2 mL Vitalyse (BioE, Inc., St. Paul, MN), 30 min, room temperature. Cell suspensions were centrifuged and washed with phosphate-buffered saline (PBS) containing 4% fetal bovine serum. Cell suspensions were centrifuged again and resuspended in PBS containing 1% paraformaldehyde.

Flow cytometric and statistical analysis

Cells were analyzed with an EPICS XL-2 flow cytometer (Beckman Coulter) within 24 hours of staining. At least 100,000 total events per sample were collected. Monocytes were gated by CD14 fluorescence and side scatter log (SS Log). Proper compensation was set by singly stained PBMC from each animal. Data analysis and graphic representations were

performed using FlowJo (Tree Star, Inc., Ashland, OR). The percent marker expression of CD14⁺ cells was derived by the number of events in the upper right (CD14⁺ double positives) quadrant.

Statistical analysis of the difference in the percent expression and mean fluorescent intensity (MFI) of activation markers on CD14^{hi} or CD14^{lo} cells between macaques that did or did not develop SIVE was performed using Student's T tests (Microsoft Excel, version 11.1.1, Redmond, WA). Mean percentage expression and MFI is displayed as mean \pm SEM. Statistical analysis of the difference between the proportions of CD14/CD16 subsets from all six macaques at baseline vs. time of infection was performed using paired Student's T tests (Prism, version 4.0b, GraphPad Software, Inc., San Diego, CA). Changes in the mean percentage of CD14/CD16 subsets as a function of duration of infection were estimated using a linear regression analysis (Prism). $P < 0.05$ was considered to be statistically significant.

3.4.4. Results

CD14 expression on pigtailed macaques monocytes can be divided into two subsets.

Based on side-scatter log and CD14 expression, monocytes can be classified as CD14^{hi} or CD14^{lo} (Figure 23). Each of these monocyte subsets was followed every two weeks throughout the course of SIV infection in six pigtailed macaques and analyzed for percentage expression and mean fluorescent intensity of a panel of activation markers. A description of each activation marker is listed in Table 5. Phenotypic changes in monocyte subsets were evaluated retrospectively in macaques that developed SIVE and compared to macaques that did not develop encephalitis.

Table 5. Description of activation markers analyzed on monocyte subsets during the course of SIV infection.

Phenotypic Marker	Other names	Ligand/ Receptor	Description and Function of Marker	Expression changes in disease states
CCR5	CD195	RANTES, MIP-1 α , MIP-1 β , HIV	β -chemokine receptor. Co-receptor for HIV and SIV entry (86). Involved in regulation of lymphocyte and phagocyte transendothelial migration to sites of inflammation and lymphocyte chemotaxis (126, 297).	Increased expression on CD14 ⁺ blood monocytes in patients with multiple sclerosis (221) and on CD4 ⁺ T cells in HIV ⁺ patients (269). Increased frequency of blood CD8 ⁺ T cells in early SIV infection (244).
CD69	Activation Inducer Molecule (AIM), EA 1, MLR3, gp34/28		Early activation marker. Pluripotent signaling molecule thought to be involved in cell aggregation, cytotoxicity, and release of cytokines (52, 248, 361).	Increased expression on CD14 ⁺ blood monocytes in patients with HAD (183, 295) and Alzheimer's Disease (184).
HLA-DR			MHC class II molecule. Found on antigen presenting cells and activated T cells.	Decreased expression on monocytes from patients with systemic lupus erythematosus (254), Hodgkin's disease (253), and acute pancreatitis (409). Increased expression on monocytes from patients in recent chronic phase of <i>Trypanosoma cruzi</i> infection (319).
CD62L	LECAM-1, L-selectin, LAM-1	CD34, GlyCAM-1, M	Involved in binding to High Endothelial Venules or peripheral lymphoid tissue (112) and in leukocyte rolling on activated endothelium (307). It is also a peripheral lymph node homing receptor (46).	Increased expression on monocytes from patients with diabetes type II (379) and PBMC from patients with rheumatoid arthritis (182).
CD40	Bp50	CD40 ligand	Involved in development of cell-mediated immune responses and control of thymus-dependent humoral immunity. Promotes cytokine production. Rescues cell from apoptosis. Involved in B cell growth, differentiation, and isotype switching. (reviewed in (19))	Increased expression on monocytes after <i>in vitro</i> treatment with interferon- β (214).
CD64	Fc γ RI	IgG	High affinity receptor for IgG. Involved in antigen capture for presentation to T cells, antibody dependent cell-mediated cytotoxicity, and receptor mediated endocytosis of IgG-antigen complexes (119).	Decreased expression on monocytes from patients with acute hemolytic uremic syndrome (106) and Bordetella pertussis infection (147). Increased expression on monocytes from patients with hemoglobin H disease.

Table continued on next page.

Table 5 continued.

CD163	Scavenger receptor, M130, GHI/61, RM3/1	Hemoglobin-haptoglobin complex	Scavenger receptor for hemoglobin-haptoglobin complexes. Expression increases as monocytes mature into macrophages (45).	Increased on patients who underwent coronary artery bypass graft surgery. (127)
CD16	FcγRIIIa	Aggregated IgG	Low-affinity receptor for IgG (119).	Increased proportion or expansion of CD14 ⁺ blood monocytes in patients with HIV (94, 362), SIV (272), HAD (183, 295), hemolytic uremic syndrome (35), bacterial infections (161), asthma (304), rheumatoid arthritis (164), acute Kawasaki Disease (161), sarcoidosis (270), liver cirrhosis (274).

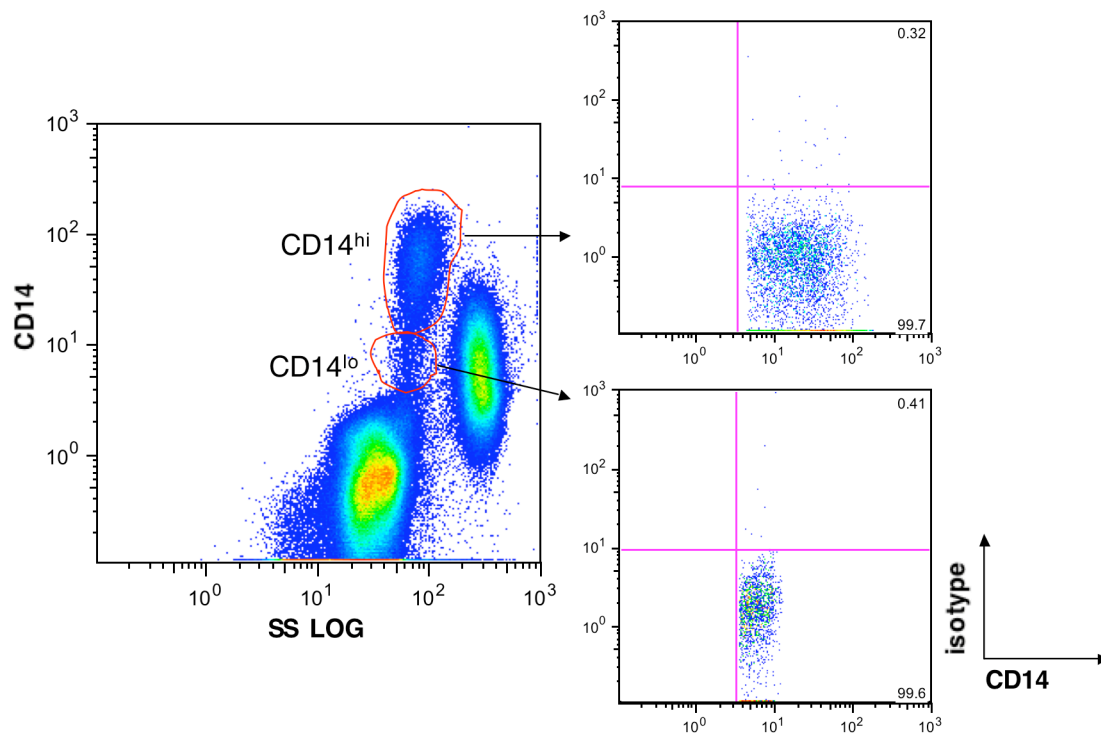


Figure 23. CD14 expression on monocytes can be divided into two subsets. Whole blood was stained with anti-CD14 and one of the antibodies listed in Table 1. Based on CD14 expression and side-scatter log characteristics, monocytes can be divided into a CD14^{hi} and CD14^{lo} subsets. Each of these gated populations was monitored for changes in expression of phenotypic markers (Table 1) throughout the course of disease in 6 SIV-infected pigtailed macaques. Isotype controls from CD14^{hi} and CD14^{lo} subsets are shown.

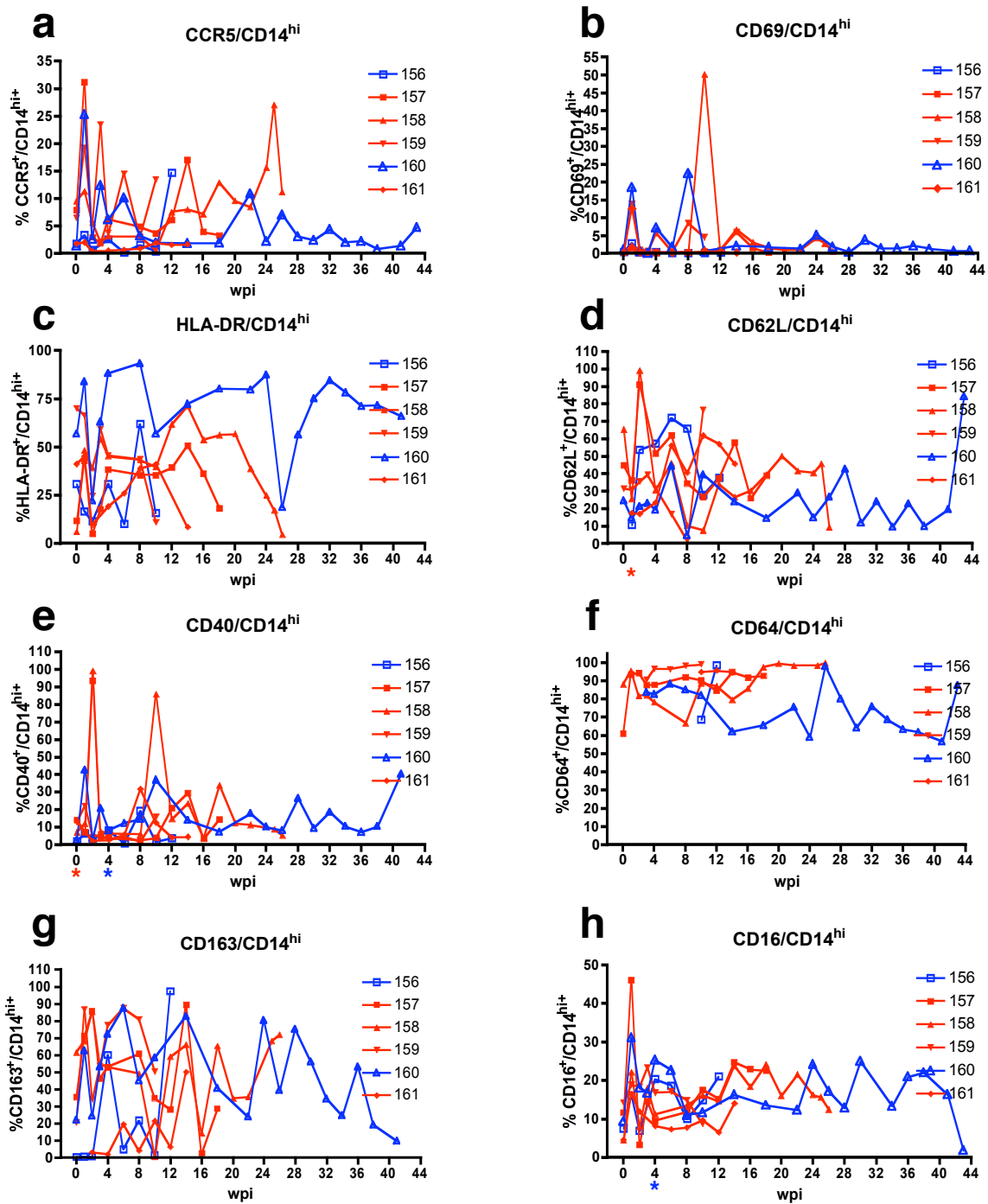


Figure 24. Proportion of CD14^{hi} cells that expressed phenotypic markers of activation during the course of infection in six pigtailed macaques infected with SIV/DeltaB670. Based on histological findings, macaques were retrospectively classified at post-mortem for presence of SIV encephalitis. Macaques that developed SIVE (M157, M158, M159, and M161) are shown in red, while macaques that did not develop SIVE (M156 and M160) are shown in blue. At each week post-infection (wpi), whole blood was stained

Figure legend continued on next page.

Figure 24 legend continued.

with anti-CD14 and the panel of antibodies listed in Table 1. CD14^{hi} cells were gated as shown in Figure 1. Shown here are longitudinal changes in percent expression of each phenotypic marker: **a.** CCR5⁺/CD14^{hi} **b.** CD69⁺/CD14^{hi} **c.** HLA-DR⁺/CD14^{hi} **d.** CD62L⁺/CD14^{hi} **e.** CD40⁺/CD14^{hi} **f.** CD64⁺/CD14^{hi} **g.** CD163⁺/CD14^{hi} **h.** CD16⁺/CD14^{hi}. Significant statistical differences between macaques that did and did not develop SIVE are shown below the corresponding time points on the x-axis. * $P < 0.05$ proportion of cells that expressed marker was greater for SIVE and * $P < 0.05$ proportion cells that expressed marker was less for SIVE (Student's t test).

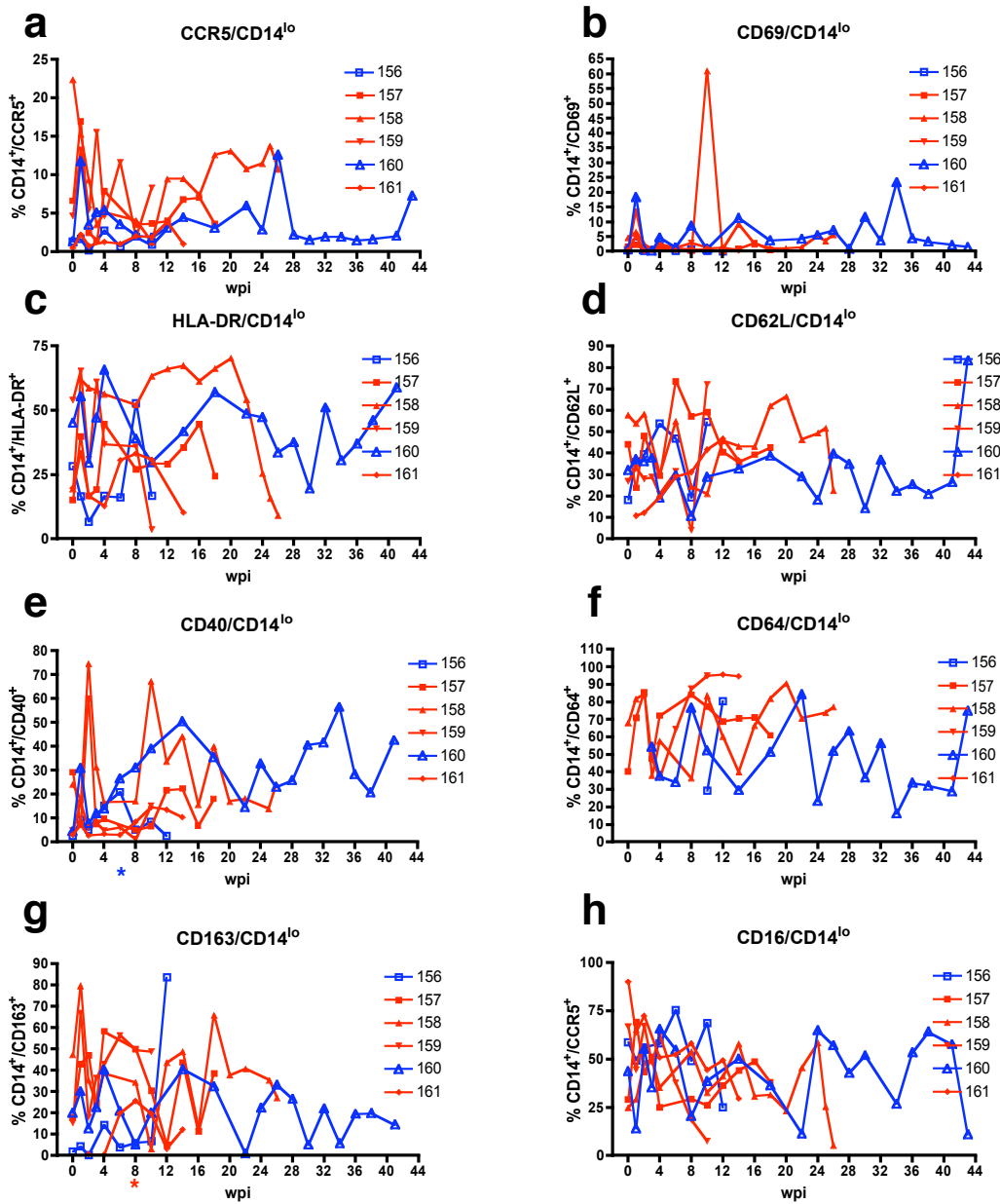


Figure 25. Proportion of CD14^{lo} cells that expressed phenotypic markers of activation during the course of infection in six pigtailed macaques infected with SIV/DeltaB670. Based on histological findings, macaques were retrospectively classified at post-mortem for presence of SIV encephalitis. Macaques that developed SIVE (M157, M158, M159, and M161) are shown in red, while macaques that did not develop SIVE (M156 and M160) are shown in blue. At each week post-infection (wpi), whole blood was stained with anti-CD14 and the panel of antibodies listed in Table 1. CD14^{lo} cells were gated as shown in Figure 1. Shown here are longitudinal changes in percent expression of each phenotypic marker: **a.** CCR5⁺/CD14^{lo} **b.** CD69⁺/CD14^{lo} **c.** HLA-DR⁺/CD14^{lo} **d.** CD62L⁺/CD14^{lo} **e.** CD40⁺/CD14^{lo} **f.** CD64⁺/CD14^{lo} **g.** CD163⁺/CD14^{lo} **h.** CD16⁺/CD14^{lo}. Significant statistical differences between macaques that did and did not develop SIVE are shown below the corresponding time points on the x-axis. * $P < 0.05$ proportion of cells that expressed marker was greater for SIVE and * $P < 0.05$ proportion cells that expressed marker was less for SIVE (Student's t test).

Macaques that would or would not develop encephalitis were not distinguished on the basis of monocyte CCR5 expression during the course of infection.

Prior to infection, 10% or less of CD14^{hi} and CD14^{lo} cells expressed CCR5 in all but one macaque (Figure 24a and 25a). Three macaques exhibited increased proportions of CD14^{hi}/CCR5⁺ cells (range = 19.2% - 31.1%, median = 15.2%, mean = 25.2 ± 3.4%) and CD14^{lo}/CCR5⁺ cells (range = 11.7%-16.9%, median = 25.3%, mean = 13.9 ± 1.5%) at one week post-infection (wpi) regardless of whether the macaque developed encephalitis (Figures 24a and 25a). In the weeks prior to death, there was a general increase in proportion of CD14^{hi}/CCR5⁺ cells in most macaques. CCR5 MFI varied during the course of infection on both CD14^{hi} (Figure 26a) and CD14^{lo} cells, but this was independent of development of encephalitis.

CD69⁺ Monocyte percentage and intensity varied during the course of infection but was independent of the development of encephalitis.

The proportion of CD14^{hi} cells that expressed CD69 at baseline was 1.12% or lower (median = 0.41, mean = 0.49 ± 0.13) for all macaques (Figure 24b), while 0.28% to 4.58% (median = 0.67, mean = 1.38 ± 0.67) of CD14^{lo} cells expressed CD69 (Figure 25b). During the first week of infection, there was a 3.3 - 57.3 fold increase in the proportion of CD14^{hi} cells that expressed CD69 and a 1.3 – 27.7 fold increase in the proportion of CD14^{lo} cells that expressed CD69 (Figures 24b and 25b). At 1 wpi, CD69 MFI on CD14^{hi} cells decreased from baseline for all macaques (Figure 26b). At two weeks before death CD69 MFI on CD14^{hi} cells was significantly lower in macaques that developed SIVE compared to macaques that did not develop SIVE ($P = 0.006$). At 8 wpi, CD69 MFI on CD14^{lo} cells was significantly increased in macaques that developed SIVE ($P = 0.01$, data not shown).

Monocyte HLA-DR MFI Was Lower in Macaques That Would Develop Encephalitis During the First Weeks of Infection.

The proportions of CD14^{hi} and CD14^{lo} cells that expressed HLA-DR were variable prior to SIV infection (median = 36%, mean = $36.1 \pm 10.2\%$, range = 6.01% - 70% and median = 24%, mean = $30.3 \pm 4.8\%$, range = 15% - 54%, respectively) (Figures 24c and 25c). At 2 wpi, all but one macaque had decreased proportions of CD14^{hi} and CD14^{lo} cells that expressed HLA-DR (Figure 24c and 25c). After acute infection, the percentage of CD14^{hi} and CD14^{lo} cells that expressed HLA-DR remained variable with all macaques showing decreased proportions of CD14^{hi}/HLA-DR⁺ and CD14^{lo}/HLA-DR⁺ cells during the weeks before death. Macaques that developed SIVE had a significantly lower proportion of CD14^{hi}/HLA-DR⁺ cells four weeks before death ($P = 0.02$). HLA-DR MFI was higher for macaques that did not develop encephalitis for the CD14^{hi} population at 1 and 8 wpi (Figure 26c) and for the CD14^{lo} subset at 1 and 4 ($P = 0.02$) wpi (data not shown).

Early in infection, macaques that would develop encephalitis showed increased proportion of CD62L⁺ monocytes.

Prior to infection, the proportion of CD14^{hi} cells that expressed CD62L was higher in macaques that developed SIVE (mean = 47.2%) than macaques that did not develop encephalitis (24.6%) (Figure 24d). Baseline CD62L expression was not available for one macaque that developed SIVE and one macaque that did not develop SIVE. At 1 wpi, the proportion of CD14^{hi} cells that expressed CD62L decreased in all macaques, however macaques that

developed SIVE had a significantly higher proportion of CD14^{hi}/CD62L⁺ cells ($P = 0.03$) (Figure 24d). The proportion of CD14^{hi}/CD62L⁺ cells was variable for the remainder of infection. Macaques that developed SIVE had significantly decreased CD62L MFI on CD14^{hi} cells at 1 wpi ($P = 0.05$) (Figure 26d).

Monocytes of macaques that would develop SIVE showed higher expression of CD40 prior to infection that decreased below that of macaques that would not develop SIVE at 4 weeks.

Prior to infection, the proportion of CD14^{hi}/CD40⁺ cells was significantly higher for macaques that developed SIVE ($P = 0.009$) (Figure 24e). After infection, the proportions of CD14^{hi}/CD40⁺ and CD14^{lo}/CD40⁺ cells were variable for most macaques (Figure 25e). Macaques that developed SIVE had significantly lower percentages of CD14^{hi}/CD40⁺ cells ($P = 0.02$) and CD14^{lo}/CD40⁺ cells ($P = 0.05$) at 4 and 6 wpi, respectively (Figures 24e and 25e). CD40 MFI was greater in macaques that developed SIVE at baseline ($P = 0.04$ for CD14^{hi} subset), during the second wpi for both CD14^{hi} and CD14^{lo} populations, and at 6 and 10 wpi for the CD14^{lo} subset ($P = 0.05$ and 0.04 , respectively) (Figure 26e and data not shown). Four weeks prior to death, macaques that developed SIVE had significantly higher CD40 MFI on CD14^{hi} cells than macaques that did not develop SIVE ($P = 0.05$).

Four weeks prior to death, macaques that would develop SIVE had greater proportion of CD64⁺/CD14⁺ cells.

The percentage of CD14^{hi} cells that expressed CD64 either increased or remained high for most macaques during the course of infection (Figure 24f). Four weeks prior to death, macaques that developed SIVE had significantly higher proportions of CD64⁺CD14^{hi} and CD64⁺CD14^{lo} cells than macaques that did not develop SIVE ($P = 0.04$ and 0.008 , respectively) (Figure 26f and data not shown).

Two weeks prior to death, CD14^{lo} monocytes of macaques that would develop SIVE had greater CD163 MFI than macaques that would not develop encephalitis.

During the first two wpi, the percentage of CD14^{lo} cells that expressed CD163 was higher in macaques that developed SIVE (Figure 25g). Both CD14^{hi} and CD14^{lo} subsets showed large increases and decreases in the proportions of cells that expressed CD163 through the length of infection (Figures 24g and 25g). Two weeks prior to death, macaques that developed SIVE had significantly higher CD163 MFI on CD14^{lo} cells than macaques that did not develop SIVE ($P = 0.04$) (data not shown).

Increased Proportions of CD14⁺/CD16⁺ Cells Occurred in All SIV-Infected Macaques Regardless of Development of Encephalitis.

Prior to infection, the mean proportion of CD14^{lo} cells that expressed CD16 was $52.19 \pm 10.1\%$ (median = 51.2%) (Figure 3h) and $8.65 \pm 1.57\%$ (median = 8.4%) for CD14^{hi} cells (Figure 24h). All macaques had an increased percentage of CD14^{hi}/CD16⁺ cells at 1 wpi (Figure 24h), while the proportion of CD14^{lo}/CD16⁺ cells decreased in four macaques at 1 wpi (Figure

25h). Regardless of development of encephalitis, the proportion of CD14^{hi}/CD16⁺ cells remained high for most time periods for the duration of infection. However, at 4 wpi, macaques that developed SIVE showed significant decreases in both proportion ($P = 0.05$) (Figure 2h) and CD16 MFI ($P = 0.008$) (Figure 26h) for the CD14^{hi}/CD16⁺ subset compared to macaques that did not develop SIVE. CD16 MFI increased in most animals at 1 and 3 wpi for both CD14^{hi} and CD14^{lo} subsets (Figure 26h and data not shown).

Figure 27a is a representative example of the changes in the proportions of CD14⁺/CD16⁺ cell populations during the course of infection. Three CD16⁺ cell populations can be observed as shown in Figure 27a, week 0; A = CD14^{hi}/CD16⁺; B = CD14^{lo}/CD16^{hi}; C = CD14⁺/CD16^{hi}. The proportion of cells in C decreased during the course of infection ($A = 0.18 \pm 0.05$, $P = 0.001$) (Figures 27a and 27d). The A and B subsets were present at smaller proportions than the C subset (means \pm SD: A = $0.53 \pm 0.15\%$; B = $0.89 \pm 0.32\%$; C = $7.77 \pm 1.95\%$), but the proportion of CD14^{hi}/CD16⁺ subset increased at least 2-3 fold or higher during the course of infection ($A = 0.05 \pm 0.01$, $P = 0.006$) for all monkeys especially during 2 and 6 wpi ($P = 0.03$ and 0.003 , respectively) (Figures 27a, b, c, d). The proportion of CD14^{lo}/CD16^{hi} cells mirrored the trend of the CD14^{hi}/CD16^{lo} population for most macaques with an increase at 1 wpi ($P = 0.058$). However, due to variability, the mean percentage as a function of duration of infection showed no estimated change ($A = 0.004 \pm 0.01$, $P = 0.774$) (Figure 27c).

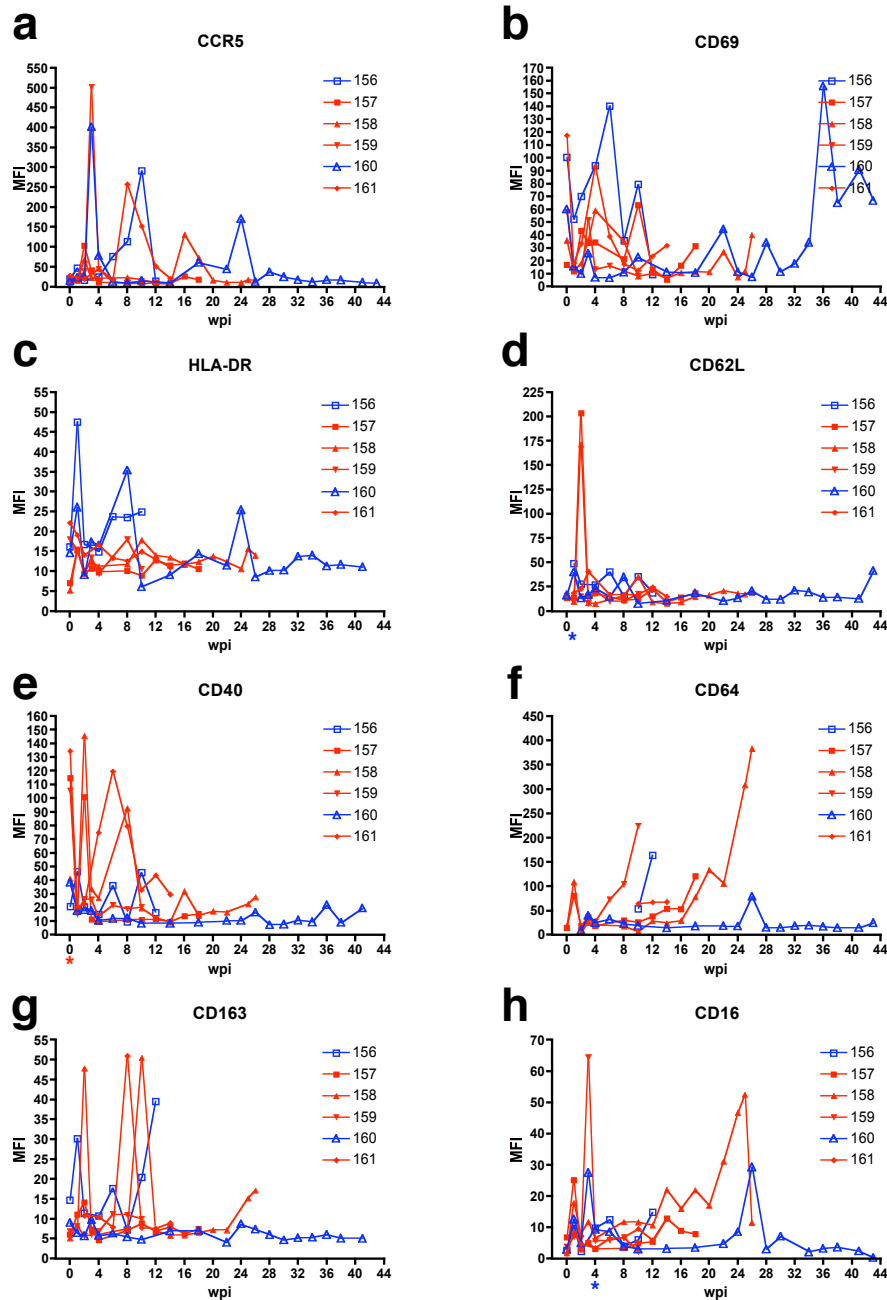


Figure 26. Mean fluorescent intensity (MFI) of activation markers on CD14^{hi} cells during the course of infection in six pigtailed macaques infected with SIV/DeltaB670. Based on histological findings, macaques were retrospectively classified at post-mortem for presence of SIV encephalitis. Macaques that developed SIVE (M157, M158, M159, and M161) are shown in red, while macaques that did not develop SIVE (M156 and M160) are shown in blue. At each week post-infection (wpi), whole blood was stained with anti-CD14 and the panel of antibodies listed in Table 5. MFI of each phenotypic marker on CD14^{hi} cells was followed every two wpi: **a.** CCR5 **b.** CD69 **c.** HLA-DR **d.** CD62L **e.** CD40 **f.** CD64 **g.** CD163 **h.** CD16. Statistically significant differences between macaques that did and did not develop SIVE are shown below the corresponding time points on the x-axis. * $P < 0.05$ = SIVE macaques with significantly greater percent marker expression. * $P < 0.05$ = SIVE macaques with significantly less percent marker expression (Student's t test).

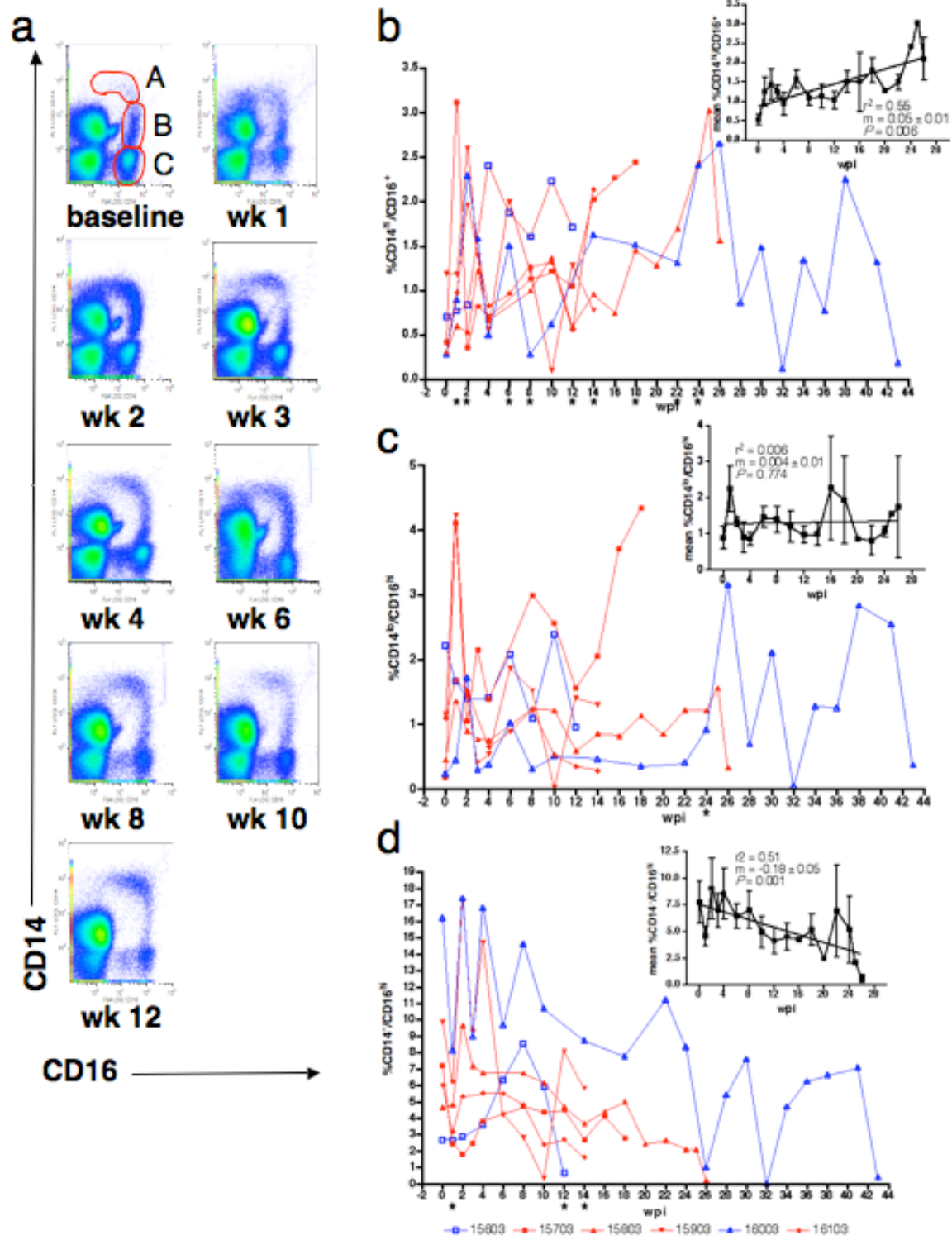


Figure 27. The proportion of CD14^{hi}/CD16⁺ cells increased while the percentage of CD14^{lo}/CD16^{hi} cells decreased during the course of infection in six pigtailed macaques infected with SIV/DeltaB670 regardless of development of encephalitis.

Figure legend continued on next page.

Figure 27 legend continued.

At each week post-infection (wpi), whole blood was stained with anti-CD14 and anti-CD16 antibodies. These representative pseudo-color plots (ungated) from M156 show the proportions of CD14^{hi}/CD16⁺ and CD14^{lo}/CD16^{hi} cells increased during the course of infection. The baseline plot shows three CD16⁺ cell populations: A = CD14^{hi}/CD16⁺; B = CD14^{lo}/CD16^{hi}; C = CD14⁻/CD16^{hi}. **b-d:** Macaques that developed SIVE (M157, M158, M159, and M161) are shown in red, while macaques that did not develop SIVE (M156 and M160) are shown in blue. The A, B, and C subsets cells were gated as shown in **a**. Insets show changes in the mean percentage of each subset as a function of duration of infection (wpi). **b: A subset.** The proportion of CD14^{hi}/CD16⁺ cells increased during the course of infection, $r^2 = 0.55$, $m = 0.05 \pm 0.01$ and $P = 0.006$. **c: B subset.** The proportion of CD14^{lo}/CD16^{hi} cells was variable during the course of infection. Most macaques showed increased proportions at 1 wpi ($P = 0.058$). However, there was no estimated change in mean percentage during the course of infection, $r^2 = 0.006$, $m = 0.004 \pm 0.01$ and $P = 0.774$. **d: C subset.** The proportion of CD14⁻/CD16^{hi} cells decreased during the course of infection, $r^2 = 0.51$, $m = -0.18 \pm 0.05$ and $P = 0.001$. Statistically significant differences between the proportions of each subset from all macaques at baseline (0 wpi) vs. time of infection are shown below the corresponding time points on the x-axis. * $P < 0.05$ (Student's t test, paired). r^2 = measure of goodness of fit. m = slope of line. Since only one animal survived after 26 wpi, the insets show data from 0-26 wpi to avoid inaccuracies of statistical analysis presented.

3.4.5. Discussion

In the past decade, it has been suggested that patients with HAD demonstrated increased CD14⁺/CD16⁺ monocytes (295). Several reports have described increases in the proportion or absolute number of CD14⁺/CD16⁺ monocytes during HIV or SIV infection (94, 295, 362, 399). During acute SIV infection of pigtailed and cynomolgus macaques, increased numbers of monocytes (152) and specifically CD14^{lo}CD16⁺ monocytes were found in the blood (272). We have performed a longitudinal analysis of CD14⁺/CD16⁺ monocyte subsets along with other phenotypic markers of activation on monocytes in a group of six SIV-infected pigtailed macaques. The SIV-infected macaque provides an excellent model to determine whether expansion of the CD14⁺/CD16⁺ monocyte subset is predictive of the development of lentiviral encephalitis.

Activation markers that distinguished macaques that would develop encephalitis from macaques that would not develop encephalitis.

Prior to SIV infection, macaques that would develop SIVE had a higher proportion of CD14^{hi} monocytes that expressed CD62L and CD40 than macaques that would not develop SIVE. CD40 MFI on CD14^{hi} monocytes was also increased in macaques that would develop SIVE compared to macaques that would not develop SIVE. Although the proportion of monocytes that expressed CD69 was similar, the MFI varied from animal to animal. Even before infection, the proportion and MFI varied greatly in all macaques.

After infection, macaques that would develop SIVE had a higher proportion of CD62L⁺CD14^{hi} monocytes than macaques that would not develop SIVE, but this was accompanied by decreased CD62L MFI. During the course of infection, the proportions of

CD40⁺CD14^{hi}, CD40⁺CD14^{lo}, and CD16⁺CD14^{hi} cells were decreased in macaques that developed SIVE. Interestingly, CD16 MFI was also decreased on CD16⁺CD14^{hi} cells, while CD40⁺CD14^{hi} cells showed increased CD40 MFI. Although these markers distinguished macaques that would develop SIVE from those that would not, differences were observed at single time points during the course of infection. All other activation markers fluctuated but showed no correlation with the development of encephalitis.

Prior to death, the proportion of CD64⁺/CD14⁺ monocytes was higher in encephalitic macaques, while the proportions of HLA-DR⁺/CD14^{hi} and HLA-DR⁺/CD14^{lo} monocytes were decreased compared to nonencephalitic macaques. MFI for CD40 and CD163 on CD14^{hi} and CD14^{lo} cells, respectively, was also increased prior to death. Decreased proportions of HLA-DR⁺/CD14^{hi} cells in the weeks before death suggests circulating cells might have trafficked into the CNS and other tissues.

Activation markers that did not distinguish macaques that would develop encephalitis from macaques that would not develop encephalitis.

Since much emphasis has been placed on potential expansion of CD14⁺/CD16⁺ monocytes being associated with presence of HAD, it is curious why the macaques that developed SIVE in this study were not distinguished from macaques that did not develop SIVE by an expansion of CD14⁺CD16⁺ cells over the course of infection. This does not rule out the possibility of increased numbers of SIV-infected CD14⁺/CD16⁺ cells in macaques that developed SIVE.

Since neither the proportion of CD14⁺/CCR5⁺ cells nor the MFI of CCR5 on CD14⁺ cells distinguished macaques that would develop SIVE from those that would not, increased presence

of SIV-infected CNS macrophages was not associated with increased proportion or intensity of CCR5 (a co-receptor for SIV associated with macrophage infection) on blood monocytes. It has also been suggested that CCR1⁺/CCR5⁺/CD14⁺ cells are the population of monocytes that are able to enter the inflamed CNS (365), but we were unable to detect such trafficking by assessing the peripheral blood. Our results in a small number of SIV-infected macaques do not support the observation that the proportion of circulating CD14⁺CD69⁺ monocytes is elevated during encephalitis (183, 295).

Activation markers that changed during the course of infection in all macaques regardless of development of encephalitis.

Interestingly, CD16 expression on ungated cells changed during the course of SIV infection in macaques that would and would not develop encephalitis. We analyzed changes in the proportion of three CD16⁺ cell populations. The CD14⁻CD16⁺ subset (population C) likely contained NK cells. We observed a decrease in the proportion of NK cells during the course of SIV infection. This corroborates reports that the frequency of the cytolytic subset of NK cells (CD16⁺) decreases during HIV infection (206, 236, 356).

The other two CD16⁺ cell populations were CD14^{hi}/CD16⁺ and CD14^{lo}/CD16^{hi}. These subsets contained the monocyte populations described in previous reports, CD14⁺⁺CD16⁺ and CD14⁺CD16⁺ (414). As others have described, our study showed that the proportion of CD14^{hi}CD16⁺ cells changed significantly as a function of duration of infection, but this was regardless of whether the macaque developed encephalitis. An increased percentage was also observed in the CD14^{lo}/CD16^{hi} subset during the course of infection, but this was not statistically significant. This was probably due to the presence of CD14⁺/CD16⁺ granulocytes. We have

expanded previous observations by following the macaques throughout the course of infection. The strength of our longitudinal study suggests that increases in the proportion of CD14⁺/CD16⁺ cells are not predictive of the development of encephalitis but rather an indication of chronic disease.

The changes in CD16⁺ populations could have arisen due to two possibilities: either these populations expanded over time (increased number of cells) or the proportions of these subsets increased because other populations were decreasing. Assuming the number of events in each subset is a rough indication of the actual number of cells in each subset, it appears that during acute infection, the increased proportion of monocytes seen was due to an expansion in the number of monocytes in both subsets. After acute infection, the increased proportion of monocytes was due to expansion of the number of monocytes alternating with times where changes in other cell populations increased the proportion of monocytes. At the last time point analyzed, approximately half of the macaques had expanded monocyte populations. Expansion of the monocyte subsets and loss of the NK cell subset did not correlate with viral load or CD4⁺ T cell counts (data not shown).

The data presented here reports the proportion of cells that expressed activation markers, not actual cell numbers. Determining absolute cell numbers by multiplying the proportion of each subset by the number of monocytes present in whole blood at each time point confirmed that both percentage and actual number of cells that expressed activation markers had similar trends (data not shown).

It is possible that we did not observe differences between activation markers on monocytes from macaques that did and did not develop SIVE because we did not look at the correct activation marker(s). We have also analyzed these activation markers along with others

on monocytes from a group of eight rhesus macaques. Longitudinal analysis of the proportion of monocytes that expressed CD49 ($\alpha 4$ integrin), CD80, CD86, CD166, and any of the markers listed in Table 5 did not reveal any differences between macaques that did and did not develop encephalitis (unpublished observations). Inclusion of CCR1 on monocytes would be germane since the chemokine ligand of this receptor is reportedly involved in monocyte CNS trafficking, but there are no commercial antibodies available to this marker.

The present study followed activation markers on blood monocytes from six SIV infected pigtailed macaques during the course of infection. Analysis of blood monocytes showed there was an expansion of CD14^{hi}/CD16⁺ and CD14^{lo}/CD16^{hi} monocytes during acute infection and at various time points during the course of infection; however, this expansion was not unique or greater in macaques that developed SIVE. The proportion of monocytes that expressed other activation markers was variable for all macaques during the course of infection and none of the tested phenotypic markers predicted development of encephalitis. Taken together, these results suggest that changes in the proportion of activated monocytes do not direct development of SIVE, but this does not rule out the importance of activated monocytes in the development of encephalitis.

3.4.6. Acknowledgements

We thank Aki Hoji for assistance with flow cytometry analysis; Dawn L. McClemens-McBride for assistance in scheduling blood draws; and LuAnn Borowski and Charles Rinaldo, Jr. for use and assistance with the flow cytometry facility.

4. DISCUSSION

HIV-infection has touched nearly every corner of the world and the epidemic remains an increasing public health problem. Approximately $\frac{1}{4}$ of AIDS patients develop HIVE, the pathologic entity associated with cognitive, motor, and behavioral deficits attributed to synaptic damage and neuronal loss. The neuropathogenesis of this disease has been studied intensely over the past 25 years, but it still remains unclear why only a subset of HIV-infected individuals develop the abundant CNS macrophage infection that characterizes HIVE. The concentration of this body of work was to study the relationship of infected and activated monocyte/macrophage elements outside of the CNS during the evolution of lentiviral encephalitis to the presence of infected macrophages in the CNS of rhesus and pigtailed macaques infected with SIV. In order to understand the pathogenesis of the development of lentiviral encephalitis, knowing whether robust production of virus in monocyte/macrophage elements is unique to the CNS or whether it is a system-wide phenomena will have beneficial public health significance by helping define therapeutic targets to halt the development or progression of lentiviral encephalitis.

The overarching hypothesis of this body of work is development of SIV encephalitis and ensuing neurologic damage is associated with increased SIV infection and activation of monocyte/macrophage elements both inside and outside of the brain. We have examined whether the presence of infected CNS macrophages or only activated macrophages is associated with neuronal damage in macaque brains with SIVE. Using SIV-infected pigtailed macaques and an antibody mediated CD8⁺ T cell depletion model in SIV-infected rhesus macaques, we longitudinally examined whether monocyte/macrophages from macaques that develop SIVE

contain more replication competent virus than macaques that do not develop SIVE during the course of infection and at necropsy. Finally, we longitudinally examined whether blood monocytes from macaques that developed SIVE would have increased proportion of monocytes expressing activation markers compared to macaques that would not develop SIVE.

CNS macrophage infection is related to neuronal damage in lentiviral encephalitis

In the field of lentiviral-associated dementia, there has been considerable controversy regarding the relationship between neurological damage and the abundance of virus in the CNS (3, 32, 85, 124, 125, 157, 187, 288, 394, 395, 397, 415, 418). Some investigators believe that the presence of activated macrophages/microglia in the CNS is a better determinant of neuronal damage than the presence of HIV-infected macrophages (124), while other studies have shown that the severity of HIV and SIV encephalitis correlates with higher viral RNA concentrations in several brain regions using sensitive, quantitative RNA assays (85, 395, 397, 418).

We used a combination of quantitative RT-PCR and quantitation of immunohistochemical staining to show that encephalitis is associated with high concentrations of SIV RNA and SIV protein in most brain regions. Brains of SIV-infected macaques with SIVE contained 5 orders of magnitude greater concentrations of SIV RNA than SIV-infected macaques without encephalitis (Figure 5). Although using quantifiable RNA assays to determine viral load in macaques with SIVE is a valuable, unbiased tool, it does not define the spatial relationship between macrophages, virus, and neurons in the microenvironment of the CNS. Macrophage and SIV envelope protein staining were elevated in all brain regions of macaques with SIVE compared to SIV-infected macaques without SIVE, especially in the midfrontal cortical gray matter and caudate (Figures 6 and 7). This suggests that neurons in midfrontal

cortex, caudate and the regions receiving projections from these areas are at greater risk from damage mediated by soluble products secreted by infected macrophages and secondary downstream events initiated in the soma of neurons.

In encephalitic regions we estimated ~70 to 80% of macrophages stain for SIVgp110. However, SIVE is a multifocal disease with significant variation between microscopic regions. There is significant variation in the abundance of infected macrophages between individual microscopic fields. This necessitates evaluating large areas of brain tissue to objectively assess the severity of SIV lesions. Despite many focal areas being free of infected macrophages, SIV RNA measurements and evaluation of infected macrophages at the microscopic level shows that infection of brain macrophages is abundant.

In order to determine whether abundant infected macrophages present in the CNS are related to neuronal damage, we examined neuronal proteins associated with both presynaptic and postsynaptic processes. Microscopic foci within brain regions of macaques with abundant macrophage infiltration and viral infection show loss of synaptic proteins (Figures 8 and 9). MAP-2 staining was decreased in the caudate, midfrontal cortex, and hippocampus of macaques with SIVE compared to macaques without SIVE. This suggests primary postsynaptic damage. Presynaptic protein synaptophysin was decreased in brain regions from both macaques with and without SIVE. Finding presynaptic damage in SIV-infected macaques independent of encephalitis and postsynaptic damage dependent on local presence of encephalitis suggests the following hypothesis: presynaptic components are susceptible to systemic toxins generated as a result of lentiviral infection, whereas postsynaptic elements are susceptible to degradation by products of locally activated and infected macrophages within the CNS.

In support for this hypothesis, SIV-infected macaques without SIVE also showed increased astrocyte (GFAP) staining compared to noninfected controls although far less than that observed with SIVE (Figure 9). This suggests that SIV-infected macaques without SIVE show presynaptic neuronal damage due to extended peripheral infection and extended periods of systemic toxins affecting the CNS as evidenced by increased astrocyte staining. Presynaptic and postsynaptic damage may progress to neuronal loss in the brains with SIVE. These studies show that without viral infected macrophages in the brain, presynaptic damage can occur in lentiviral encephalitic individuals; but viral infected macrophages clearly are important in mediating structural neuronal damage crucial to the pathogenesis of neurodegeneration in this encephalitides.

Antibody-mediated CD8⁺ T cell depletion of rhesus macaques

Antibody-mediated CD8⁺ T cell depletion of macaques has been used to show the importance CD8⁺ T cells in controlling SIV replication and subsequently length of disease (154, 323). Development of SIVE has been associated with rapid disease progression (391). Therefore, we hypothesized that antibody-mediated CD8⁺ T cell depletion, which leads to rapid disease progression, would lead to greater incidence of encephalitis. If validated, this would provide a useful model that because of decreased time to disease would be cost-efficient. Of the eight CD8-depleted macaques that progressed to AIDS, 38% developed SIVE (Table 3). This is not strikingly different compared to non-depleted macaques; however, the three macaques that developed SIVE progressed to AIDS in 8-14 weeks. Given model variability, it is unclear what percentage of SIV-infected macaques developed SIVE in these studies (399).

Two of the CD8-depleted macaques that did not develop SIVE had meningitis with SIV-infected cells. Two additional CD8-depleted macaques were sacrificed at two and four weeks post-infection, and the macaque sacrificed at 4 weeks post-infection showed meningitis with SIV-infected cells. The macaque sacrificed at 2 weeks post-infection had an accidental needle nick in the brainstem during a routine CSF draw. Remarkably, none of the 3-day old infiltrate was infected with SIV despite considerable plasma viremia. These data suggest that few infected macrophages can be found in the CNS at acute stages of infection. These results indicate that development of SIVE involves mechanisms beyond massive viremia, BBB breaches, and SIV-infected cells in the meninges.

The rapidity of the CD8 depletion model may result in death before SIVE or other organs show massive infection (Figure 15). Since pigtailed macaques have higher percentages of animals that develop SIVE naturally, this may ultimately be a better model to answer questions regarding neuropathogenesis than the more manipulated depletion model.

Monocyte-associated SIV DNA and capability to produce virus during development of SIVE

One of the most interesting findings of this work is that MDM from macaques that developed SIVE produced more virus *ex vivo* than SIV-infected macaques that did not develop SIVE in both rhesus and pigtailed models (Figures 13 and 19). Peak MDM SIV production was observed at different time points post-infection, usually early or mid-infection, indicating there is variability in disease progression even among animals that develop encephalitis. The capability of monocytes to produce virus upon differentiation did not appear to be directly related to the monocyte-associated SIV DNA viral load. In pigtailed macaques, three of the macaques that

developed SIVE had higher numbers of SIV DNA copies than the SIV-infected macaques that did not develop SIVE (Figure 19). However, in the CD8-depleted rhesus macaques, the number of SIV DNA copies in monocytes was not consistently higher in macaques that developed SIVE compared to macaques that did not develop SIVE (Figure 13). Additionally, peak monocyte-associated viral loads and peak SIV production from MDM did not coincide during the same time points. This suggests that even though infected monocytes are in circulation, they might be poor producers of virus. When MDM are producing high levels of virus, it appears that a few monocytes are capable of producing more virus. These data suggest there are inherent differences in the individual macaque monocytes to harbor virus and to produce virus during the course of infection. These differences are associated with development of encephalitis.

Interestingly, CSF viral load increased during the same time periods after infection (4-8 weeks post-infection) (Figure 12) as *ex vivo* production was increased in cultured MDM in CD8-depleted rhesus macaques that eventually developed SIVE. Further studies are needed to determine if this association is indicative of the time period when encephalitis develops.

In pigtailed macaques, nonadherent PBMC containing CD4⁺ T cells produced more virus *ex vivo* in macaques that developed SIVE compared to SIV-infected macaques that did not develop SIVE (Figure 19). While in CD8-depleted rhesus macaque, there was no observable or statistical difference in SIV p27 production in nonadherent PBMC cultures (Figure 13); however, SIV production was increased in two of the macaques in the SIVE group at two and six weeks post-infection. Both MDM and nonadherent PBMC produce more virus earlier infection than prior to death, suggesting the ability of cells to produce virus during earlier time points of infection is more important in the development of encephalitis. These data leave open the possibility that development of SIVE could be associated with the magnitude of total viral

production rather than number of circulating infected monocytes. Differential capability of replicating virus during development of SIVE suggests an inherent difference in the ability of individual host monocytes to become infected and/or to produce virus.

Phenotypic monocyte-activation markers during the development of SIVE

Past reports have suggested that patients with HIVD demonstrated increased CD14⁺/CD16⁺ monocytes (295). We performed analysis of CD14⁺/CD16⁺ monocyte subsets along with other phenotypic markers of activation on monocytes during the course of disease in a group of six SIV-infected pigtailed macaques. Some markers, such as CD62L, CD40, CD16, CD64, HLA-DR, and CD163, were expressed on different proportions of monocyte subsets or with different MFI in macaques that would develop SIVE compared to those that did not (Figures 24, 25, 26). However, these differences were observed at single time points during the course of infection. Many activation markers fluctuated but showed no correlation with the development of encephalitis, including viral co-receptor CCR5.

The strength of our longitudinal study suggests that increases in the proportion of CD14⁺/CD16⁺ cells are not predictive of the development of encephalitis but rather an indication of chronic disease (Figure 27). Although CD16 expression on monocyte subsets did not distinguish macaques that did and did not develop SIVE, it is still plausible that macaques that develop SIVE contain increased numbers of SIV-infected CD14⁺/CD16⁺ cells since these cells are associated with an activated phenotype that may be more susceptible to infection in a fraction of animals. We determined that none of the tested phenotypic markers predicted development of encephalitis.

Peripheral macrophage infection in macaques with SIVE

In animals that develop SIVE, it is not clear whether the presence of abundant infected macrophages is unique to the CNS or whether infected macrophages are abundant in peripheral organs. In pigtailed macaques, animals with SIVE exhibit greater numbers of infected macrophages in all peripheral organs except lymph nodes compared to macaques without SIVE (Figure 21). Unexpectedly, we did not observe a clear relationship between systemic macrophage infection and CNS infection in CD8-depleted rhesus macaques (Figure 15). The difference between these models is difficult to interpret, but it may be due to death of CD8-depleted animals before peripheral organs show massive infection. Few infected CD3⁺ T cells were observed in any organ including secondary lymphoid tissue, but this may simply reflect severe depletion of CD4⁺ T cells in tissues at the end stages of disease (276, 308, 381). These data suggest that the ability of pigtailed macaque macrophages to produce virus in the CNS and other organs is related to the development of encephalitis.

Immune response to CNS macrophage infection

The ability for macrophages to produce more virus in the CNS of macaques that develop encephalitis might be due to differential immune response, divergent evolution of viral strains that better infect macrophages, or disparate host factors. Although we did not analyze the immune response to peripheral infected monocyte/macrophages during the course of infection, we performed an initial survey of cells with cytolytic potential in the brain of SIV-infected pigtailed macaques. In macaques with SIVE, the number of T cells with cytotoxic potential was significantly higher than SIV-infected macaques without encephalitis (Figure 22). Numbers of NK cells and T cells without cytotoxic granules were also elevated in macaques with SIVE.

Interestingly, analysis of cells with cytolytic potential in humans with HSV encephalitis shows that other viral encephalitides (e.g. West Nile Virus encephalitis) induce a much greater local T cell response than SIVE. In the future, it will be necessary to determine whether the CNS immune response during asymptomatic infection or in animals that do not develop SIVE is sufficient to contain viral production or whether development of encephalitis is determined by other host factors.

Summary of correlates of SIVE

In our studies, we continue to observe elevated CSF viral loads in macaques that developed SIVE compared to SIV-infected macaques that did not develop SIVE as in previous studies (397, 418). Macaques with SIVE have higher SIV RNA concentration in brain tissue than macaques without SIVE. Although macaques without SIVE have mild gliosis, SIVE is accompanied by widespread gliosis. Although others have reported that the number of activated macrophages is a better indication of the extent of neuronal damage than the number of infected macrophages in HIV-infected individuals (124), the presence of abundant infected macrophages in the CNS is related to postsynaptic neuronal damage in macaques with SIVE. Brains with SIVE have greater numbers of T cells and NK cells with cytotoxic potential.

Compared to macaques that did not develop SIVE, the monocyte associated SIV-DNA load of monocytes and the capability of MDM and nonadherent PBMC to produce virus *ex vivo* was increased in macaques that developed SIVE. Pigtailed macaques with SIVE had increased virus production *ex vivo* in nonadherent PBMC. The number of infected macrophages in

peripheral organs was greater in pigtailed macaques with SIV with the exception of lymph nodes. Finally, the percentage of CD4⁺/CD29⁺ T cells decreased more rapidly in macaques that developed SIVE compared to macaques that did not develop encephalitis.

Summary of factors that did not correlate with development of SIVE

Although plasma viremia was significantly higher in CD8-depleted macaques that developed encephalitis at 1 and 3 weeks post-infection, there is no consistent increase in plasma viremia in macaques that develop SIVE compared to those that do not develop SIVE. There is no correlation between CD4⁺ and CD8⁺ T cell count dynamics and development of encephalitis. In our study group, antibody mediated CD8⁺ T cell depletion did not lead to an increased incidence of SIVE. None of the tested phenotypic activation markers on monocytes predicted development of encephalitis. The number of infected macrophages in lymph nodes during the course of disease was not different in macaques that did and did not develop SIVE. Post-synaptic neuronal damage was present in both macaques with and without SIVE.

Future directions

We found that MDM and macrophages in systemic tissues produced more virus in macaques that developed SIVE compared to SIV-infected macaques that did not develop SIVE. A number of questions arise from this finding. First, do the monocytes that are capable of producing more virus and harbor more monocyte-associated SIV DNA selectively traffic to the CNS or other peripheral organs? It would be interesting to determine whether development of SIVE is the result of recent entry of infected monocytes that are capable of producing more virus by labeling blood monocytes and following their trafficking. This could be potentially done in a

couple of different ways. Monocytes take up intravenously administered superparamagnetic iron oxide. Monocytes that traffic to organs or brain can be detected *in vivo* by magnetic resonance scanning and potentially immunohistochemistry (84, 174, 405, 410). Endogenous hemosiderin precludes detection of iron by immunohistochemistry, but the sugars present on the superparamagnetic iron oxide are not found in mammalian bodies. Use of quantum dots, nano-sized fluorophores with cadmium-based cores, could be used *in vivo* by intravenous delivery. Alternatively, isolated monocytes could be labeled *ex vivo* and autologous cells intravenously delivered (243, 351). If trafficking of monocytes to the CNS were determined by these methods, it would provide a valuable tool to determine if therapies to block cell trafficking into the CNS were effective.

Secondly, administration of an antibody against the $\alpha 4$ integrin on leukocytes to SIV-infected macaques may halt the development of SIVE by preventing the accumulation of leukocytes in the CNS. $\alpha 4\beta 1$ integrin interactions with VCAM-1 on brain endothelial cells are thought to be important in mediating monocyte adhesion in SIV infection (318). Administration of a monoclonal antibody that binds the $\alpha 4$ integrin subunit has shown promise in preventing or ameliorating relapses in clinical trials in humans with multiple sclerosis (MS) (26). However, two treated MS patients developed progressive multifocal leukoencephalopathy caused by JC virus production in the CNS (26), suggesting that immune cells responsible for containing JC virus infection were unable to gain access to the CNS. Treatment of SIV-infected macaques at different points post-infection will produce valuable insights to the kinetics and pathogenesis of lentiviral encephalitis.

Thirdly, future studies will be needed to elucidate by which mechanisms monocyte/macrophages from macaques that develop SIVE are more susceptible to infection or to produce virus. We have already observed there was no difference in the proportion of cells expressing co-receptor CCR5 in animals that did or did not develop SIVE. By comparing the viral life cycle in macaques that will or will not develop encephalitis, we can systematically dissect at what point in the viral life cycle infected macrophages might be different between encephalitic and non-encephalitic macaques. This will yield valuable insights to host factors that potentially mediate differential virus production in macrophages and subsequent development of encephalitis. Host factors such as APOBEC family members (211, 408), mutant MCP-1 alleles (130), TRIM-5 α (350), C/EBP β (383), reverse transcription efficiency, or the ability to disseminate virus during acute infection may be important during the development of encephalitis.

Lastly, extending observations of the immune response to CNS and systemic macrophage infection in macaques that will and will not develop encephalitis will determine whether differential ability to control virus production is related to the development of encephalitis. A few observations have been made regarding CD8⁺ T cell, NK cell, and antibody response in macaques with neuro-involvement during SIV infection (95, 169, 335, 340, 347, 388), but detailed analysis has not been preformed. One interesting area to begin would be to determine why the immune responses differ in magnitude in different types of encephalitides.

Summary

These studies have provided a better understanding of the relationship between the ability of monocyte/macrophage elements to produce virus and the development of encephalitis. The presence of abundant infected macrophages in the CNS is related to postsynaptic neuronal damage in macaques with SIVE. At the same time CSF viral load increased in macaques that developed encephalitis, we observed that monocyte-derived macrophages from these macaques produced more virus *ex vivo* than macaques that did not develop encephalitis. Compared to macaques that did not develop SIVE, the monocyte associated SIV-DNA load of monocytes was elevated in macaques that developed SIVE. Macaques with SIVE had more infected macrophages in peripheral organs with the important exception of lymph nodes. Antibody-mediated CD8⁺ T cell depletion did not increase the incidence of SIVE in infected rhesus macaques. Brains with SIVE have greater numbers of T cells and NK cells with cytotoxic potential; however, other encephalitides induced a more robust T cell and NK cell infiltration. In conclusion, these findings support the hypothesis that inherent differences in host monocyte viral production or immune response to macrophage infection are associated with the development of encephalitis.

BIBLIOGRAPHY

1. Current Protocols in Molecular Biology, p. 12.11.1-12.11.8. *In* F. M. Ausubel, R. Brent, R. E. Kingston, D. D. Moore, J. G. Seidman, J. A. Smith, and K. Struhl (ed.). 1994. John Wiley and Sons, Inc., New York.
2. Abramo, F., S. Bo, M. G. Canese, and A. Poli. 1995. Regional distribution of lesions in the central nervous system of cats infected with feline immunodeficiency virus. *AIDS Res Hum Retroviruses* 11:1247-53.
3. Achim, C. L., R. Wang, D. K. Miners, and C. A. Wiley. 1994. Brain viral burden in HIV infection. *J Neuropathol Exp Neurol* 53:284-94.
4. Achim, C. L., and C. A. Wiley. 1992. Expression of major histocompatibility complex antigens in the brains of patients with progressive multifocal leukoencephalopathy. *J Neuropathol Exp Neurol* 51:257-63.
5. Achim, C. L., and C. A. Wiley. 1996. Inflammation in AIDS and the role of the macrophage in brain pathology. *Current Opinion in Neurology* 9:xxx.
6. Adamson, D. C., K. L. Kopnisky, T. M. Dawson, and V. L. Dawson. 1999. Mechanisms and structural determinants of HIV-1 coat protein, gp41-induced neurotoxicity. *Journal of Neuroscience* 19:64-71.
7. Alkhatib, G., C. Combadiere, C. C. Broder, Y. Feng, P. E. Kennedy, P. M. Murphy, and E. A. Berger. 1996. CC CKR5: a RANTES, MIP-1alpha, MIP-1beta receptor as a fusion cofactor for macrophage-tropic HIV-1. *Science* 272:1955-8.
8. Alvarez Losada, S., C. Canto-Nogues, and M. A. Munoz-Fernandez. 2002. A new possible mechanism of human immunodeficiency virus type 1 infection of neural cells. *Neurobiol Dis* 11:469-78.
9. An, S. F., M. Groves, F. Gray, and F. Scaravilli. 1999. Early entry and widespread cellular involvement of HIV-1 DNA in brains of HIV-1 positive asymptomatic individuals. *J Neuropathol Exp Neurol* 58:1156-62.
10. Anderson, P. 1995. TIA-1: structural and functional studies on a new class of cytolytic effector molecule. *Curr Top Microbiol Immunol* 198:131-43.
11. Appleman, M. E., D. W. Marshall, R. L. Brey, R. W. Houk, D. C. Beatty, R. E. Winn, G. P. Melcher, M. G. Wise, C. V. Sumaya, and R. N. Boswell. 1988. Cerebrospinal fluid

- abnormalities in patients without AIDS who are seropositive for the human immunodeficiency virus. *J Infect Dis* 158:193-199.
12. Aquaro, S., C. F. Perno, E. Balestra, J. Balzarini, A. Cenci, M. Francesconi, S. Panti, F. Serra, N. Villani, and R. Calio. 1997. Inhibition of replication of HIV in primary monocyte/macrophages by different antiviral drugs and comparative efficacy in lymphocytes. *Journal of Leukocyte Biology* 62:138-43.
 13. Ausubel, F. M., R. Brent, R. E. Kingston, D. D. Moore, J. G. Seidman, J. A. Smith, and K. Struhl (ed.). 1994. *Current Protocols in Molecular Biology*. John Wiley and Sons, Inc., New York.
 14. Babas, T., E. Vieler, D. A. Hauer, R. J. Adams, P. M. Tarwater, K. Fox, J. E. Clements, and M. C. Zink. 2001. Pathogenesis of SIV pneumonia: selective replication of viral genotypes in the lung. *Virology* 287:371-81.
 15. Bacellar, H., A. Munoz, E. N. Miller, B. A. Cohen, D. Besley, O. A. Selnes, J. T. Becker, and J. C. McArthur. 1994. Temporal trends in the incidence of HIV-1-related neurologic diseases: Multicenter AIDS cohort study, 1985-1992. *Neurology* 44:1892-1900.
 16. Bagasra, O., S. P. Hauptman, H. W. Lischner, M. Sachs, and R. J. Pomerantz. 1992. Detection of human immunodeficiency virus type 1 provirus in mononuclear cells by in situ polymerase chain reaction. *N Engl J Med* 326:1385-91.
 17. Bagasra, O., T. Seshamma, J. W. Oakes, and R. J. Pomerantz. 1993. High percentages of CD4-positive lymphocytes harbor the HIV-1 provirus in the blood of certain infected individuals. *Aids* 7:1419-25.
 18. Baltimore, D. 1970. RNA-dependent DNA polymerase in virions of RNA tumour viruses. *Nature* 226:1209-11.
 19. Banchereau, J., F. Bazan, D. Blanchard, F. Briere, J. P. Galizzi, C. van Kooten, Y. J. Liu, F. Rousset, and S. Saeland. 1994. The CD40 antigen and its ligand. *Annu Rev Immunol* 12:881-922.
 20. Banks, W. A., E. O. Freed, K. M. Wolf, S. M. Robinson, M. Franko, and V. B. Kumar. 2001. Transport of human immunodeficiency virus type 1 pseudoviruses across the blood-brain barrier: role of envelope proteins and adsorptive endocytosis. *J Virol* 75:4681-91.
 21. Barre-Sinoussi, F., J. C. Chermann, F. Rey, M. T. Nugeyre, S. Chamaret, J. Gruest, C. Dauguet, C. Axler-Blin, F. Vezinet-Brun, C. Rouzioux, W. Rozenbaum, and L. Montagnier. 1983. Isolation of a T-lymphotropic retrovirus from a patient at risk for acquired immune deficiency syndrome (AIDS). *Science* 220:868-71.
 22. Baskin, G. B., M. Murphey-Corb, E. D. Roberts, P. J. Didier, and L. N. Martin. 1992. Correlates of SIV encephalitis in rhesus monkeys. *J Med Primatol* 21:59-63.

23. Baszler, T. V., and J. F. Zachary. 1990. Murine retroviral-induced spongiform neuronal degeneration parallels resident microglial cell infection: ultrastructural findings. *Lab. Invest.* 63:612-623.
24. Benos, D. J., B. H. Hahn, J. K. Buben, S. K. Ghosh, N. A. Mashburn, M. A. Chaikin, G. M. Shaw, and E. N. Benveniste. 1994. Envelope glycoprotein gp120 of human-immunodeficiency-virus type-1 alters ion-transport in astrocytes - implications for aids dementia complex. *Proceedings Of The National Academy Of Sciences Of The United States Of America* 91:494-498.
25. Berger, E. A., P. M. Murphy, and J. M. Farber. 1999. Chemokine receptors as HIV-1 coreceptors: roles in viral entry, tropism, and disease. *Annu Rev Immunol* 17:657-700.
26. Berger, T., and F. Deisenhammer. 2005. Progressive multifocal leukoencephalopathy, natalizumab, and multiple sclerosis. *N Engl J Med* 353:1744-6; author reply 1744-6.
27. Bezzi, P., M. Domercq, L. Brambilla, R. Galli, D. Schols, E. De Clercq, A. Vescovi, G. Bagetta, G. Kollias, J. Meldolesi, and A. Volterra. 2001. CXCR4-activated astrocyte glutamate release via TNFalpha: amplification by microglia triggers neurotoxicity. *Nat Neurosci* 4:702-10.
28. Bissel, S. J., G. Wang, M. Ghosh, T. A. Reinhart, S. Capuano, 3rd, K. Stefano Cole, M. Murphey-Corb, M. J. Piatak, J. D. Lifson, and C. A. Wiley. 2002. Macrophages relate presynaptic and postsynaptic damage in simian immunodeficiency virus encephalitis. *Am J Pathol* 160:927-41.
29. Bissel, S. J., G. Wang, A. M. Trichel, M. Murphey-Corb, and C. A. Wiley. submitted. Longitudinal Analysis of Monocyte/Macrophage Infection in Simian Immunodeficiency Virus-Infected, CD8+ T Cell-Depleted Macaques that Develop Lentiviral Encephalitis. *Am J Pathol*.
30. Bissel, S. J., and C. A. Wiley. 2004. Human immunodeficiency virus infection of the brain: pitfalls in evaluating infected/affected cell populations. *Brain Pathol* 14:97-108.
31. Boche, D., M. Hurtrel, F. Gray, M. A. Claessens-Maire, J. P. Ganiere, L. Montagnier, and B. Hurtrel. 1996. Virus load and neuropathology in the FIV model. *J Neurovirol* 2:377-87.
32. Boche, D., E. Khatissian, F. Gray, P. Falanga, L. Montagnier, and B. Hurtrel. 1999. Viral load and neuropathology in the SIV model. *Journal of Neurovirology* 5:232-40.
33. Bontrop, R. E., N. Otting, H. Niphuis, R. Noort, V. Teeuwssen, and J. L. Heeney. 1996. The role of major histocompatibility complex polymorphisms on SIV infection in rhesus macaques. *Immunol Lett* 51:35-8.
34. Borda, J. T., X. Alvarez, I. Kondova, P. Aye, M. A. Simon, R. C. Desrosiers, and A. A. Lackner. 2004. Cell tropism of simian immunodeficiency virus in culture is not predictive of in vivo tropism or pathogenesis. *Am J Pathol* 165:2111-22.

35. Brauner, A., Y. Lu, G. Hallden, B. Hylander, and J. Lundahl. 1998. Difference in the blood monocyte phenotype between uremic patients and healthy controls: its relation to monocyte differentiation into macrophages in the peritoneal cavity. *Inflammation* 22:55-66.
36. Brew, B. J. 1999. AIDS dementia complex. *Neurologic Clinics* 17:861-81.
37. Brew, B. J., and G. Dore. 2000. Decreasing incidence of CNS AIDS defining events associated with antiretroviral therapy. *Neurology* 55:1424.
38. Brew, B. J., M. Rosenblum, K. Cronin, and R. W. Price. 1995. AIDS dementia complex and HIV-1 brain infection: clinical-virological correlations [see comments]. *Annals of Neurology* 38:563-70.
39. Brinchmann, J. E., J. Albert, and F. Vartdal. 1991. Few infected CD4+ T cells but a high proportion of replication-competent provirus copies in asymptomatic human immunodeficiency virus type 1 infection. *J Virol* 65:2019-23.
40. Brooks, B. R., J. R. Swarz, and R. T. Johnson. 1980. Spongiform polioencephalomyelopathy caused by a murine retrovirus. I. Pathogenesis of infection in newborn mice. *Lab Invest* 43:480-6.
41. Brouwers, P., M. P. Heyes, H. A. Moss, P. L. Wolters, D. G. Poplack, S. P. Markey, and P. A. Pizzo. 1993. Quinolinic acid in the cerebrospinal fluid of children with symptomatic human immunodeficiency virus type 1 disease: relationships to clinical status and therapeutic response. *Journal of Infectious Diseases* 168:1380-6.
42. Budka, H. 1991. Neuropathology of human immunodeficiency virus infection. *Brain Pathology* 1:163-175.
43. Budka, H., G. Costanzi, S. Cristina, A. Lechi, C. Parravicini, R. Trabattoni, and L. Vago. 1987. Brain pathology induced by infection with the human immunodeficiency virus (HIV). A histological, immunocytochemical, and electron microscopical study of 100 autopsy cases. *Acta Neuropathol.(Berl)*. 75:185-198.
44. Budka, H., C. A. Wiley, P. Kleihues, J. Artigas, A. K. Asbury, E.-S. Cho, D. R. Cornblath, M. C. Dal Canto, U. DeGirolami, D. Dickson, L. G. Epstein, M. M. Esiri, F. Giangaspero, G. Gosztonyi, F. Gray, J. W. Griffin, D. Henin, Y. Iwasaki, R. S. Janssen, R. T. Johnson, P. L. Lantos, W. D. Lyman, J. C. McArthur, K. Nagashima, N. Peres, C. K. Petit, R. W. Price, R. H. Rhodes, M. Rosenblum, G. Said, F. Scaravilli, L. R. Sharer, and H. V. Vinters. 1991. HIV-associated disease of the nervous system: Review of nomenclature and proposal for neuropathology-based terminology. *Brain Pathology* 1:143-152.
45. Buechler, C., M. Ritter, E. Orso, T. Langmann, J. Klucken, and G. Schmitz. 2000. Regulation of scavenger receptor CD163 expression in human monocytes and macrophages by pro- and antiinflammatory stimuli. *J Leukoc Biol* 67:97-103.

46. Butcher, E. C., and L. J. Picker. 1996. Lymphocyte homing and homeostasis. *Science* 272:60-6.
47. Buttini, M., M. Orth, S. Bellosta, H. Akeefe, R. E. Pitas, T. Wyss-Coray, L. Mucke, and R. W. Mahley. 1999. Expression of human apolipoprotein E3 or E4 in the brains of Apoe^{-/-} mice: isoform-specific effects on neurodegeneration. *J Neurosci* 19:4867-80.
48. Buttner, A., P. Mehraein, and S. Weis. 1996. Vascular changes in the cerebral cortex in HIV-1 infection. II. An immunohistochemical and lectin histochemical investigation. *Acta Neuropathol (Berl)* 92:35-41.
49. Cameron, P. U., P. S. Freudenthal, J. M. Barker, S. Gezelter, K. Inaba, and R. M. Steinman. 1992. Dendritic cells exposed to human immunodeficiency virus type-1 transmit a vigorous cytopathic infection to CD4⁺ T cells. *Science* 257:383-7.
50. Cao, Y. Z., D. Dieterich, P. A. Thomas, Y. X. Huang, M. Mirabile, and D. D. Ho. 1992. Identification and quantitation of HIV-1 in the liver of patients with AIDS. *Aids* 6:65-70.
51. Carrington, M., G. W. Nelson, M. P. Martin, T. Kissner, D. Vlahov, J. J. Goedert, R. Kaslow, S. Buchbinder, K. Hoots, and S. J. O'Brien. 1999. HLA and HIV-1: heterozygote advantage and B*35-Cw*04 disadvantage. *Science* 283:1748-52.
52. Cebrian, M., E. Yague, M. Rincon, M. Lopez-Botet, M. O. de Landazuri, and F. Sanchez-Madrid. 1988. Triggering of T cell proliferation through AIM, an activation inducer molecule expressed on activated human lymphocytes. *J Exp Med* 168:1621-37.
53. Chackerian, B., L. M. Rudensey, and J. Overbaugh. 1997. Specific N-linked and O-linked glycosylation modifications in the envelope V1 domain of simian immunodeficiency virus variants that evolve in the host alter recognition by neutralizing antibodies. *J Virol* 71:7719-27.
54. Chakrabarti, L., M. Hurtrel, M. A. Maire, R. Vazeux, D. Dormont, L. Montagnier, and B. Hurtrel. 1991. Early viral replication in the brain of SIV-infected rhesus monkeys. *Am.J.Pathol.* 139:1273-1280.
55. Chakrabarti, L. A. 2004. The paradox of simian immunodeficiency virus infection in sooty mangabeys: active viral replication without disease progression. *Front Biosci* 9:521-39.
56. Chakrabarti, L. A., S. R. Lewin, L. Zhang, A. Gettie, A. Luckay, L. N. Martin, E. Skulsky, D. D. Ho, C. Cheng-Mayer, and P. A. Marx. 2000. Normal T-cell turnover in sooty mangabeys harboring active simian immunodeficiency virus infection. *J Virol* 74:1209-23.
57. Charman, H. P., S. Bladen, R. V. Gilden, and L. Coggins. 1976. Equine Infectious anemia virus: evidence favoring classification as a retrovirus. *J Virol* 19:1073-1079.

58. Cherner, M., E. Masliah, R. J. Ellis, T. D. Marcotte, D. J. Moore, I. Grant, and R. K. Heaton. 2002. Neurocognitive dysfunction predicts postmortem findings of HIV encephalitis. *Neurology* 59:1563-7.
59. Choudhary, S., K. Joshi, and K. D. Gill. 2001. Possible role of enhanced microtubule phosphorylation in dichlorvos induced delayed neurotoxicity in rat. *Brain Res* 897:60-70.
60. Chuluyan, H. E., and A. C. Issekutz. 1993. VLA-4 integrin can mediate CD11/CD18-independent transendothelial migration of human monocytes. *J Clin Invest* 92:2768-77.
61. Cinque, P., P. Scarpellini, L. Vago, A. Linde, and A. Lazzarin. 1997. Diagnosis Of Central Nervous System Complications In Hiv-Infected Patients - Cerebrospinal Fluid Analysis By the Polymerase Chain Reaction. *Aids* 11:1-17.
62. Cinque, P., L. Vago, D. Ceresa, F. Mainini, M. R. Terreni, A. Vagani, W. Torri, S. Bossolasco, and A. Lazzarin. 1998. Cerebrospinal fluid HIV-1 RNA levels: correlation with HIV encephalitis. *Aids* 12:389-394.
63. Cinque, P., L. Vago, M. Mengozzi, V. Torri, D. Ceresa, E. Vicenzi, P. Transidico, A. Vagani, S. Sozzani, A. Mantovani, A. Lazzarin, and G. Poli. 1998. Elevated cerebrospinal fluid levels of monocyte chemotactic protein-1 correlate with HIV-1 encephalitis and local viral replication. *Aids* 12:1327-32.
64. Clapham, P. R., and A. McKnight. 2002. Cell surface receptors, virus entry and tropism of primate lentiviruses. *J Gen Virol* 83:1809-29.
65. Clavel, F., D. Guetard, F. Brun-Vezinet, S. Chamaret, M. A. Rey, M. O. Santos-Ferreira, A. G. Laurent, C. Dauguet, C. Katlama, C. Rouzioux, and et al. 1986. Isolation of a new human retrovirus from West African patients with AIDS. *Science* 233:343-6.
66. Clements, J. E., T. Babas, J. L. Mankowski, K. Suryanarayana, M. J. Piatak, P. M. Tarwater, J. D. Lifson, and M. C. Zink. 2002. The central nervous system as a reservoir for simian immunodeficiency virus (SIV): steady-state levels of SIV DNA in brain from acute through asymptomatic infection. *J Infect Dis* 186:905-13.
67. Clynes, R., J. S. Maizes, R. Guinamard, M. Ono, T. Takai, and J. V. Ravetch. 1999. Modulation of immune complex-induced inflammation in vivo by the coordinate expression of activation and inhibitory Fc receptors. *J Exp Med* 189:179-85.
68. Coffin, J. M. 1996. Retroviridae: The viruses and their replication., p. 763-843. *In* B. N. Fields, D. M. Knipe, and P. M. Howley (ed.), *Fundamental Virology*, 3 ed. Lippincott-Raven, Philadelphia.
69. Coffin, J. M., M. Essex, R. Gallo, T. M. Graf, Y. Hinuma, E. Hunter, R. Jaenisch, R. Nusse, S. Oroszlan, J. Svoboda, N. Teich, K. Toyoshima, and H. Varmus. 2002. Presented at the International Committee on Taxonomy of Viruses.

70. Cohen, O., D. Weissman, and A. S. Fauci. 1999. *The Immunopathogenesis of HIV Infection*. Lippincott-Raven, Philadelphia.
71. Collman, R., N. F. Hassan, R. Walker, B. Godfrey, J. Cutilli, J. C. Hastings, H. Friedman, S. D. Douglas, and N. Nathanson. 1989. Infection of monocyte-derived macrophages with human immunodeficiency virus type 1 (HIV-1). Monocyte-tropic and lymphocyte-tropic strains of HIV-1 show distinctive patterns of replication in a panel of cell types. *J Exp Med* 170:1149-63.
72. Connor, R. I., and D. D. Ho. 1994. Human immunodeficiency virus type 1 variants with increased replicative capacity develop during the asymptomatic stage before disease progression. *J Virol* 68:4400-8.
73. Cosenza, M. A., M. L. Zhao, Q. Si, and S. C. Lee. 2002. Human brain parenchymal microglia express CD14 and CD45 and are productively infected by HIV-1 in HIV-1 encephalitis. *Brain Pathol* 12:442-55.
74. Crowe, S. M. 1995. Role of macrophages in the pathogenesis of human immunodeficiency virus (HIV) infection. *Australian & New Zealand Journal of Medicine* 25:777-83.
75. Czub, S., J. G. Muller, M. Czub, and H. K. Muller-Hermelink. 1996. Impact of various simian immunodeficiency virus variants on induction and nature of neuropathology in macaques. *Research in Virology* 147:165-70.
76. Dalgleish, A. G., P. C. Beverley, P. R. Clapham, D. H. Crawford, M. F. Greaves, and R. A. Weiss. 1984. The CD4 (T4) antigen is an essential component of the receptor for the AIDS retrovirus. *Nature* 312:763-7.
77. Dalpan, G. J., H. Farzadegan, O. Selnes, D. R. Hoover, E. N. Miller, R. L. Skolasky, T. E. Nancesproson, and J. C. McArthur. 1998. Sustained Cognitive Decline In Hiv Infection - Relationship to Cd4+ Cell Count, Plasma Viremia and P24 Antigenemia. *Journal of Neurovirology* 4:95-99.
78. Daniel, M. D., N. L. Letvin, N. W. King, M. Kannagi, P. K. Sehgal, R. D. Hunt, P. J. Kanki, M. Essex, and R. C. Desrosiers. 1985. Isolation of T-cell tropic HTLV-III-like retrovirus from macaques. *Science* 228:1201-4.
79. Davies, J., I. P. Everall, S. Weich, J. McLaughlin, F. Scaravilli, and P. L. Lantos. 1997. HIV-associated brain pathology in the United Kingdom: an epidemiological study. *AIDS* 11:1145-50.
80. Davis, L. E., B. L. Hjelle, V. E. Miller, D. L. Palmer, A. L. Llewellyn, T. L. Merlin, S. A. Young, R. G. Mills, W. Wachsmann, and C. A. Wiley. 1992. Early viral brain invasion in iatrogenic human immunodeficiency virus infection. *Neurology* 42:1736-9.

81. Dawson, V. L., T. M. Dawson, G. R. Uhl, and S. H. Snyder. 1993. Human immunodeficiency virus type 1 coat protein neurotoxicity mediated by nitric oxide in primary cortical cultures. *Proc Natl Acad Sci U S A* 90:3256-9.
82. Dean, M., M. Carrington, C. Winkler, G. A. Huttley, M. W. Smith, R. Allikmets, J. J. Goedert, S. P. Buchbinder, E. Vittinghoff, E. Gomperts, S. Donfield, D. Vlahov, R. Kaslow, A. Saah, C. Rinaldo, R. Detels, and S. J. O'Brien. 1996. Genetic restriction of HIV-1 infection and progression to AIDS by a deletion allele of the *CCR5* structural gene. Hemophilia Growth and Development Study, Multicenter AIDS Cohort Study, Multicenter Hemophilia Cohort Study, San Francisco City Cohort, ALIVE Study. *Science* 273:1856-62.
83. del Arco, A., M. A. Martinez, J. M. Pena, C. Gamallo, J. J. Gonzalez, F. J. Barbado, and J. J. Vazquez. 1993. Thrombotic thrombocytopenic purpura associated with human immunodeficiency virus infection: demonstration of p24 antigen in endothelial cells. *Clin Infect Dis* 17:360-3.
84. Deloire, M. S., T. Touil, B. Brochet, V. Dousset, J. M. Caille, and K. G. Petry. 2004. Macrophage brain infiltration in experimental autoimmune encephalomyelitis is not completely compromised by suppressed T-cell invasion: in vivo magnetic resonance imaging illustration in effective anti-VLA-4 antibody treatment. *Mult Scler* 10:540-8.
85. Demuth, M., S. Czub, U. Sauer, E. Koutsilieri, P. Haft, J. Heeney, C. Stahl-Hennig, V. ter Meulen, and S. Sopper. 2000. Relationship between viral load in blood, cerebrospinal fluid, brain tissue and isolated microglia with neurological disease in macaques infected with different strains of SIV. *J Neurovirol* 6:187-201.
86. Deng, H. K., R. Liu, W. Ellmeier, S. Choe, D. Unutmaz, M. Burkhart, P. Dimarzio, S. Marmon, R. E. Sutton, C. M. Hill, C. B. Davis, S. C. Peiper, T. J. Schall, D. R. Littman, and N. R. Landau. 1996. Identification Of a Major Co-Receptor For Primary Isolates Of Hiv-1. *Nature* 381:661-666.
87. Desrosiers, R. C., A. Hansen-Moosa, K. Mori, D. P. Bouvier, N. W. King, M. D. Daniel, and D. J. Ringler. 1991. Macrophage-tropic variants of SIV are associated with specific AIDS-related lesions but are not essential for the development of AIDS. *Am J Pathol* 139:29-35.
88. Dickson, D. W., S. C. Lee, L. A. Mattiace, S. H. Yen, and C. Brosnan. 1993. Microglia and cytokines in neurological disease, with special reference to AIDS and Alzheimer's disease. *Glia* 7:75-83.
89. Donaldson, Y. K., J. E. Bell, J. W. Ironside, R. P. Brettell, J. R. Robertson, A. Busuttill, and P. Simmonds. 1994. Redistribution of HIV outside the lymphoid system with onset of AIDS. *Lancet* 343:383-5.
90. Dore, G. J., P. K. Correll, Y. Li, J. M. Kaldor, D. A. Cooper, and B. J. Brew. 1999. Changes to AIDS dementia complex in the era of highly active antiretroviral therapy. *Aids* 13:1249-53.

91. Dragic, T., V. Litwin, G. P. Allaway, S. R. Martin, Y. X. Huang, K. A. Nagashima, C. Cayanan, P. J. Maddon, R. A. Koup, J. P. Moore, and W. A. Paxton. 1996. Hiv-1 Entry Into Cd4(+) Cells Is Mediated By the Chemokine Receptor Cc-Ckr-5. *Nature* 381:667-673.
92. Dreyer, E. B., P. K. Kaiser, J. T. Offermann, and S. A. Lipton. 1990. HIV-1 coat protein neurotoxicity prevented by calcium channel antagonists [see comments]. *Science* 248:364-367.
93. Dumonceaux, J., S. Nisole, C. Chanel, L. Quivet, A. Amara, F. Baleux, P. Briand, and U. Hazan. 1998. Spontaneous mutations in the env gene of the human immunodeficiency virus type 1 NDK isolate are associated with a CD4-independent entry phenotype. *Journal of Virology* 72:512-9.
94. Dunne, J., C. Feighery, and A. Whelan. 1996. Beta-2-microglobulin, neopterin and monocyte Fc gamma receptors in opportunistic infections of HIV-positive patients. *Br J Biomed Sci* 53:263-9.
95. Dykhuizen, M., J. L. Mitchen, D. C. Montefiori, J. Thomson, L. Acker, H. Lardy, and C. D. Pauza. 1998. Determinants of disease in the simian immunodeficiency virus-infected rhesus macaque: characterizing animals with low antibody responses and rapid progression. *J Gen Virol* 79 (Pt 10):2461-7.
96. Eastwood, S. L., P. W. Burnet, B. McDonald, J. Clinton, and P. J. Harrison. 1994. Synaptophysin gene expression in human brain: a quantitative in situ hybridization and immunocytochemical study. *Neuroscience* 59:881-92.
97. Ebert, L. M., P. Schaerli, and B. Moser. 2005. Chemokine-mediated control of T cell traffic in lymphoid and peripheral tissues. *Mol Immunol* 42:799-809.
98. Edinger, A. L., J. L. Mankowski, B. J. Doranz, B. J. Margulies, B. Lee, J. Rucker, M. Sharron, T. L. Hoffman, J. F. Berson, M. C. Zink, V. M. Hirsch, J. E. Clements, and R. W. Doms. 1997. CD4-independent, CCR5-dependent infection of brain capillary endothelial cells by a neurovirulent simian immunodeficiency virus strain. *Proceedings of the National Academy of Sciences of the United States of America* 94:14742-7.
99. Embretson, J., M. Zupancic, J. L. Ribas, A. Burke, P. Racz, R. K. Tenner, and A. T. Haase. 1993. Massive covert infection of helper T lymphocytes and macrophages by HIV during the incubation period of AIDS [see comments]. *Nature* 362:359-62.
100. Ensoli, F., A. Cafaro, V. Fiorelli, B. Vannelli, B. Ensoli, and C. J. Thiele. 1995. HIV-1 infection of primary human neuroblasts. *Virology* 210:221-5.
101. Epstein, L. G., J. Goudsmit, D. A. Paul, S. H. Morrison, E. M. Connor, J. M. Oleske, and B. Holland. 1987. Expression of human immunodeficiency virus in cerebrospinal fluid of children with progressive encephalopathy. *Ann Neurol* 21:397-401.

102. Overall, I., P. Luthert, and P. Lantos. 1993. A review of neuronal damage in human immunodeficiency virus infection: its assessment, possible mechanism and relationship to dementia. *J Neuropathol Exp Neurol* 52:561-6.
103. Overall, I. P., P. J. Luthert, and P. L. Lantos. 1991. Neuronal loss in the frontal cortex in HIV infection. *Lancet* 337:1119-1121.
104. Fauci, A. S. 1988. The human immunodeficiency virus: infectivity and mechanisms of pathogenesis. *Science* 239:617-22.
105. Feng, Y., C. C. Broder, P. E. Kennedy, and E. A. Berger. 1996. HIV-1 entry cofactor: functional cDNA cloning of a seven-transmembrane, G protein-coupled receptor. *Science* 272:872-7.
106. Fernandez, G. C., M. V. Ramos, S. A. Gomez, G. I. Dran, R. Exeni, M. Alduncin, I. Grimoldi, G. Vallejo, C. Elias-Costa, M. A. Isturiz, and M. S. Palermo. 2005. Differential expression of function-related antigens on blood monocytes in children with hemolytic uremic syndrome. *J Leukoc Biol* 78:853-61.
107. Fleuridor, R., B. Wilson, R. Hou, A. Landay, H. Kessler, and L. Al-Harthi. 2003. CD1d-restricted natural killer T cells are potent targets for human immunodeficiency virus infection. *Immunology* 108:3-9.
108. Freed, E. O. 1998. HIV-1 gag proteins: diverse functions in the virus life cycle. *Virology* 251:1-15.
109. Fuller, D. H., P. A. Rajakumar, L. A. Wilson, A. M. Trichel, J. T. Fuller, T. Shipley, M. S. Wu, K. Weis, C. R. Rinaldo, J. R. Haynes, and M. Murphey-Corb. 2002. Induction of mucosal protection against primary, heterologous simian immunodeficiency virus by a DNA vaccine. *J Virol* 76:3309-17.
110. Funke, I., A. Hahn, E. P. Rieber, E. Weiss, and G. Riethmuller. 1987. The cellular receptor (CD4) of the human immunodeficiency virus is expressed on neurons and glial cells in human brain. *J Exp Med* 165:1230-5.
111. Gabriel, H., A. Urhausen, L. Brechtel, H. J. Muller, and W. Kindermann. 1994. Alterations of regular and mature monocytes are distinct, and dependent of intensity and duration of exercise. *Eur J Appl Physiol Occup Physiol* 69:179-81.
112. Gallatin, W. M., I. L. Weissman, and E. C. Butcher. 1983. A cell-surface molecule involved in organ-specific homing of lymphocytes. *Nature* 304:30-4.
113. Gandhi, R. T., and B. D. Walker. 2002. Immunologic control of HIV-1. *Annu Rev Med* 53:149-72.
114. Gelbard, H. A., H. S. Nottet, S. Swindells, M. Jett, K. A. Dzenko, P. Genis, R. White, L. Wang, Y. B. Choi, D. Zhang, and et al. 1994. Platelet-activating factor: a candidate human immunodeficiency virus type 1-induced neurotoxin. *J Virol* 68:4628-35.

115. Gendelman, H. E., O. Narayan, S. Kennedy-Stoskopf, P. G. Kennedy, Z. Ghotbi, J. Clements, J. Stanley, and G. Pezeshkpour. 1986. Tropism of sheep lentiviruses for monocytes: susceptibility to infection and virus gene expression increase during maturation of monocytes to macrophages. *J Virol.* 58:67-74.
116. Gendelman, H. E., O. Narayan, S. Molineaux, J. E. Clements, and Z. Ghotbi. 1985. Slow, persistent replication of lentiviruses: role of tissue macrophages and macrophage precursors in bone marrow. *Proc Natl Acad Sci U S A* 82:7086-90.
117. Gendelman, H. E., Y. Persidsky, A. Ghorpade, J. Limoges, M. Stins, M. Fiala, and R. Morrisett. 1997. The neuropathogenesis of the AIDS dementia complex. *Aids* 11 Suppl A:S35-45.
118. Geraci, A. P., and D. M. Simpson. 2001. Neurological manifestations of HIV-1 infection in the HAART era. *Compr Ther* 27:232-41.
119. Gerber, J. S., and D. M. Mosser. 2001. Stimulatory and inhibitory signals originating from the macrophage Fcγ receptors. *Microbes Infect* 3:131-9.
120. Giovannoni, G., R. F. Miller, S. J. Heales, J. M. Land, M. J. Harrison, and E. J. Thompson. 1998. Elevated cerebrospinal fluid and serum nitrate and nitrite levels in patients with central nervous system complications of HIV-1 infection: a correlation with blood-brain-barrier dysfunction. *J Neurol Sci* 156:53-8.
121. Gisslen, M., D. Fuchs, B. Svennerholm, and L. Hagberg. 1999. Cerebrospinal fluid viral load, intrathecal immunoactivation, and cerebrospinal fluid monocytic cell count in HIV-1 infection. *J Acquir Immune Defic Syndr* 21:271-6.
122. Giulian, D., E. Wendt, K. Vaca, and C. A. Noonan. 1993. The envelope glycoprotein of human immunodeficiency virus type 1 stimulates release of neurotoxins from monocytes. *Proc Natl Acad Sci U S A* 90:2769-73.
123. Giulian, D., J. Yu, X. Li, D. Tom, J. Li, E. Wendt, S. N. Lin, R. Schwarcz, and C. Noonan. 1996. Study of receptor-mediated neurotoxins released by HIV-1-infected mononuclear phagocytes found in human brain. *Journal Of Neuroscience* 16:3139-3153.
124. Glass, J. D., H. Fedor, S. L. Wesselingh, and J. C. McArthur. 1995. Immunocytochemical quantitation of Human-Immunodeficiency-Virus in the brain - Correlations with dementia. *Annals of Neurology* 38:755-762.
125. Glass, J. D., S. L. Wesselingh, O. A. Selnes, and J. C. McArthur. 1993. Clinical-neuropathologic correlation in HIV-associated dementia. *Neurology* 43:2230-7.
126. Godiska, R., D. Chantry, C. J. Raport, S. Sozzani, P. Allavena, D. Leviten, A. Mantovani, and P. W. Gray. 1997. Human macrophage-derived chemokine (MDC), a novel chemoattractant for monocytes, monocyte-derived dendritic cells, and natural killer cells. *J Exp Med* 185:1595-604.

127. Goldstein, J. I., K. A. Goldstein, K. Wardwell, S. L. Fahrner, K. E. Goonan, M. D. Cheney, M. P. Yeager, and P. M. Guyre. 2003. Increase in plasma and surface CD163 levels in patients undergoing coronary artery bypass graft surgery. *Atherosclerosis* 170:325-32.
128. Goldstein, S., C. R. Brown, H. Dehghani, J. D. Lifson, and V. M. Hirsch. 2000. Intrinsic susceptibility of rhesus macaque peripheral CD4(+) T cells to simian immunodeficiency virus in vitro is predictive of in vivo viral replication. *Journal of Virology* 74:9388-95.
129. Gonzalez, E., H. Kulkarni, H. Bolivar, A. Mangano, R. Sanchez, G. Catano, R. J. Nibbs, B. I. Freedman, M. P. Quinones, M. J. Bamshad, K. K. Murthy, B. H. Rovin, W. Bradley, R. A. Clark, S. A. Anderson, J. O'Connell R, B. K. Agan, S. S. Ahuja, R. Bologna, L. Sen, M. J. Dolan, and S. K. Ahuja. 2005. The influence of CCL3L1 gene-containing segmental duplications on HIV-1/AIDS susceptibility. *Science* 307:1434-40.
130. Gonzalez, E., B. H. Rovin, L. Sen, G. Cooke, R. Dhanda, S. Mummidi, H. Kulkarni, M. J. Bamshad, V. Telles, S. A. Anderson, E. A. Walter, K. T. Stephan, M. Deucher, A. Mangano, R. Bologna, S. S. Ahuja, M. J. Dolan, and S. K. Ahuja. 2002. HIV-1 infection and AIDS dementia are influenced by a mutant MCP-1 allele linked to increased monocyte infiltration of tissues and MCP-1 levels. *Proc Natl Acad Sci U S A* 99:13795-800.
131. Gonzalez, R. G., L. L. Cheng, S. V. Westmoreland, K. E. Sakaie, L. R. Becerra, P. L. Lee, E. Masliah, and A. A. Lackner. 2000. Early brain injury in the SIV-macaque model of AIDS. *Aids* 14:2841-9.
132. Gonzalez-Scarano, F., and J. Martin-Garcia. 2005. The neuropathogenesis of AIDS. *Nat Rev Immunol* 5:69-81.
133. Gorry, P. R., G. Bristol, J. A. Zack, K. Ritola, R. Swanstrom, C. J. Birch, J. E. Bell, N. Bannert, K. Crawford, H. Wang, D. Schols, E. De Clercq, K. Kunstman, S. M. Wolinsky, and D. Gabuzda. 2001. Macrophage tropism of human immunodeficiency virus type 1 isolates from brain and lymphoid tissues predicts neurotropism independent of coreceptor specificity. *J Virol* 75:10073-89.
134. Gosztonyi, G., J. Artigas, L. Lamperth, and H. D. Webster. 1994. Human immunodeficiency virus (HIV) distribution in HIV encephalitis: study of 19 cases with combined use of in situ hybridization and immunocytochemistry. *J Neuropathol Exp Neurol* 53:521-34.
135. Gravel, C., D. G. Kay, and P. Jolicoeur. 1993. Identification of the infected target cell type in spongiform myeloencephalopathy induced by the neurotropic Cas-Br-E murine leukemia virus. *Journal of Virology* 67:6648-58.
136. Gray, F., H. Adle-Biassette, F. Chretien, G. Lorin de la Grandmaison, G. Force, and C. Keohane. 2001. Neuropathology and neurodegeneration in human immunodeficiency virus infection. Pathogenesis of HIV-induced lesions of the brain, correlations with HIV-

- associated disorders and modifications according to treatments. *Clin Neuropathol* 20:146-55.
137. Gray, F., F. Chretien, A. V. Vallat-Decouvelaere, and F. Scaravilli. 2003. The changing pattern of HIV neuropathology in the HAART era. *J Neuropathol Exp Neurol* 62:429-40.
 138. Griffin, D. E., S. L. Wesselingh, and J. C. McArthur. 1994. Elevated central nervous system prostaglandins in human immunodeficiency virus-associated dementia. *Annals of Neurology* 35:592-7.
 139. Harouse, J. M., C. Kunsch, H. T. Hartle, M. A. Laughlin, J. A. Hoxie, B. Wigdahl, and F. Gonzalez-Scarano. 1989. CD4-independent infection of human neural cells by human immunodeficiency virus type 1. *J Virol* 63:2527-33.
 140. Hayman, M., G. Arbuthnott, G. Harkiss, H. Brace, P. Filippi, V. Philippon, D. Thomson, R. Vigne, and A. Wright. 1993. Neurotoxicity of peptide analogues of the transactivating protein tat from Maedi-Visna virus and human immunodeficiency virus. *Neuroscience* 53:1-6.
 141. Henderson, A. J., and K. L. Calame. 1997. CCAAT/enhancer binding protein (C/EBP) sites are required for HIV-1 replication in primary macrophages but not CD4(+) T cells. *Proc Natl Acad Sci U S A* 94:8714-9.
 142. Heyes, M. P., K. Saito, A. Lackner, C. A. Wiley, C. L. Achim, and S. P. Markey. 1998. Sources of the neurotoxin quinolinic acid in the brain of HIV-1-infected patients and retrovirus-infected macaques. *Faseb J* 12:881-96.
 143. Hickey, W. F. 1999. Leukocyte traffic in the central nervous system: the participants and their roles. *Semin Immunol* 11:125-37.
 144. Hill, J. M., R. F. Mervis, R. Avidor, T. W. Moody, and D. E. Brenneman. 1993. HIV envelope protein-induced neuronal damage and retardation of behavioral development in rat neonates. *Brain Res* 603:222-33.
 145. Hirsch, V. M. 2004. What can natural infection of African monkeys with simian immunodeficiency virus tell us about the pathogenesis of AIDS? *AIDS Rev* 6:40-53.
 146. Hirsch, V. M., and P. R. Johnson. 1994. Pathogenic diversity of simian immunodeficiency viruses. *Virus Res* 32:183-203.
 147. Hodge, G., S. Hodge, C. Markus, A. Lawrence, and P. Han. 2003. A marked decrease in L-selectin expression by leucocytes in infants with *Bordetella pertussis* infection: leucocytosis explained? *Respirology* 8:157-62.
 148. Honda, Y., L. Rogers, K. Nakata, B. Y. Zhao, R. Pine, Y. Nakai, K. Kurosu, W. N. Rom, and M. Weiden. 1998. Type I interferon induces inhibitory 16-kD CCAAT/ enhancer binding protein (C/EBP)beta, repressing the HIV-1 long terminal repeat in macrophages:

- pulmonary tuberculosis alters C/EBP expression, enhancing HIV-1 replication. *J Exp Med* 188:1255-65.
149. Hsia, K., and S. A. Spector. 1991. Human immunodeficiency virus DNA is present in a high percentage of CD4⁺ lymphocytes of seropositive individuals. *J Infect Dis* 164:470-5.
 150. Huang, Y., W. A. Paxton, S. M. Wolinsky, A. U. Neumann, L. Zhang, T. He, S. Kang, D. Ceradini, Z. Jin, K. Yazdanbakhsh, K. Kunstman, D. Erickson, E. Dragon, N. R. Landau, J. Phair, D. D. Ho, and R. A. Koup. 1996. The role of a mutant CCR5 allele in HIV-1 transmission and disease progression. *Nat Med* 2:1240-3.
 151. Hume, D. A., I. L. Ross, S. R. Himes, R. T. Sasmono, C. A. Wells, and T. Ravasi. 2002. The mononuclear phagocyte system revisited. *J Leukoc Biol* 72:621-7.
 152. Israel, Z. R., G. A. Dean, D. H. Maul, S. P. O'Neil, M. J. Dreitz, J. I. Mullins, P. N. Fultz, and E. A. Hoover. 1993. Early pathogenesis of disease caused by SIVsmmPBj14 molecular clone 1.9 in macaques. *AIDS Res Hum Retroviruses* 9:277-86.
 153. Issekutz, A. C., and T. B. Issekutz. 1995. Monocyte migration to arthritis in the rat utilizes both CD11/CD18 and very late activation antigen 4 integrin mechanisms. *J Exp Med* 181:1197-203.
 154. Jin, X., D. E. Bauer, S. E. Tuttleton, S. Lewin, A. Gettie, J. Blanchard, C. E. Irwin, J. T. Safrit, J. Mittler, L. Weinberger, L. G. Kostrikis, L. Zhang, A. S. Perelson, and D. D. Ho. 1999. Dramatic rise in plasma viremia after CD8(+) T cell depletion in simian immunodeficiency virus-infected macaques. *Journal of Experimental Medicine* 189:991-8.
 155. Joag, S. V., E. B. Stephens, D. Galbreath, G. W. Zhu, Z. Li, L. Foresman, L. J. Zhao, D. M. Pinson, and O. Narayan. 1995. Simian immunodeficiency virus SIVmac chimeric virus whose env gene was derived from SIV-encephalitic brain is macrophage-tropic but not neurovirulent. *Journal of Virology* 69:1367-1369.
 156. Johnson, R. T. 1998. *Viral Infections of the Nervous System*. Raven Press, New York.
 157. Johnson, R. T., J. D. Glass, J. C. McArthur, and B. W. Chesebro. 1996. Quantitation of human immunodeficiency virus in brains of demented and nondemented patients with acquired immunodeficiency syndrome. *Annals of Neurology* 39:392-5.
 158. Jordan-Sciutto, K. L., G. Wang, M. Murphey-Corb, and C. A. Wiley. 2002. Cell cycle proteins exhibit altered expression patterns in lentiviral-associated encephalitis. *J Neurosci* 22:2185-95.
 159. Jordan-Sciutto, K. L., G. Wang, M. Murphey-Corb, and C. A. Wiley. 2000. Induction of cell cycle regulators in simian immunodeficiency virus encephalitis. *American Journal of Pathology* 157:497-507.

160. Kaiser, P. K., J. T. Offermann, and S. A. Lipton. 1990. Neuronal injury due to HIV-1 envelope protein is blocked by anti-gp120 antibodies but not by anti-CD4 antibodies. *Neurology* 40:1757-1761.
161. Katayama, K., T. Matsubara, M. Fujiwara, M. Koga, and S. Furukawa. 2000. CD14+CD16+ monocyte subpopulation in Kawasaki disease. *Clin Exp Immunol* 121:566-70.
162. Kaufmann, A., R. Salentin, D. Gemsa, and H. Sprenger. 2001. Increase of CCR1 and CCR5 expression and enhanced functional response to MIP-1 alpha during differentiation of human monocytes to macrophages. *J Leukoc Biol* 69:248-52.
163. Kaul, M., G. A. Garden, and S. A. Lipton. 2001. Pathways to neuronal injury and apoptosis in HIV-associated dementia. *Nature* 410:988-94.
164. Kawanaka, N., M. Yamamura, T. Aita, Y. Morita, A. Okamoto, M. Kawashima, M. Iwahashi, A. Ueno, Y. Ohmoto, and H. Makino. 2002. CD14+,CD16+ blood monocytes and joint inflammation in rheumatoid arthritis. *Arthritis Rheum* 46:2578-86.
165. Kennedy, P. G., O. Narayan, Z. Ghotbi, J. Hopkins, H. E. Gendelman, and J. E. Clements. 1985. Persistent expression of Ia antigen and viral genome in visna-maedi virus-induced inflammatory cells. Possible role of lentivirus-induced interferon. *J Exp Med* 162:1970-82.
166. Ketzler, S., S. Weis, H. Haug, and H. Budka. 1990. Loss of neurons in the frontal cortex in AIDS brains. *Acta Neuropathol (Berl)* 80:92-4.
167. Kilby, J. M., and J. J. Eron. 2003. Novel therapies based on mechanisms of HIV-1 cell entry. *N Engl J Med* 348:2228-38.
168. Kim, S. Y., R. Byrn, J. Groopman, and D. Baltimore. 1989. Temporal aspects of DNA and RNA synthesis during human immunodeficiency virus infection: evidence for differential gene expression. *J Virol* 63:3708-13.
169. Kim, W. K., S. Corey, G. Chesney, H. Knight, S. Klumpp, C. Wuthrich, N. Letvin, I. Koralnik, A. Lackner, R. Veasey, and K. Williams. 2004. Identification of T lymphocytes in simian immunodeficiency virus encephalitis: distribution of CD8+ T cells in association with central nervous system vessels and virus. *J Neurovirol* 10:315-25.
170. Kindt, T. J., V. M. Hirsch, P. R. Johnson, and S. Sawasdikosol. 1992. Animal models for acquired immunodeficiency syndrome. *Adv Immunol* 52:425-74.
171. Kirchhoff, F., T. C. Greenough, D. B. Brettler, J. L. Sullivan, and R. C. Desrosiers. 1995. Brief report: absence of intact nef sequences in a long-term survivor with nonprogressive HIV-1 infection. *N Engl J Med* 332:228-32.
172. Kivisakk, P., C. Trebst, Z. Liu, B. H. Tucky, T. L. Sorensen, R. A. Rudick, M. Mack, and R. M. Ransohoff. 2002. T-cells in the cerebrospinal fluid express a similar repertoire of

- inflammatory chemokine receptors in the absence or presence of CNS inflammation: implications for CNS trafficking. *Clin Exp Immunol* 129:510-8.
173. Klatzmann, D., E. Champagne, S. Chamaret, J. Gruest, D. Guetard, T. Hercend, J. C. Gluckman, and L. Montagnier. 1984. T-lymphocyte T4 molecule behaves as the receptor for human retrovirus LAV. *Nature* 312:767-8.
 174. Kleinschnitz, C., M. Bendszus, M. Frank, L. Solymosi, K. V. Toyka, and G. Stoll. 2003. In vivo monitoring of macrophage infiltration in experimental ischemic brain lesions by magnetic resonance imaging. *J Cereb Blood Flow Metab* 23:1356-61.
 175. Kodama, T., K. Mori, T. Kawahara, D. J. Ringler, and R. C. Desrosiers. 1993. Analysis of simian immunodeficiency virus sequence variation in tissues of rhesus macaques with simian AIDS. *J Virol* 67:6522-34.
 176. Kong, L. Y., B. C. Wilson, M. K. McMillian, G. Y. Bing, P. M. Hudson, and J. S. Hong. 1996. The Effects Of the Hiv-1 Envelope Protein Gp120 On the Production Of Nitric Oxide and Proinflammatory Cytokines In Mixed Glial Cell Cultures. *Cellular Immunology* 172:77-83.
 177. Kootstra, N. A., and H. Schuitemaker. 1998. Proliferation-Dependent Replication in Primary Macrophages of Macrophage-Tropic Hiv Type 1 Variants. *AIDS Research & Human Retroviruses* 14:339-345.
 178. Koup, R. A., J. T. Safrit, Y. Cao, C. A. Andrews, G. McLeod, W. Borkowsky, C. Farthing, and D. D. Ho. 1994. Temporal association of cellular immune responses with the initial control of viremia in primary human immunodeficiency virus type 1 syndrome. *J Virol* 68:4650-5.
 179. Koyanagi, Y., S. Miles, R. T. Mitsuyasu, J. E. Merrill, H. V. Vinters, and I. S. Chen. 1987. Dual infection of the central nervous system by AIDS viruses with distinct cellular tropisms. *Science* 236:819-822.
 180. Krivine, A., G. Force, J. Servan, A. Cabee, F. Rozenberg, L. Dighiero, F. Marguet, and P. Lebon. 1999. Measuring HIV-1 RNA and interferon-alpha in the cerebrospinal fluid of AIDS patients: insights into the pathogenesis of AIDS Dementia Complex. *Journal of Neurovirology* 5:500-6.
 181. Kure, K., K. M. Weidenheim, W. D. Lyman, and D. W. Dickson. 1990. Morphology and distribution of HIV-1 gp41-positive microglia in subacute AIDS encephalitis. Pattern of involvement resembling a multisystem degeneration. *Acta Neuropathol.(Berl)*. 80:393-400.
 182. Kurohori, Y., K. Sato, S. Suzuki, and S. Kashiwazaki. 1995. Adhesion molecule expression on peripheral blood mononuclear cells in rheumatoid arthritis: positive correlation between the proportion of L-selectin and disease activity. *Clin Rheumatol* 14:335-41.

183. Kusdra, L., D. McGuire, and L. Pulliam. 2002. Changes in monocyte/macrophage neurotoxicity in the era of HAART: implications for HIV-associated dementia. *Aids* 16:31-8.
184. Kusdra, L., H. Rempel, K. Yaffe, and L. Pulliam. 2000. Elevation of CD69+ monocyte/macrophages in patients with Alzheimer's disease. *Immunobiology* 202:26-33.
185. Kustova, Y., M. G. Espey, E. G. Sung, D. Morse, Y. Sei, and A. S. Basile. 1998. Evidence of neuronal degeneration in C57B1/6 mice infected with the LP-BM5 leukemia retrovirus mixture. *Mol Chem Neuropathol* 35:39-59.
186. Lackner, A. 1994. Pathology of simian immunodeficiency virus infection. *Curr Top Microbiol Immunol* 188:35-64.
187. Lackner, A. A., M. O. Smith, R. J. Munn, D. J. Martfeld, M. B. Gardner, P. A. Marx, and S. Dandekar. 1991. Localization of simian immunodeficiency virus in the central nervous system of rhesus monkeys. *Am J Pathol* 139:609-21.
188. Lane, J. H., V. G. Sasseville, M. O. Smith, P. Vogel, D. R. Pauley, M. P. Heyes, and A. A. Lackner. 1996. Neuroinvasion by simian immunodeficiency virus coincides with increased numbers of perivascular macrophages/microglia and intrathecal immune activation. *J Neurovirol* 2:423-32.
189. Langford, D., A. Adame, A. Grigorian, I. Grant, J. A. McCutchan, R. J. Ellis, T. D. Marcotte, and E. Masliah. 2003. Patterns of selective neuronal damage in methamphetamine-user AIDS patients. *J Acquir Immune Defic Syndr* 34:467-74.
190. Langford, T. D., S. L. Letendre, G. J. Larrea, and E. Masliah. 2003. Changing patterns in the neuropathogenesis of HIV during the HAART era. *Brain Pathol* 13:195-210.
191. Lavi, E., J. M. Strizki, A. M. Ulrich, W. Zhang, L. Fu, Q. Wang, M. O'Connor, J. A. Hoxie, and F. Gonzalez-Scarano. 1997. CXCR-4 (Fusin), a co-receptor for the type 1 human immunodeficiency virus (HIV-1), is expressed in the human brain in a variety of cell types, including microglia and neurons. *American Journal of Pathology* 151:1035-42.
192. Lee, E. S., D. Sarma, H. Zhou, and A. J. Henderson. 2002. CCAAT/enhancer binding proteins are not required for HIV-1 entry but regulate proviral transcription by recruiting coactivators to the long-terminal repeat in monocytic cells. *Virology* 299:20-31.
193. Levy, J. A. 1994. *HIV and the Pathogenesis of AIDS*. American Society for Microbiology, Washington, D.C.
194. Levy, J. A., C. E. Mackewicz, and E. Barker. 1996. Controlling HIV pathogenesis: the role of the noncytotoxic anti-HIV response of CD8+ T cells. *Immunol Today* 17:217-24.
195. Lifson, J. D., M. A. Nowak, S. Goldstein, J. L. Rossio, A. Kinter, G. Vasquez, T. A. Wiltout, C. Brown, D. Schneider, L. Wahl, A. L. Lloyd, J. Williams, W. R. Elkins, A. S. Fauci, and V. M. Hirsch. 1997. The extent of early viral replication is a critical

- determinant of the natural history of simian immunodeficiency virus infection. *J Virol* 71:9508-14.
196. Lipton, S. A. 1991. Calcium channel antagonists and human immunodeficiency virus coat protein-mediated neuronal injury. *Ann.Neurol.* 30:110-114.
 197. Lipton, S. A. 1993. Human immunodeficiency virus-infected macrophages, gp120, and N-methyl-D-aspartate receptor-mediated neurotoxicity [letter]. *Ann Neurol* 33:227-8.
 198. Lipton, S. A. 1992. Requirement for macrophages in neuronal injury induced by HIV envelope protein gp120. *Neuroreport* 3:913-5.
 199. Lipton, S. A., N. J. Sucher, P. K. Kaiser, and E. B. Dreyer. 1991. Synergistic effects of HIV coat protein and NMDA receptor-mediated neurotoxicity. *Neuron.* 7:111-118.
 200. Liu, N. Q., A. S. Lossinsky, W. Popik, X. Li, C. Gujuluva, B. Kriederman, J. Roberts, T. Pushkarsky, M. Bukrinsky, M. Witte, M. Weinand, and M. Fiala. 2002. Human immunodeficiency virus type 1 enters brain microvascular endothelia by macropinocytosis dependent on lipid rafts and the mitogen-activated protein kinase signaling pathway. *J Virol* 76:6689-700.
 201. Liu, S. L., T. Schacker, L. Musey, D. Shriner, M. J. McElrath, L. Corey, and J. I. Mullins. 1997. Divergent patterns of progression to AIDS after infection from the same source: human immunodeficiency virus type 1 evolution and antiviral responses. *J Virol* 71:4284-95.
 202. Livingstone, W. J., M. Moore, D. Innes, J. E. Bell, and P. Simmonds. 1996. Frequent infection of peripheral blood CD8-positive T-lymphocytes with HIV-1. Edinburgh Heterosexual Transmission Study Group. *Lancet* 348:649-54.
 203. Llansola, M., R. Saez, and V. Felipo. 2001. NMDA-induced phosphorylation of the microtubule-associated protein MAP-2 is mediated by activation of nitric oxide synthase and MAP kinase. *Eur J Neurosci* 13:1283-91.
 204. Lo, T. M., C. J. Fallert, T. M. Piser, and S. A. Thayer. 1992. HIV-1 envelope protein evokes intracellular calcium oscillations in rat hippocampal neurons. *Brain Res* 594:189-96.
 205. Lobb, R. R., and M. E. Hemler. 1994. The pathophysiologic role of alpha 4 integrins in vivo. *J Clin Invest* 94:1722-8.
 206. Lucia, B., C. Jennings, R. Cauda, L. Ortona, and A. L. Landay. 1995. Evidence of a selective depletion of a CD16+ CD56+ CD8+ natural killer cell subset during HIV infection. *Cytometry* 22:10-5.
 207. Mabrouk, K., J. Van Rietschoten, E. Vives, H. Darbon, H. Rochat, and J. M. Sabatier. 1991. Lethal neurotoxicity in mice of the basic domains of HIV and SIV Rev proteins. Study of these regions by circular dichroism. *FEBS Lett.* 289:13-17.

208. MacDonald, K. S., K. R. Fowke, J. Kimani, V. A. Dunand, N. J. Nagelkerke, T. B. Ball, J. Oyugi, E. Njagi, L. K. Gaur, R. C. Brunham, J. Wade, M. A. Luscher, P. Krausa, S. Rowland-Jones, E. Ngugi, J. J. Bwayo, and F. A. Plummer. 2000. Influence of HLA supertypes on susceptibility and resistance to human immunodeficiency virus type 1 infection. *J Infect Dis* 181:1581-9.
209. Maehlen, J., O. Dunlop, K. Liestol, J. H. Dobloug, A. K. Goplen, and A. Torvik. 1995. Changing incidence of HIV-induced brain lesions in Oslo, 1983-1994: effects of zidovudine treatment. *AIDS* 9:1165-1169.
210. Magnuson, D. S., B. E. Knudsen, J. D. Geiger, R. M. Brownstone, and A. Nath. 1995. Human immunodeficiency virus type 1 tat activates non-N-methyl-D-aspartate excitatory amino acid receptors and causes neurotoxicity. *Annals of Neurology* 37:373-80.
211. Mangeat, B., P. Turelli, G. Caron, M. Friedli, L. Perrin, and D. Trono. 2003. Broad antiretroviral defence by human APOBEC3G through lethal editing of nascent reverse transcripts. *Nature* 424:99-103.
212. Mankowski, J. L., J. E. Clements, and M. C. Zink. 2002. Searching for clues: tracking the pathogenesis of human immunodeficiency virus central nervous system disease by use of an accelerated, consistent simian immunodeficiency virus macaque model. *J Infect Dis* 186 Suppl 2:S199-208.
213. Mankowski, J. L., M. T. Flaherty, J. P. Spelman, D. A. Hauer, P. J. Didier, A. M. Amedee, M. Murphey-Corb, L. M. Kirstein, A. Munoz, J. E. Clements, and M. C. Zink. 1997. Pathogenesis of simian immunodeficiency virus encephalitis: viral determinants of neurovirulence. *Journal of Virology* 71:6055-60.
214. Marckmann, S., E. Wiesemann, R. Hilse, C. Trebst, M. Stangel, and A. Windhagen. 2004. Interferon-beta up-regulates the expression of co-stimulatory molecules CD80, CD86 and CD40 on monocytes: significance for treatment of multiple sclerosis. *Clin Exp Immunol* 138:499-506.
215. Marcondes, M. C., E. M. Burudi, S. Huitron-Resendiz, M. Sanchez-Alavez, D. Watry, M. Zandonatti, S. J. Henriksen, and H. S. Fox. 2001. Highly activated CD8(+) T cells in the brain correlate with early central nervous system dysfunction in simian immunodeficiency virus infection. *J Immunol* 167:5429-38.
216. Marras, D., L. A. Bruggeman, F. Gao, N. Tanji, M. M. Mansukhani, A. Cara, M. D. Ross, G. L. Gusella, G. Benson, V. D. D'Agati, B. H. Hahn, M. E. Klotman, and P. E. Klotman. 2002. Replication and compartmentalization of HIV-1 in kidney epithelium of patients with HIV-associated nephropathy. *Nat Med* 8:522-6.
217. Martin, K. A., R. Wyatt, M. Farzan, H. Choe, L. Marcon, E. Desjardins, J. Robinson, J. Sodroski, C. Gerard, and N. P. Gerard. 1997. CD4-independent binding of SIV gp120 to rhesus CCR5. *Science* 278:1470-3.

218. Martin, L. N., M. Murphey-Corb, P. Mack, G. B. Baskin, G. Pantaleo, M. Vaccarezza, C. H. Fox, and A. S. Fauci. 1997. Cyclosporin A modulation of early virologic and immunologic events during primary simian immunodeficiency virus infection in rhesus monkeys. *J Infect Dis* 176:374-83.
219. Martin, L. N., M. Murphey-Corb, K. F. Soike, B. Davison-Fairburn, and G. B. Baskin. 1993. Effects of initiation of 3'-azido,3'-deoxythymidine (zidovudine) treatment at different times after infection of rhesus monkeys with simian immunodeficiency virus. *Journal of Infectious Diseases* 168:825-35.
220. Martin, L. N., K. F. Soike, M. Murphey-Corb, R. P. Bohm, E. D. Roberts, T. J. Kakuk, S. Thaisrivongs, T. J. Vidmar, M. J. Ruwart, S. R. Davio, and W. G. Tarpley. 1994. Effects of U-75875, a peptidomimetic inhibitor of retroviral proteases, on simian immunodeficiency virus infection in rhesus monkeys. *Antimicrob Agents Chemother* 38:1277-83.
221. Martinez-Caceres, E. M., C. Espejo, L. Brieva, I. Pericot, M. Tintore, I. Saez-Torres, and X. Montalban. 2002. Expression of chemokine receptors in the different clinical forms of multiple sclerosis. *Mult Scler* 8:390-5.
222. Masliah, E., C. L. Achim, N. Ge, R. DeTeresa, R. D. Terry, and C. A. Wiley. 1992. Spectrum of human immunodeficiency virus-associated neocortical damage. *Annals of Neurology* 32:321-9.
223. Masliah, E., R. M. DeTeresa, M. E. Mallory, and L. A. Hansen. 2000. Changes in pathological findings at autopsy in AIDS cases for the last 15 years. *Aids* 14:69-74.
224. Masliah, E., N. Ge, C. L. Achim, R. DeTeresa, and C. A. Wiley. 1996. Patterns of neurodegeneration in HIV encephalitis. *Journal of NeuroAIDS* 1:161-173.
225. Masliah, E., N. Ge, and L. Mucke. 1996. Pathogenesis of HIV-1 associated neurodegeneration. *Critical Reviews in Neurobiology* 10:57-67.
226. Masliah, E., R. K. Heaton, T. D. Marcotte, R. J. Ellis, C. A. Wiley, M. Mallory, C. L. Achim, J. A. McCutchan, J. A. Nelson, J. H. Atkinson, and I. Grant. 1997. Dendritic injury is a pathological substrate for human immunodeficiency virus-related cognitive disorders. HNRC Group. The HIV Neurobehavioral Research Center. *Annals of Neurology* 42:963-72.
227. Masliah, E., M. Mallory, M. Alford, R. DeTeresa, L. A. Hansen, D. W. McKeel, Jr., and J. C. Morris. 2001. Altered expression of synaptic proteins occurs early during progression of Alzheimer's disease. *Neurology* 56:127-9.
228. Masliah, E., M. Mallory, L. Hansen, R. DeTeresa, M. Alford, and R. Terry. 1994. Synaptic and neuritic alterations during the progression of Alzheimer's disease. *Neurosci Lett* 174:67-72.

229. Masliah, E., R. D. Terry, M. Alford, and R. M. DeTeresa. 1990. Quantitative immunohistochemistry of synaptophysin in human neocortex: an alternative method to estimate density of presynaptic terminals in paraffin sections. *J Histochem.Cytochem.* 38:837-844.
230. Matesic, D. F., and R. C. Lin. 1994. Microtubule-associated protein 2 as an early indicator of ischemia-induced neurodegeneration in the gerbil forebrain. *J Neurochem* 63:1012-20.
231. Mazer, C., J. Muneyyirci, K. Taheny, N. Raio, A. Borella, and P. Whitaker-Azmitia. 1997. Serotonin depletion during synaptogenesis leads to decreased synaptic density and learning deficits in the adult rat: a possible model of neurodevelopmental disorders with cognitive deficits. *Brain Res* 760:68-73.
232. McArthur, J. C., D. R. McClernon, M. F. Cronin, T. E. Nance-Sproson, A. J. Saah, M. St Clair, and E. R. Lanier. 1997. Relationship between human immunodeficiency virus-associated dementia and viral load in cerebrospinal fluid and brain [see comments]. *Annals of Neurology* 42:689-98.
233. McArthur, J. C., D. R. McClernon, M. F. Cronin, T. E. Nance-Sproson, A. J. Saah, M. St.Clair, and E. R. Lanier. 1997. Relationship between human immunodeficiency virus-associated dementia and viral load in cerebrospinal fluid and brain. *Annals of Neurology* 42:689-698.
234. Medina-Flores, R., G. Wang, S. J. Bissel, M. Murphey-Corb, and C. A. Wiley. 2004. Destruction of extracellular matrix proteoglycans is pervasive in simian retroviral neuroinfection. *Neurobiol Dis* 16:604-16.
235. Meerschaert, J., and M. B. Furie. 1994. Monocytes use either CD11/CD18 or VLA-4 to migrate across human endothelium in vitro. *J Immunol* 152:1915-26.
236. Meier, U. C., R. E. Owen, E. Taylor, A. Worth, N. Naoumov, C. Willberg, K. Tang, P. Newton, P. Pellegrino, I. Williams, P. Klenerman, and P. Borrow. 2005. Shared alterations in NK cell frequency, phenotype, and function in chronic human immunodeficiency virus and hepatitis C virus infections. *J Virol* 79:12365-74.
237. Mellors, J. W., C. R. Rinaldo, P. Gupta, R. M. White, J. A. Todd, and L. A. Kingsley. 1996. Prognosis In HIV-1 infection predicted by the quantity of virus in plasma. *Science* 272:1167-1170.
238. Merrill, J. E., and I. S. Chen. 1991. HIV-1, macrophages, glial cells, and cytokines in AIDS nervous system disease. *FASEB Journal* 5:2391-2397.
239. Meucci, O., and R. J. Miller. 1996. Gp120-Induced Neurotoxicity In Hippocampal Pyramidal Neuron Cultures - Protective Action Of Tgf-Beta-1. *Journal of Neuroscience* 16:4080-4088.

240. Meyer, L., M. Magierowska, J. B. Hubert, C. Rouzioux, C. Deveau, F. Sanson, P. Debre, J. F. Delfraissy, and I. Theodorou. 1997. Early protective effect of CCR-5 delta 32 heterozygosity on HIV-1 disease progression: relationship with viral load. The SEROCO Study Group. *Aids* 11:F73-8.
241. Meyerhoff, D. J., M. W. Weiner, and G. Fein. 1996. Deep gray matter structures in HIV infection: a proton MR spectroscopic study. *Ajnr: American Journal of Neuroradiology* 17:973-8.
242. Michael, N. L., G. Chang, L. G. Louie, J. R. Mascola, D. Dondero, D. L. Birx, and H. W. Sheppard. 1997. The role of viral phenotype and CCR-5 gene defects in HIV-1 transmission and disease progression. *Nat Med* 3:338-40.
243. Michalet, X., F. F. Pinaud, L. A. Bentolila, J. M. Tsay, S. Doose, J. J. Li, G. Sundaresan, A. M. Wu, S. S. Gambhir, and S. Weiss. 2005. Quantum dots for live cells, in vivo imaging, and diagnostics. *Science* 307:538-44.
244. Monceaux, V., L. Viollet, F. Petit, R. Ho Tsong Fang, M. C. Cumont, J. Zaunders, B. Hurtrel, and J. Estaquier. 2005. CD8+ T cell dynamics during primary simian immunodeficiency virus infection in macaques: relationship of effector cell differentiation with the extent of viral replication. *J Immunol* 174:6898-908.
245. Moniuszko, M., C. Brown, R. Pal, E. Trynieszewska, W. P. Tsai, V. M. Hirsch, and G. Franchini. 2003. High frequency of virus-specific CD8+ T cells in the central nervous system of macaques chronically infected with simian immunodeficiency virus SIVmac251. *J Virol* 77:12346-51.
246. Montgomery, M. M., A. F. Dean, F. Taffs, E. J. Stott, P. L. Lantos, and P. J. Luthert. 1999. Progressive dendritic pathology in cynomolgus macaques infected with simian immunodeficiency virus. *Neuropathol Appl Neurobiol* 25:11-9.
247. Mook-Jung, I., H. S. Hong, J. H. Boo, K. H. Lee, S. H. Yun, M. Y. Cheong, I. Joo, K. Huh, and M. W. Jung. 2001. Ginsenoside Rb1 and Rg1 improve spatial learning and increase hippocampal synaptophysin level in mice. *J Neurosci Res* 63:509-15.
248. Moretta, A., A. Poggi, D. Pende, G. Tripodi, A. M. Orengo, N. Pella, R. Augugliaro, C. Bottino, E. Ciccone, and L. Moretta. 1991. CD69-mediated pathway of lymphocyte activation: anti-CD69 monoclonal antibodies trigger the cytolytic activity of different lymphoid effector cells with the exception of cytolytic T lymphocytes expressing T cell receptor alpha/beta. *J Exp Med* 174:1393-8.
249. Moses, A. V., F. E. Bloom, C. D. Pauza, and J. A. Nelson. 1993. Human immunodeficiency virus infection of human brain capillary endothelial cells occurs via a CD4/galactosylceramide-independent mechanism. *Proceedings of the National Academy of Sciences of the United States of America* 90:10474-8.
250. Moses, A. V., S. Williams, M. L. Heneveld, J. Strussenberg, M. Rarick, M. Loveless, G. Bagby, and J. A. Nelson. 1996. Human immunodeficiency virus infection of bone

- marrow endothelium reduces induction of stromal hematopoietic growth factors. *Blood* 87:919-25.
251. Murphey-Corb, M., L. N. Martin, S. R. Rangan, G. B. Baskin, B. J. Gormus, R. H. Wolf, W. A. Andes, M. West, and R. C. Montelaro. 1986. Isolation of an HTLV-III-related retrovirus from macaques with simian AIDS and its possible origin in asymptomatic mangabeys. *Nature* 321:435-7.
 252. Murray, E. A., D. M. Rausch, J. Lendvay, L. R. Sharer, and L. E. Eiden. 1992. Cognitive and motor impairments associated with SIV infection in rhesus monkeys. *Science* 255:1246-1249.
 253. Nagai, H., R. I. Fisher, J. Cossman, and J. J. Oppenheim. 1986. Decreased expression of class II major histocompatibility antigens on monocytes from patients with Hodgkin's disease. *J Leukoc Biol* 39:313-21.
 254. Nagai, H., M. B. Szein, P. S. Steeg, J. J. Hooks, J. J. Oppenheim, and A. D. Steinberg. 1984. Diminished peripheral blood monocyte DR antigen expression in systemic lupus erythematosus. *Clin Exp Rheumatol* 2:131-7.
 255. Naif, H. M., S. Li, M. Alali, J. Chang, C. Mayne, J. Sullivan, and A. L. Cunningham. 1999. Definition of the stage of host cell genetic restriction of replication of human immunodeficiency virus type 1 in monocytes and monocyte-derived macrophages by using twins. *J Virol* 73:4866-81.
 256. Narayan, O., D. Sheffer, J. Clements, and G. Tennekoon. 1985. Restricted replication of lentiviruses: visna viruses induce a unique interferon during interaction between lymphocytes and infected macrophages. *J.Exp.Med.* 162:1954-1969.
 257. Nath, A., R. A. Padua, and J. D. Geiger. 1995. Hiv-1 Coat Protein Gp120-Induced Increases In Levels Of Intrasyntosomal Calcium. *Brain Research* 678:200-206.
 258. Nath, A., K. Psooy, C. Martin, B. Knudsen, D. S. Magnuson, N. Haughey, and J. D. Geiger. 1996. Identification of a human immunodeficiency virus type 1 Tat epitope that is neuroexcitatory and neurotoxic. *J Virol* 70:1475-80.
 259. Navia, B. A., E. S. Cho, C. K. Petito, and R. W. Price. 1986. The AIDS dementia complex: II. Neuropathology. *Annals of Neurology* 19:525-535.
 260. Neil, S., F. Martin, Y. Ikeda, and M. Collins. 2001. Postentry restriction to human immunodeficiency virus-based vector transduction in human monocytes. *J Virol* 75:5448-56.
 261. Nelson, J. A., C. A. Wiley, C. Reynolds-Kohler, C. E. Reese, W. Margaretten, and J. A. Levy. 1988. Human immunodeficiency virus detected in bowel epithelium from patients with gastrointestinal symptoms. *Lancet* 1:259-62.

262. Nottet, H., D. R. Bar, H. van Hassel, J. Verhoef, and L. A. Boven. 1997. Cellular aspects of HIV-1 infection of macrophages leading to neuronal dysfunction in in vitro models for HIV-1 encephalitis. *Journal of Leukocyte Biology* 62:107-116.
263. Nottet, H., Y. Persidsky, V. G. Sasseville, A. N. Nukuna, P. Bock, Q. H. Zhai, L. R. Sharer, R. D. McComb, S. Swindells, C. Soderland, and H. E. Gendelman. 1996. Mechanisms For the Transendothelial Migration Of Hiv-1-Infected Monocytes Into Brain. *Journal Of Immunology* 156:1284-1295.
264. Nottet, H. S., D. R. Bar, H. van Hassel, J. Verhoef, and L. A. Boven. 1997. Cellular aspects of HIV-1 infection of macrophages leading to neuronal dysfunction in in vitro models for HIV-1 encephalitis. *Journal of Leukocyte Biology* 62:107-16.
265. Nottet, H. S., E. M. Flanagan, C. R. Flanagan, H. A. Gelbard, H. E. Gendelman, and J. F. Reinhard, Jr. 1996. The regulation of quinolinic acid in human immunodeficiency virus-infected monocytes. *Journal of Neurovirology* 2:111-7.
266. Nuovo, G. J., J. Becker, M. W. Burk, M. Margiotta, J. Fuhrer, and R. T. Steigbigel. 1994. In situ detection of PCR-amplified HIV-1 nucleic acids in lymph nodes and peripheral blood in patients with asymptomatic HIV-1 infection and advanced-stage AIDS. *J Acquir Immune Defic Syndr* 7:916-23.
267. Nuovo, G. J., F. Gallery, P. MacConnell, and A. Braun. 1994. In situ detection of polymerase chain reaction-amplified HIV-1 nucleic acids and tumor necrosis factor-alpha RNA in the central nervous system. *Am J Pathol* 144:659-66.
268. O'Neil, S. P., C. Suwyn, D. C. Anderson, G. Niedziela, J. Bradley, F. J. Novembre, J. G. Herndon, and H. M. McClure. 2004. Correlation of acute humoral response with brain virus burden and survival time in pig-tailed macaques infected with the neurovirulent simian immunodeficiency virus SIVsmmFGb. *Am J Pathol* 164:1157-72.
269. Oishi, K., M. Hayano, H. Yoshimine, S. B. Tugume, A. Kebba, R. Mugerwa, P. Mugenyi, A. Kumatori, K. Matsushima, and T. Nagatake. 2000. Expression of chemokine receptors on CD4+ T cells in peripheral blood from HIV-infected individuals in Uganda. *J Interferon Cytokine Res* 20:597-602.
270. Okamoto, H., K. Mizuno, and T. Horio. 2003. Circulating CD14+ CD16+ monocytes are expanded in sarcoidosis patients. *J Dermatol* 30:503-9.
271. Orenstein, J. M., M. S. Meltzer, T. Phipps, and H. E. Gendelman. 1988. Cytoplasmic assembly and accumulation of human immunodeficiency virus types 1 and 2 in recombinant human colony-stimulating factor-1-treated human monocytes: an ultrastructural study. *J Virol* 62:2578-86.
272. Otani, I., H. Akari, K. H. Nam, K. Mori, E. Suzuki, H. Shibata, K. Doi, K. Terao, and Y. Yosikawa. 1998. Phenotypic changes in peripheral blood monocytes of cynomolgus monkeys acutely infected with simian immunodeficiency virus. *AIDS Res Hum Retroviruses* 14:1181-6.

273. Overbaugh, J., A. D. Miller, and M. V. Eiden. 2001. Receptors and entry cofactors for retroviruses include single and multiple transmembrane-spanning proteins as well as newly described glycoposphatidylinositol-anchored and secreted proteins. *Microbiol Mol Biol Rev* 65:371-89, table of contents.
274. Panasiuk, A., J. Zak, E. Kasprzycka, K. Janicka, and D. Prokopowicz. 2005. Blood platelet and monocyte activations and relation to stages of liver cirrhosis. *World J Gastroenterol* 11:2754-8.
275. Pantaleo, G., and A. S. Fauci. 1996. Immunopathogenesis of HIV infection. *Ann Rev Microbiol* 50:825-854.
276. Pantaleo, G., C. Graziosi, J. F. Demarest, L. Butini, M. Montroni, C. H. Fox, J. M. Orenstein, D. P. Kotler, and A. S. Fauci. 1993. HIV infection is active and progressive in lymphoid tissue during the clinically latent stage of disease. *Nature* 362:355-8.
277. Paquette, Y., Z. Hanna, P. Savard, R. Brousseau, Y. Robitaille, and P. Jolicoeur. 1989. Retrovirus-induced murine motor neuron disease: mapping the determinant of spongiform degeneration within the envelope gene. *Proc Natl Acad Sci U S A* 86:3896-900.
278. Parren, P. W., J. P. Moore, D. R. Burton, and Q. J. Sattentau. 1999. The neutralizing antibody response to HIV-1: viral evasion and escape from humoral immunity. *Aids* 13 Suppl A:S137-62.
279. Patel, C. A., M. Mukhtar, and R. J. Pomerantz. 2000. Human immunodeficiency virus type 1 Vpr induces apoptosis in human neuronal cells. *J Virol* 74:9717-26.
280. Patterson, B. K., M. Till, P. Otto, C. Goolsby, M. R. Furtado, L. J. McBride, and S. M. Wolinsky. 1993. Detection of HIV-1 DNA and messenger RNA in individual cells by PCR-driven in situ hybridization and flow cytometry. *Science* 260:976-9.
281. Peluso, R., A. Haase, L. Stowring, M. Edwards, and P. Ventura. 1985. A Trojan Horse mechanism for the spread of visna virus in monocytes. *Virology* 147:231-236.
282. Persidsky, Y., A. Ghorpade, J. Rasmussen, J. Limoges, X. J. Liu, M. Stins, M. Fiala, D. Way, K. S. Kim, M. H. Witte, M. Weinand, L. Carhart, and H. E. Gendelman. 1999. Microglial and astrocyte chemokines regulate monocyte migration through the blood-brain barrier in human immunodeficiency virus-1 encephalitis. *American Journal of Pathology* 155:1599-611.
283. Petit, C. K., and K. S. Cash. 1992. Blood-brain barrier abnormalities in the acquired immunodeficiency syndrome: immunohistochemical localization of serum proteins in postmortem brain. *Ann Neurol* 32:658-66.
284. Petursson, G., N. Nathanson, G. Georgsson, H. Panitch, and P. A. Palsson. 1976. Pathogenesis of visna. I. Sequential virologic, serologic, and pathologic studies. *Lab Invest* 35:402-12.

285. Pietschmann, P., J. J. Cush, P. E. Lipsky, and N. Oppenheimer-Marks. 1992. Identification of subsets of human T cells capable of enhanced transendothelial migration. *J Immunol* 149:1170-8.
286. Portegies, P., R. H. Enting, J. de Gans, P. R. Algra, M. M. Derix, J. M. Lange, and J. Goudsmit. 1993. Presentation and course of AIDS dementia complex: 10 years of follow-up in Amsterdam, The Netherlands. *Aids* 7:669-75.
287. Power, C., P. A. Kong, T. O. Crawford, S. Wesselingh, J. D. Glass, J. C. McArthur, and B. D. Trapp. 1993. Cerebral white matter changes in acquired immunodeficiency syndrome dementia: alterations of the blood-brain barrier. *Annals of Neurology* 34:339-50.
288. Power, C., J. C. McArthur, R. T. Johnson, D. E. Griffin, J. D. Glass, S. Perryman, and B. Chesebro. 1994. Demented and nondemented patients with AIDS differ in brain-derived human-immunodeficiency-virus type-1 envelope sequences. *Journal of Virology* 68:4643-4649.
289. Power, C., J. C. McArthur, A. Nath, K. Wehrly, M. Mayne, J. Nishio, T. Langelier, R. T. Johnson, and B. Chesebro. 1998. Neuronal death induced by brain-derived human immunodeficiency virus type 1 envelope genes differs between demented and nondemented AIDS patients. *Journal of Virology* 72:9045-53.
290. Price, R. W. 1994. Understanding the AIDS dementia complex (ADC). The challenge of HIV and its effects on the central nervous system., p. 1-45. *In* R. W. Price and S. W. I. Perry (ed.), *HIV, AIDS, and the brain*. Raven Press, New York.
291. Price, R. W., B. Brew, J. Sidtis, M. Rosenblum, A. C. Scheck, and P. Cleary. 1988. The brain in AIDS: central nervous system HIV-1 infection and AIDS dementia complex. *Science* 239:586-592.
292. Psallidopoulos, M. C., S. M. Schnittman, L. M. Thompson, 3rd, M. Baseler, A. S. Fauci, H. C. Lane, and N. P. Salzman. 1989. Integrated proviral human immunodeficiency virus type 1 is present in CD4+ peripheral blood lymphocytes in healthy seropositive individuals. *J Virol* 63:4626-31.
293. Pulliam, L., J. A. Clarke, M. S. McGrath, D. Moore, and D. McGuire. 1996. Monokine products as predictors of AIDS dementia. *Aids* 10:1495-500.
294. Pulliam, L., J. A. Clarke, D. McGuire, and M. S. McGrath. 1994. Investigation of HIV-infected macrophage neurotoxin production from patients with AIDS dementia. *Advances in Neuroimmunology* 4:195-8.
295. Pulliam, L., R. Gascon, M. Stubblebine, D. McGuire, and M. S. McGrath. 1997. Unique monocyte subset in patients with AIDS dementia. *Lancet* 349:692-5.
296. Pulliam, L., B. G. Herndier, N. M. Tang, and M. S. McGrath. 1991. Human immunodeficiency virus-infected macrophages produce soluble factors that cause

- histological and neurochemical alterations in cultured human brains. *J.Clin.Invest.* 87:503-512.
297. Qin, S., J. B. Rottman, P. Myers, N. Kassam, M. Weinblatt, M. Loetscher, A. E. Koch, B. Moser, and C. R. Mackay. 1998. The chemokine receptors CXCR3 and CCR5 mark subsets of T cells associated with certain inflammatory reactions. *J Clin Invest* 101:746-54.
 298. Ranki, A., M. Nyberg, V. Ovod, M. Haltia, I. Elovaara, R. Raininko, H. Haapasalo, and K. Krohn. 1995. Abundant expression of HIV nef and rev proteins in brain astrocytes in vivo is associated with dementia. *AIDS* 9:1001-1008.
 299. Reece, J. C., A. J. Handley, E. J. Anstee, W. A. Morrison, S. M. Crowe, and P. U. Cameron. 1998. HIV-1 selection by epidermal dendritic cells during transmission across human skin. *J Exp Med* 187:1623-31.
 300. Reinhart, T. A., M. J. Rogan, D. Huddleston, D. M. Rausch, L. E. Eiden, and A. T. Haase. 1997. Simian immunodeficiency virus burden in tissues and cellular compartments during clinical latency and AIDS. *Journal of Infectious Diseases* 176:1198-1208.
 301. Reitter, J. N., R. E. Means, and R. C. Desrosiers. 1998. A role for carbohydrates in immune evasion in AIDS. *Nat Med* 4:679-84.
 302. Resnick, L., J. R. Berger, P. Shapshak, and W. W. Tourtelotte. 1988. Early penetration of the blood-brain-barrier by HIV. *Neurology* 38:9-14.
 303. Rich, E. A., I. S. Chen, J. A. Zack, M. L. Leonard, and W. A. O'Brien. 1992. Increased susceptibility of differentiated mononuclear phagocytes to productive infection with human immunodeficiency virus-1 (HIV-1). *J Clin Invest* 89:176-83.
 304. Rivier, A., J. Pene, H. Rabesandratana, P. Chanez, J. Bousquet, and A. M. Campbell. 1995. Blood monocytes of untreated asthmatics exhibit some features of tissue macrophages. *Clin Exp Immunol* 100:314-8.
 305. Robison, P. M., J. A. Clemens, E. B. Smalstig, D. Stephenson, and P. C. May. 1993. Decrease in amyloid precursor protein precedes hippocampal degeneration in rat brain following transient global ischemia. *Brain Res* 608:334-7.
 306. Rodriguez, E. R., S. Nasim, J. Hsia, R. L. Sandin, A. Ferreira, B. A. Hilliard, A. M. Ross, and C. T. Garrett. 1991. Cardiac myocytes and dendritic cells harbor human immunodeficiency virus in infected patients with and without cardiac dysfunction: detection by multiplex, nested, polymerase chain reaction in individually microdissected cells from right ventricular endomyocardial biopsy tissue. *Am J Cardiol* 68:1511-20.
 307. Rosen, S. D. 2004. Ligands for L-selectin: homing, inflammation, and beyond. *Annu Rev Immunol* 22:129-56.

308. Rosenberg, Y. J., P. M. Zack, B. D. White, S. F. Papermaster, W. R. Elkins, G. A. Eddy, and M. G. Lewis. 1993. Decline in the CD4⁺ lymphocyte population in the blood of SIV-infected macaques is not reflected in lymph nodes. *AIDS Res Hum Retroviruses* 9:639-46.
309. Ross, M. D., L. A. Bruggeman, B. Hanss, M. Sunamoto, D. Marras, M. E. Klotman, and P. E. Klotman. 2003. Podocan, a novel small leucine-rich repeat protein expressed in the sclerotic glomerular lesion of experimental HIV-associated nephropathy. *J Biol Chem* 278:33248-55.
310. Rottman, J. B., K. P. Ganley, K. Williams, L. Wu, C. R. Mackay, and D. J. Ringler. 1997. Cellular localization of the chemokine receptor CCR5. Correlation to cellular targets of HIV-1 infection. *Am J Pathol* 151:1341-51.
311. Sabatier, J. M., E. Vives, K. Mabrouk, A. Benjouad, H. Rochat, A. Duval, B. Hue, and E. Bahraoui. 1991. Evidence for neurotoxic activity of tat from human immunodeficiency virus type 1. *J Virol.* 65:961-967.
312. Sacktor, N., R. H. Lyles, R. Skolasky, C. Kleeberger, O. A. Selnes, E. N. Miller, J. T. Becker, B. Cohen, and J. C. McArthur. 2001. HIV-associated neurologic disease incidence changes: Multicenter AIDS Cohort Study, 1990-1998. *Neurology* 56:257-60.
313. Sacktor, N., M. P. McDermott, K. Marder, G. Schifitto, O. A. Selnes, J. C. McArthur, Y. Stern, S. Albert, D. Palumbo, K. Kiebertz, J. A. De Marcaida, B. Cohen, and L. Epstein. 2002. HIV-associated cognitive impairment before and after the advent of combination therapy. *J Neurovirol* 8:136-42.
314. Saito, S., S. Kobayashi, Y. Ohashi, M. Igarashi, Y. Komiya, and S. Ando. 1994. Decreased synaptic density in aged brains and its prevention by rearing under enriched environment as revealed by synaptophysin contents. *J Neurosci Res* 39:57-62.
315. Saland, L. C., D. Thomas, M. Morales, and J. Gaddy. 1998. Synaptophysin immunoreactivity in the rat pituitary: alterations after 6-hydroxydopamine treatment. *Endocrine* 9:201-6.
316. Samson, M., F. Libert, B. J. Doranz, J. Rucker, C. Liesnard, C. M. Farber, S. Saragosti, C. Lapoumeroulie, J. Cognaux, C. Forceille, G. Muyldermans, C. Verhofstede, G. Burtonboy, M. Georges, T. Imai, S. Rana, Y. Yi, R. J. Smyth, R. G. Collman, R. W. Doms, G. Vassart, and M. Parmentier. 1996. Resistance to HIV-1 infection in caucasian individuals bearing mutant alleles of the CCR-5 chemokine receptor gene. *Nature* 382:722-5.
317. Sanders, V. J., C. A. Pittman, M. G. White, W. G., C. A. Wiley, and C. L. Achim. 1998. Chemokines and receptors in HIV encephalitis. *AIDS* 12:1021-1026.
318. Sasseville, V. G., W. Newman, S. J. Brodie, P. Hesterberg, D. Pauley, and D. J. Ringler. 1994. Monocyte adhesion to endothelium in simian immunodeficiency virus-induced aids

- encephalitis is mediated by vascular cell-adhesion molecule-1/ α -4- β -1 integrin interactions. *American Journal Of Pathology* 144:27-40.
319. Sathler-Avelar, R., E. M. Lemos, D. D. Reis, N. Medrano-Mercado, T. C. Araujo-Jorge, P. R. Antas, R. Correa-Oliveira, A. Teixeira-Carvalho, S. M. Eloi-Santos, D. Favato, and O. A. Martins-Filho. 2003. Phenotypic features of peripheral blood leucocytes during early stages of human infection with *Trypanosoma cruzi*. *Scand J Immunol* 58:655-63.
 320. Savio, T., and G. Levi. 1993. Neurotoxicity of HIV coat protein gp120, NMDA receptors, and protein kinase C: a study with rat cerebellar granule cell cultures. *J Neurosci Res* 34:265-72.
 321. Schacker, T., S. Little, E. Connick, K. Gebhard, Z. Q. Zhang, J. Krieger, J. Pryor, D. Havlir, J. K. Wong, R. T. Schooley, D. Richman, L. Corey, and A. T. Haase. 2001. Productive infection of T cells in lymphoid tissues during primary and early human immunodeficiency virus infection. *J Infect Dis* 183:555-62.
 322. Schlitt, A., G. H. Heine, S. Blankenberg, C. Espinola-Klein, J. F. Dopheide, C. Bickel, K. J. Lackner, M. Iz, J. Meyer, H. Darius, and H. J. Rupprecht. 2004. CD14+CD16+ monocytes in coronary artery disease and their relationship to serum TNF-alpha levels. *Thromb Haemost* 92:419-24.
 323. Schmitz, J. E., M. J. Kuroda, S. Santra, V. G. Sasseville, M. A. Simon, M. A. Lifton, P. Racz, K. Tenner-Racz, M. Dalesandro, B. J. Scallon, J. Ghrayeb, M. A. Forman, D. C. Montefiori, E. P. Rieber, N. L. Letvin, and K. A. Reimann. 1999. Control of viremia in simian immunodeficiency virus infection by CD8+ lymphocytes. *Science* 283:857-60.
 324. Schmitz, J. E., M. A. Simon, M. J. Kuroda, M. A. Lifton, M. W. Ollert, C. W. Vogel, P. Racz, K. Tenner-Racz, B. J. Scallon, M. Dalesandro, J. Ghrayeb, E. P. Rieber, V. G. Sasseville, and K. A. Reimann. 1999. A nonhuman primate model for the selective elimination of CD8+ lymphocytes using a mouse-human chimeric monoclonal antibody. *American Journal of Pathology* 154:1923-32.
 325. Schnittman, S. M., M. C. Psallidopoulos, H. C. Lane, L. Thompson, M. Baseler, F. Massari, C. H. Fox, N. P. Salzman, and A. S. Fauci. 1989. The reservoir for HIV-1 in human peripheral blood is a T cell that maintains expression of CD4. *Science* 245:305-8.
 326. Schuitemaker, H. 1994. Macrophage-tropic HIV-1 variants: initiators of infection and AIDS pathogenesis? *Journal of Leukocyte Biology* 56:218-24.
 327. Sei, Y., P. H. Tsang, F. N. Chu, I. Wallace, J. P. Roboz, P. S. Sarin, and J. G. Bekesi. 1989. Inverse relationship between HIV-1 p24 antigenemia, anti-p24 antibody and neutralizing antibody response in all stages of HIV-1 infection. *Immunol Lett* 20:223-30.
 328. Seidman, R., N. S. Peress, and G. J. Nuovo. 1994. In situ detection of polymerase chain reaction-amplified HIV-1 nucleic acids in skeletal muscle in patients with myopathy. *Mod Pathol* 7:369-75.

329. Seman, A. L., W. F. Pewen, L. F. Fresh, L. N. Martin, and M. Murphey-Corb. 2000. The replicative capacity of rhesus macaque peripheral blood mononuclear cells for simian immunodeficiency virus in vitro is predictive of the rate of progression to AIDS in vivo. *J Gen Virol* 81:2441-9.
330. Shang, X. Z., and A. C. Issekutz. 1998. Contribution of CD11a/CD18, CD11b/CD18, ICAM-1 (CD54) and -2 (CD102) to human monocyte migration through endothelium and connective tissue fibroblast barriers. *Eur J Immunol* 28:1970-9.
331. Shapshak, P., D. M. Segal, K. A. Crandall, R. K. Fujimura, B. T. Zhang, K. Q. Xin, K. Okuda, C. K. Petito, C. Eisdorfer, and K. Goodkin. 1999. Independent evolution of HIV type 1 in different brain regions. *AIDS Res Hum Retroviruses* 15:811-20.
332. Sharer, L. R., E. S. Cho, and L. G. Epstein. 1985. Multinucleated giant cells and HTLV-III in AIDS encephalopathy. *Hum Pathol* 16:760.
333. Sharer, L. R., J. Michaels, C. M. Murphey, F. S. Hu, D. J. Kuebler, L. N. Martin, and G. B. Baskin. 1991. Serial pathogenesis study of SIV brain infection. *J Med Primatol* 20:211-7.
334. Shi, B., J. Raina, A. Lorenzo, J. Busciglio, and D. Gabuzda. 1998. Neuronal apoptosis induced by HIV-1 Tat protein and TNF-alpha: potentiation of neurotoxicity mediated by oxidative stress and implications for HIV-1 dementia. *Journal of Neurovirology* 4:281-90.
335. Shieh, T. M., D. L. Carter, R. L. Blosser, J. L. Mankowski, M. C. Zink, and J. E. Clements. 2001. Functional analyses of natural killer cells in macaques infected with neurovirulent simian immunodeficiency virus. *J Neurovirology* 7:11-24.
336. Shin, H. D., C. Winkler, J. C. Stephens, J. Bream, H. Young, J. J. Goedert, T. R. O'Brien, D. Vlahov, S. Buchbinder, J. Giorgi, C. Rinaldo, S. Donfield, A. Willoughby, S. J. O'Brien, and M. W. Smith. 2000. Genetic restriction of HIV-1 pathogenesis to AIDS by promoter alleles of IL10. *Proc Natl Acad Sci U S A* 97:14467-72.
337. Silvestri, G., D. L. Sodora, R. A. Koup, M. Paiardini, S. P. O'Neil, H. M. McClure, S. I. Staprans, and M. B. Feinberg. 2003. Nonpathogenic SIV infection of sooty mangabeys is characterized by limited bystander immunopathology despite chronic high-level viremia. *Immunity* 18:441-52.
338. Simmonds, P., P. Balfe, J. F. Peutherer, C. A. Ludlam, J. O. Bishop, and A. J. Brown. 1990. Human immunodeficiency virus-infected individuals contain provirus in small numbers of peripheral mononuclear cells and at low copy numbers. *J Virol* 64:864-72.
339. Smith, M. Z., Z. Nagy, L. Barnetson, E. M. King, and M. M. Esiri. 2000. Coexisting pathologies in the brain: influence of vascular disease and Parkinson's disease on Alzheimer's pathology in the hippocampus. *Acta Neuropathol (Berl)* 100:87-94.

340. Smith, S. M., B. Holland, C. Russo, P. J. Dailey, P. A. Marx, and R. I. Connor. 1999. Retrospective analysis of viral load and SIV antibody responses in rhesus macaques infected with pathogenic SIV: predictive value for disease progression. *AIDS Res Hum Retroviruses* 15:1691-701.
341. Sonnerborg, A. B., A. C. Ehrnst, S. K. Bergdahl, P. O. Pehrson, B. R. Skoldenberg, and O. O. Strannegard. 1988. HIV isolation from cerebrospinal fluid in relation to immunological deficiency and neurological symptoms. *AIDS* 2:89-93.
342. Sonza, S., A. Maerz, N. Deacon, J. Meanger, J. Mills, and S. Crowe. 1996. Human Immunodeficiency Virus Type 1 Replication Is Blocked Prior to Reverse Transcription and Integration In Freshly Isolated Peripheral Blood Monocytes. *Journal of Virology* 70:3863-3869.
343. Soontornniyomkij, V., J. A. Nieto-Rodriguez, A. J. Martinez, L. A. Kingsley, A. C.L., and C. A. Wiley. 1998. Brain HIV burden and length of survival after AIDS diagnosis. *Clinical Neuropathology* 17:95-99.
344. Sopper, S., U. Sauer, S. Hemm, M. Demuth, J. Muller, C. Stahl-Hennig, G. Hunsmann, V. ter Meulen, and R. Dorries. 1998. Protective role of the virus-specific immune response for development of severe neurologic signs in simian immunodeficiency virus-infected macaques. *Journal of Virology* 72:9940-7.
345. Spencer, D. C., and R. W. Price. 1992. Human immunodeficiency virus and the central nervous system. [Review]. *Annual Review of Microbiology* 46:655-93.
346. Stahl-Hennig, C., R. M. Steinman, K. Tenner-Racz, M. Pope, N. Stolte, K. Matz-Rensing, G. Grobschupff, B. Raschdorff, G. Hunsmann, and P. Racz. 1999. Rapid infection of oral mucosal-associated lymphoid tissue with simian immunodeficiency virus. *Science* 285:1261-5.
347. Staprans, S. I., P. J. Dailey, A. Rosenthal, C. Horton, R. M. Grant, N. Lerche, and M. B. Feinberg. 1999. Simian immunodeficiency virus disease course is predicted by the extent of virus replication during primary infection. *J Virol* 73:4829-39.
348. Stevenson, M. 2003. HIV-1 pathogenesis. *Nat Med* 9:853-60.
349. Strelow, L. I., D. D. Watry, H. S. Fox, and J. A. Nelson. 1998. Efficient infection of brain microvascular endothelial cells by an in vivo-selected neuroinvasive SIVmac variant. *Journal of Neurovirology* 4:269-80.
350. Stremlau, M., C. M. Owens, M. J. Perron, M. Kiessling, P. Autissier, and J. Sodroski. 2004. The cytoplasmic body component TRIM5alpha restricts HIV-1 infection in Old World monkeys. *Nature* 427:848-53.
351. Stroh, M., J. P. Zimmer, D. G. Duda, T. S. Levchenko, K. S. Cohen, E. B. Brown, D. T. Scadden, V. P. Torchilin, M. G. Bawendi, D. Fukumura, and R. K. Jain. 2005. Quantum

- dots spectrally distinguish multiple species within the tumor milieu in vivo. *Nat Med* 11:678-82.
352. Subbramanian, R. A., A. Kessous-Elbaz, R. Lodge, J. Forget, X. J. Yao, D. Bergeron, and E. A. Cohen. 1998. Human immunodeficiency virus type 1 Vpr is a positive regulator of viral transcription and infectivity in primary human macrophages. *J Exp Med* 187:1103-11.
 353. Swingler, S., B. Brichacek, J. M. Jacque, C. Ulich, J. Zhou, and M. Stevenson. 2003. HIV-1 Nef intersects the macrophage CD40L signalling pathway to promote resting-cell infection. *Nature* 424:213-9.
 354. Takahashi, K., S. L. Wesselingh, D. E. Griffin, J. C. McArthur, J. R.T., and G. J.D. 1996. Localization of HIV-1 in human brain using PCR/in situ hybridization and immunocytochemistry. *Annals of Neurology*.
 355. Tanaka, S., M. Saito, M. Morimatsu, and E. Ohama. 2000. Immunohistochemical studies of the PrP(CJD) deposition in Creutzfeldt-Jakob disease. *Neuropathology* 20:124-33.
 356. Tarazona, R., J. G. Casado, O. Delarosa, J. Torre-Cisneros, J. L. Villanueva, B. Sanchez, M. D. Galiani, R. Gonzalez, R. Solana, and J. Pena. 2002. Selective depletion of CD56(dim) NK cell subsets and maintenance of CD56(bright) NK cells in treatment-naive HIV-1-seropositive individuals. *J Clin Immunol* 22:176-83.
 357. Temin, H. M. 1992. Origin and General Nature of Retroviruses., p. 1-17. *In* J. A. Levy (ed.), *The Retroviridae*, vol. 1. Plenum Press, New York.
 358. Temin, H. M., and D. Baltimore. 1972. RNA-directed DNA synthesis and RNA tumor viruses. *Adv Virus Res* 17:129-86.
 359. Temin, H. M., and S. Mizutani. 1970. RNA-dependent DNA polymerase in virions of Rous sarcoma virus. *Nature* 226:1211-3.
 360. Teo, I., C. Veryard, H. Barnes, S. F. An, M. Jones, P. L. Lantos, P. Luthert, and S. Shaunak. 1997. Circular forms of unintegrated human immunodeficiency virus type 1 DNA and high levels of viral protein expression: association with dementia and multinucleated giant cells in the brains of patients with AIDS. *Journal of Virology* 71:2928-33.
 361. Testi, R., D. D'Ambrosio, R. De Maria, and A. Santoni. 1994. The CD69 receptor: a multipurpose cell-surface trigger for hematopoietic cells. *Immunol Today* 15:479-83.
 362. Thieblemont, N., L. Weiss, H. M. Sadeghi, C. Estcourt, and N. Haeffner-Cavaillon. 1995. CD14^{low}CD16^{high}: a cytokine-producing monocyte subset which expands during human immunodeficiency virus infection. *Eur J Immunol* 25:3418-24.
 363. Tornatore, C., R. Chandra, J. R. Berger, and E. O. Major. 1994. HIV-1 infection of subcortical astrocytes in the pediatric central-nervous-system. *Neurology* 44:481-487.

364. Torres-Munoz, J., P. Stockton, N. Tacoronte, B. Roberts, R. R. Maronpot, and C. K. Petito. 2001. Detection of HIV-1 gene sequences in hippocampal neurons isolated from postmortem AIDS brains by laser capture microdissection. *J Neuropathol Exp Neurol* 60:885-92.
365. Trebst, C., T. L. Sorensen, P. Kivisakk, M. K. Cathcart, J. Hesselgesser, R. Horuk, F. Sellebjerg, H. Lassmann, and R. M. Ransohoff. 2001. CCR1+/CCR5+ mononuclear phagocytes accumulate in the central nervous system of patients with multiple sclerosis. *Am J Pathol* 159:1701-10.
366. Trebst, C., S. M. Staugaitis, B. Tucky, T. Wei, K. Suzuki, K. D. Aldape, C. A. Pardo, J. Troncoso, H. Lassmann, and R. M. Ransohoff. 2003. Chemokine receptors on infiltrating leucocytes in inflammatory pathologies of the central nervous system (CNS). *Neuropathol Appl Neurobiol* 29:584-95.
367. Trichel, A. M., P. A. Rajakumar, and M. Murphey-Corb. 2002. Species-specific variation in SIV disease progression between Chinese and Indian subspecies of rhesus macaque. *J Med Primatol* 31:171-8.
368. Tridandapani, S., K. Siefker, J. L. Teillaud, J. E. Carter, M. D. Wewers, and C. L. Anderson. 2002. Regulated expression and inhibitory function of Fcgamma RIIb in human monocytic cells. *J Biol Chem* 277:5082-9.
369. Trillo-Pazos, G., A. Diamanturos, L. Rislove, T. Menza, W. Chao, P. Belem, S. Sadiq, S. Morgello, L. Sharer, and D. J. Volsky. 2003. Detection of HIV-1 DNA in microglia/macrophages, astrocytes and neurons isolated from brain tissue with HIV-1 encephalitis by laser capture microdissection. *Brain Pathol* 13:144-54.
370. Trillo-Pazos, G., E. McFarlane-Abdulla, I. C. Campbell, G. J. Pilkington, and I. P. Everall. 2000. Recombinant nef HIV-IIIb protein is toxic to human neurons in culture. *Brain Res* 864:315-26.
371. Tyor, W. R., J. D. Glass, N. Baumrind, J. C. McArthur, J. W. Griffin, P. S. Becker, and D. E. Griffin. 1993. Cytokine expression of macrophages in HIV-1-associated vacuolar myelopathy. *Neurology* 43:1002-9.
372. UNAIDS. 2004. AIDS epidemic update: 2004. Joint United Nations Programme on HIV/AIDS and World Health Organization.
373. Valcour, V. G., C. M. Shikuma, M. R. Watters, and N. C. Sacktor. 2004. Cognitive impairment in older HIV-1-seropositive individuals: prevalence and potential mechanisms. *Aids* 18 Suppl 1:S79-86.
374. Valentin, A., M. Rosati, D. J. Patenaude, A. Hatzakis, L. G. Kostrikis, M. Lazanas, K. M. Wyvill, R. Yarchoan, and G. N. Pavlakis. 2002. Persistent HIV-1 infection of natural killer cells in patients receiving highly active antiretroviral therapy. *Proc Natl Acad Sci U S A* 99:7015-20.

375. Valle, H., and H. Carre. 1904. Sur l'anemie infectieuse du cheval. C.R. Acad. Sci. 139:1239-1241.
376. van de Bovenkamp, M., H. S. Nottet, and C. F. Pereira. 2002. Interactions of human immunodeficiency virus-1 proteins with neurons: possible role in the development of human immunodeficiency virus-1-associated dementia. *Eur J Clin Invest* 32:619-27.
377. van Furth, R. 1992. Production and migration of monocytes and kinetics of macrophages. Kluwer Academic Publishers, Dordrecht.
378. van Marle, G., S. Henry, T. Todoruk, A. Sullivan, C. Silva, S. B. Rourke, J. Holden, J. C. McArthur, M. J. Gill, and C. Power. 2004. Human immunodeficiency virus type 1 Nef protein mediates neural cell death: a neurotoxic role for IP-10. *Virology* 329:302-18.
379. van Oostrom, A. J., J. P. van Wijk, T. P. Sijmonsma, T. J. Rabelink, and M. Castro Cabezas. 2004. Increased expression of activation markers on monocytes and neutrophils in type 2 diabetes. *Neth J Med* 62:320-5.
380. van't Wout, A. B., N. A. Kootstra, G. A. Mulder-Kampinga, N. Albrecht-van Lent, H. J. Scherpbier, J. Veenstra, K. Boer, R. A. Coutinho, F. Miedema, and H. Schuitemaker. 1994. Macrophage-tropic variants initiate human immunodeficiency virus type 1 infection after sexual, parenteral, and vertical transmission. *J Clin Invest* 94:2060-7.
381. Veazey, R. S., M. DeMaria, L. V. Chalifoux, D. E. Shvetz, D. R. Pauley, H. L. Knight, M. Rosenzweig, R. P. Johnson, R. C. Desrosiers, and A. A. Lackner. 1998. Gastrointestinal tract as a major site of CD4+ T cell depletion and viral replication in SIV infection. *Science* 280:427-31.
382. Vella, C., and R. S. Daniels. 2003. CD8+ T-cell-mediated non-cytolytic suppression of human immuno-deficiency viruses. *Curr Drug Targets Infect Disord* 3:97-113.
383. Verani, A., G. Gras, and G. Pancino. 2005. Macrophages and HIV-1: dangerous liaisons. *Mol Immunol* 42:195-212.
384. Verdegaal, E. M., H. Beekhuizen, I. Blokland, and R. van Furth. 1993. Increased adhesion of human monocytes to IL-4-stimulated human venous endothelial cells via CD11/CD18, and very late antigen-4 (VLA-4)/vascular cell adhesion molecule-1 (VCAM-1)-dependent mechanisms. *Clin Exp Immunol* 93:292-8.
385. Wagner, L., O. O. Yang, E. A. Garcia-Zepeda, Y. Ge, S. A. Kalams, B. D. Walker, M. S. Pasternack, and A. D. Luster. 1998. Beta-chemokines are released from HIV-1-specific cytolytic T-cell granules complexed to proteoglycans. *Nature* 391:908-11.
386. Wang, G., C. L. Achim, R. L. Hamilton, C. A. Wiley, and V. Soontornniyomkij. 1999. Tyramide signal amplification method in multiple-label immunofluorescence confocal microscopy. *Methods* 18:459-64.

387. Ward, J. M., T. J. O'Leary, G. B. Baskin, R. Benveniste, C. A. Harris, P. L. Nara, and R. H. Rhodes. 1987. Immunohistochemical localization of human and simian immunodeficiency viral antigens in fixed tissue sections. *Am J Pathol* 127:199-205.
388. Watson, A., J. Ranchalis, B. Travis, J. McClure, W. Sutton, P. R. Johnson, S. L. Hu, and N. L. Haigwood. 1997. Plasma viremia in macaques infected with simian immunodeficiency virus: plasma viral load early in infection predicts survival. *J Virol* 71:284-90.
389. Weiden, M., N. Tanaka, Y. Qiao, B. Y. Zhao, Y. Honda, K. Nakata, A. Canova, D. E. Levy, W. N. Rom, and R. Pine. 2000. Differentiation of monocytes to macrophages switches the Mycobacterium tuberculosis effect on HIV-1 replication from stimulation to inhibition: modulation of interferon response and CCAAT/enhancer binding protein beta expression. *J Immunol* 165:2028-39.
390. Weinberg, J. B., T. J. Matthews, B. R. Cullen, and M. H. Malim. 1991. Productive human immunodeficiency virus type 1 (HIV-1) infection of nonproliferating human monocytes. *J Exp Med* 174:1477-82.
391. Westmoreland, S. V., E. Halpern, and A. A. Lackner. 1998. Simian immunodeficiency virus encephalitis in rhesus macaques is associated with rapid disease progression. *Journal of Neurovirology* 4:260-8.
392. Wiley, C., R. D. Schrier, J. A. Nelson, P. W. Lampert, and M. B. Oldstone. 1986. Cellular localization of human immunodeficiency virus infection within the brains of acquired immune deficiency syndrome patients. *Proc.Natl.Acad.Sci.USA.* 83:7089-7093.
393. Wiley, C. A. 2003. Detection of HIV-1 DNA in microglia/macrophages, astrocytes and neurons isolated from brain tissue with HIV-1 encephalitis by laser capture microdissection. *Brain Pathol* 13:415; author reply 415-6.
394. Wiley, C. A., and C. Achim. 1994. Human immunodeficiency virus encephalitis is the pathological correlate of dementia in acquired immunodeficiency syndrome. *Annals of Neurology* 36:673-6.
395. Wiley, C. A., C. L. Achim, C. Christopherson, Y. Kidane, S. Kwok, E. Masliah, J. Mellors, L. Radhakrishnan, G. Wang, and V. Soontornniyomkij. 1999. HIV mediates a productive infection of the brain. *AIDS* 13:2055-2059.
396. Wiley, C. A., E. Masliah, M. Morey, C. Lemere, R. DeTeresa, M. Grafe, L. Hansen, and R. Terry. 1991. Neocortical damage during HIV infection. *Annals of Neurology* 29:651-7.
397. Wiley, C. A., V. Soontornniyomkij, L. Radhakrishnan, E. Masliah, J. Mellors, S. A. Hermann, P. Dailey, and C. L. Achim. 1998. Distribution of brain HIV load in AIDS. *Brain Pathol* 8:277-84.

398. Williams, K., X. Alvarez, and A. A. Lackner. 2001. Central nervous system perivascular cells are immunoregulatory cells that connect the CNS with the peripheral immune system. *Glia* 36:156-64.
399. Williams, K., S. Westmoreland, J. Greco, E. Ratai, M. Lentz, W. K. Kim, R. A. Fuller, J. P. Kim, P. Autissier, P. K. Sehgal, R. F. Schinazi, N. Bischofberger, M. Piatak, J. D. Lifson, E. Masliah, and R. G. Gonzalez. 2005. Magnetic resonance spectroscopy reveals that activated monocytes contribute to neuronal injury in SIV neuroAIDS. *J Clin Invest* 115:2534-2545.
400. Williams, K. C., S. Corey, S. V. Westmoreland, D. Pauley, H. Knight, C. deBakker, X. Alvarez, and A. A. Lackner. 2001. Perivascular macrophages are the primary cell type productively infected by simian immunodeficiency virus in the brains of macaques: implications for the neuropathogenesis of AIDS. *J Exp Med* 193:905-15.
401. Williams, K. C., and W. F. Hickey. 2002. Central nervous system damage, monocytes and macrophages, and neurological disorders in AIDS. *Annu Rev Neurosci* 25:537-62.
402. Williams, K. C., and W. F. Hickey. 1995. Traffic of hematogenous cells through the central nervous system. *Current Topics in Microbiology & Immunology* 202:221-45.
403. Wyatt, R., and J. Sodroski. 1998. The HIV-1 envelope glycoproteins: fusogens, antigens, and immunogens. *Science* 280:1884-8.
404. Xiong, H., Y. C. Zeng, J. Zheng, M. Thylin, and H. E. Gendelman. 1999. Soluble HIV-1 infected macrophage secretory products mediate blockade of long-term potentiation: a mechanism for cognitive dysfunction in HIV-1-associated dementia. *Journal of Neurovirology* 5:519-28.
405. Xu, S., E. K. Jordan, S. Brocke, J. W. Bulte, L. Quigley, N. Tresser, J. L. Ostuni, Y. Yang, H. F. McFarland, and J. A. Frank. 1998. Study of relapsing remitting experimental allergic encephalomyelitis SJL mouse model using MION-46L enhanced in vivo MRI: early histopathological correlation. *J Neurosci Res* 52:549-58.
406. Yang, O. O., S. A. Kalams, M. Rosenzweig, A. Trocha, N. Jones, M. Koziel, B. D. Walker, and R. P. Johnson. 1996. Efficient lysis of human immunodeficiency virus type 1-infected cells by cytotoxic T lymphocytes. *J Virol* 70:5799-806.
407. Yeung, M. C., L. Pulliam, and A. S. Lau. 1995. The Hiv Envelope Protein Gp120 Is Toxic to Human Brain-Cell Cultures Through the Induction Of Interleukin-6 and Tumor-Necrosis-Factor-Alpha. *Aids* 9:137-143.
408. Yu, Q., D. Chen, R. Konig, R. Mariani, D. Unutmaz, and N. R. Landau. 2004. APOBEC3B and APOBEC3C are potent inhibitors of simian immunodeficiency virus replication. *J Biol Chem* 279:53379-86.
409. Yu, W. K., W. Q. Li, N. Li, and J. S. Li. 2004. Mononuclear histocompatibility leukocyte antigen-DR expression in the early phase of acute pancreatitis. *Pancreatology* 4:233-43.

410. Zelivyanskaya, M. L., J. A. Nelson, L. Poluektova, M. Uberti, M. Mellon, H. E. Gendelman, and M. D. Boska. 2003. Tracking superparamagnetic iron oxide labeled monocytes in brain by high-field magnetic resonance imaging. *J Neurosci Res* 73:284-95.
411. Zhang, J. Y., L. N. Martin, E. A. Watson, R. C. Montelaro, M. West, L. Epstein, and M. Murphey-Corb. 1988. Simian immunodeficiency virus/delta-induced immunodeficiency disease in rhesus monkeys: relation of antibody response and antigenemia. *J Infect Dis* 158:1277-86.
412. Zhu, T., H. Mo, N. Wang, D. S. Nam, Y. Cao, R. A. Koup, and D. D. Ho. 1993. Genotypic and phenotypic characterization of HIV-1 patients with primary infection. *Science* 261:1179-81.
413. Zhu, T., D. Muthui, S. Holte, D. Nickle, F. Feng, S. Brodie, Y. Hwangbo, J. I. Mullins, and L. Corey. 2002. Evidence for human immunodeficiency virus type 1 replication in vivo in CD14(+) monocytes and its potential role as a source of virus in patients on highly active antiretroviral therapy. *J Virol* 76:707-16.
414. Ziegler-Heitbrock, H. W. 2000. Definition of human blood monocytes. *J Leukoc Biol* 67:603-6.
415. Zink, M. C., A. M. Amedee, J. L. Mankowski, L. Craig, P. Didier, D. L. Carter, A. Munoz, M. Murphey-Corb, and J. E. Clements. 1997. Pathogenesis of SIV encephalitis. Selection and replication of neurovirulent SIV. *Am J Pathol* 151:793-803.
416. Zink, M. C., and J. E. Clements. 2002. A novel simian immunodeficiency virus model that provides insight into mechanisms of human immunodeficiency virus central nervous system disease. *J Neurovirol* 8 Suppl 2:42-8.
417. Zink, M. C., J. P. Spelman, R. B. Robinson, and J. E. Clements. 1998. SIV infection of macaques--modeling the progression to AIDS dementia. *Journal of Neurovirology* 4:249-59.
418. Zink, M. C., K. Suryanarayana, J. L. Mankowski, A. Shen, M. J. Piatak, J. P. Spelman, D. L. Carter, R. J. Adams, J. D. Lifson, and J. E. Clements. 1999. High viral load in the cerebrospinal fluid and brain correlates with severity of simian immunodeficiency virus encephalitis. *Journal of Virology* 73:10480-8.